



Characterizing the involvement of NMDA receptors in Alzheimer's disease

Doctoral Thesis presented by

Sergio Escamilla Ruiz

Thesis Director:

Dr. Inmaculada Cuchillo Ibáñez

Thesis Co-Director:

Dr. Javier Sáez Valero

PhD Program in Neuroscience

Neurosciences Institute

Miguel Hernández University of Elche

- 2024 -



This Doctoral Thesis, entitled "Characterizing the involvement of NMDA receptors in Alzheimer's disease" is presented under the compendium of publications form with the following quality indications:

- Escamilla, S.; Badillos, R; Comella, JX; Solé, M; Pérez-Otaño, I; Sánchez-Mut, JS; Sáez-Valero, J.; Cuchillo-Ibáñez, I. Synaptic and extrasynaptic distribution of NMDA receptors in cortex of Alzheimer's disease patients. *Alzheimer's Dement.* 2024. DOI: 10.1002/alz.14125
- Escamilla, S.; Sáez-Valero, J.; Cuchillo-Ibáñez, I. NMDARs in Alzheimer's Disease: Between Synaptic and Extrasynaptic Membranes. *Int. J. Mol. Sci.* 2024, 25, 10220. DOI: 10.3390/ijms251810220

Sant Joan d'Alacant, 21 October 2024

Dr. Inmaculada Cuchillo Ibáñez, Director, and Dr. Javier Sáez Valero, co-director of the doctoral thesis entitled **“Characterizing the involvement of NMDA receptors in Alzheimer’s disease”**.

INFORMAN:

That Mr. Sergio Escamilla Ruiz has carried out under our supervision the work entitled **"Characterizing the involvement of NMDA receptors in Alzheimer’s disease"** in accordance with the terms and conditions defined in his Research Plan and in accordance with the Code of Good Practice of the Miguel Hernández University of Elche, satisfactorily fulfilling the objectives foreseen for its public defence as a doctoral thesis.

We sign for appropriate purposes, at San Juan de Alicante to 21 from October from 2024

Thesis supervisor

Dr. Inmaculada Cuchillo Ibáñez

Thesis co-director

Dr Javier Sáez Valero

Sant Joan d'Alacant, 21st October 2024

Ms. Cruz Morenilla Palao, Coordinator of the Neurosciences PhD programme at the Institute of Neurosciences in Alicante, a joint centre of the Miguel Hernández University (UMH) and the Spanish National Research Council (CSIC),

INFORMA:

That Mr. Sergio Escamilla Ruiz has carried out under the supervision of our PhD Programme the work entitled "Characterizing the involvement of NMDA receptors in Alzheimer's disease" in accordance with the terms and conditions defined in its Research Plan and in accordance with the Code of Good Practice of the University Miguel Hernández de Elche, fulfilling the objectives satisfactorily for its public defence as a doctoral thesis.

Which I sign for the appropriate purposes, at San Juan de Alicante to 21st October 2024.

And for the record, for all due purposes, I sign this certificate.

Dra. Cruz Morenilla Palao

Coordinator of the PhD Programme in Neurosciences

E-mail: cruz@umh.es

www.in.umh.es

Tel: +34 34 965 919295

Av Ramón y Cajal s/n

SANT JOAN CAMPUS

03550 SANT JOAN D'ALACANT- SPAIN



2014 - 2027

This thesis has been funded by fellowship PFIS (Contratos predoctorales de formación en investigación en salud) associated to project PI19/01359 from Instituto de Salud Carlos III.



Index

1. Introduction.....	12
1.1 Alzheimer's disease (AD)	12
1.1.1 AD epidemiology	12
1.1.2 AD symptoms	12
1.1.3 AD pathogenesis.....	13
1.1.4 Genetics of AD	14
1.1.5 The amyloid cascade hypothesis	14
1.1.6 Other AD hypotheses	15
1.2 NMDA receptors (NMDARs)	17
1.2.1 Structure and signaling of NMDARs	17
1.2.2 Maturation of NMDARs	18
1.2.3 Regulation of NMDARs	19
1.2.4 Synaptic versus extrasynaptic signaling of NMDARs	19
1.2.5 Synaptic and extrasynaptic NMDARs in AD	21
1.3 AD biomarkers in CSF	22
1.3.1 Soluble NMDARs as a read-out of brain changes.....	23
1.4 Research models of AD	24
1.4.1 The need for human-relevant models.....	25
1.4.2 The use of iPSC-derived neurons for the study of NMDARs in AD	25
1.5 Proteomics of the AD brain	26
2. Objectives	28
3. Methods	29
3.1 Human samples.....	29
3.2 Brain samples	29
3.3 Human CSF samples	31
3.4 Cell culture	35
3.5 Mice.....	36
3.6 CSF extraction from mice	36
3.7 Subcellular fractionation protocol.....	36
3.8 Western blotting.....	37
3.9 Immunoprecipitation assays	37
3.10 Enzymatic deglycosylation assays.....	38
3.11 Lectin binding assays	38
3.12 Cell Immunocytochemistry (ICC).....	38

3.13 Fluorescence-activated Cell Sorting (FACS)	39
3.14 Extracellular vesicles isolation	39
3.15 RT-qPCR	39
3.16 Proteomics.....	40
3.17 Statistical analysis.....	42
4. Results	43
4.1. Fractionation protocol: Synaptic (SynF) and Extrasynaptic fractions (ExsynF) from human cortex.....	43
4.2 Synaptic and extrasynaptic distribution of NMDA receptors in cortex of AD patients	47
4.2.1 SynF and ExsynF characterization of NMDAR subunits	47
4.2.2 Identification of GluN2B and GluN2A glycoforms	49
4.2.3 Tyr1336 is the main site for GluN2B phosphorylation	50
4.2.4 Synaptic and extrasynaptic distribution of NMDAR subunits in control and AD cortex	51
4.2.5 Low Tyr1472 phosphorylation at synaptic GluN2B in AD cortex.....	54
4.2.6 N-glycosylation is altered in extrasynaptic GluN2B and GluN2A in AD cortex	55
4.2.7 NMDAR subunits distribution in mice models	57
4.3 NMDA receptor subunits characterization in the CSF of AD	61
4.3.1 NMDAR subunits GluN1, GluN2A, GluN2B, and GluN3A are present in human CSF	61
4.3.2 GluN2A subunit levels are lower in CSF from AD patients	63
4.3.3 GluN3A is increased in CSF samples from Huntington's disease subjects.....	65
4.4 iNeurons as a model for the study of NMDARs in the context of AD.....	67
4.4.1 Characterization of iNeurons from an individual with sporadic AD in BPM and NMM	69
4.4.2 Evidence for GluN2B-GluN2A switch in iNeurons	75
4.4.3 Increment of synaptic NMDARs along neuron maturation	77
4.4.4 Astrocytes also express NMDARs in BPM and NMM	79
4.4.5 Effect of A β on GluN2B and GluN2A in iNeurons	81
4.5 The synaptic and extrasynaptic proteome of the AD brain.....	84
4.5.1 Experimental design	84
4.5.2 Proteomic analysis: differentially expressed proteins in SynF and ExsynF.....	85
4.5.3 Proteomic analysis: Underexpressed proteins in SynF.....	97
4.5.4 Proteomic analysis: Overexpressed proteins in SynF	99
4.5.5 Proteomic analysis: Underexpressed proteins in ExsynF	101
4.5.6 Proteomic analysis: Overexpressed proteins in ExsynF.....	102
4.5.7 Comparative analysis between SynF and ExsynF	104
5. Discussion.....	106

5.1 Synaptic and extrasynaptic distribution of NMDA receptors in cortex of AD patients ...	106
5.2 NMDA receptor subunits characterization in the CSF of AD	109
5.3 To study the suitability of iNeurons for the study of NMDARs in the context of AD	112
5.4 The synaptic and extrasynaptic proteome of the AD brain.....	116
5.1.1 Validation of differentially expressed proteins in AD	116
5.1.2 Synaptic-related differentially expressed proteins.....	118
5.1.3 Mitochondria-related differentially expressed proteins	120
5.1.4 Metabolism-related differentially expressed proteins	122
5.1.3 Limitations	123
5.5 General discussion.....	124
6. Conclusions.....	127
7. References	129
8. Annex.....	149
9. Agradecimientos.....	186

List of abbreviations

ACH: amyloid cascade hypothesis

AD: Alzheimer's disease

APP: Amyloid precursor protein

A β : amyloid beta peptide

CaMKII: Calcium/calmodulin-stimulated protein kinase II

CSF: cerebrospinal fluid

DEP: Differentially expressed proteins

EOAD: Early onset Alzheimer's disease

FAD: Familial Alzheimer's disease

LOAD: Late onset Alzheimer's disease

NFT: Neurofibrillary tangle

NMDAR: N-methyl-D-aspartate receptors

MAGUK: Membrane-associated guanylate kinases

PSD: Postsynaptic density

SAD: Sporadic Alzheimer's disease

WHO: World Health Organization

RESUMEN

Los receptores NMDA (NMDAR) son fundamentales para la fisiología cerebral y la plasticidad sináptica, y su mal funcionamiento se ha asociado con la enfermedad de Alzheimer (EA). Específicamente, estudios realizados en modelos animales y celulares muestran que, mientras que la activación de los NMDAR sinápticos promueve señales de supervivencia, la activación de los NMDAR extrasinápticos produce neurotoxicidad y muerte celular. En esta tesis, llevamos a cabo un protocolo bioquímico para aislar las membranas sinápticas y extrasinápticas del cerebro humano. Mostramos que las subunidades de NMDAR GluN2A y GluN2B estaban reducidas en la fracción sináptica, mientras que GluN2B estaba aumentada en la fracción extrasináptica de la corteza con EA. Descubrimos una nueva glicoforma de 160 kDa de GluN2B y GluN2A que estaba aumentada en la fracción extrasináptica de la corteza con EA, y la N-glicosilación de GluN2B y GluN2A estaba alterada en la EA. El desequilibrio de subunidades de NMDAR en la EA podría inducir el fallo en la transmisión sináptica y la excitotoxicidad observada en la EA.

También describimos por primera vez la presencia de NMDAR en el líquido cefalorraquídeo humano y reportamos niveles reducidos de GluN2A e incrementados de GluN3A en la EA y la enfermedad de Huntington (EH), respectivamente. Este descubrimiento podría abrir el camino para futuros enfoques de biomarcadores en enfermedades neurológicas.

Finalmente, nos propusimos evaluar la idoneidad de las neuronas derivadas de células madre pluripotentes inducidas (iNeurons) para el estudio de los NMDAR en la EA. Utilizamos dos protocolos alternativos -Brainphys (BPM) y Neural Maintenance Media (NMM)- para estudiar si dos procesos clave del desarrollo -a saber, la incorporación de NMDAR en la sinapsis y el cambio de GluN2B a GluN2A- ocurren en las iNeurons. Saber si estos procesos del desarrollo ocurren en las iNeurons es fundamental para comprender sus limitaciones cuando los investigadores están interesados en modelar enfermedades relacionadas con el envejecimiento, como la EA. Encontramos que ambos protocolos incrementan sus NMDAR sinápticos con la maduración, pero solo BPM muestra signos que sugieren el cambio de GluN2B a GluN2A. Luego, intentamos modular el sistema NMDAR con tratamiento de A β para simular un entorno similar a la EA. El A β redujo los niveles de ARNm de GluN2B y GluN2A y la proporción de NMDAR sinápticos en NMM, pero no en BPM.

En conjunto, estos hallazgos subrayan la importancia de los NMDAR como moduladores clave de la EA y proporcionan un marco para futuras investigaciones orientadas a frenar la progresión de esta devastadora enfermedad.

ABSTRACT

NMDA receptors (NMDARs) are fundamental for brain physiology and synaptic plasticity, and their malfunctioning has been associated with Alzheimer's disease (AD). Specifically, studies performed in animal and cellular models show that while the activation of synaptic NMDARs promotes prosurvival signaling, the activation of extrasynaptic NMDARs leads to neurotoxicity and cell death. In this thesis, we perform a biochemical protocol to isolate the synaptic and extrasynaptic membranes from the human brain. We show that NMDAR subunits GluN2A and GluN2B were reduced in the synaptic fraction, whereas GluN2B was increased in the extrasynaptic fraction of AD cortex. We discovered a new GluN2B and GluN2A 160 kDa glycoform that were increased in the extrasynaptic fraction of the AD cortex, and N-glycosylation of GluN2B and GluN2A was altered in AD. The NMDAR subunit imbalance in AD could induce synaptic transmission failure and excitotoxicity found in AD.

We also described the presence of NMDARs in the human cerebrospinal fluid for the first time and reported decreased levels of GluN2A and increased GluN3A in AD and Huntington's disease, respectively. This discovery could pave the way for future biomarker approaches in neurological conditions.

Finally, we aimed to assess the suitability of iPSC-derived neurons (iNeurons) for the study of NMDARs in AD. We employed two alternative protocols -Brainphys (BPM) and Neural Maintenance Media (NMM)- to study whether two key developmental processes -namely, the incorporation of NMDARs into the synapse and the GluN2B-GluN2A switch- occur in iNeurons. Knowing whether these developmental processes occur in iNeurons is fundamental to understanding their limitations when researchers are interested in modeling aging-related diseases, such as AD. We found that both protocols increase their synaptic NMDARs with maturation, but only BPM shows signs suggesting the GluN2B-GluN2A switch. Then, we aimed to modulate the NMDAR system with A β treatment as an AD-like environment. A β reduced the mRNA levels of GluN2B and GluN2A and the proportion of synaptic NMDARs in NMM but not in BPM.

Taken together, these findings underscore the importance of NMDARs as key modulators of AD and provide a framework for future research aimed at slowing the progression of this devastating disease.

1. Introduction

1.1 Alzheimer's disease (AD)

1.1.1 AD epidemiology

The brain is probably the most important organ in the body. This is not only because it orchestrates and coordinates the rest of the body but also because it is the source of behavior, emotions, cognition, mind, and consciousness. Brain diseases fear us because they can perturbate our inner, mental life. Surely, brain diseases related to aging are particularly thrilling because aging is unavoidable. Among aging-related diseases, dementia is probably the most important one. According to the World Health Organization (WHO), dementia was one of the most relevant causes of death in high-income countries in 2021 (only after ischaemic heart disease, COVID-19, and stroke) [<https://www.who.int/data/gho/data/themes/mortality-and-global-health-estimates/ghe-leading-causes-of-death>].

Alzheimer's disease (AD) is the most common form of dementia [1], accounting for 50-70% of cases [2]. Aging is the most important risk factor for AD, and as life expectancy increases every decade, the prevalence of AD has been increasing over the years [3]. Today, more than 50 million people suffer from dementia worldwide, and this number is expected to triple by 2050 [4].

The importance of AD is not only social and medical but also economical. A study performed in a cohort of 1222 patients from the USA, Spain, Sweden, and the UK estimated that the total cost of caring for a patient with dementia and a low level of autonomy was up to 72,000€ per year [5]. This cost is shared between medical care and the caregiver's costs, the latter being more cost-consuming than the former [6, 7].

In 2015, the first WHO meeting took place in Switzerland to acknowledge and emphasize that AD and other dementias are global public health priorities [8]. Therefore, the efforts to deepen our understanding of the disease are necessary and should increase.

1.1.2 AD symptoms

The first symptom of AD is a short-term memory problem accompanied by spatial disorientation, some language difficulties, mood changes and both decision-making and problem-solving impairment. The second stage can be differentiated by increased forgetfulness, severe language problems, and difficulty dealing with day-to-day activities [2, 9].

Finally, at the late stages of the disease, long-term memory is also affected [10]. The patient becomes totally dependent, and there is a severe absence of activity or active behavior [2, 9].

1.1.3 AD pathogenesis

AD is characterized by the aggregation of two major proteins: the amyloid-beta peptide ($A\beta$), which aggregates in the form of amyloid plaques, and tau, which aggregates in the form of neurofibrillary tangles (NFTs). Both protein aggregates are tightly associated with the disease, and the spatial progression of each aggregate through different brain structures gives rise to two different progression scales: 1) extracellular deposition of $A\beta$, that ranges from 0 (no plaques) to A, B, C and D stages according to the accumulation of plaques [11, 12]; and 2) the intracellular deposition of NFTs, ranging from “Braak stage” I to VI [12-14].

$A\beta$ is a metabolic product of the amyloid precursor protein (APP). The transmembrane APP can be cleaved by β -secretase and γ -secretase in the so-called amyloidogenic pathway, releasing $A\beta$ to the extracellular space. In contrast, the action of α -secretase followed by γ -secretase does not form $A\beta$, constituting the non-amyloidogenic pathway [15].

$A\beta$ aggregates build up the so-called amyloid plaques, typical in the brain parenchyma of individuals with AD. $A\beta$ starts to aggregate in the neocortex, preferentially in layers II, III, IV, and V. Then, $A\beta$ deposits appear in the hippocampal formation, including the entorhinal cortex. As the disease progresses, $A\beta$ spreads throughout subcortical regions such as the striatum, thalamus, hypothalamus, and white matter. In the final stages of the disease, $A\beta$ deposits invade the cerebellum and brainstem [15, 16].

Tau, the microtubule-associated protein, plays an important function in stabilizing the cytoskeletal microtubules [17]. Tau aggregates form NFTs, which deposition occurs mainly inside neurons [18]. The first NFTs appear in transentorhinal regions, rapidly followed by entorhinal cortex and subiculum (Braak stages I and II). In Braak stage II, the hippocampus is affected, especially CA1. At this point, it may also start some sparse NFTs appearance in the neocortex. Some subcortical areas like the amygdala, the thalamus, or the hypothalamus can also be affected. In stage III, deposition increases in the same areas. In stage IV, the hippocampus is severely affected, and NFTs spread through subcortical regions, reaching the claustrum, the nucleus accumbens, and the striatum. In stage V, the entire hippocampal formation is severely affected. Still, the main feature is that the neocortex is seriously affected, with primary sensory and motor areas the less affected. Finally, stage VI is characterized by a severe worsening of the areas affected and a profound neuronal loss. Given the devastating

affectation of the neocortex at this stage, it is sometimes known as the “isocortex stage” [13, 19].

In addition to the spatial progression of protein aggregates, it is important to indicate that the progressive accumulation of tau correlates better with cognitive impairment than A β deposition [20].

1.1.4 Genetics of AD

The genetic architecture and heritability of AD are complex. However, it can be summarized as follows. Around 95% of cases are identified in individuals above 65 years of age, which is known as late-onset AD (LOAD). Accordingly, only 5% of cases develop before age 65, constituting early-onset AD (EOAD) [21]. While the genetic component of LOAD cases is considered to be less crucial, many EOAD cases carry genetic variants that increase the probability of developing AD. Approximately 11% of EOAD cases (0.6% of total AD cases) carry mutations in *APP*, *PSEN1*, or *PSEN2* genes. *PSEN1* and *PSEN2* codify presenilin 1 and 2, two members of the γ -secretase that cleaves APP, producing A β [22]. These cases are known as familial AD (FAD), in contrast to the remaining cases, which are termed sporadic AD (SAD) [23, 24].

While the heritability of FAD is autosomal dominant, the heritability of SAD is variable. According to twin studies, the heritability of SAD can be up to 70%, and the number of genetic variants associated with the disease is increasing as new genetic studies are performed [25-27]. The function of these genes is mainly involved in immune function but also in processes such as endocytosis and cell adhesion [28].

However, a gene has been associated with SAD more than any other: *APOE*. The gene *APOE* exists in three allelic variants in the human population: *APOE2*, *APOE3*, and *APOE4*. The genetic variant *APOE4* is the main genetic risk factor for SAD [29-31]. The *APOE4* gene encodes a lipoprotein that loses its normal ability to dimerize [32], affecting its various functions, including a crucial role in A β clearance [33], promoting A β aggregation into amyloid plaques [34]. Other alternative mechanisms that could increase the probability of developing AD include synaptic deficits, mitochondrial dysfunction, tau aggregation, and neuroinflammation [35].

1.1.5 The amyloid cascade hypothesis

The amyloid cascade hypothesis (ACH) is the leading and most influential theoretical framework in AD research. It accommodates evidence from different sources, and it has been a

way to gather efforts, test other hypotheses, and develop therapeutic strategies [36]. ACH was formulated in 1992 in a seminal paper by John A. Hardy and Gerald A. Higgins [37]. ACH proposes that A β deposition is the upstream causative agent that induces other pathological molecular alterations such as NFT formation and, ultimately, neuronal death and dementia.

ACH can account for three critical empirical facts: 1) A β deposition in brain parenchyma is strongly associated with AD, 2) A β deposition occurs before neuronal death and dementia, and 3) mutations associated with FAD cause A β deposition [36]. However, the ACH is not exempt from criticisms, and at least two points are debatable: A β deposition is a criterion for AD diagnosis, so it is a circular argument, and the causative role of A β in FAD could not be translatable to SAD or LOAD [36].

Even though it is accepted that the cause of FAD is the inheritance of genetic variants leading to increased production of A β (mutations in *APP*, *PSEN1*, and *PSEN2*), these cases represent less than 1% of cases [15]. In comparison, 99% are considered SAD and this is not caused by these mutations. In the SAD cases, it is thought that A β clearance rather than production is affected, and it is the driving mechanism that leads to amyloid pathology [36, 38], although other mechanisms could be in play.

1.1.6 Other AD hypotheses

The ACH is still the leading hypothesis in the AD research field. However, other hypotheses have been created to accommodate a plethora of empirical facts and endow the field with new perspectives [36, 39, 40]. The different alternative hypotheses are summarized.

1) The *synaptopathy hypothesis* states that synapses are the biological units that primarily suffer the pathological effects of A β and tau [41-43]. This is supported by several pieces of evidence. First, synapse deterioration and synapse loss correlate with cognitive decline, even before neuronal loss [44, 45]. Additionally, synaptic failure driven by A β or tau can be explained by numerous mechanisms [42, 46, 47] and can explain the abnormal oscillatory and hypersynchronous activity of neuronal networks in the AD brain [48, 49]. Furthermore, many scientists propose synapses as the therapeutic target in AD [50, 51]. Indeed, available drugs against AD are targeted to synaptic proteins (memantine [52, 53], an open channel blocker of N-methyl-D-aspartate receptors (NMDARs), and Acetylcholinesterase inhibitors [54]).

2) The *mitochondrial cascade hypothesis* states that an age-related mitochondrial dysfunction would lead to AD [55]. Mitochondrial energy production is lower in the AD brain than in age-matched healthy individuals [56, 57]. Also, mitochondrial dysfunction promotes APP

metabolism and A β production [58, 59]. This and other pieces of evidence, such as that genetic variants in the mitochondrial genome promote the development of AD [60, 61], have established the mitochondrial cascade hypothesis as an alternative to explain LOAD [62, 63].

3) The *dual pathway hypothesis* states that tau would be as important as A β in AD. Pathologic changes in tau and A β would be a consequence of one or several upstream causes [36, 64].

4) The *metabolism hypothesis* states that glucose metabolism impairment through distinct mechanisms, including insulin resistance in the brain, would be the upstream cause of AD-related molecular hallmarks, such as A β and tau accumulation [65, 66].

5) The *vascular hypothesis* states that vascular malfunctioning is crucial in AD progression [67-69]. It is supported by studies in humans showing impaired vascularization in the brain of AD patients [67] and studies in mice models that develop amyloid plaques, showing that up to 90% of plaques develop around blood vessels [70]. However, the cause-effect relationship remains controversial: does a vascular deficit lead to A β deposition? Or does A β deposition lead to a vascular deficit [36]?

6) The *A β oligomer hypothesis* states that soluble A β oligomers rather than insoluble amyloid plaques or A β monomers (which is the ACH) exert the pathologic effect. It may be considered as an extension of ACH rather than a different hypothesis [36, 71].

7) The *neuroinflammation hypothesis* emphasizes the microglial dysfunction. Given the abundant empirical data supporting it, it is currently the most compelling hypothesis [72-75]. This hypothesis states that microglia would detect misfolded proteins and develop a pathological sustained pro-inflammatory state through the innate response, contributing to the disease progression [72]. The sustained activation of microglia leads to the release of reactive oxygen species, compromising brain cells function [72]. Some authors argue that, primarily through Triggering receptor expressed on myeloid cells 2 (TREM2) signaling, microglial cells could be a mechanistic link between amyloid plaques and tau pathology [36, 72, 76]. In fact, genetic variants in *TREM2* [77] and other genes related to the immune system predispose to the development of AD [78, 79].

8) The *hormonal hypothesis*. This hypothesis claims that hormonal dysregulation may be a causative agent of some of the metabolic perturbations that characterize AD [80, 81]. An imbalance in hormones such as follicle-stimulating hormone (FSH) [82, 83] or sexual hormones such as estrogen [84] and testosterone [85] have been linked to a greater probability of

developing AD. However, thyroid hormone is probably the hormone most commonly associated with AD [86-91].

1.2 NMDA receptors (NMDARs)

1.2.1 Structure and signaling of NMDARs

NMDARs are glutamate-binding ionic channels [92]. The main subunits are GluN1, GluN2 (A-D) and GluN3 (A-B) [93]. The mandatory subunit is GluN1, while the others can be arranged as di or tri-heteromers [94-97]. The different subunits of NMDARs are expressed in various developmental stages and brain areas. For example, GluN2C expression is specific to the adult cerebellum [98], whereas GluN2D is expressed early in development, and its expression is restricted to the mesencephalon and the spinal cord [99]. The most important subunits expressed in the mouse and human adult cerebral cortex and hippocampus are GluN1, GluN2A, and GluN2B [92, 93].

When the four subunits are correctly assembled, the inner part of the receptor forms an ion channel that is blocked by extracellular Mg^{2+} when the plasma membrane is at a resting state [100]. After membrane depolarization, the Mg^{2+} leaves the pore, allowing the flux of sodium, potassium, and calcium into the cell [93].

The NMDAR blockade by Mg^{2+} is voltage-dependent and acts as a detector of simultaneous activation of the pre and postsynaptic neuron. Indeed, both pre and postsynaptic neurons must be simultaneously stimulated to activate NMDARs and induce the ion flux. Presynaptic activity is needed to release glutamate, which binds to GluN2 subunits, whereas postsynaptic activity is required to depolarize the membrane and promote Mg^{2+} to leave the receptor. Besides this, a third requisite is needed to activate NMDARs: the binding of the co-agonist D-serine to GluN1 subunits [101, 102]. It is worth mentioning that GluN3A subunits do not bind glutamate but glycine [103] and that GluN2B can bind both D-serine and glycine [104].

GluN subunits have a large N-terminal extracellular domain containing the glutamate and D-serine binding sites. The C-terminal domain is critical for the interaction with other partners, such as proteins of the family membrane-associated guanylate kinases (MAGUK) like the scaffolding protein PSD95 (postsynaptic density protein-95) or the receptor for signaling proteins reelin and apoE, apoER2/LRP8 [105-107]. The C-terminal domain of NMDAR subunits can be regulated through different post-translational modifications, including phosphorylation.

Specifically, they contain residues that can be phosphorylated by the SCR kinases family [108, 109].

NMDAR activation is intimately related to synaptic plasticity mechanisms underlying learning and memory processes [110-113]. When a synapse is repeatedly activated, NMDAR-mediated calcium influx induces local modifications such as phosphorylation of kinases like Calcium/calmodulin-stimulated protein kinase II (CaMKII) [114], which leads to the incorporation of new synaptic proteins that strengthen the synapse. Moreover, NMDAR activity also induces some chemical signaling that reaches the nucleus [115], leading to a whole-cell strengthening, known as homeostatic plasticity (translocation of the protein Jacob to the nucleus and phosphorylation of CREB are key mechanisms of this plasticity [116-118]).

1.2.2 Maturation of NMDARs

Maturation of NMDARs occurs through a complex pathway. When NMDAR subunits are translated in the ribosome/endoplasmic reticulum, they undergo co-translational modifications such as N-glycosylation [119-121]. After translation, they undergo numerous post-translational modifications, including further glycosylation and phosphorylations, until they are finally assembled as tetramers in the endoplasmic reticulum [121, 122]. Subsequently, NMDARs are transported to their ultimate location, mainly in the dendritic compartment.

To build a mature synapse, a developmental switch between NMDAR subunits is needed to occur [123]. During development, immature synapses in the mice cerebral cortex are mainly populated by GluN2B, while GluN2A resides in the extrasynaptic membranes. This constitutes de so-called silent synapses. During the second postnatal week in the cortex and hippocampus, GluN2B gradually leaves the synapse and populate mainly the extrasynaptic membranes, while GluN2A does the opposite, enters the synapse and is stabilized at the postsynaptic density (PSD), a protein-dense molecular ultrastructure attached to the post-synaptic membrane [93, 96, 123]. This natural switch triggered by sensory input is recapitulated in mice primary cortical cultures after two weeks *in vitro*, although it has been a matter of debate [123-126]. The use of different techniques (electrophysiology and pharmacology, microscopy imaging, or biochemistry), different animal models, or different days-in-vitro in primary cultures may explain the diversity in the obtained results [127, 128]. This “entering and leaving” movement of NMDARs at the synapse is not a process restricted to the developmental stage. In adulthood, these dynamics are thought to constitute some mechanisms underlying learning and memory-related synaptic plasticity phenomena [129, 130].

1.2.3 Regulation of NMDARs

As mentioned above, an essential mechanism of NMDAR regulation is phosphorylation [131]. The interplay between kinases and phosphatases allows local and fast regulation of many synaptic proteins [132]. Both GluN2A and GluN2B can be extensively phosphorylated [131], but the phosphorylation of the residue (tyrosine) Y1472 of GluN2B is one of the most important. First, because it is the main phosphorylation site of the GluN2B subunit [133], and second, because of its functional implications [134]. The phosphorylation of this residue by the kinase Fyn of the SRC family [135] leads to the anchoring of GluN2B in the synapse. The residue Y1472 is located within an internalization motif that, when interacting with the adaptor AP-2 (a multimeric protein that works on the cell membrane to internalize cargo in clathrin-mediated endocytosis), leads to its endocytosis [136]. When Y1472 is phosphorylated, the binding to the adaptor is inhibited, and the interaction of the PDZ binding domain (a short common structural domain at the C-terminus found in signaling proteins that regulate protein interactions) of GluN2B to the scaffolding protein PSD95 is favored. Phosphorylation of Y1472 leads to GluN2B retaining in the synapse [137], while dephosphorylation allows the receptor to be endocytosed or to move freely and eventually leave the synaptic space and enter into the extrasynaptic membranes by lateral diffusion [138]. Hence, the intracellular C-terminal domain of GluN subunits through the PDZ-binding site can be modified to mediate the binding to MAGUK scaffolding proteins [93]. Interestingly, when the PDZ domain of GluN2B is removed, the number of subunits within the synapse dramatically decreases [137], suggesting that protein-protein interaction is needed to retain GluN subunits in the PSD. In addition, it is thought that GluN2B subunits are more mobile than GluN2A ones [138], meaning that GluN2A dwells in the synapse while GluN2B moves in and out.

GluN2A and GluN2B have different electrophysiological kinetics [139-141] and partner repertoires [115], and this has an impact on their functions. In the adult, GluN2A-containing NMDARs were thought to be present mainly at synaptic membranes, whereas GluN2B-containing ones were believed to reside in the extrasynaptic space [138]. It is known that this model is oversimplified and needs to be overcome, although some current studies still endorse it [142]. Both GluN2A and GluN2B are in the synaptic and extrasynaptic membranes [143-146], and complex dynamics and interplay between these two subcellular localizations occur.

1.2.4 Synaptic versus extrasynaptic signaling of NMDARs

Although NMDARs can be expressed by astrocytes [147, 148], oligodendrocytes [149], and microglia [150], most NMDARs are expressed by neurons [94]. NMDARs have been reported in

inhibitory GABAergic interneurons [151] and in the presynaptic compartment of excitatory neurons [152]. However, the most important population of NMDARs are those in postsynaptic membranes located at the PSD [94], receiving the name of synaptic NMDARs (SynNMDARs).

NMDARs located outside the synapses are defined as extrasynaptic NMDARs (ExsynNMDARs) and are present at a lower density compared to SynNMDARs [144]. This criterion includes the peri-synaptic space, such as the dendritic spine neck, and places further from synapses located in the dendritic shaft, the soma, or the axon [128, 144, 153]. Relying on morphological criteria, receptors are considered extrasynaptic when located at 100 nm or more from the PSD [8]. To put it in perspective, the PSD is around 30 nm thick and 300 nm long [154].

SynNMDARs and ExsynNMDARs show different kinetics with respect to glutamate release. The presynaptic neuron releases glutamate in the synapse, but several mechanisms rapidly eliminate the glutamate in the synaptic space. This leads to a fast kinetics in the glutamate-binding dynamics in the synapses. On the contrary, ExsynNMDARs are activated by high levels of glutamate in the extracellular environment, leading to chronic activation instead of transient activation [155].

In 2002, it was demonstrated that the activation of SynNMDARs induced synaptic plasticity and pro-survival signaling, whereas activation of ExsynNMDARs led to pro-death signaling and cell death [117]. The mechanism that mediates the toxicity of ExsynNMDARs is not likely dependent on the calcium current *per se* since similar calcium transients through SynNMDARs and ExsynNMDARs trigger antagonistic responses [117]. A compelling explanation for solving this paradoxical antagonism of SynNMDARs versus ExsynNMDARs activations comes from transcriptomic studies. The selective activation of SynNMDARs induces transcriptomic changes toward neuroprotective genes, such as *Atf3*, *Bcl6*, and *Btg2* [155]. At the same time, this leads to the suppression of pro-death genes such as *Puma* and pro-caspase-9 [117]. Instead, activation of ExsynNMDARs promotes the inhibition of the master transcription factor CREB. Besides, other pathologic activities could occur, such as the inactivation of the ERK1/2 pathway [156], the inversion of the mitochondrial potential [157, 158], toxic synapse-to-nucleus communication [118, 159], the activation of the death gene *FOXO* [155] or sustained influx of calcium [160, 161].

Some researchers have proposed a subunit specificity relating to these processes, where GluN2A is linked to pro-survival and GluN2B to pro-death signaling [162]. However, the accumulation of different evidence led to the assumption that such subunit specificity does not

exist [155], and instead, both GluN2A and GluN2B are part of NMDAR related to pro-survival and pro-death signaling [163-165].

1.2.5 Synaptic and extrasynaptic NMDARs in AD

It is assumed that an imbalance between SynNMDARs and ExsynNMDARs activation could be part of the aetiology of neurodegenerative diseases such as AD [127, 166-168], where the homeostasis of glutamate is dysregulated [169-171]. However, there is little information about alterations in the distribution of NMDARs in synaptic and extrasynaptic membranes in the brains of individuals with AD. In the clinic, one of the few drugs used in AD therapy, memantine, is an open-channel blocker of ExsynNMDARs [172-175]. Memantine is currently used in combination with acetylcholinesterase inhibitors [176], and despite the clinical effects are still controversial [52], data in clinical studies suggest that it has a positive impact on improving AD symptoms [177].

Chronic activation of ExsynNMDARs could be a contributing effector of AD [166, 178-180]. *In vitro* and *in vivo* studies suggest an excessive release of glutamate from astrocytes in AD would activate ExsynNMDARs in neurons [181]. Besides, sustained activation of ExsynNMDARs increases the production of A β [182] and increases the expression [183-185] and phosphorylation [181] of tau, the main pathological hallmarks of AD. Accordingly, the pharmacological targeting of GluN2B and GluN2A *in vivo* ameliorates excitotoxicity [146]. On the other hand, stimulation of SynNMDARs increases the non-amyloidogenic processing of APP by α -secretase, thus decreasing the release of A β [186].

Many researchers have measured total NMDAR protein levels in the cerebral cortex of individuals with AD [187-192], and mRNA levels by Real-Time Quantitative Reverse Transcription (qPCR) [187, 189, 193, 194] or RNAseq (a deep-sequencing technology) [195-198], most of them leading to the same observation: NMDAR levels are lower in the AD brain. However, it has not been performed a systematic study of NMDAR subunits -GluN1, GluN2B, GluN2A, and GluN3A- distribution discriminating synaptic and extrasynaptic membranes in the cerebral cortex of individuals with AD, despite this, can shed light on the role of these receptors in the pathology. Accordingly, this constitutes an **objective** of this thesis: To characterize the NMDARs population in synaptic and extrasynaptic membranes, evaluating the subunits GluN1, GluN2B, GluN2A, and GluN3A in control and AD human cortex.

1.3 AD biomarkers in CSF

Molecular alterations such as A β and tau deposition begin in the brain many years, even decades before the clinical phase of AD appears [15]. Therefore, the need for early biomarkers is crucial since once the symptoms appear, neurodegeneration is too advanced to have an optimal therapeutic opportunity [15, 199]. To have available biomarkers is desirable for a better diagnosis, disease state assessment, mechanism of action, dose optimization, and drug response monitoring, among other interests [200]. Although neuroimaging biomarkers exist [201], fluid biomarkers are more extended because they are less expensive, need less equipment, can be easily implemented, and several biomarkers can be analyzed in the same cerebrospinal fluid (CSF) or blood sample [202].

Blood is the most desirable fluid from which to obtain biomarkers because it requires a minimally invasive procedure. However, the first stage of discovering new biomarkers usually relies on the CSF, given that it is the fluid that wash out brain metabolites [203]. This is ideal since CSF could serve as a read-out of the neurodegenerative processes that could be happening in the brains of AD individuals [204].

Since A β and tau constitute two crucial proteins in AD pathogenesis, they were candidates for being CSF biomarkers since the beginning. In 1999, the first paper showed that individuals with high total tau and low A β ₄₂ (the more amyloidogenic form of A β) were more likely to develop AD [205]. In 2006, a new study presented the so-called “AD core biomarkers” in CSF [206]. In this study, authors showed a 95% diagnostic sensitivity for the combination of low A β ₄₂ levels and high total-tau/phospho-tau ratio to predict individuals that would develop AD from early stages of the disease. When these important results were replicated in other studies [207-209], the core biomarkers became so important that they became part of the AD biological definition [210-212]. Notwithstanding, scientists are constantly seeking new biomarkers to reflect other aspects of the disease, to stratify patients, or to provide biomarkers independent of A β and tau [213].

Hence, the search for new biomarkers in the CSF of individuals with AD is still needed. This search can be either unbiased or hypothesis-driven. The unbiased search relies on omic techniques, such as proteomics or metabolomics [214-216], whereas the hypothesis-driven search considers a core hypothesis in AD pathophysiology and tries to find a related molecule as a biomarker. For example, researchers interested in the role of vascular dysfunction in AD have sought vascular-related biomarkers, such as Heart-type fatty acid binding protein [228, 229], while scientists interested in neuroinflammation have looked for related proteins, such as

TREM2 [217, 218]. These new biomarkers do not look to replace the core biomarkers but to use them as a confirmatory or supportive diagnosis, as well as to stratify the heterogeneity of AD patients, among other uses [200]. In addition, the heterogeneity of the pathological mechanisms behind some LOAD cases demands an extended list beyond the core biomarkers that may reflect additional features of the disease [213].

Interestingly, synaptic proteins have received much attention as AD biomarkers in CSF in recent years. This is probably because synaptic degeneration is a central process in AD [42, 46, 219]. Furthermore, synapses suffer plastic changes in the short term that may reflect pathologic changes and serve as a read-out of the synaptic degeneration processes occurring in the brain [213].

While hypothesis-driven search has found that synaptic proteins such as Neurogranin [165, 166] and SNAP-25 [220] are altered in the AD CSF, new unbiased approaches have revealed that changes in several synaptic proteins precede neurodegeneration. Specifically, researchers discovered using shotgun proteomics that six synaptic proteins (Calsyntenin-1, GluR4, Neurexin-2A, Neurexin-3A, Syntaxin-1B and Thy-1) were reduced in preclinical AD [214].

1.3.1 Soluble NMDARs as a read-out of brain changes

Motivated by these findings, we wondered if measuring NMDAR levels in CSF could provide a read-out of the synaptic degenerative processes that occur in the brains of individuals with AD. The existence of multipass membrane proteins in CSF, as fragments or full-length forms proteolytically unprocessed, cannot be discounted since several transmembrane proteins that retain their transmembrane and intracellular domains, such as APP [221], BACE1 [222], ADAM10 [223] or the ACE2 receptor [224], have been found in human CSF and plasma, also including subunits of membranes multipass protein complexes such as presenilin-1 [225]. To our knowledge, the presence of NMDAR subunits in the human CSF has not been investigated until now.

Accordingly, this constitutes an **objective** of this thesis, to characterize the presence of NMDARs in the CSF from individuals with AD, as well as from other diseases such as Huntington's disease (HD), where GluN3A is increased in the striatum of human HD patients [224], and anti-NMDAR encephalitis, an autoimmune encephalitis characterized by the presence of Immunoglobulin G (IgG) antibodies against the GluN1 subunit in the central nervous system (CNS) [226, 227].

1.4 Research models of AD

The availability of good models of human diseases is crucial for advancing our understanding of their pathophysiology. Unfortunately, AD is particularly difficult to replicate in animal models because there are no sporadic AD cases in nature (although some non-human primates may develop a similar pathology [228]). Second, because the well-established genetic mutations behind the FAD cases account for only 1% of total cases, and the aetiology of the rest, considered as SAD [15, 229], is not known [15, 36].

The strategies for developing animal models of AD are focused on recapitulating the two hallmarks of AD: amyloid plaques and NFTs. The most used models in AD research are the transgenic mice models that develop amyloid plaques [228, 230], such as the APP^{V717F} (Indiana mutation) [231] or the Tg2576 APP^{K670N/M671L} (Swedish mutation) [232]. Wild-type mouse APP has 97% sequence homology with human APP. The main differences reside in key residues involved in the sequence of A β , which could explain why mice do not develop amyloid plaques. The genetic AD mice models usually carry human *APP* and/or *PSEN1* or *PSEN2* and are considered models of early AD or amyloidosis [228, 230]. Thus, these mice constituted FAD and not SAD models.

The wild-type mouse *Tau* gene has 88% homology with the human gene and expresses mouse-specific isoforms [230]. Similarly to amyloidosis models, endogenous mice tau do not form NFTs. This implies that to model a tau pathology, these transgenic mice express human Tau, and this human Tau has to be mutated to form NFTs [233]. The most common mutations are P301S and P301L, where a proline amino acid is replaced by serine or leucine, which leads to tau aggregation [234]. There is a concern about whether these models resemble the pathological alterations that the human Tau suffers in the brain of patients with AD since these mutations are not present in AD patients, only in patients with other tauopathies such as frontotemporal dementia and Parkinson's linked to chromosome 17. Thus, these models may not be as representative of the disease as desired [230]. Tau pathology can also be induced by injecting okadaic acid [235], a protein phosphatase inhibitor that leads to tau hyperphosphorylation and aggregation.

In many cases, the use of knock-in mice has replaced transgenic mice, especially for amyloidosis models. *APP* knock-in mice have the same expression levels as the endogenous gene, expressed by the physiological cells and brain regions [236]. This is a step forward to model specific aspects of AD in a more physiologically relevant manner [230]. Even though

mice are the most used models, other animals have been used to develop specific aspects of the disease, such as zebrafish, worms, and fruit flies [2, 228, 230].

1.4.1 The need for human-relevant models

The use of animal models in AD research has allowed a profound study of amyloid and tau pathology [2]. However, even though the recapitulation of AD-like pathology in mice has been improved and therapies have been tested successfully, there is still a remarkable lack of disease-modifier drugs for humans [5, 230].

One possible explanation for this mismatch between animal modeling and the clinic may reside in the amyloid and tau pathology, which could be endpoints of different pathologic mechanisms rather than the origin of the disease [36]. This explanation is not entirely satisfactory, and anyhow, we need to study human tissues directly or through human-relevant models to capture the complexity that defines this pathology [237].

In this regard, AD models derived from induced pluripotent stem cells (iPSCs) have impacted the field [238, 239]. With this technology, researchers can reprogram somatic cells (e.g., fibroblasts) to iPSCs, which can be differentiated into almost any kind of cell [240, 241].

iPSC lines from patients with SAD/EOAD or FAD/LOAD and differentiated to neuronal cultures display some AD biochemical features, such as increased production of A β or hyperphosphorylated tau [242, 243]. iPSCs can also be differentiated into other cell types relevant to AD, such as astrocytes or microglia [244, 245]. This allows researchers to study how the different cells are implicated in the pathology in a human-relevant manner. Furthermore, there is a rapid development in stem cell technologies, and the creation of 3D cerebral organoids represents a significant advance in modeling AD [246].

1.4.2 The use of iPSC-derived neurons for the study of NMDARs in AD

Our understanding of the role of NMDARs in AD has grown over the years using animal models. However, the emergence of iPSC-derived neurons (iNeurons) prompted many researchers to explore this *in vitro* human model. The use of iPSC and specifically of iNeurons entailed a dramatic step forward to model AD [238, 247, 248], not only the familial forms [249, 250] but also the sporadic cases [251-254].

iNeurons have allowed us to gain insight into proteins and pathological mechanisms related to AD, and there are still many important gaps to which this technique can contribute in a valuable manner, as those related to NMDARs function. In this regard, understanding the

timing of the GluN2B-GluN2A switch in iNeurons is crucial, as it was mentioned previously in this thesis for murine primary cultures [93, 96, 123]. It is essential to ensure that the iNeurons used in experiments worldwide contain mature synapses. The presence of mature synapses in iNeurons is crucial to consider this culture suitable specifically for the study of aging-related pathologies as AD.

However, it is not well described in the literature the type of differentiation or the days of maturation needed for the GluN2B-GluN2A switch to occur in iNeurons.

The evaluate of the suitability of iNeurons for the study of NMDARs in the context of AD constitutes an **objective** of this thesis.

1.5 Proteomics of the AD brain

Most biological functions are performed by proteins [255], and many proteins have been described to be altered in AD. This is why high-throughput proteomics through mass spectrometry (MS) is a very powerful technique for researchers interested in AD [256-258]. Proteomics can be defined as the set of experimental and data analysis techniques that allow researchers to study the protein composition, structure, expression, modification status, and protein-protein interactions in a biological sample [259, 260].

In this regard, a recent study that gathered differentially expressed proteins (DEP) in different proteomic studies indicates that 1,484 proteins are upregulated and 1,214 proteins are downregulated in the AD brain [258]. Interestingly, some DEP in AD match with genes identified as linked to AD through Genome-Whole-Association-Studies (GWAS). Integrating genomic with proteomic data led to the discovery of 11 causal genes that lead to AD [261].

Furthermore, proteomic analysis allows researchers to cluster proteins and predict which functional pathways could be affected [258]. A recent study revealed that the most affected pathways in the left frontal AD cortex are those related to metabolic processes, translation, synapses, actin-cytoskeleton regulation, signal transduction, and protein transport [262].

As previously stated, AD is a synaptopathy [41, 42, 46], which means that many molecular alterations that characterize the disease occur in the synaptic compartment. However, most proteomic studies of the AD brain are performed on the whole tissue. A protein can perform different functions depending on its subcellular location or post-translational status [263, 264]. In fact, proteins prone to suffer abundant post-translational modifications are more involved in diseases [265]. Thus, an analysis of whole tissue could mask subtle pathological

changes in synaptic proteins since only the more abundant or differentially expressed are analyzed [266].

Spatial proteomics aims to disentangle the proteomic influence of different organelles or subcellular locations to uncover specific, subtle changes that proteins could suffer in pathological conditions. Spatial proteomics takes profit from biochemical fractionation protocols, which allow researchers to purify different fractions from a tissue, where each fraction is enriched in specific subcellular compartments or organelles [267].

Embracing the synaptopathy hypothesis, we aim to analyze and compare the proteome of both the synaptic and the extrasynaptic fractions from the frontal cortex of control and AD individuals. We employed label-free shotgun proteomics, an unbiased approach to uncover the whole synaptic and extrasynaptic proteome. Accordingly, this constitutes an **objective** of this thesis, to uncover the proteome of synaptic and extrasynaptic fractions in control and AD human cortex.

2. Objectives

This thesis aims to reach the following objectives:

Objective 1: To characterize NMDARs population in synaptic and extrasynaptic membranes, from control and AD human cortex.

Objective 2: To characterize the presence of NMDARs in the CSF from individuals with AD.

Objective 3: To evaluate the suitability of iNeurons for the study of NMDARs in AD.

Objective 4: To describe the proteome of synaptic and extrasynaptic fractions in control and AD human cortex.

3. Methods

3.1 Human samples

The projects included in this thesis have been approved by the ethics committee of the Universidad Miguel Hernández de Elche and the Hospital General Universitario de Alicante-ISABIAL (Spain) and it was carried out in accordance with the WMA Declaration of Helsinki.

3.2 Brain samples

Brain samples (frontal cortex, Brodmann area 8) were provided by the Biobank HUB-ICO-IDIBELL (PT20/00171), integrated in the ISC-III Biobanks and Biomodels Platform. Samples were processed following standard operating procedures. Cases with AD-related pathology were considered those showing NFTs and/or amyloid plaques with the distribution established by Braak and Braak at the post-mortem neuropathological examination [14]. These were categorized as Braak stages I–II, $n = 8$, 1 female/7 males, 63 ± 5 years; Braak stages III–IV, $n = 9$, 4 females/5 males, 78 ± 7 years; and Braak stages V–VI, $n = 8$, 3 females/5 males, 76 ± 6 years. Taking together from Braak I to VI $n = 25$, 8 females/17 males, 72 ± 9 years. Cases at stages I, II, and III did not have cognitive impairment; three cases at stage IV had moderate cognitive impairment, and cases at stages V and VI all suffered dementia. Special care was taken not to include cases with combined pathologies to avoid bias in the pathological series. Samples from controls, $n = 14$, 4 females/10 males, 56 ± 10 years, corresponded to individuals with no evidence of brain pathology and no clinical dementia. The mean post-mortem interval of the tissue was 7.1 h in all cases, with no significant difference between the subgroups. See **Table 1** for summarized details.

Human brain samples

Age (y)	Gender	PM (h)	HUSPIR Index	Braak stage	Aβ stage
50	F	14	2.3	Control	0
52	M	4	2.2	Control	0
58	M	4	6.7	Control	0
59	M	4	5.2	Control	0
62	M	3	4	Control	0

64	F	5	2.7	Control	0
75	F	3	4.3	Control	0
44	M	6.4	2.2	Control	0
46	M	15	5.1	Control	0
53	M	3	5.6	Control	0
47	M	5	6.4	Control	0
52	F	6	2.6	Control	0
52	F	5	5.0	Control	0
79	M	7	3.2	Control	0
68	M	11	8	I	0
67	M	14	3.1	I	0
53	M	6	4.1	I	A
67	M	7	3.3	II	0
57	M	4	4.7	II	0
60	F	9	2.9	II	A
69	M	3	4.8	II	A
77	M	4	4.1	III	0
68	F	4	1.9	III	A
82	F	5	2.2	III	A
71	M	7	4.1	III	0
90	F	4	3.9	III	B
77	M	5	5.9	III	A
79	M	5	3.2	III	A
81	F	5	3.3	IV	C

85	M	14	2.8	IV	B
72	M	2	5.1	V	C
73	M	4	4.1	V	B
67	F	8	4.7	V	C
81	F	5	4.5	V	C
78	M	17	2.8	V	O
77	M	16	7.8	VI	C
86	F	20	3.5	VI	C
75	M	12	7.3	VI	B

Table 1. Control and Alzheimer's disease (AD) frontal cortex cases from Biobank HUB-ICO-IDIBELL (PT20/00171). Subjects were categorized according to the Braak stage of neurofibrillary tangle (NFT) pathology. Age (y= years), gender (M=male, F=female), Post-mortem (PM, h=hours). HUSPIR Index >1 [268] ensures that post-mortem cortical samples are optimally preserved for biochemical evaluation of synaptic proteins. Stage of disease progression was measured according to NFT [13, 14] and amyloid accumulation [11].

3.3 Human CSF samples

CSF samples were obtained from the Clinical Neurochemistry Laboratory (Mölnådal, Sweden) from patients who sought medical advice because of cognitive impairment. Patients were designated as AD or controls according to CSF biomarker levels. AD patients had a CSF biomarker profile indicative of AD, including increased total tau and phosphorylated tau and low A β 42 concentrations in CSF. Age-matched control individuals had normal levels of all three CSF biomarkers; cut-offs >90% specific for AD [206]. The collection for the AD study was composed of n = 20 control and n = 15 AD individuals. The average age of control subjects is 73.1 ± 6.7 years. The average age of AD is 74.2 ± 6.9 years (see **Table 2**).

Human AD CSF samples

<i>Age (y)</i>	<i>Gender</i>	<i>Tau (ng/ml)</i>	<i>Aβ (ng/ml)</i>	<i>pTau (ng/mL)</i>	<i>Diagnosis</i>
68	M	211	645	26	Control
59	F	317	1730	41	Control

70	F	366	1220	40	Control
74	M	306	1120	38	Control
64	M	289	894	27	Control
75	M	322	784	58	Control
24	M	315	858	24	Control
77	M	297	940	42	Control
83	F	244	765	34	Control
71	F	170	879	23	Control
77	M	284	1060	32	Control
76	M	375	744	46	Control
86	M	310	705	39	Control
65	M	284	751	31	Control
84	F	197	708	22	Control
76	M	189	969	28	Control
76	M	259	1070	40	Control
67	M	193	938	26	Control
73	M	681	490	88	AD
76	F	1130	569	148	AD
73	M	780	462	105	AD
66	F	412	566	62	AD
75	M	495	561	75	AD
80	F	784	539	116	AD
74	M	493	512	79	AD
82	M	429	473	153	AD
85	M	637	522	104	AD
68	M	618	538	74	AD
69	F	1080	456	154	AD
53	M	974	613	143	AD
67	F	455	545	65	AD
67	M	585	512	89	AD
71	M	452	535	79	AD
60	F	685	514	98	AD
80	M	664	568	88	AD

76	M	721	603	103	AD
78	F	898	612	130	AD
81	F	990	520	135	AD

Table 2. Control and AD CSF samples from the Clinical Neurochemistry Laboratory (Möln dal, Sweden). The core biomarkers Tau (ng/ml), A β (ng/ml) and pTau (ng/mL) were measured in all samples. Age (y= years), gender (M= male, F= female). Diagnosis: either control or AD.

The CSF study included a cohort with samples from HD patients from Hospital Sant Pau (Barcelona, Spain). The cohort was composed of n = 9 control individuals with no signs of dementia (5 males/4 females, 40 ± 15 years), a group of n = 10 in the asymptomatic phase (H0) (5 males/5 females, 40 ± 8 years), and a group of n = 9 in the symptomatic phase (H1) (4 males/5 females, 53 ± 12 years) [269]. The age of both groups was not significantly different. In H0 patients, the number of CAG repeats in the smaller allele was 18.9 ± 2.8 , and the number of CAG repeats in the larger allele was 42.5 ± 2.0 . Disease burden or CAG score (CAG repeats x age), a parameter that reflects disease severity [270], was 349.4 ± 72.4 in H0 patients. In H1 patients, the number of CAG repeats in the smaller allele was 20.8 ± 6.5 , the number of CAG repeats in the larger allele was 43.6 ± 2.7 , and Disease burden (CAG repeats x age) was 541.8 ± 225.9 . See **Table 3** for summarized details.

Human CSF HD samples

Age(y)	Gender	CAG repeats smaller allele	CAG repeats larger allele	Manifest	Disease burden (CAG repeats x age)
38	F	24	44	H0	399.36
45	F	17	43	H0	428.09
41	M	16	41	H0	304.86
50	F	22	39	H0	272.12
38	M	18	45	H0	437.00
33	M		43	H0	319.39
50	M	17	40	H0	322.90
41	M	17	44	H0	427.18
42	F	21	42	H0	356.72
21	F	18	44	H0	226.40
47	M		46	H1	584.45
42	F	22	43	H1	402.48

67	M	24	41	H1	499.13
37	M	35	45	H1	431.71
41	F	15	43	H1	394.04
47	F	18	48	H1	677.20
70	M	18	40	H1	451.70
65	F	17	41	H1	486.34
45	F	17	45	H1	514.71
61	M	20	47	H1	818.22
58	F	control			
30	M	control			
24	M	control			
38	M	control			
38	M	control			
50	F	control			
61	F	control			
63	M	control			
24	F	control			
30	M	control			

Table 3. Control and Huntington's disease (HD) CSF samples from Hospital Sant Pau (Barcelona, Spain). Subjects were categorized according to CAG repeats of the smaller and larger allele, manifestation of the disease (H0 asymptomatic, H1 symptomatic) and Disease burden (CAG repeats x age) [270]. Age (y= years), gender (M=male, F=female).

Moreover, CSF samples from patients with encephalitis were included for analysis. All clinical analyses were performed at the Neurology Unit, Department of Neurosciences, Biomedicine and Movement Sciences, University of Verona (Italy). Each subject underwent brain magnetic resonance imaging, standard electroencephalography, thyroid function and antibodies (anti-thyroglobulin, anti-thyroid peroxidase), IgM, and IgG for *Borrelia burgdorferi*. CSF viral screening included herpes simplex virus (HSV-1, HSV-2, HSV-6, HSV-8, CMV, Epstein-Barr virus, varicella zoster virus), adenovirus and enterovirus; and standard immunological screening, which included antibodies against NMDARs, LGI1, CASPR2, GABAbR, AMPARs, DPPX, Ri, Yo, Ma2, CV2, Hu, amphiphysin, titin (Euroline and Mosaic kit, Euroimmun, Luebeck) and MOG (live cell-based assay). Samples were subgrouped between anti-NMDARs encephalitis and

other types of encephalitis. The average age of anti-NMDAR encephalitis subjects is 48.5 ± 11.0 years. The average age of viral encephalitis subjects is 60.2 ± 24.7 years. See **Table 4** for summarized details.

Human CSF Encephalitis samples

Diagnosis	Age (y)
Anti-NMDARs encephalitis	32
Anti-NMDARs encephalitis	54
Anti-NMDARs encephalitis	55
Anti-NMDARs encephalitis	53
Anti-LG1 encephalitis	67
Anti-LG1 encephalitis	75
Anti-LG1 encephalitis	76
Anti-Yo encephalitis	82
Viral encephalitis	45
Viral encephalitis	62
Viral encephalitis	17
Viral encephalitis (HSV-1)	75

Table 4. Viral and anti-NMDARs encephalitis CSF samples from the University of Verona (Italy). Different types of encephalitis were categorized into anti-NMDARs and viral. Age (y= years).

3.4 Cell culture

The iPSC line used in this thesis was the N1-001iC2 hPSCreg name UGOTSAi002-B, provided by Prof. Henrik Zetterberg (Institute of Neuroscience and Physiology, University of Gothenburg, Sweden) (<https://hpscereg.eu/cell-line/UGOTSAi002-B>). The donor was a male of 75-79 years old at collection with SAD. iPSC line was maintained in Matrigel-coated P6 plaques and fed with mTeSR+1 (StemCell Technologies) at 37°C, 5% CO₂. Passages were done every 3-4 days (80% confluence) using ReLeSR™ solution (StemCell Technologies). Lines were routinely screened for the absence of mycoplasma.

iPSCs were differentiated into neural progenitor cells (NPCs) using the STEMdiff™ SMADi Neural Induction Kit (StemCell Technologies). Then, NPCs were expanded and matured using STEMdiff™ Neural Progenitor Medium (StemCell Technologies). From NPCs, cells were differentiated into neurons using two alternative protocols: Neural Maintenance Media

(NMM), which yields a neuronal culture with a small percentage of astrocytes, and BrainPhys media (BPM), which yields a higher percentage of astrocytes [271-273]. During the neural induction period, the expression of Nestin and PAX6 was checked as makers of neuroprogenitors and the expression of MAP2 as a marker of mature neurons. NPCs were passed using accutase.

iPSC were differentiated from NPC to astrocytes using STEMdiff™ Astrocyte Differentiation Kit. Mature astrocytes were achieved using STEMdiff™ Astrocyte Maturation Kit.

3.5 Mice

The APP/PS1 mouse model of AD initiates A β deposits, astrogliosis and learning deficits at 6 months of age, all of which increase with age. In this thesis, APPswe, PSEN1dE9 mice of 12 months of age were used. These mice develop amyloid deposits, neuritic plaques, synaptic loss, astrogliosis, and microgliosis [231].

The TauP301S mouse model of tauopathy accumulates pTau/Tau at 6 months of age in the hippocampus, but until 9 months, when these mice were used, there is no substantial neural loss and hippocampal and entorhinal atrophy [274]. Synapse loss measured by synaptophysin staining starts to decrease by month 3 of age [274]. These mice suffer from cognitive impairment since 6 months of age [275].

The *Grin3a* knockout strain was generated by back-crossing F1 hybrids 8 into a C57Bl6/J background for more than 12 generations [276].

3.6 CSF extraction from mice

CSF was extracted from WT and *Grin3a* knockout mice by puncturing the cisterna magna [225] using a needle BD Micro-Fine™+Demi 0.3 mL. Around 4 μ L were extracted from each animal.

3.7 Subcellular fractionation protocol

Human frozen frontal cortex was cut into pieces (100 mg) trying to avoid white matter and excess of vascular tissue. When the protocol was performed in mouse brain tissue, whole frontal cortices were used (~ 20 mg). Each piece was homogenized in 100 μ L for human samples or 200 μ L for mouse samples of homogenization buffer (ice-cold sucrose buffer containing 0.32 M sucrose, 10 mM Tris–HCl (pH 7.4), 1 mM Na₃VO₄, 1 mM NaF, 1mM HEPES, 1 mM EDTA, 1 mM EGTA, protease (cOmplete™, Roche) and phosphatase inhibitors (PhosSTOP™, Roche)) in a 1.5 mL eppendorf using a Heidolf homogenizer (10 strokes). The subsequent

centrifugations were all performed at 4°C. Cortical homogenates (Ho) were centrifuged at 1,000×g for 10 min to obtain a nuclear-free supernatant (S1) and a pellet (P1) containing the nucleus. Further centrifugation of S1 at 10,000×g for 15 min resulted in a supernatant that contained cell cytosol and microsomes (S2) and a pellet (P2) of plasma membranes. P2 was incubated with homogenization buffer containing 1% TX-100 (w/v) for 20 minutes in rotation at 4°C and then centrifuged at 32,000×g for 20 minutes. The supernatant fraction collected contained extrasynaptic membranes, which include non-synaptic membranes and presynaptic membranes (extrasynaptic fraction, ExsynF); the pellet fraction, containing the insoluble fraction, was solubilized in RIPA buffer. This pellet was mainly composed of post-synaptic densities and, therefore, post-synaptic membranes (synaptic fraction, SynF). Finally, ultracentrifugation at 100,000×g for 1h of S2 fraction made it possible to discriminate microsomal (solubilized in RIPA buffer, P3) and cytosolic fractions (S3).

3.8 Western blotting

Brain fractions were run on SDS-PAGE (7.5% Tris-glycine) after boiling at 98°C for 5 minutes in 6× Laemmli sample buffer. Proteins were transferred by electrophoresis to nitrocellulose membranes for 2.5 h at 300 mA. Primary antibodies were used against GluN2B C-terminal (mouse, 1:800, Invitrogen MA1-2014), GluN2B N-terminal (rabbit, 1:800, Alomone AGC-003), GluN2A C-terminal (rabbit, 1:800, Invitrogen A6473), GluN2A C-terminal (rabbit, 1:800, Millipore 07-632) phospho-Tyr1472-GluN2B (rabbit, 1:800, Phosphosolutions, p1516-1472), phospho-Tyr1336-GluN2B (rabbit, 1:800, Phosphosolutions p1516-1336), GluN1 N-terminal (guinea pig, 1:1000, Alomone AGP-046), GluN1 C-terminal (mouse, 1:800, Millipore 05-432) GluN3A C-terminal (rabbit, 1:1000, Millipore 07-356), GluN3A N-terminal (rabbit, 1:800, Alomone AGC-030) PSD-95 (goat, 1:1500, Abcam ab12093), synaptophysin (mouse, 1:1000, Proteintech 60191-1-Ig), CaMKII α (rabbit, 1:1000, Proteintech 20666-1-AP), TGN46 (rabbit, 1:1000, Proteintech AB10597396), GFAP (mouse, 1:1000, Thermofischer MA5-12023), EEA1 (mouse: 1:1000, Hybridoma Bank PCRP-EEA1-1F8), Alix (mouse, 1:1000, Cell Signaling #2171) and finally α -tubulin (1:4000, Sigma-Aldrich), as a loading control. Primary antibody binding was visualized with fluorescent secondary antibodies (IRDye, 1: 10000, Bioss), and images were acquired using an Odyssey CLx Infrared Imaging system (LI-COR Biosciences GmbH).

3.9 Immunoprecipitation assays

Brain extracts (100 μ g in 500 μ L PBS) or CSF (50-400 μ L) were incubated on a roller overnight at 4°C with Protein A Sepharose CL-4B (100 μ L, Cytiva 17078001) coupled to antibodies against

GluN2B N-terminal (rabbit, 15 μ L, Alomone AGC-003), GluN2B N-terminal (mouse, 10 μ L, NeuroMab 75-097 Clone N59/20), GluN2A N-terminal (mouse, 10 μ L, Hybridoma Bank N327/95), GluN3A N-terminal (rabbit, 10 μ L, Alomone, AGC-030) or GluN1 N-terminal (mouse, 10 μ L, Hybridoma Bank N308/48). The same amount of beads without coupled antibodies was used as a negative control. The input, bound, and unbound fractions were analyzed by western blotting using antibodies against the GluN2B C-terminal (Invitrogen MA1-2014), GluN2A C-terminal (Invitrogen A6473), and GluN1 N-terminal (Alomone AGP-046).

3.10 Enzymatic deglycosylation assays

Enzymatic deglycosylation was performed using an Agilent Enzymatic Deglycosylation Kit (Agilent Technologies, GK80110) following the manufacturer's instructions. Briefly, 100 μ g of control or AD brain extract (SynF or ExsynF) was mixed with 10 μ L incubation buffer and 2.5 μ L denaturing buffer (both provided by the kit) and heated at 100°C for 5 min. Then, samples were cooled down to room temperature and 2.5 μ L of detergent (15% w/v, NP-40) was added while mixing gently. Sialidase (1 μ L), O-glycanase (1 μ L) or N-glycanase (1 μ L) enzymes were added to the samples and then heated at 37°C for 3 h.

3.11 Lectin binding assays

SynF and ExsynF samples (50 μ g) were incubated overnight at 4 °C with lectins immobilized in agarose beads (100 μ L), either Con A lectin (from *Canavalia ensiformis*; Sigma) or WGA lectin (from *Triticum vulgaris*, Sigma). After centrifugation at 3,000 \times g for 1 min, the supernatant containing the unbound fraction was analysed by western blot. The proportion of unbound protein was calculated respect to the total input.

3.12 Cell Immunocytochemistry (ICC)

Cells were fixed in 4% paraformaldehyde for 15 min and stored in phosphate buffered saline (PBS) at 4 °C until immunostaining was performed. Cells were washed in PBS once and permeabilized using 0.1% triton-X-100 in PBS for 10 min and blocked in 1% bovine serum albumin in PBS for 1 h. Then, cells were incubated with primary antibodies in blocking solution overnight. Primary antibodies used were S100 β (rabbit, 1:500, Proteintech 15146-1-AP), GFAP (mouse, 1:500, thermofischer MA5-12023), TUJ1 (beta-3-tubulin)(mouse, 1:500, abcam ab14545), MAP2 (chicken, 1:500, thermofischer PA1-10005), Synaptophysin (rabbit, 1:250, thermofischer MA5-14532), PAX6 (rabbit, 1:500, thermofischer 42-6600), Nanog (mouse,

1:500, BioLegend 674002), OCT4 (rabbit, 1:500, thermofischer MA5-14845), GluN1 N-terminal (rabbit, 1:500, Alomone AGP-046).

After three washes with PBS, secondary antibodies (Alexa Fluor™ 647 goat anti-rabbit IgG (H+L), Cy3™ goat anti-mouse IgG (H+L), Alexa Fluor™ 488 goat anti-guinea pig IgG (H+L), Alexa Fluor™ 488 goat anti-chicken IgY (H+L), Thermo Scientific) were added in blocking solution for 1 h in the dark. 4',6-diamidino-2-phenylindole (DAPI, 1 µM) was added as a nuclear counterstain before the last wash with PBS. Cells were mounted on slides using ProLong™ Diamond Antifade Mountant (Invitrogen, P36961). Images were taken by a Leica SPEII and visualized using Imaris.

3.13 Fluorescence-activated Cell Sorting (FACS)

Cells were collected using Gentle Cell Dissociation Reagent (StemCell Technologies) to dissociate them into single cells. Cells were counted and distributed 200.000 cells/15 ml falcon. Cells were centrifuged at 1000 rpm for 3 min and fixed in PFS 4% for 10 min at room temperature. Then, cells were centrifuged at 1000 rpm for 3 min and resuspended in PBS. Then, cells were distributed in Eppendorf, centrifuged at the same speed and time, and incubated with conjugated antibodies for 30 min at RT (5 µL conjugated antibodies + 100 µL PBS + Triton-X-100 0,01% (w/v) (for 4 tubes). Then, cells were centrifuged and resuspended in PBS until analysis. A negative control was always included, as well as single conjugated antibodies when the assay included more than one simultaneous marker. FACS was performed with FACS Aria III.

3.14 Extracellular vesicles isolation

CSF samples were processed by differential ultracentrifugation as described earlier [277]. Briefly, CSF aliquots were thawed and subjected to subsequent centrifugation steps: 3,500 g for 10 min, two times 4,500 g for 10 min, 12,000 g for 35 min, and finally at 100,000 g for 70 min to pellet EVs. The supernatant was saved, and the EV pellet was washed in 1 ml of 1X PBS and centrifuged again at 100,000 g for 70 min. The EV pellet, as well as the pellet obtained after the 12,000 g centrifugation and an aliquot of the kept supernatant, were prepared in loading buffer 1x for Western blot analysis.

3.15 RT-qPCR

RNA was extracted from NPCs, NMM or BPM iNeurons using the PureLink™ Micro Total RNA Purification System (Life Technologies, Carlsbad, CA, USA) following the manufacturer's

instructions. SuperScript™ III Reverse Transcriptase (Life Technologies, Carlsbad, CA, USA) was used to synthesize cDNAs from this total RNA (2 µg) using random primers according to the manufacturer's instructions. Real time Quantitative PCR (RT-qPCR) amplification was performed on a QuantStudio3 (Applied Biosystems, Thermo Fisher Scientific, Rockford, USA) with ThermoFisher Scientific TaqMan probes specific for human *GRIN1* (assay ID: Hs00609557_m1), *GRIN2B* (assay ID: Hs01002012_m1), *GRIN2A* (assay ID: Hs00168219_m1), *MAP2* (assay ID: Hs00258900_m1), *CAMKIIβ* (assay ID: Hs00365799_m1), *GRIA1* (assay ID: Hs00181348_m1), *GFAP* (assay ID: Hs00909233_m1), *PAX6* (assay ID: Hs01088114_m1), *APP* (assay ID: Hs05510637_m1) and human *GAPDH* as a housekeeping gene (assay ID: Hs02786624_g1) to normalize the expression levels of the target gene by the ΔC_t method curves.

3.16 Proteomics

The proteomics analysis was performed through a biotechnological company (ainia). For sample analysis, a microLC Eksigent 425 system was used in conjunction with a high-resolution mass spectrometer, the SCIEX TripleTOF 6600+. A total of 4.8 µg was injected using a 60-minute linear chromatographic gradient. Mobile phase A consisted of Water + 0.1% formic acid (FA), while mobile phase B consisted of Acetonitrile + 0.1% FA, with a nanoEase m/z peptide C18 column (Waters). Data acquisition was performed using Data Dependent Acquisition (DDA) settings with inclusion parameters of m/z 350-1500 in TOFMS and 100-1500 in MS/MS, charge states ranging from +2 to +5, and selection of 30 precursors per cycle. PEP was used as QC (quality control) and for internal mass calibration.

Data Processing and Protein Identification

After data acquisition, the information was processed using the ProteinPilot software (SCIEX). This software employs the Paragon algorithm and assigns MS/MS spectra to peptide sequences, which are then further assigned to proteins in the database. The algorithm parameters for the search included cysteine carbamidomethylation by iodoacetamide, trypsin digestion, and methionine oxidation. The search was performed using a '*Homo sapiens*' database obtained from UniProt. An additional search was performed using a *Homo sapiens* database filtered by the keyword 'brain' obtained from UniProt. The assignment of MS/MS spectra to peptides and peptides to proteins was validated using a False Discovery Rate (FDR) analysis, setting the filter at 1%.

Label-free Quantification

Raw mass spectrometry data were processed with MaxQuant software. The process included converting raw data into peak list files, searching for sequences in a protein database, assigning peptide and protein identifications, and quantifying based on MS1 peak intensity.

Quantification was performed using the LFQ algorithm with standard parameters, selecting a maximum of 2 peptides for quantification. The "Match between runs" option was applied to normalize retention times between chromatographic runs.

Complex Data Analysis, Statistical Analysis, GO Term Annotation, Expression Analysis, and Data Visualization

Quantitative data were processed using the Perseus statistical package (Max Planck Institute of Biochemistry). LFQ intensity data were transformed to $\text{Log}_2(X)$, and data normality was verified. Missing values between replicates were corrected by applying a normal distribution.

Two-sample t-tests were used to determine significant differences between the two treatments. PCAs, volcano plots, histograms, hierarchical clusters, and scatter plots were represented using the same software.

For the functional annotation of differentially expressed proteins, GO (Gene Ontology) term assignment was performed using the Metascape platform. Enrichment and interaction analyses were conducted by calculating cumulative hypergeometric p -values and enrichment factors for filtering. Specifically, the analysis focused on biological functions, processes, and cellular components potentially associated with differentially expressed proteins.

Graph interpretation

- **Volcano plot.** The X-axis represents the fold change in protein abundance between controls and AD, and it is represented as the \log_2 of the fold change. Proteins at the extreme of the X-axis will be the most differentially expressed (according to fold-change). The Y-axis represents the statistical significance as the negative \log_{10} of the p -value derived from a t-test (control vs AD). Proteins at the extreme of the Y-axis will be the most differentially expressed (according to statistical significance). Proteins underexpressed in AD are placed in the left part of the plot, while overexpressed proteins are at the right [278, 279].

- **Heat map.** Illustrates the differentially expressed proteins (DEP) in AD respect to control according to a code color: green means overexpression and red underexpression. Moreover, the darker the color, the greater the statistical significance. The heatmap was created through a hierarchical clustering algorithm, providing different clusters of DEP in control and AD samples.

In the Y-axis, proteins were grouped by similarity, where similar proteins are closer to each other [259, 280].

- **Enrichment analysis.** The enrichment analysis assigns Gene Ontology (GO) terms to the differentially expressed proteins. This aims to determine whether specific biological processes, functions, or pathways represented as GO terms are significantly overrepresented in the list of DEP. Although the most used ontology is GO, other ontologies utilized were KEGG Pathway, Reactome Gene Sets and WikiPathways. Enrichment analysis provides the **Enrichment Ontology Cluster** plot, which identifies the most statistically significant GO terms represented in the list of DEP. This provides information about the biological processes that may be altered according to the DEP. Each cluster is represented in a list in order of statistical significance [281].

3.17 Statistical analysis

The distribution of data has been tested for normality using a D'Agostino-Pearson test. ANOVA has been used for parametric variables and the Kruskal-Wallis test for non-parametric variables for comparison between groups. A Student's t-test for parametric variables and a Mann-Whitney U test for non-parametric variables were employed to compare the two groups and determine p values. For the unpaired Student's t-test, a Welch's correction was employed for data with different standard deviations. Correlations were performed by Pearson correlation coefficients for parametric distributions and Spearman correlation coefficients for non-parametric distributions. When considered, the results are presented as the means \pm SEM, and all the analyses were performed using GraphPad Prism (version 7; GraphPad Software, Inc). p-value < 0.05 is considered significant.

4. Results

4.1. Fractionation protocol: Synaptic (SynF) and Extrasynaptic fractions (ExsynF) from human cortex

The study of proteins involved in AD from whole brain extracts from AD individuals has reported valuable data. However, our interest was to examine the pathological changes that occur between the synaptic and extrasynaptic membranes for the NMDAR. With this aim, we developed a protocol to isolate the synaptic and extrasynaptic fractions (SynF and ExsynF) from frozen pieces of human frontal cortex.

We first tried different fractionation protocols based on centrifugations and detergent digestion [282], as well as sucrose gradients [283], that were reported for other groups for fresh mouse brain. However, these protocols did not work properly for frozen samples of post-mortem human brains. Based on previous protocols [282, 284], we have designed and validated an effective fractionation protocol to obtain synaptic and extrasynaptic membranes from frozen human cortex. We have modified specific parameters such as Triton X-100 concentration, use of acetone, and incubation times in key steps.

In our protocol, described in Methods and in **Figure 1A**, cortical brain pieces were first homogenized to obtain a supernatant that contained cell cytosol and microsomes (S2) and a P2 fraction of plasma membranes. P2 was incubated with 1% (w/v) Triton X-100 and centrifuged to get a supernatant fraction containing extrasynaptic membranes, which includes non-synaptic membranes and presynaptic membranes (extrasynaptic fraction, ExsynF); the pellet fraction was solubilized in RIPA buffer to collect post-synaptic membranes (synaptic fraction, SynF). Ultracentrifugation of S2 fraction was used to discriminate microsomal (P3) from cytosolic fractions (S3).

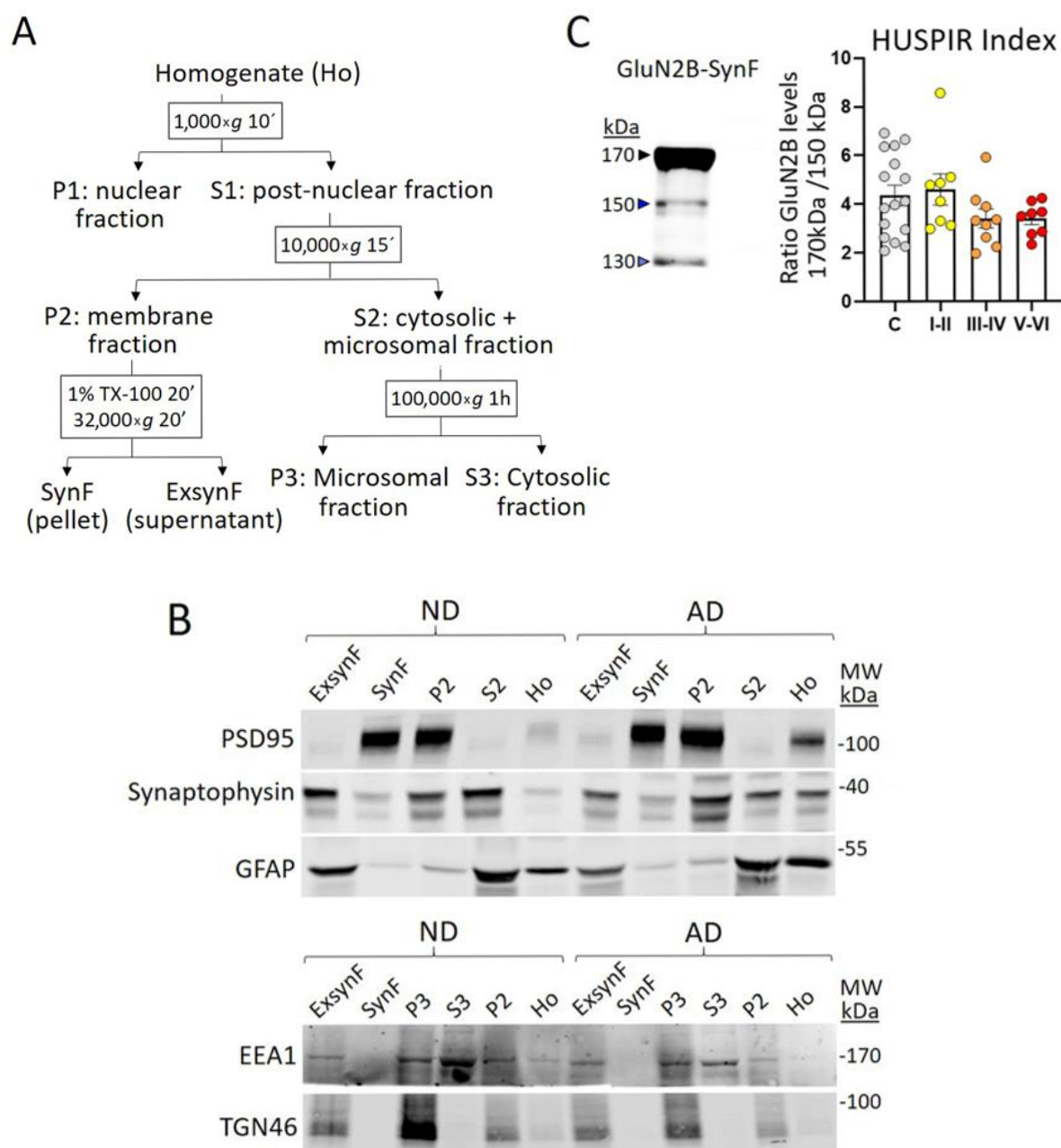


Figure 1. Validation of the fractionation protocol in human post-mortem cortex. A) Scheme of the fractionation procedure indicating the centrifugation steps and the fractions resulting from each one. P: pellet. S: supernatant. Cortical homogenates (Ho) were centrifuged at 1,000×g to obtain a nuclear-free supernatant (S1) and a pellet (P1) containing the nucleus. Centrifugation at 10,000×g of S1 resolved a supernatant that contained cell cytosol and microsomes (S2) and a pellet (P2) of plasma membranes. P2 was incubated with 1% (w/v) Triton X-100 and centrifuged at 32,000×g to obtain a supernatant fraction collected contained extrasynaptic membranes (ExsynF); the pellet fraction was solubilized in RIPA buffer to obtain the post-synaptic

membranes (synaptic fraction, SynF). Ultracentrifugation at 100,000×g of S2 fraction served to obtain microsomal (P3) and cytosolic fractions (S3). **B)** Western blot of different fractions from the fractionation protocol revealed with antibodies against synaptic-related proteins (PSD95, synaptophysin), astroglial cells (GFAP) and no synaptic proteins associated to early endosome-associated protein (EEA1) and to Golgi apparatus (TGN46), in control and AD samples. **C)** Representative western blot of the NMDAR subunit GluN2B, revealed with an antibody against the C-terminal of GluN2B, of a synaptic fraction from a control sample and the quantification of the HUSPIR index for all samples (Controls n=16, Braak I-II n=8, Braak III-IV n=9 and Braak V-VI n=8).

To validate this fractionation protocol in frontal cortices from controls and AD samples, synaptic and non-synaptic markers were examined by western blots (**Figure 1B**). PSD95, a classical marker of PSD, was mainly present in P2 and SynF, the fractions containing synaptic membranes. Synaptophysin, a presynaptic protein, was mainly observed in P2 and ExsynF, the fractions containing extrasynaptic membranes, but also at the cytosolic fraction (S2). The astrocytic glial fibrillary acidic protein (GFAP), a marker for glial cells, was mainly present at S2 and ExsynF. Non-synaptic-related proteins, such as the early endosome-associated protein (EEA1) and the trans-Golgi network integral membrane protein 2 (detected with the TGN46 antibody), were enriched in S3 and P3, respectively, and not detected in SynF. Therefore, our protocol showed a high efficiency in discriminating cell compartments and specifically, synaptic and extrasynaptic membranes.

Since our goal was to characterize the synaptic and extrasynaptic proteome in the human cortex, it was compulsory to ensure the integrity and preservation of the post-mortem samples prior to the analysis. For this purpose, we estimated the HUman Synapse Proteome Integrity Ratio or “HUSPIR index” [268], which measures the ratio of proteolytic fragments of the NMDAR subunit GluN2B in SynF by immunoblots (**Figure 1C**). In human brain samples, particularly at synaptic membranes, GluN2B is present as a ~170 kDa full-length protein, but also detectable as ~150 kDa and ~130 kDa species. These two shorter bands correspond to proteolytic fragments which levels increase during post-mortem degradation [188]. A GluN2B full-length-170 kDa/fragment-150 kDa ratio, or HUSPIR index, above 1 indicates a good synaptic structure integrity, which is more commonly found in post-mortem cortical regions respect to non-cortical regions [268]. The HUSPIR index of our brain cortical samples averaged 3.85 ± 1.5 (controls: 4.19 ± 0.4 ; AD: 3.65 ± 0.25 , $p = 0.29$; no differences were found when comparing AD

samples sub-grouped by Braak stages). This index indicates that our control and AD samples maintain a high synaptic structural integrity and an optimal quality for our biochemical analysis. Samples with a HUSPIR index ≤ 1 were removed from the study.

4.2 Synaptic and extrasynaptic distribution of NMDA receptors in cortex of AD patients

4.2.1 SynF and ExsynF characterization of NMDAR subunits

The evaluation of NMDAR subunits distribution in SynF and ExsynF was performed by western blots as a tool that makes possible to discriminate these two fractions. When same amounts of SynF and ExsynF (10 µg) were loaded, it was clearly observed that NMDAR subunits were more abundant in synaptic membranes. Therefore, to allow a quantitative analysis of less abundant extrasynaptic NMDAR subunits we used a concentration five times higher (50 µg) of ExsynF in western blots, onwards.

We first characterized the expression of NMDAR subunits in brain cortices from controls in S2 (50 µg; containing the cytosol and therefore predictably low levels), P2 (10 µg), SynF (10 µg) and ExsynF (50 µg, **Figure 2A**). GluN2B and GluN2A full-length subunits were present at SynF with the expected ~170 kDa molecular mass. At ExsynF, GluN2B and GluN2A immunoreactivity showed an additional ~160 kDa band each one. GluN1 was observed as ~120 kDa band and GluN3A as ~130 kDa band, both with the same apparent molecular mass in SynF and ExsynF. Remarkably, GluN3A seemed to be an exception with respect to the rest of the NMDAR subunits, as it was more abundant at extrasynaptic membranes, as reported by other groups in mouse brains [285, 286]. To confirm the identity of GluN2B, GluN2A, and GluN1, in SynF and ExsynF, we performed immunoprecipitations to pull down the NMDAR subunits, resolving with alternative antibodies that verified the identity of the bands (**Figure 2B**). To verify the identity of the GluN3A band, we employed mice lacking GluN3A (*Grin3a*^{-/-}). The absence of the GluN3A-130 kDa band in *Grin3a*^{-/-} brain extracts, but not in those from the wild-type, validated the identity of the GluN3A subunit (**Figure 2C**).

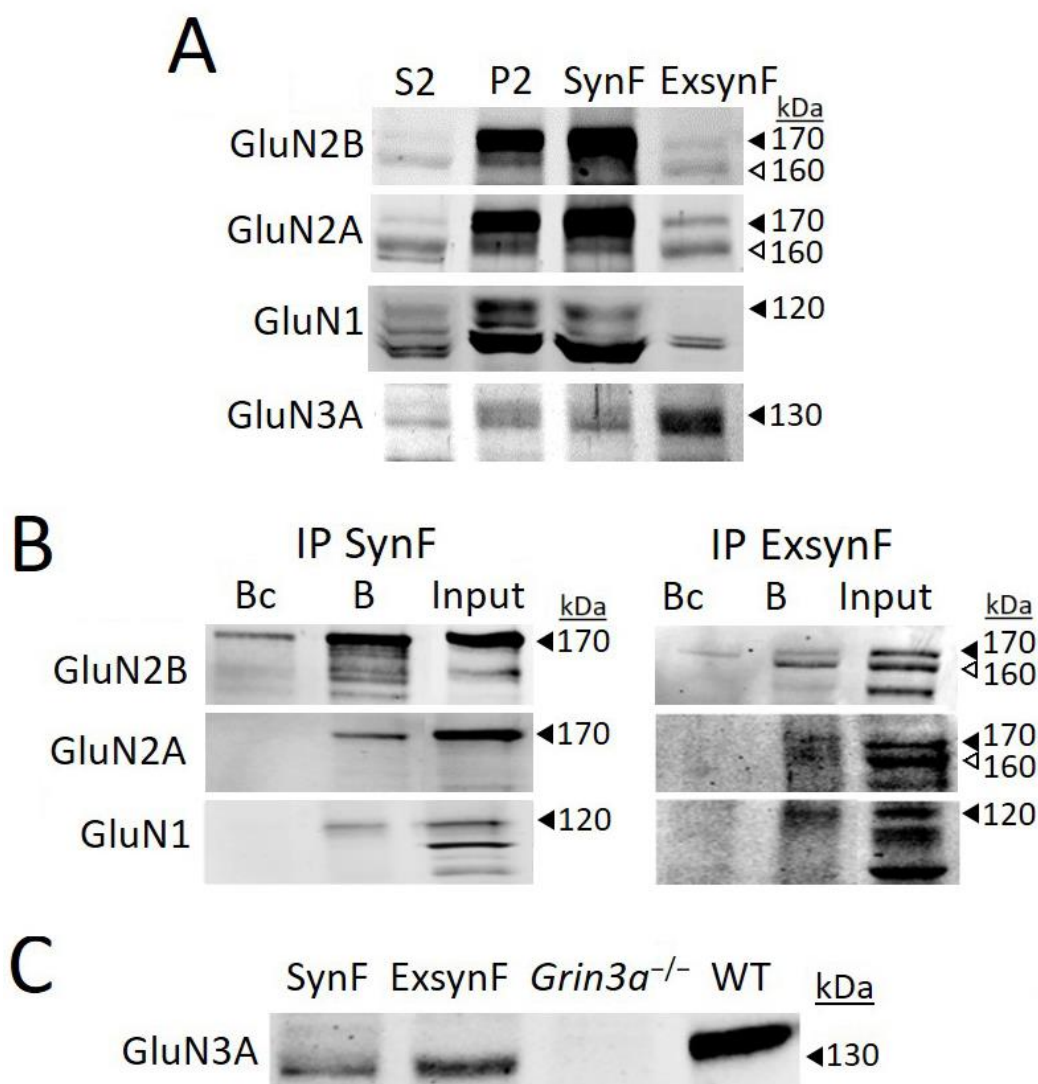


Figure 2. Characterization of NMDAR subunits in SynF and ExsynF. A) Representative blots of the NMDAR subunits GluN2B, GluN2A, GluN1 and GluN3A from different fractions of the fractionation protocol (50 μ g for S2 and ExsynF; 10 μ g for P2 and SynF). Black arrowheads indicate bands corresponding to ~170 kDa GluN2B, ~170 kDa GluN2A, ~120 kDa GluN1 and ~130 kDa GluN3A in each blot. White arrowheads indicate ~160 kDa bands of GluN2B and GluN2A. **B)** Immunoprecipitations (IP) of SynF and ExsynF of control samples. IP of GluN2B (antibody GluN2B N-terminal, rabbit, 10 μ l, Alomone AGC-003); revealed with antibody against GluN2B C-terminal (mouse, 1:800, Invitrogen MA1-2014). IP of GluN2A (antibody GluN2A N-terminal, mouse, 100 μ l supernatant, HybridomaBank N327/95) revealed with antibody against GluN2A C-terminal (rabbit, 1:800, Invitrogen A6473). IP of GluN1 (antibody GluN1 N-terminal, guinea pig, 10 μ l, Alomone AGP-046) revealed with antibody against GluN1 N-terminal (mouse, 30 μ l supernatant, HybridomaBank, N308/48). Bc: bound from control IP (IgG), B: bound fraction from the IP, Input: SynF or ExsynF. **C)** Western blot of brain homogenates from a wild-

type mouse (WT), a mouse lacking GluN3A (*Grin3a*^{-/-}) and from control human samples (SynF and ExsynF) revealed with a C-terminal GluN3A antibody (rabbit, 1:1000, Millipore 07-356).

4.2.2 Identification of GluN2B and GluN2A glycoforms

We aimed to understand why GluN2B and GluN2A subunits appeared as two distinct species in extrasynaptic membranes. NMDAR subunits are post-translationally modified by glycosylation, an adjustment key for their function and sorting [121, 287, 288]. Therefore, we hypothesized that extrasynaptic GluN2B-160 kDa and GluN2A-160 kDa could represent different glycoforms of the synaptic subunits. To test this, we performed an enzymatic deglycosylation assay in control and AD samples. Enzymatic deglycosylation (N-glycanase + sialidase + O-glycanase) of synaptic membranes induced a change in the electrophoretic mobility of GluN2A and GluN2B as a result of the removal of sugars. Remarkably, it was only in the presence of N-glycanase when the mobility of these subunits was affected, which suggests that their glycosylation was mainly due to N-glycosylation. In ExsynF, the N-deglycosylation simplified the 170 and 160 kDa bands of GluN2B and GluN2A to a single immunoreactive band, the 160 kDa band (**Figure 3A**). This indicated that GluN2B and GluN2A are expressed as two different glycoforms. The 170 kDa form would be predominantly at synaptic membranes and correspond to fully glycosylated subunits, likely mature forms that harbor N-linked sugars. The 160 kDa glycoform would be almost exclusively at extrasynaptic membranes and could represent different glycoforms of synaptic GluN2B and GluN2A. When N-deglycosylation was performed in AD fractions, the NMDAR subunits exhibited similar migration change as in controls, in both SynF and ExsynF (**Figure 3B**).

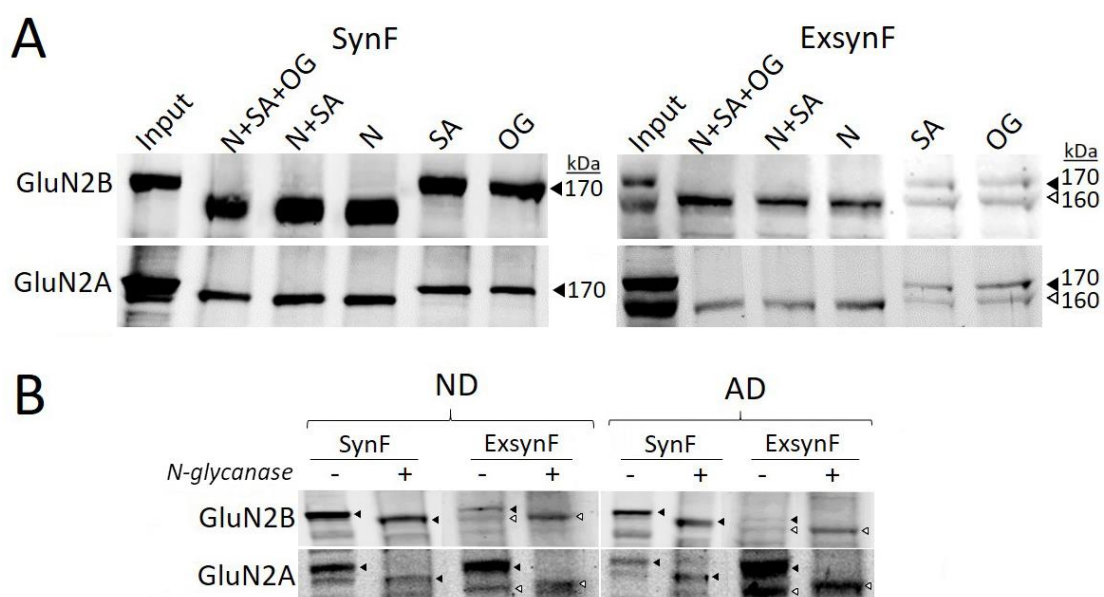


Figure 3. Glycosylation of NMDAR subunits. A) Enzymatic deglycosylation of SynF and ExsynF (3B) with N-glycanase (N), sialidase (SA), O-glycanase (OG) or a combination of them in control samples, revealed with antibodies against GluN2B C-terminal (Invitrogen MA1-2014) and GluN2A C-terminal (Invitrogen A6473). Black arrowheads indicate bands corresponding to ~170 kDa GluN2B and ~170 kDa GluN2A. White arrowheads indicate ~160 kDa bands of GluN2B and GluN2A. **B)** NMDAR subunits in SynF and ExsynF fractions from control and AD cases, after N-deglycosylation (+) or in unprocessed samples (-), revealed with antibodies against the C-terminal of GluN2B and GluN2A.

4.2.3 Tyr1336 is the main site for GluN2B phosphorylation

GluN2B-170 kDa phosphorylation at Tyr1472 and Tyr1336 was analyzed in SynF and ExsynF to evaluate whether there is a preferential phosphorylation site associated with each membrane fraction (**Figure 4A**). In SynF from control and AD cases (Braak stage V-VI), GluN2B was phosphorylated at Tyr1472 and Tyr1336, showing higher levels of the last. Interestingly, phosphorylation at Tyr1472 was identified only in synaptic membranes and was almost undetectable in extrasynaptic membranes (**Figure 4B**). This indicated that GluN2B is phosphorylated at Tyr1472 almost exclusively at synapses, while phosphorylation at Tyr1336 occurs in synaptic and extrasynaptic membranes.

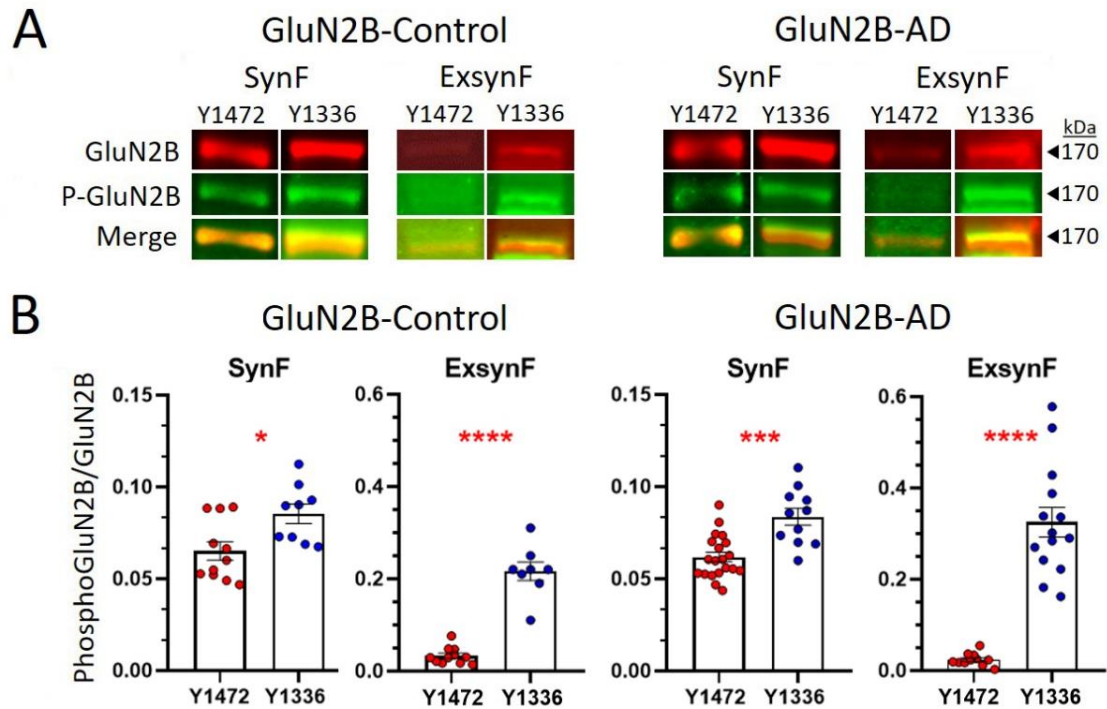


Figure 4. Comparison of GluN2B phosphorylation in SynF and ExsynF between control and AD cases. **A)** Representative blots and **B)** quantification of GluN2B (total protein resolved with mouse C-terminal antibody MA1-2014) and GluN2B phosphorylation (P-GluN2B) at Tyr1472 (rabbit antibody p1516-1472) and at Tyr1336 (rabbit antibody p1516-1336) in synaptic and extrasynaptic GluN2B-170 kDa from control and AD samples (Braak V-VI). The fluorescence of the secondary antibodies (IRDye 680RD goat anti-mouse, red; IRDye 800CW goat anti-rabbit, green) was detected with the Odyssey CLx Infrared Imaging system (LI-COR); merge fluorescence shows co-localization (yellow). Levels of phosphorylated GluN2B were normalized to total GluN2B. Cases control SynF $n = 9-11$; control ExsynF $n = 8-11$; AD SynF $n = 11-20$; AD ExsynF $n = 11-14$. Observe the different Y scale for ExsynF graphs. * $p < 0.05$, ** $p < 0.001$ respect to control, t-test.

4.2.4 Synaptic and extrasynaptic distribution of NMDAR subunits in control and AD cortex

We next compared NMDAR subunit levels in control and AD cases sub-grouped by different Braak stages of neurodegeneration related to AD. Quantitative infrared western blotting has a bigger linear range of detection than the more widely used chemiluminescent technique; however, due to the large differences in the levels of NMDAR subunits between membrane fractions, we analysed P2, SynF and ExsynF samples in separate blots to make the analysis feasible and more reproducible. We observed the same banding pattern in synaptic

membranes and extrasynaptic membranes for all the NMDAR subunits when comparing control and AD samples (**Figure 5A**). Quantification (**Figure 5B**) revealed that P2 fractions expressed significantly lower levels of GluN2B in AD than control tissues when pooling all Braak stages ($58.2 \pm 37.0\%$; $p = 0.0009$) and in each independent stage, except for Braak III-IV, that showed a tendency ($67.0 \pm 25.6\%$; $p = 0.072$). Similarly, GluN2A levels were significantly lower in AD when pooling all Braak stages ($57.2 \pm 53.7\%$; $p = 0.0006$) and in each independent stage, except for Braak I-II ($86.6 \pm 75.0\%$; $p = 0.087$). GluN1 levels were significantly lower in AD than in controls when taking all Braak stages ($80.3 \pm 25.2\%$; $p = 0.039$), and in Braak V-VI. As previously reported, [289] GluN3A levels did not change between control and AD fractions. Since SynF contributes more to P2 signal than ExsynF, synaptic membrane levels of NMDAR subunits mirrored the decrease observed in P2. Both GluN2B and GluN2A levels were significantly lower in all Braak stages overall relative to controls ($67.3 \pm 43.0\%$, $p = 0.022$; $63.2 \pm 44.5\%$, $p = 0.017$ respectively), and in Braak V-VI stage for GluN2B and Braak III-IV and V-VI stages for GluN2A. GluN1 and GluN3A levels did not change in AD in overall or individual Braak stages relative to controls.

Interestingly, NMDAR subunit levels in extrasynaptic membranes displayed an opposite trend to those observed in synaptic membranes, suggesting a subcellular redistribution in AD cases (**Figure 5B**). Extrasynaptic GluN2B-170 kDa levels were higher in AD in overall ($146.5 \pm 55.6\%$; $p = 0.016$) and most individual Braak stages than controls, and the glycoform GluN2B-160 kDa displayed higher levels only at Braak V-VI ($169.5 \pm 58.0\%$; $p = 0.010$). Extrasynaptic GluN2A-170 kDa levels showed a tendency to be higher in overall AD than controls ($134.8 \pm 56.8\%$; $p = 0.098$), and the 160 kDa glycoform was significantly more abundant in Braak stages I-II, compared with controls ($123.5 \pm 30.8\%$; $p = 0.050$) and a tendency in Braak stage V-VI ($120.4 \pm 27.7\%$; $p = 0.076$). Extrasynaptic GluN1 was significantly higher in overall AD ($137.3 \pm 49.9\%$; $p = 0.039$). Remarkably, GluN3A, the unique NMDAR subunit more abundant in ExsynF membranes than in SynF, did not show any change in ExsynF from AD tissues.

To confirm that changes in NMDAR subunit levels were related to the pathology of each group rather than to the age, we performed correlations in controls and at each Braak stage. No association between age and the levels of any NMDAR subunit was found in P2 and SynF in control or Braak stages. In ExsynF, a positive correlation was found in Braak V-VI for GluN2A ($p = 0.037$) and GluN2B-160 kDa ($p = 0.008$). This indicated that the higher levels of these subunits were found in the oldest subjects at the late stages of the pathology. In control ExsynF GluN2A-160 kDa and control and Braak I-II stage ExsynF GluN3A, levels correlated with age ($p = 0.036$; positive correlation; $p = 0.050$, negative correlation; $p = 0.037$, negative correlation,

respectively) although it seemed not to affect quantification (see **Figure 5**). We also analyzed the correlation between NMDAR subunit levels and the gender of the individuals, but no association was found in any group. There was no correlation neither between age and GluN2B phosphorylation at Tyr1472 or Tyr1336 in any group.

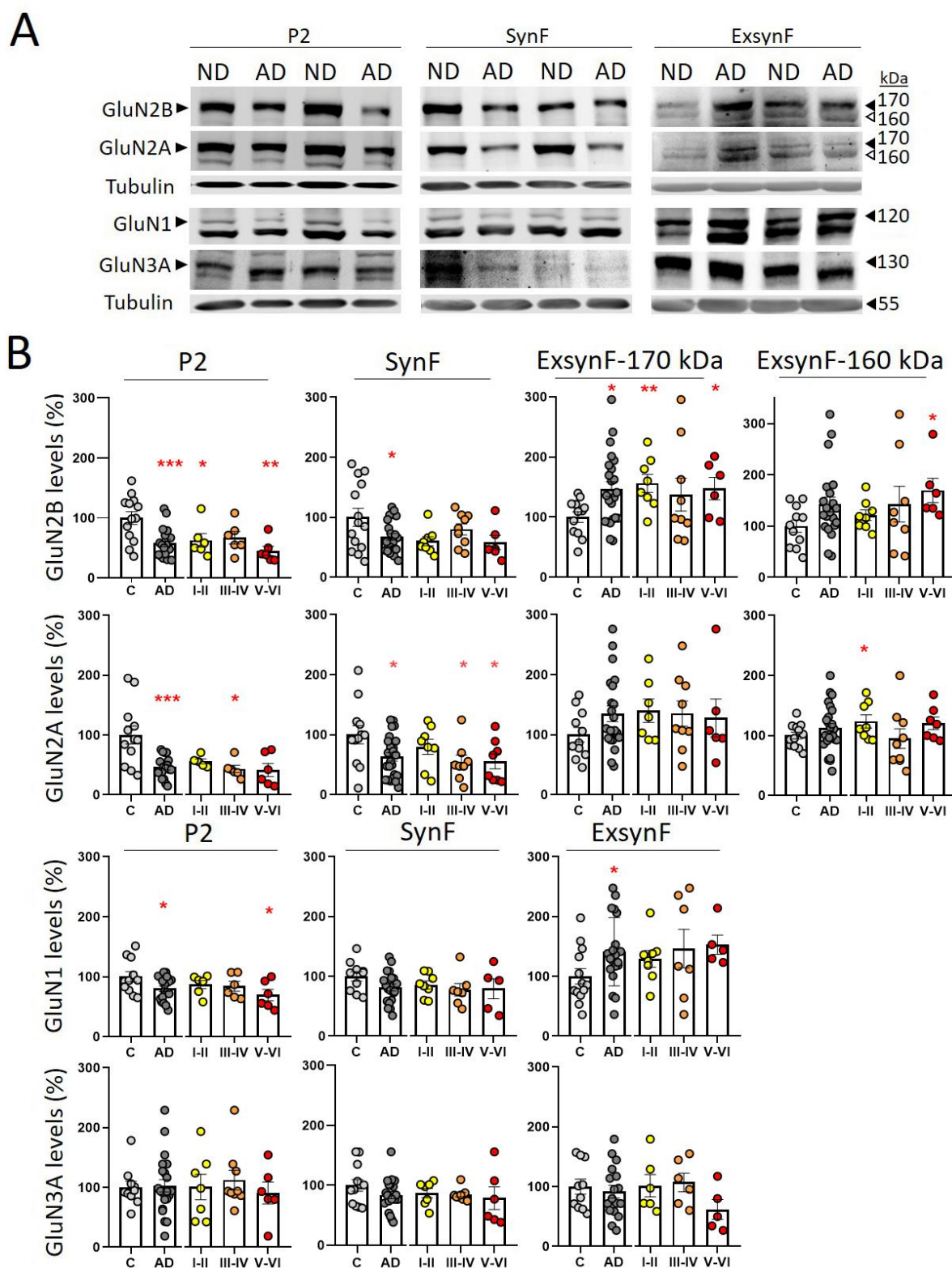


Figure 5. Distribution of NMDAR subunits in membrane-containing fractions from control and AD cases. A) Representative western blots of NMDAR subunits in membrane fraction (P2, 10 µg), synaptic fraction (SynF, 10 µg) and extrasynaptic fractions (ExsynF, 50 µg) from control and AD samples (Braak V-VI). Tubulin was used to normalize quantifications. **B)** Quantification of NMDAR subunits levels at different Braak stages and all Braak stages together (AD: Braak stages I-VI) expressed as percentage respect to controls. GluN2B-170 kDa and GluN2A-170 kDa levels were measured in P2, SynF and ExsynF; GluN2B-160 kDa and GluN2A-160 kDa were measured in ExsynF only. * $p < 0.05$, ** $p < 0.01$, *** $p < 0.001$ respect to control, t-test; # $p < 0.01$ ANOVA one-way comparing control and all Braak stages. Cases control P2, $n = 10-13$; control SynF, $n = 10-14$; control ExsynF, $n = 10-12$; AD P2, $n = 18-22$; AD SynF, $n = 21-24$; AD ExsynF, $n = 17-24$.

4.2.5 Low Tyr1472 phosphorylation at synaptic GluN2B in AD cortex

We then examined the phosphorylation pattern of GluN2B-170kDa between controls and different Braak stages of AD (**Figure 6A**). The only significant difference was an overall lower GluN2B phosphorylation at Tyr1472 in SynF of AD tissue relative to controls ($88.1 \pm 15.3\%$; $p = 0.043$); phosphorylation at Tyr1336 remained unchanged. In ExsynF, no changes were observed between control and AD fractions in Tyr1336 phosphorylation (**Figure 6B**). Phosphorylation at Tyr1472 was too weak to be evaluated in ExsynF, as mentioned before. This finding suggests that the stabilization of GluN2B at synapses could be compromised in AD due to low levels of Tyr1472 phosphorylation.

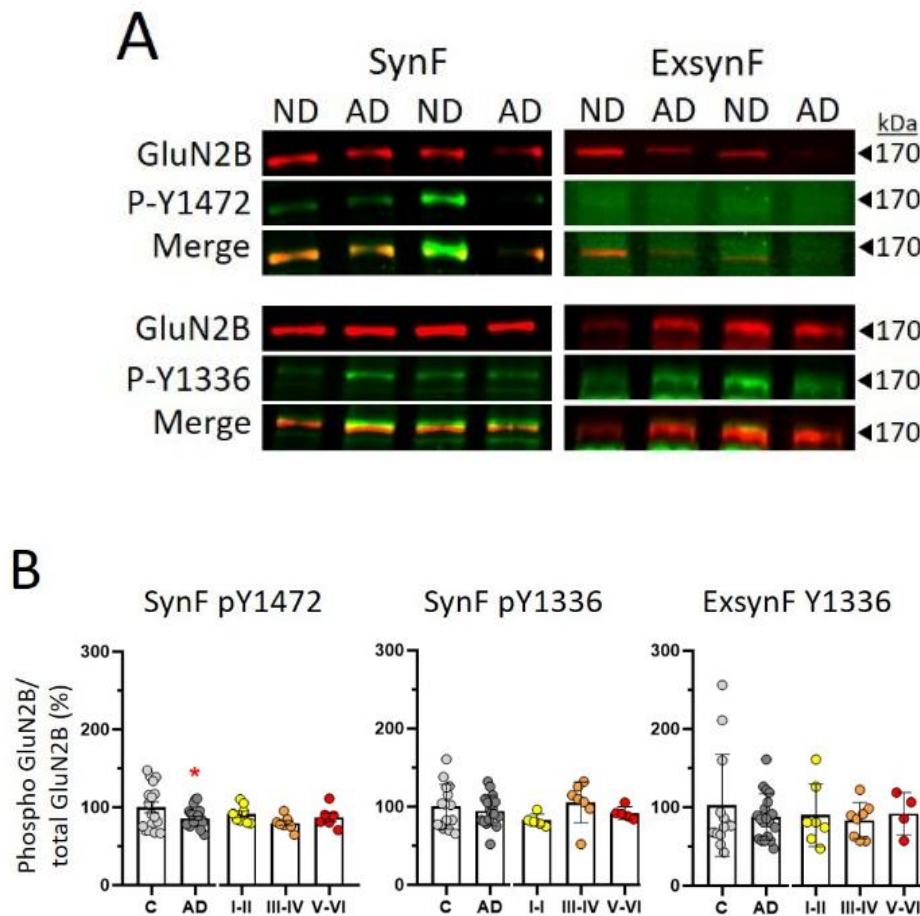


Figure 6. GluN2B phosphorylation from control and AD cases comparing SynF and ExsynF. A)

Representative western blots of GluN2B, phospho GluN2B Tyr1472 and phospho GluN2B Tyr1336 in SynF and ExsynF of controls and AD (Braak V-VI) samples. **B)** Quantification of GluN2B-170kDa phosphorylation at SynF (phospho Tyr1472, phospho Tyr1336) and at ExsynF (phospho Tyr1336). Levels of phosphorylated GluN2B were normalized to total GluN2B and estimated as in Fig. 4. * $p < 0.05$ AD v control, t-test. Cases control SynF $n = 15-17$; control ExsynF $n = 13$; AD SynF $n = 17-22$; AD ExsynF $n = 19$.

4.2.6 N-glycosylation is altered in extrasynaptic GluN2B and GluN2A in AD cortex

Modifications of N-glycosylation have been reported in AD for many glycoproteins, and consequently, we evaluated whether glycosylation of NMDAR subunits is affected. To this end, SynF and ExsynF from controls and AD samples (Braak V-VI) were incubated with lectins, which bind to specific carbohydrates linked to protein residues. We employed two agarose-immobilized lectins, Con A (binds mannose/glucose) and WGA (binds N-acetyl-D-glucosamine

and sialic acid residues), that previously have demonstrated a saccharide-specificity and high affinity for NMDAR subunits [287]. After incubation, the levels of unbound glycoforms were determined by western blot (**Figure 7A**) and quantified for each lectin. The unbound fractions of GluN2B-170 kDa and GluN2A-170 kDa were measured only in SynF, as the affinities of either Con A or WGA lectins for these subunits were so high in ExsynF that made it difficult to quantify the unbound fraction, due its weakness in the immunoblot. In SynF, the percentages of GluN2B, GluN2A, and GluN1 unbound to lectins showed no differences among controls and AD (**Figure 7B**). Likewise, ExsynF GluN1 unbound fraction to ConA and WGA was similar in controls and AD. GluN3A affinity for Con A and WGA lectins was so high in SynF and ExsynF from control and AD samples that the unbound fraction was quite weak, and therefore, we did not quantify it either. We found statistical differences only in the ExsynF GluN2B-160 kDa and GluN2A-160 kDa, both with lower unbound percentages to Con A in AD fractions with respect to controls, indicating a higher affinity for this lectin. This suggests a specific AD-related alteration in the glycosylation of these extrasynaptic GluN2B and GluN2A glycoforms.

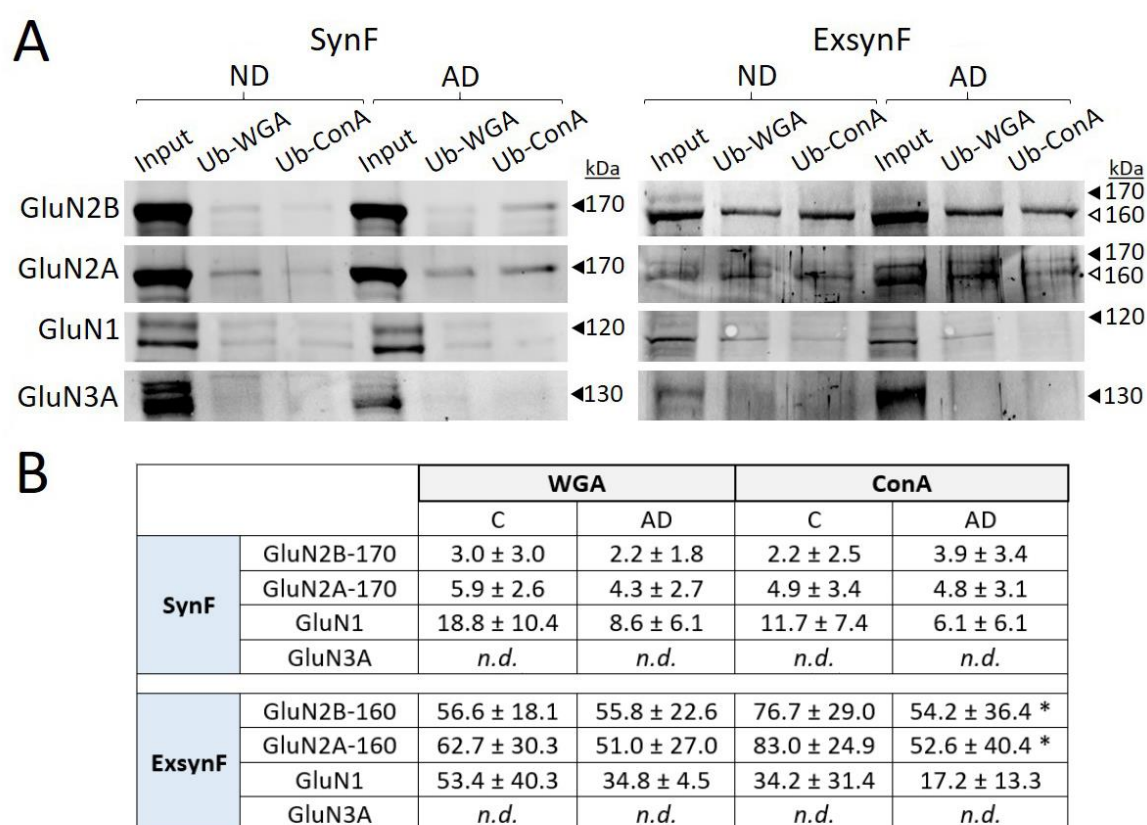
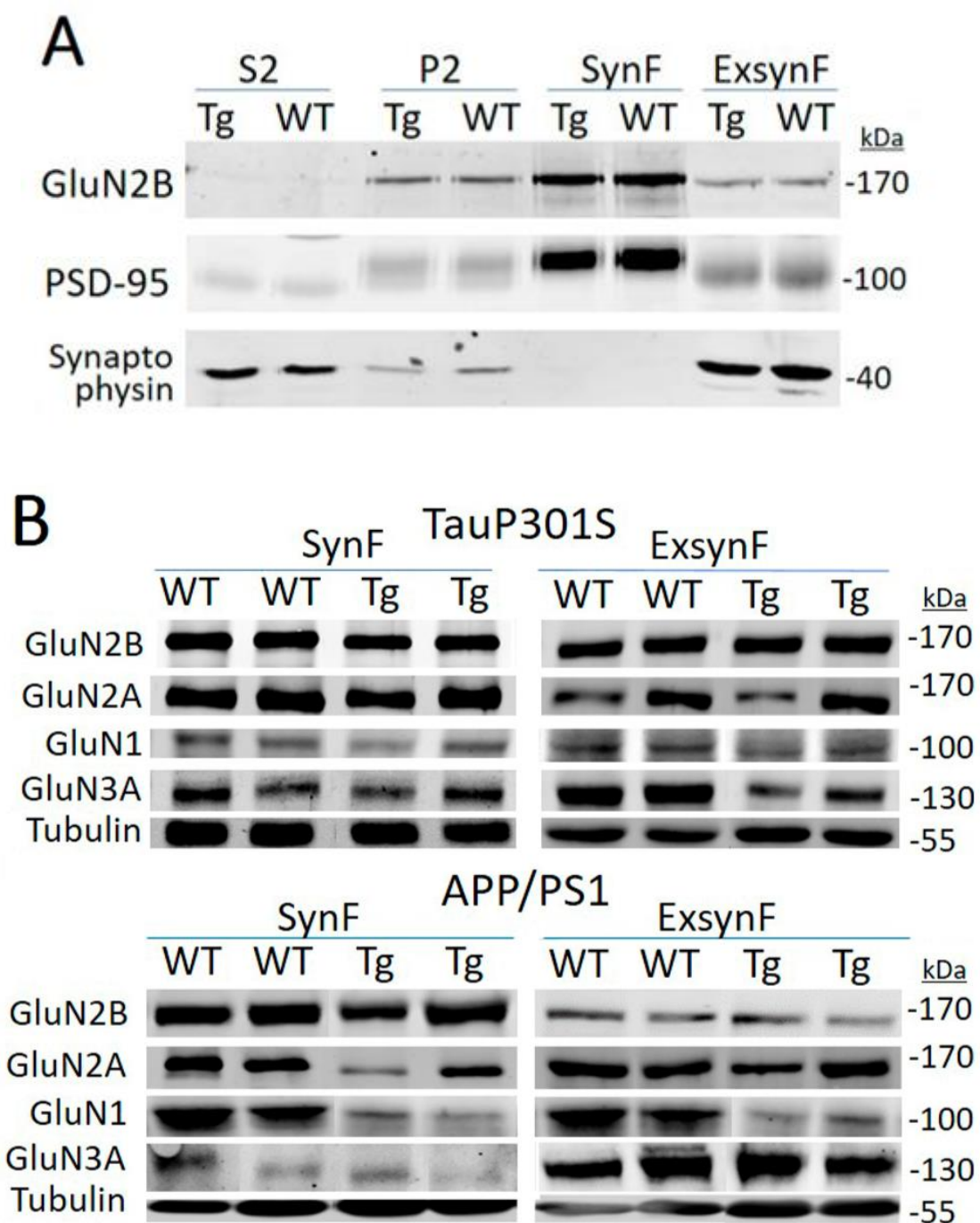


Figure 7. NMDAR subunits interaction with N-glycan lectins. A) Representative western blots for GluN2B, GluN2A, GluN1, and GluN3A of unbound and inputs of SynF and ExsynF fractions after incubation with WGA and Con A lectins from control (C) and AD Braak stage V-VI samples.

B) Quantification of SynF and ExsynF unbound fraction to WGA or Con A lectins from control and AD samples, respect to the input fraction (SynF or ExsynF respectively) expressed as percentage (%). Data represent SynF GluN2B-170 kDa, SynF GluN2A-170 kDa, SynF GluN1, ExsynF GluN2B-160 kDa, ExsynF GluN2A-160 kDa and ExsynF GluN1. Values represent % unbound \pm standard deviation. Control SynF n = 5, controls ExsynF n = 7; Braak V-VI SynF n = 6, Braak V-VI ExsynF n = 7. nd = not determined. * $p < 0.05$ AD vs control, t-test.

4.2.7 NMDAR subunits distribution in mice models

Finally, we used two mouse models to determine whether dysfunction in AD key proteins, tau and APP, may be related to changes in NMDAR subunit distribution among synaptic and extrasynaptic membranes. The same fractionation protocol was used, yielding a high discrimination among cytosolic, synaptic, and extrasynaptic fractions (**Figure 8**). In all immunoblots, mouse NMDAR subunits were identified at a molecular mass similar to that of human samples, but ExsynF GluN2B and GluN2A were resolved as a unique band. The first transgenic line used, TauP301S, is a tauopathy model that expresses the human P301S mutant tau protein and is characterized by neurofibrillary pathology and neurological manifestations [233]. At nine months of age, a decrease was observed in SynF GluN2B ($62.3 \pm 27.6\%$; $p = 0.009$), SynF GluN1 ($65.9 \pm 25.1\%$; $p = 0.020$), and ExsynF GluN3A levels ($62.2 \pm 31.3\%$; $p = 0.014$) when compared with those in wild-type mice (**Figure 8B, C**). This somehow resembles what occurs in AD samples and suggests that tau phosphorylation could be involved in GluN2B and GluN3A retention at their main synaptic locations. A second transgenic model, the APP/PS1 mouse [290], develops amyloid plaque pathology, astrogliosis, and learning deficits starting at seven months of age [291, 292]. In this model, at 12 months of age, only GluN1 levels were affected, in both SynF ($33.2 \pm 4.3\%$; $p = 0.0317$) and ExsynF ($57.3 \pm 24.6\%$; $p = 0.003$), compared with wild-type controls (**Figure 8B, D**). In any of these mouse models, phosphorylation of GluN2B was affected.



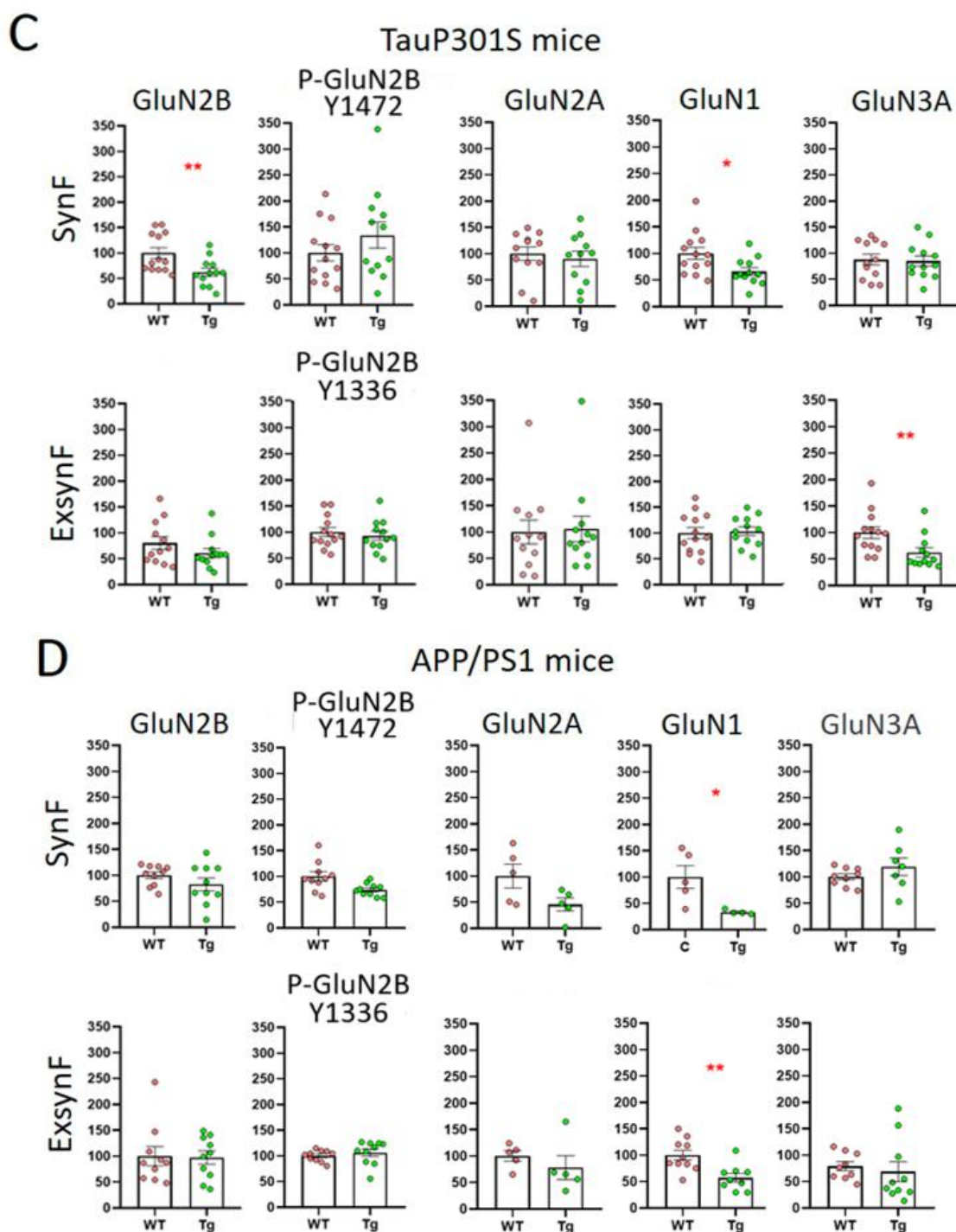


Figure 8. NMDAR subunit levels and GluN2B phosphorylation in AD mouse models TauP301S and APP/PS1. A) The fractionation protocol in wild-type mice (WT) and transgenic mice (Tg) cortex was the same as described for human samples in **Figure 1**. Representative western blot of S2, P2, SynF, and ExsynF fractions from WT and TauP301S mice (Tg) revealed antibodies against GluN2B, PSD95, Synaptophysin, and glial fibrillary astrocytic protein (GFAP); similar patterns were obtained for APP/PS1 mice (not shown). **B)** Representative western blots of NMDAR subunits in SynF and ExsynF from wild-type (WT) and TauP301S mice (Tg); and from

wild-type (WT) and APP/PS1 mice (Tg), as indicated. **C)** Quantification of GluN2B, Tyr1472 phosphorylation of GluN2B (P-GluN2B Tyr1472), Tyr1336 phosphorylation of GluN2B (P-GluN2B Tyr1472), GluN2A, GluN1 and GluN3A levels in SynF and ExsynF from WT and TauP301S mice (Tg). WT SynF n = 6-13, WT ExsynF n = 12-13, Tg SynF n = 6-12, Tg ExsynF nn= 12. **D)** Quantification of GluN2B, Tyr1472 phosphorylation of GluN2B (P-GluN2B Tyr1472), Tyr1336 phosphorylation of GluN2B (P-GluN2B Tyr1472), GluN2A, GluN1 and GluN3A levels in SynF and ExsynF from WT and APP/PS1 mice (Tg). WT SynF n = 5-10, WT ExsynF n = 5-10, Tg SynF n = 5-10; Tg ExsynF n = 5-10. * $p < 0.05$, ** $p < 0.01$ respect to WT.

The research conducted in this section constitutes a paper accepted for publication [426].

4.3 NMDA receptor subunits characterization in the CSF of AD

We were interested in expanding the study and characterization of this receptor to the CSF. To our knowledge, NMDARs have never been characterized in the CSF. Detecting NMDAR subunits in CSF can be a valuable diagnostic tool for certain neurological conditions and could be used as a read-out of the neurodegenerative processes that occur in the brains of these patients (objective 2 of the thesis).

4.3.1 NMDAR subunits GluN1, GluN2A, GluN2B, and GluN3A are present in human CSF

To assess whether NMDAR subunits are present in CSF, we performed immunoprecipitation assays and resolved by western blot with alternative C-terminal antibodies. We detected the presence of GluN1, GluN2A, GluN2B, and GluN3A immunoreactivities in human CSF compatible with the full-length species, which originally were resident membrane proteins (**Figure 9A**).

Thus, we wondered whether NMDARs could be present in the CSF as a transmembrane protein of extracellular vesicles (EVs). To examine this, EVs were isolated following a specific protocol [277] that separates different fractions: a supernatant where no EVs are present, a first pellet (P10K) that contains mainly cellular fragments and big vesicles, and a final pellet (P100K) that contains the EVs. We stained against the EVs marker Alix to ensure that EVs are only present in the P100K [293]. We failed to find GluN1, GluN2A, GluN2B, and GluN3A in the P100K, meaning that NMDAR subunits are not part of the CSF EVs; the four NMDAR subunits reside in the supernatant fraction (**Figure 9B**).

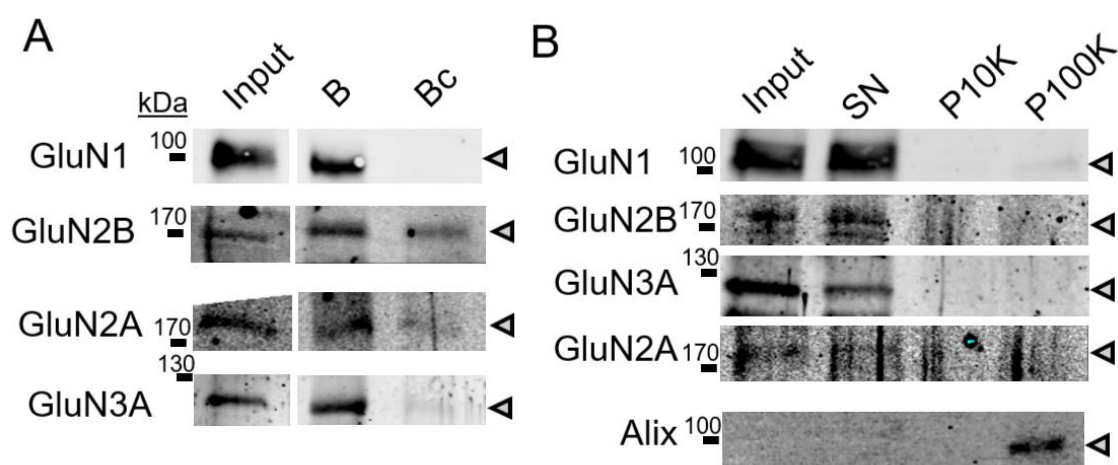


Figure 9. NMDAR subunits GluN2A, GluN2B, GluN1, and GluN3A are present in human CSF. A)

Immunoprecipitation (IP) of control CSF against the four different subunits using alternative antibodies to IP and reveal the western blot. IP of GluN1 N-terminal; revealed with antibody against GluN1 C-terminal. IP of GluN2B N-terminal; revealed with antibody against GluN2B C-terminal. IP of GluN2A C-terminal; revealed with antibody against GluN2A C-terminal. IP of GluN3A N-terminal; revealed with GluN3A C-terminal. Together with the input and the bound fraction, a control IP (Bc) was also revealed, corresponding to the IP performed with an irrelevant IgG of the same animal species as the specific anti-NMDAR antibody. **B)** Western blot against the four different subunits using input CSF and three different fractions of the extracellular vesicles (EVs) fractionation protocol. Supernatant (SN) did not contain any EVs. Pellet P10K was obtained after centrifugation of 10,000×g and contained cellular fragments and big vesicles. Pellet P100K was obtained after an ultracentrifugation of 100,000×g and contained the EVs. The presence of the EVs marker Alix in P100K demonstrates that this is the only fraction that contains EVs.

To provide further evidence for the specificity of NMDAR subunits, we determined the GluN1 subunit in the CSF from patients with anti-NMDAR encephalitis, an auto-immune that target directly GluN1 [294], and viral encephalitis from the University of Verona (Verona, Italy; see **Table 4** in Methods). The CSF from anti-NMDAR encephalitis individuals exhibited lower levels of GluN1 subunit (in 79%) than the CSF from subjects with viral encephalitis (**Figure 10A**). We also analyzed CSF from WT and *GluN3a* KO mice to provide further evidence for immunoreactive band specificity. Although the immunoreactive band attributed to GluN3A is found in the mice CSF from WT, this is absent in the KO (**Figure 10B**).

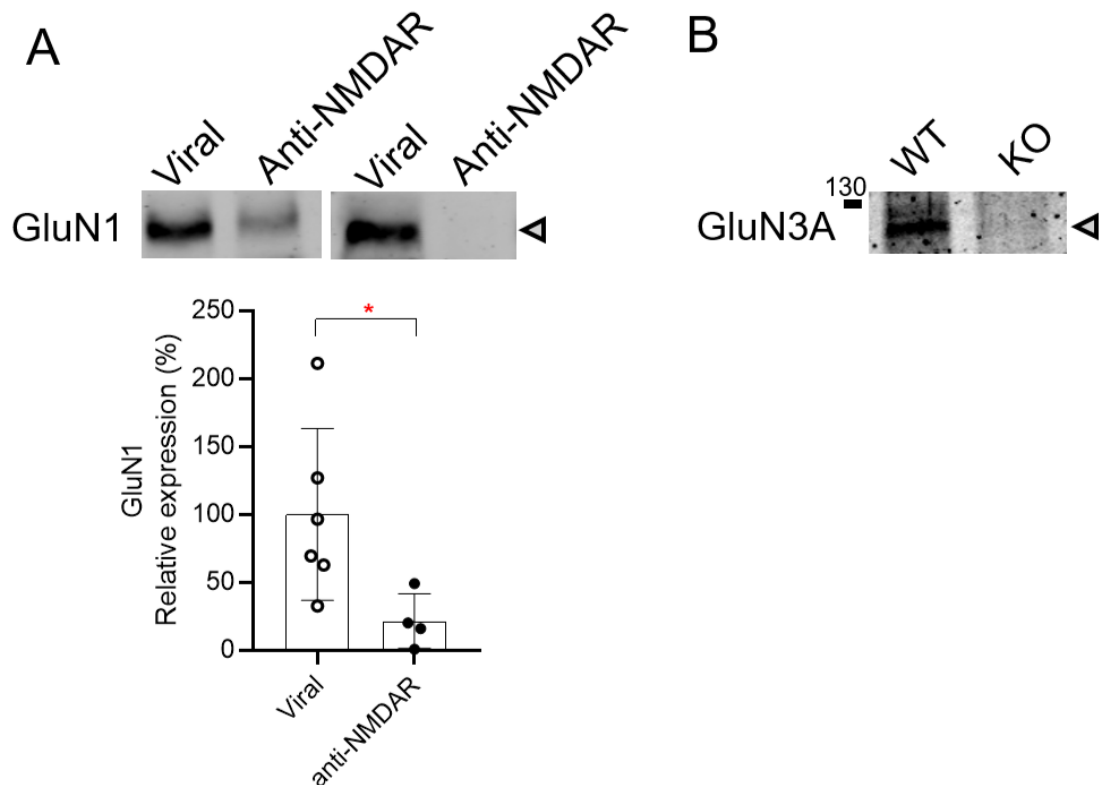


Figure 10. NMDAR subunit GluN1 is depleted in the CSF from individuals with anti-NMDAR encephalitis and GluN3A is depleted in the CSF of a mice *Grin3a* KO model. A) Representative blot and quantification of the GluN1 subunit in the CSF from individuals with anti-NMDAR encephalitis and viral encephalitis. * $p < 0.05$, Mann-Whitney test. **B)** Western blot of CSF (a mix from 3-4 animals) from wild-type mouse (WT), and a mouse KO for *Grin3a* (GluN3A subunit).

4.3.2 GluN2A subunit levels are lower in CSF from AD patients

As we obtained significant changes in the synaptic/extrasynaptic balance of GluN2B and GluN2A in the cortex of AD patients, we also explored whether these changes are reflected in CSF from AD patients. GluN2A and GluN2B levels were determined in samples from a cohort of AD and control individuals from the University of Gothenburg (Gothenburg, Sweden; see **Table 2** in Methods) by western blot with parallel staining for GluN1 (to which GluN2A and GluN2B levels were referred to normalized subunit-specific changes) (**Figure 11A**); with a control sample to ensure normalization among different blots (previously aliquoted to avoid freezing-thawing cycles). GluN2A displayed lower levels related to GluN1 in AD than in non-AD control samples (47%; $p = 0.002$; **Figure 11B**), whereas GluN2B did not show differences between control and AD samples (**Figure 11C**). No statistically significant correlations were found between GluN2A or GluN2B levels and tau, P-tau or A β 42 levels, or age or related with gender.

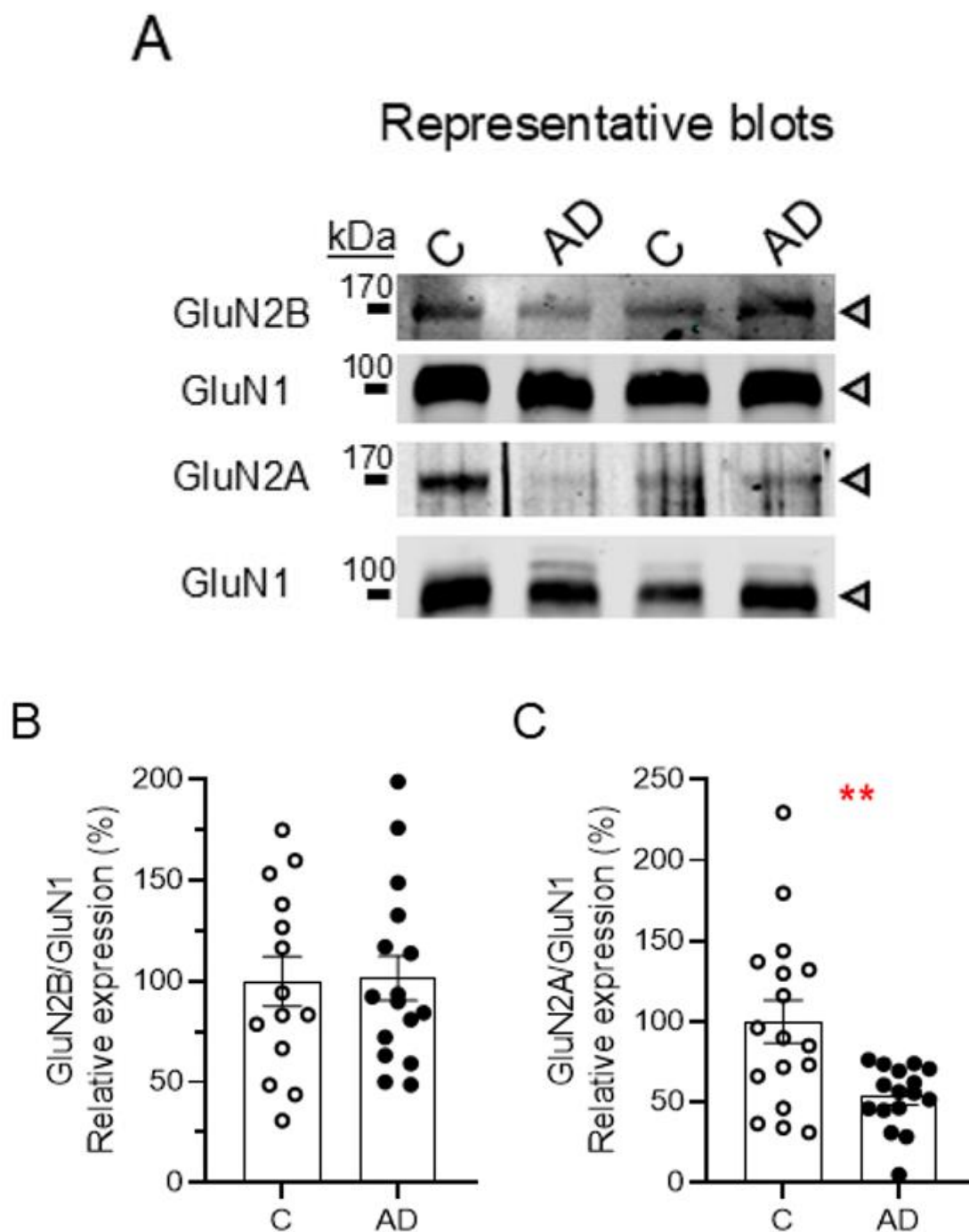


Figure 11. NMDAR subunits GluN2A and GluN2B levels in the CSF of patients with AD. A)

Representative western blots of GluN2A, GluN2B, and GluN1 subunits in human CSF (30 μ l). An internal sample was used to normalize among different membranes. **B)** Quantification of GluN2B and **C)** GluN2A subunit levels were normalized to the GluN1 subunit. Data are expressed as percentages with respect to controls. * $p < 0.05$, ** $p < 0.01$, t-test. Cases control $n = 14$, and AD $n = 16$.

4.3.3 GluN3A is increased in CSF samples from Huntington's disease subjects

Elevated GluN3A expression has been confirmed in a variety of HD mouse models and in patients [295]. Thus, we considered the possibility that these increased levels are reflected in CSF from HD patients. Accordingly, GluN3A levels were determined by western blot in H0, H1 and control samples from a cohort obtained from the Hospital Sant Pau (Barcelona, Spain; see **Table 3** in Methods), as well the levels of the GluN1 compulsory subunit present in all NMDAR complexes. Thus, the same blot was stained against GluN1, to which GluN3A levels were referred to normalized subunit-specific changes. A control sample (previously aliquoted to avoid freezing-thawing cycles) was included in each blot to serve as a loading reference and for normalizing the immunoreactivity signal between blots (**Figure 12A**).

In HD, two stages have been described: the asymptomatic (H0) and the symptomatic phase (H1) [269]. GluN3A normalized to GluN1 levels were higher in samples from H0 (118%; $p = 0.001$) and from H1 (56%; $p = 0.011$) compared to those from control samples (**Figure 12B**). No statistically significant correlations were found between GluN3A levels and age, gender, CAG repetitions, or disease burden.

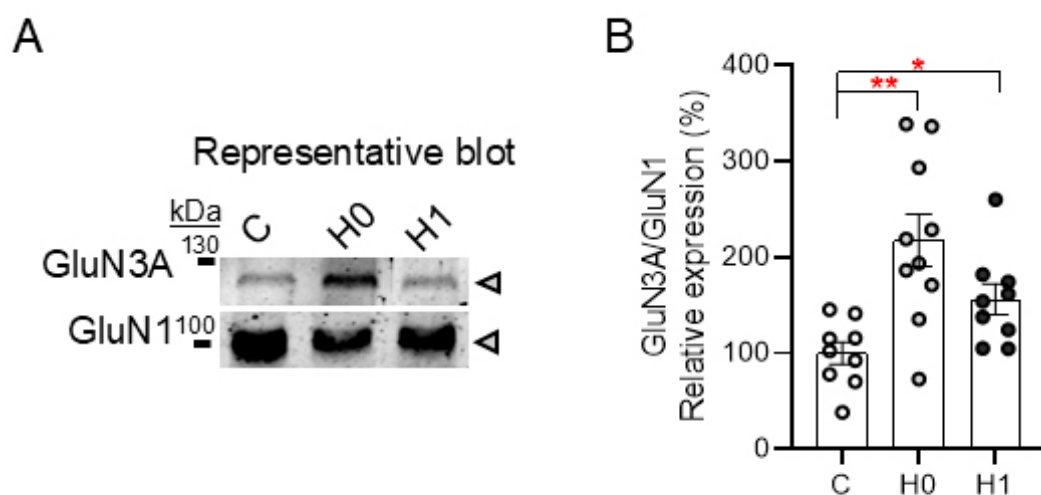


Figure 12. NMDAR subunit GluN3A levels in the CSF of patients with HD. A) Representative western blots of GluN3A and GluN1 subunits in cases control ($n = 9$), cases of Huntington's disease (HD) in the asymptomatic phase (H0; $n = 10$), and cases of HD in the symptomatic phase (H1; $n = 9$). **B)** Quantification of GluN3A subunit levels was normalized to the GluN1

subunit. An internal sample was used to normalize among different membranes. Data are expressed as percentages with respect to controls. * $p < 0.05$, ** $p < 0.01$, t-test.

Overall, this suggests that the measurement of NMDAR subunits can serve as a read-out of brain changes in several diseases, such as autoimmune NMDAR encephalitis, HD, and AD.

4.4 iNeurons as a model for the study of NMDARs in the context of AD

The third objective of the thesis is “To evaluate the suitability of iNeurons for the study of NMDARs”. Differentiating induced pluripotent stem cells (iPSCs) towards iNeurons enables *in vitro* mechanistic studies on NMDAR involvement in AD. Here, we particularly investigated the GluN2B-GluN2A switch and the incorporation of NMDARs into the synapse during differentiation of human iPSCs towards iNeurons over a large period, to determine the appropriate timing to modulate AD-like changes by A β treatment.

To obtain iPSCs-derived neurons (iNeurons) we followed a protocol described in **Figure 13**, and used an iPSC line from an individual with LOAD, to further modulate with A β . During the culture period, the iPSC colonies appeared healthy and showed signs of pluripotency, such as compact cells, smooth edges (**Figure 14A**), and the presence of classical pluripotency markers (OCT4 and Nanog) evaluated by ICC and FACS (>80% double positive for OCT4 and Nanog) (**Figure 14B, C**). We differentiated iPSC to neural progenitor cells (NPCs) using the STEMdiff™ Neural Induction Medium (StemCells Technologies). We checked the presence of NPC markers (PAX6 and Nestin) throughout the protocol. NPCs were expanded using the STEMdiff™ Neural Progenitor Medium (StemCells Technologies). From NPCs, cells were differentiated into neurons using two alternative protocols: Neural Maintenance Media (NMM) and Brainphys (BPM). Although NMM is the classic medium for neurodifferentiation [296], BPM has emerged as an alternative. The use of BPM provides faster neural and synaptic maturation [273], increasing the number of astrocytes, which interact with neurons to regulate synaptic function. Additionally, in the context of AD, the BPM medium achieves a greater secretion of A β species [271].

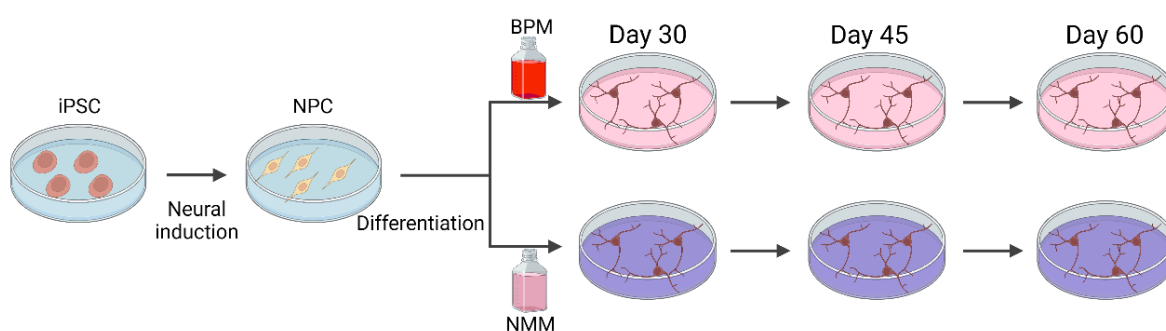


Figure 13. Schematic illustration of the experimental design. The process of iPSCs differentiation to neural progenitor cells (NPCs) is called Neural induction. The process from NPCs to mature neurons is named neural differentiation. The latter was performed through

two different media: Brainphys (BPM) and Neural Maintenance Media (NMM). We established three time points to recollect neural cells: days of differentiation 30, 45, and 60.

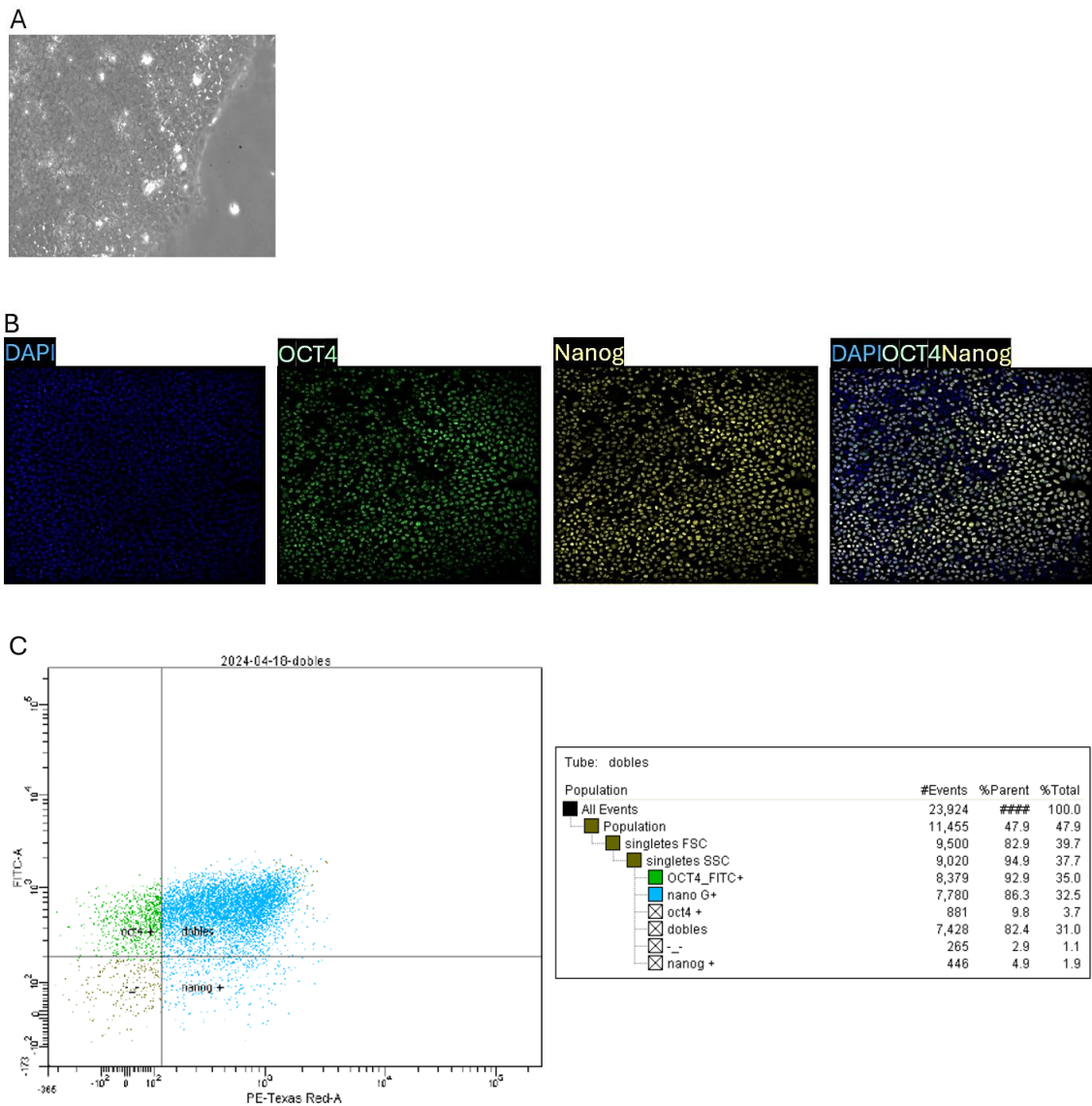


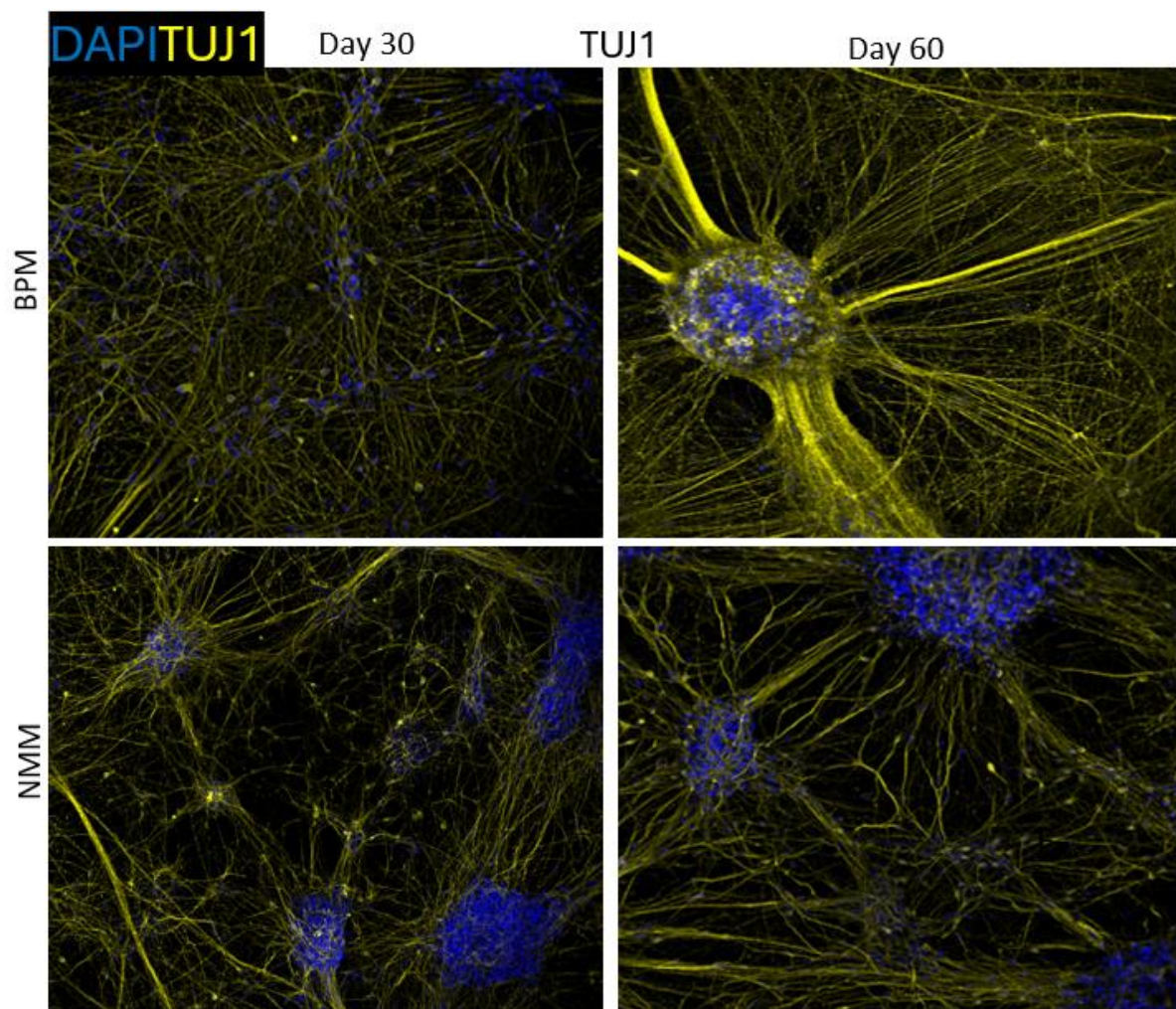
Figure 14. iPSCs characterization. **A)** Image taken from a wide field microscope showing a compacted colony with smooth edges, a sign of a healthy, pluripotent colony. **B)** Image taken from a confocal microscope showing DAPI (blue), Nanog (yellow), and OCT4 (green), which are markers for pluripotency. **C)** FACS analysis showing the number and percentage of singles and doublets for Nanog and OCT4, markers for pluripotency.

4.4.1 Characterization of iNeurons from an individual with sporadic AD in BPM and NMM

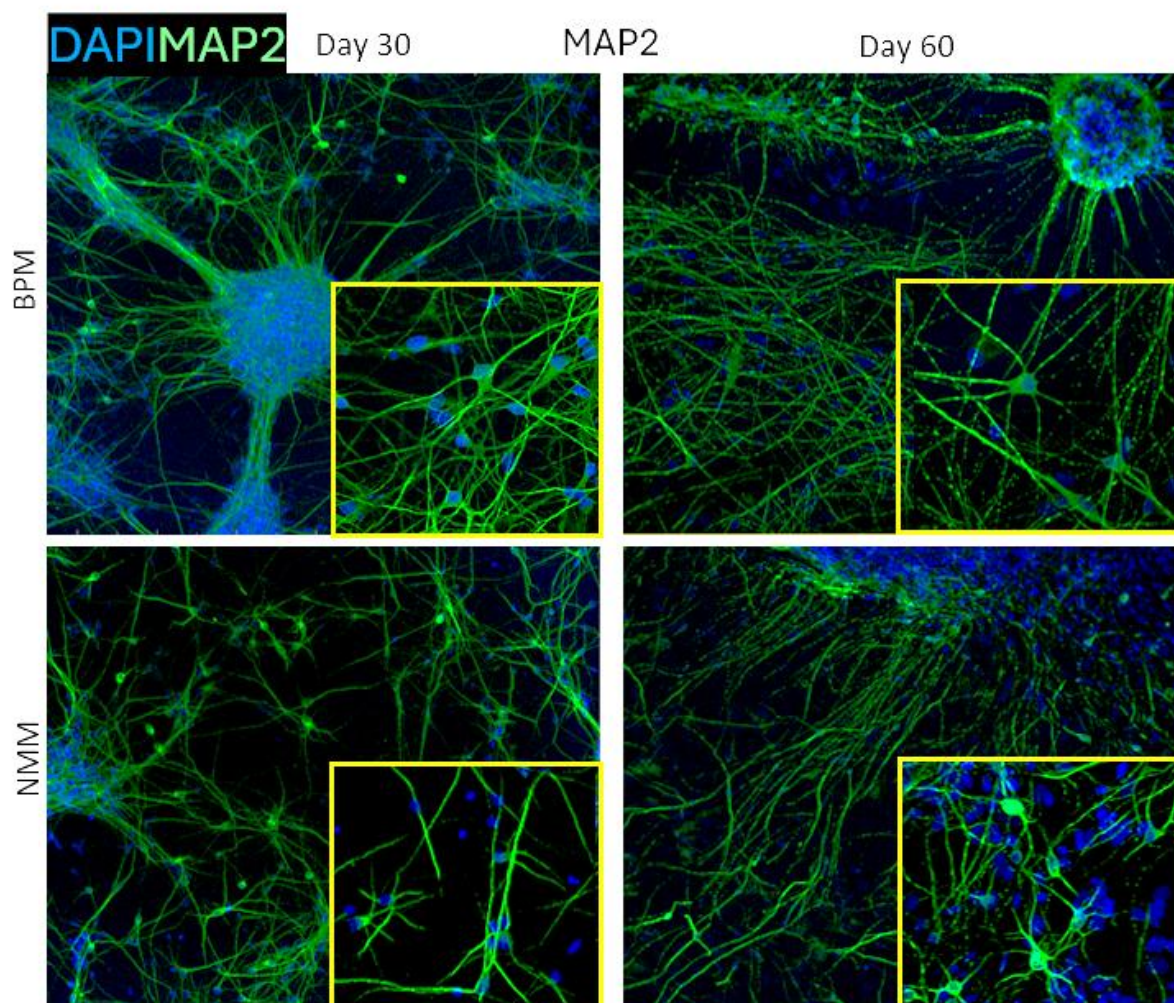
We aimed to find a suitable model for studying the role of NMDARs in AD. To do so, we performed the differentiation of NPCs to iNeurons using either NMM or BPM, and evaluated the effects of these two protocols at three different time points: 30, 45, and 60 days of neurodifferentiation. We considered day 0 the neuroprogenitor state. It is important to note that some neurodifferentiation protocols start to count days from neural induction, but we start to count when NPCs are plated in either BPM or NMM.

The immunostaining of TUJ1, a marker of post-mitotic neurons [297, 298], revealed a highly dense and interconnected neuronal network (**Figure 15A**) in cultures differentiated with both BPM and NMM and at days 30 and 60. The staining of MAP2 (a marker of mature neurons) showed a more complex morphology with BPM than NMM, in terms of number of processes and branching, at day 30. This complexity increased at day 60 in both protocols (**Figure 15B**). A crucial difference between the two protocols was the number of astrocytes. This appeared to be higher when using BPM, which was confirmed by immunostaining using the astrocyte marker GFAP (**Figure 15C**).

A



B



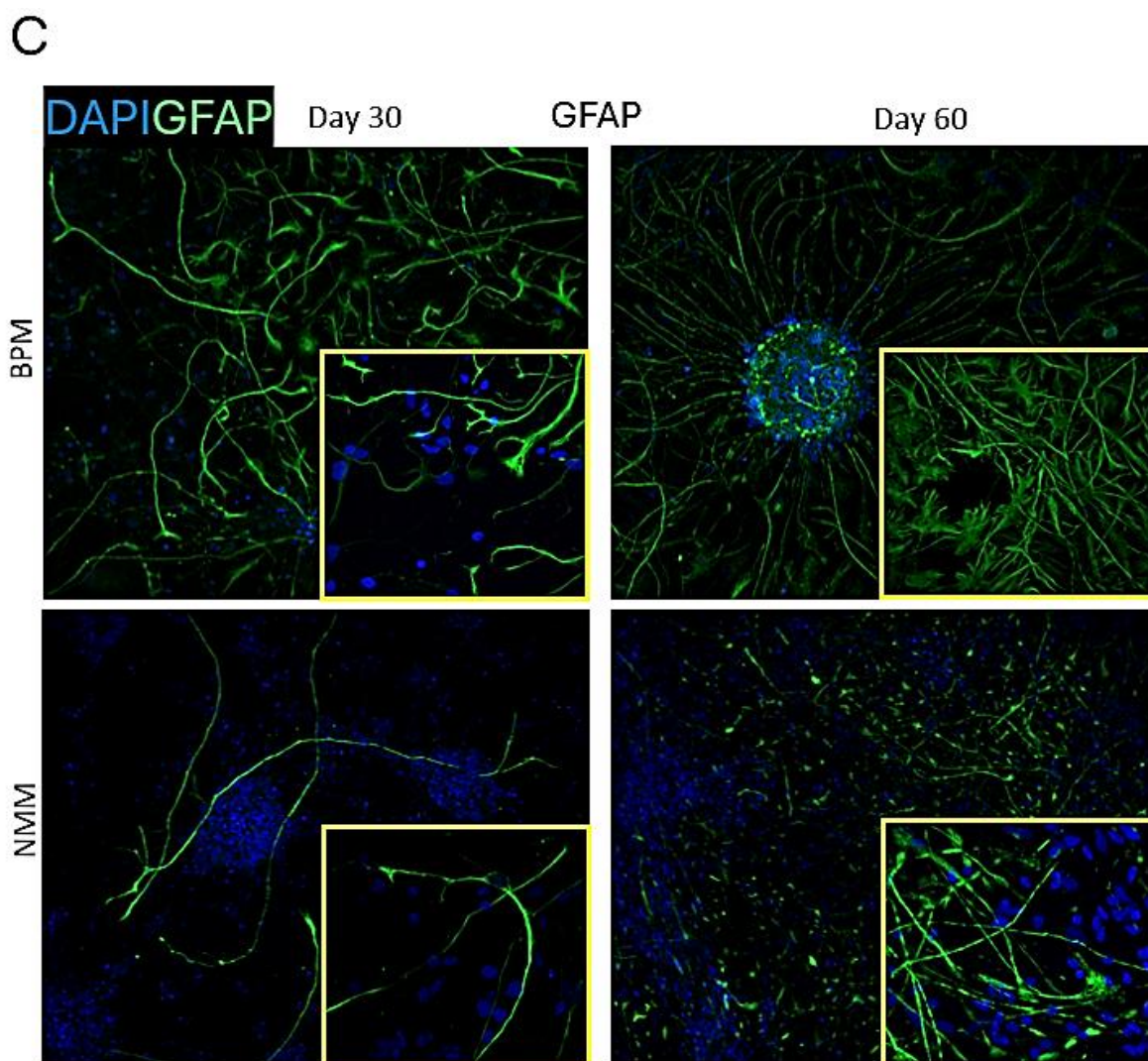


Figure 15. Characterization of NMM and BPM cultures by confocal microscopy. **A)** 10x magnification image showing DAPI (blue) and TUJ1 (yellow, a marker for post-mitotic neurons) at days 30 and 60 of neurons differentiated with BPM (up) and NMM (down). **B)** 10x magnification image with an inset in the low right corner at 40x magnification showing DAPI (blue) and MAP2 (green, marker for mature neurons) at days 30 and 60 of neuronal cultures differentiated with Brainphys media (BPM) (up) and Neural Maintenance Media (NMM) (down). **C)** 10x magnification image with an inset at 40x magnification showing DAPI (blue) and GFAP (green, marker of astrocytes) at days 30 and 60 of neuronal cultures differentiated with BPM (up) and NMM (down).

At this point, we were concerned about the identity of GFAP+ cells. GFAP is used as a marker of astrocytes [271, 299, 300], but radial glial cells (RGCs, considered as the NPCs of the brain) can also express GFAP [301-303]. Since some of our GFAP+ cells had a morphology that could

resemble RGCs, we wondered if they could be RGC or NPC instead of astrocytes. PAX6 is a recognized marker for RGCs or NPCs [304-306] (**Figure 16A**) and, therefore, was used to identify the presence of these cells. We observed only a small number of PAX6-positive cells in cultures differentiated with BPM and NMM, and, importantly, PAX6+ cells were not GFAP+ cells, confirming that our GFAP+ cells are not RGCs or NPCs (**Figure 16B**). Notwithstanding, to double-check it, we used another well-known marker of astrocytes: S100 β [300, 307]. In the mice brain, astrocytes positive for S100 β exhibit less extended branching and are more mature than other GFAP+ cells [308-310]. Our BPM and NMM cultures at day 60 had double positive GFAP+ and S100 β + staining (**Figure 16C**), indicating that these cells were, indeed, astrocytes.

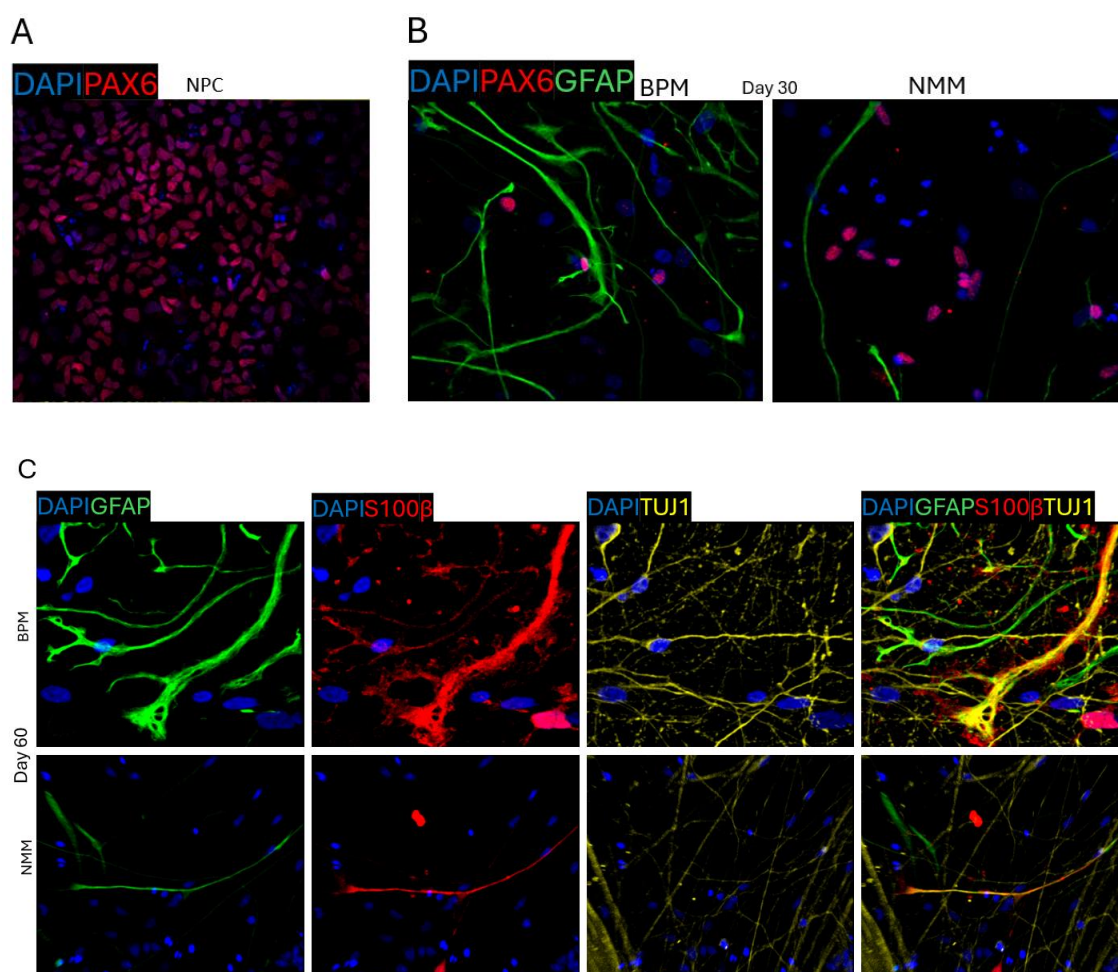


Figure 16. Identity of GFAP+ cells characterized by confocal microscopy. A) 20x magnification image of neuroprogenitor cells (NPC) showing that most nuclei (DAPI, blue) are stained for PAX6 (red, a marker for neuroprogenitor cells). **B)** 40x magnification images showing DAPI (blue), GFAP (green) and PAX6 (red) of neuronal cultures differentiated with BPM (left) and NMM (right) at day 30. **C)** 63x magnification images showing DAPI (blue), GFAP (green, a

general marker for astrocytes) and S100 β (red, marker of mature astrocytes) of neuronal cultures differentiated with BPM (top) and NMM (bottom) at day 60.

As part of the characterization, the transcript levels of a set of genes relevant to our research were measured by qPCR along differentiation. The mRNA expression of the neuronal marker *MAP2* peaked on day 30 and decreased on days 45 and 60, with no significant differences between BPM and NMM (**Figure 17A**). *CAMKIIB*, a synaptic marker, followed a similar trend. Expression of *GRIA1* mRNA, a subunit of the synaptic AMPA receptors (AMPA), also decayed along the differentiation, but it was significantly smoother in BPM than in NMM. Note that *GFAP* mRNA levels were dramatically higher in BPM than in NMM (**Figure 17A**), in accordance with immunostaining assays (**Figure 16C**) and previous studies [271, 273]. The expression of the NPC marker *PAX6* peaked at day 0 (NPC stage) and then decreased to a baseline that was not set at zero. Finally, *APP* transcript levels followed a trend similar to *MAP2* and *CAMKIIB*, but its decay resembled that of *GRIA1*, as it was significantly slower with BPM.

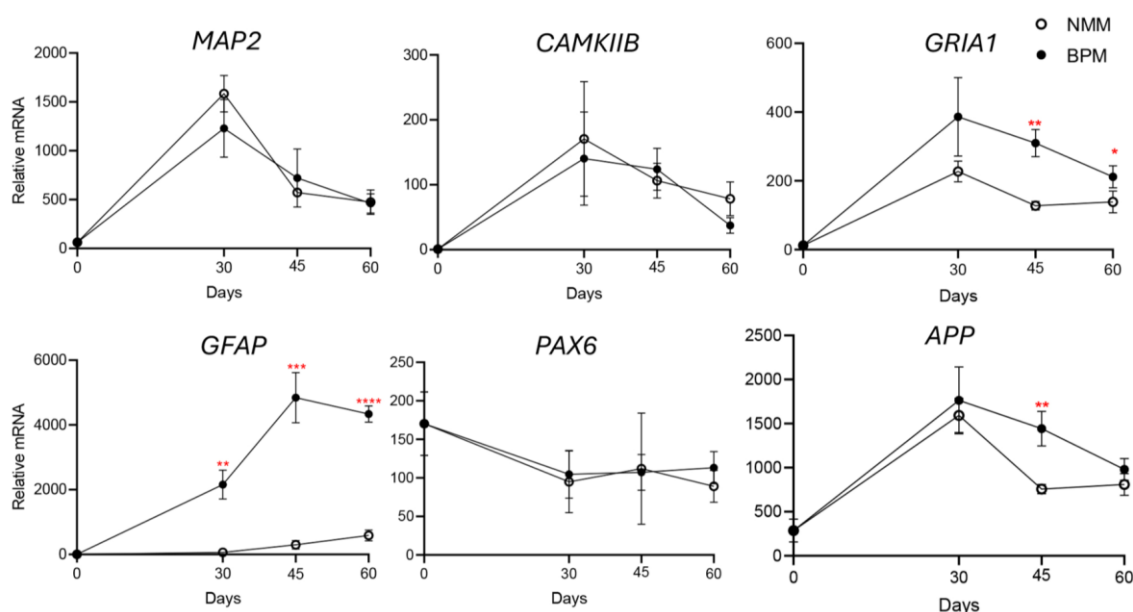


Figure 17. Characterization of NMM and BPM cultures by RT-qPCR. A) Panel of mRNA expression analysis by RT-qPCR of *MAP2*, *CAMKIIB*, *GRIA1*, *GFAP*, *PAX6* and *APP* at days 30, 45 and 60. Each point in the graph is the mean of three different samples, and each sample is a pool of three different wells of a 24-well plate. Asterisks (*) indicate statistical significance between BPM and NMM. * $p < 0.05$, ** $p < 0.005$, *** $p < 0.0001$, **** $p < 0.00001$.

4.4.2 Evidence for GluN2B-GluN2A switch in iNeurons

The characterization of our neuronal cultures has shown the presence of mature neurons and astrocytes, the latter in higher numbers when cultured with BPM. We next examined whether the switch between the expression of GluN2B and GluN2A occurs as part of the maturation in iNeurons differentiated with BPM and NMM.

We first evaluated the mRNA expression of NMDAR subunits. *GRIN2B* mRNA levels followed a similar trend to synaptic markers *CAMK1B* and *GRIA1*: a peak of expression at day 30 and a lower expression level on days 45 and 60 (**Figure 18A**). *GRIN2B* levels were significantly higher in BPM than in NMM on day 45 ($p < 0.0001$). Expression of *GRIN2A* displayed a completely different trend. *GRIN2A* mRNA levels were always significantly higher with BPM than with NMM at all time points (**Figure 18A**). Finally, *GRIN1* levels (GluN1 is the mandatory subunit for all NMDARs) were much higher in BPM than in NMM on day 30 ($p = 0.001$) (**Figure 18A**), and afterward, the levels fell in BPM, as *GRIN2B*.

To better visualize whether the differentiation with BPM and NMM affects the mRNA expression of *GRIN2B* and *GRIN2A*, the same data were plotted in a different manner. In this representation, it can be easily observed that with NMM, *GRIN2B* mRNA levels drop from day 30 to 45. *GRIN2A* expression does not change over time. However, BPM induces a drop in *GRIN2B* expression from day 30 to day 45, which is even sharper from day 45 to day 60. Simultaneously, *GRIN2A* levels increase from day 45 to day 60 (**Figure 18B**). This is in agreement with a GluN2B-GluN2A switch at the level of mRNA in BPM but not in NMM.

When GluN2B and GluN2A protein levels were determined by western blot, it was observed that GluN2B protein levels did not change across time points (and there was no difference between BPM and NMM). Remarkably, GluN2A protein levels in BPM increased from day 45 to day 60 ($p = 0.001$). Moreover, the GluN2A protein levels were higher at day 60 in BPM than in NMM ($p = 0.046$) (**Figure 18C**). These data supported the hypothesis of a GluN2B-GluN2A switch at day 60 in BPM but not in NMM, not only at the mRNA level but also at the protein level.

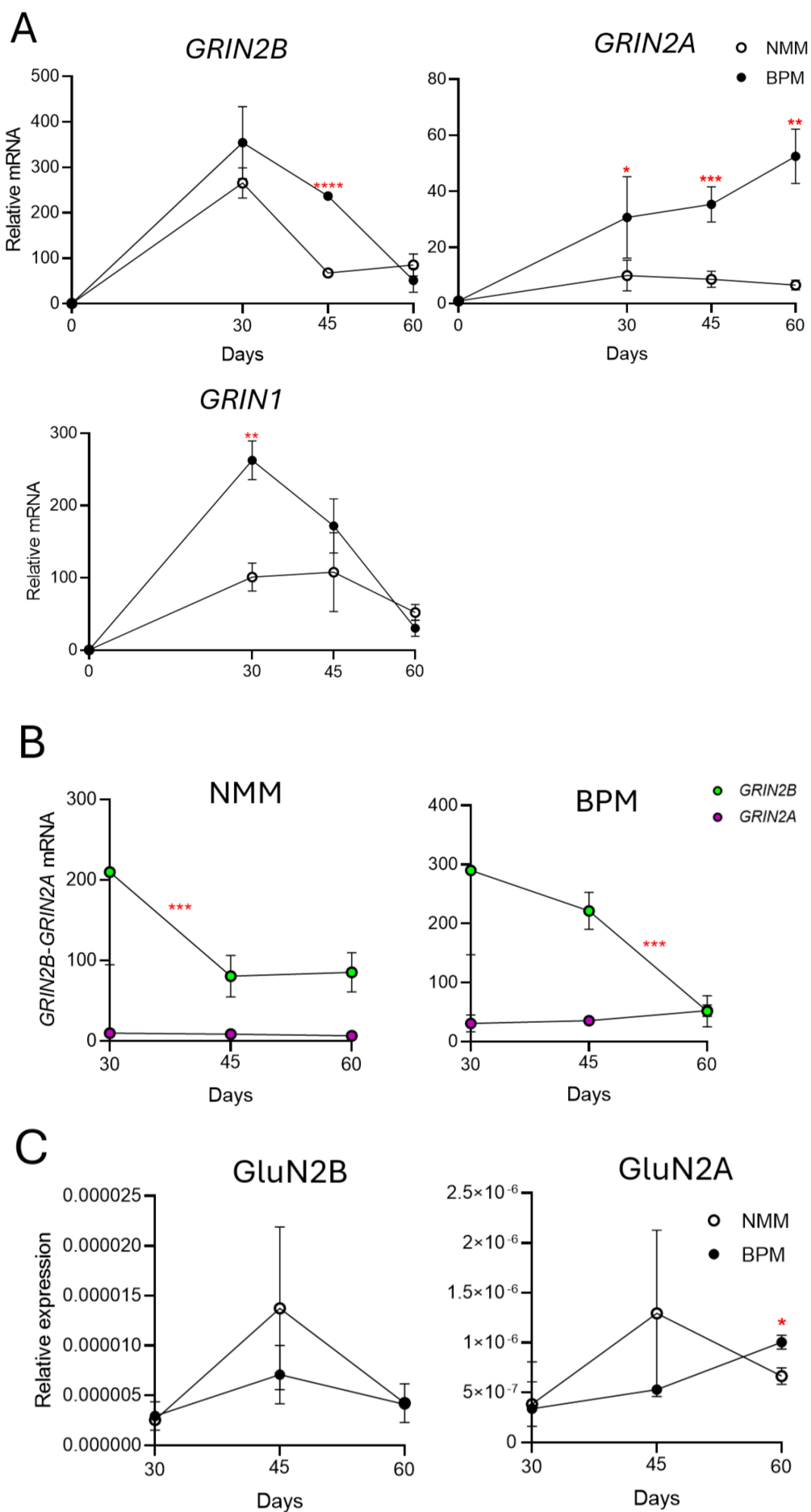


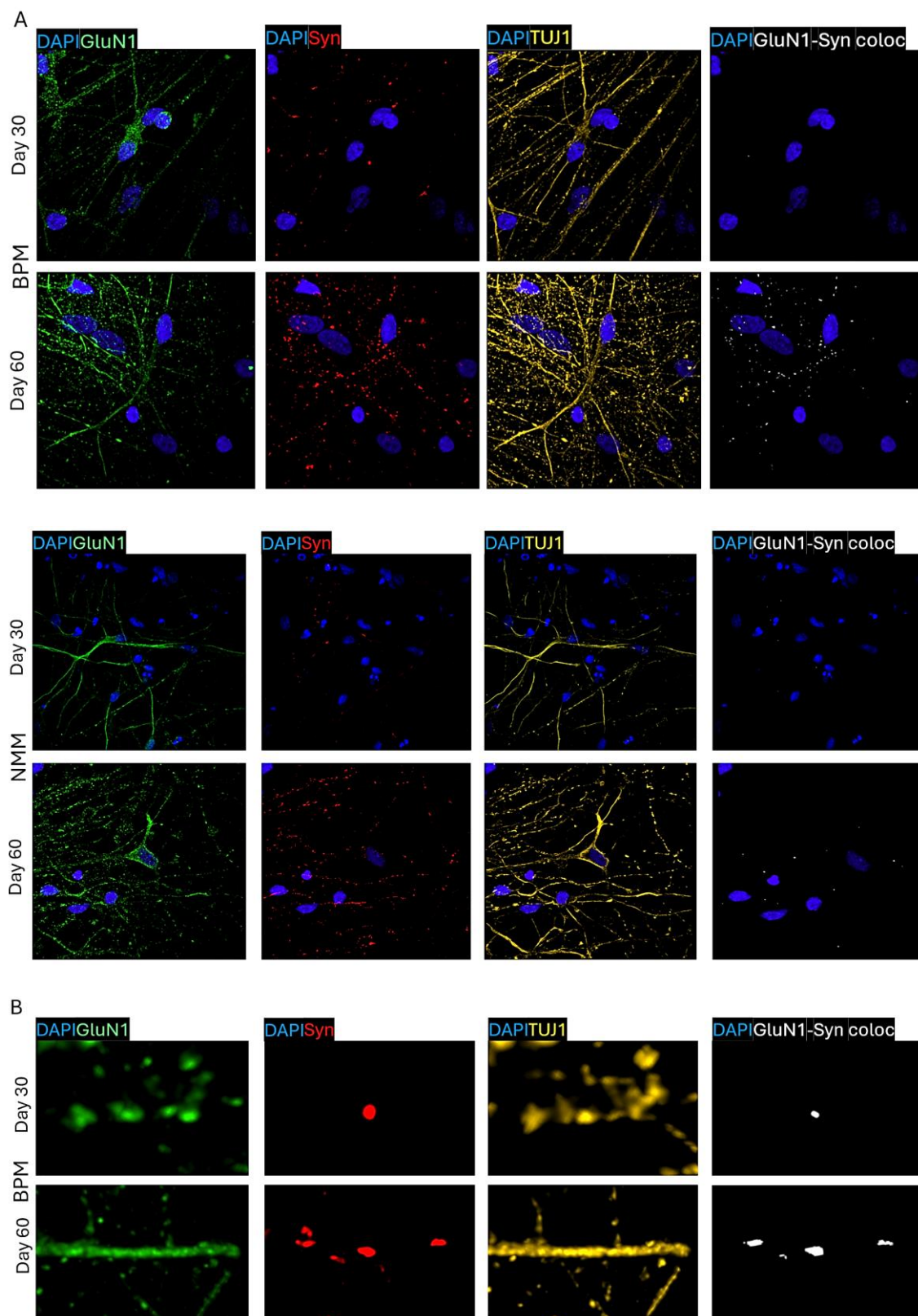
Figure 18. Evidence for GluN2B-GluN2A switch according to mRNA and protein levels. A)

Panel of mRNA expression by qPCR of *GRIN2B* (left) and *GRIN2A* (right) at days 30, 45 and 60 after differentiation with NMM (o) or with BPM (•). **B)** Alternative representation of the same data. *GRIN2B* is represented as green dots and *GRIN2A* as purple dots. Asterisks (*) indicate significant differences between time points for each media, NMM or BPM. **C)** Plots comparing the protein levels by western blot on days 30, 45, and 60 of GluN2B and GluN2A, after differentiation with NMM (o) or BMP (•). * $p < 0.05$; ** $p < 0.005$; *** $p < 0.0005$.

4.4.3 Increment of synaptic NMDARs along neuron maturation

A critical step in synaptic maturation is the insertion of NMDARs in the synapse. Previous reports in primary mice cultures indicate that after 7 weeks *in vitro*, around 90% of NMDARs localize at extrasynaptic membranes, while this number reduces to 50% or less after two weeks [128, 138, 156, 311-313]. As AD is an aging-related neurodegenerative disease, having mature synapsis in iNeurons is a crucial factor to achieve a human-relevant model. However, this process has not been extensively studied in iNeurons [314].

We analyzed the proportion of NMDARs at synapses by immunostaining. We used antibodies against the mandatory subunit GluN1 and against the presynaptic protein synaptophysin, a classical synaptic marker. The colocalization of GluN1 with synaptophysin is a widespread method for measuring SynNMDARs [315-317]. Hence, those NMDARs that do not colocalize with synaptophysin are defined as ExsynNMDARs. In **Figure 19A** and **B**, the colocalization channel is shown in white (SynNMDARs). Quantification reveals that the number of SynNMDARs increases by 9-fold from day 30 to day 60 in both NMM and BPM (**Figure 19C**). This dramatic increase in SynNMDARs on day 60 demonstrates that NMDARs are highly localized at the synapsis.



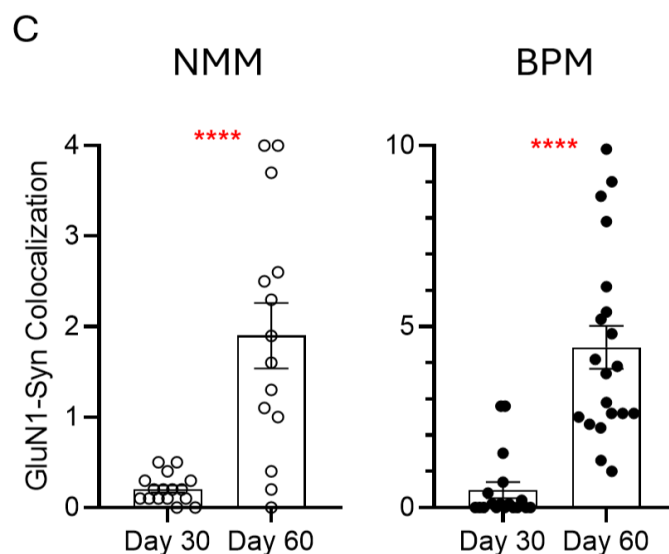
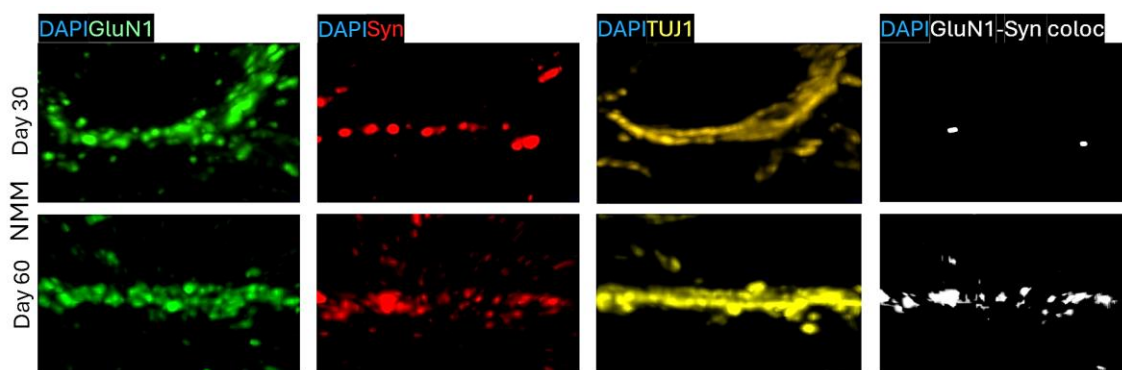


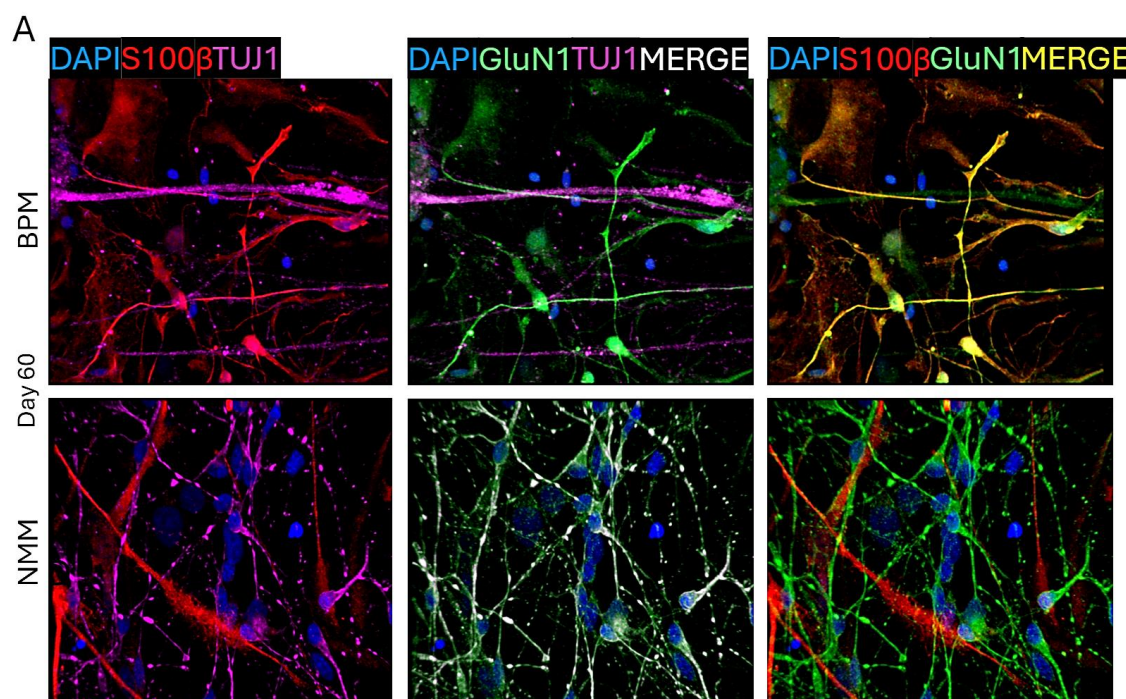
Figure 19. Increment of synaptic NMDARs along maturation. A) 63x images of DAPI (blue), GluN1 (green), Synaptophysin (Syn, red), and TUJ1 (yellow) at days 30 and 60 in BPM and NMM conditions. GluN1-Syn colocalization channel was built (white). **B)** 63x zoom images of DAPI (blue), GluN1 (green), Synaptophysin (Syn, red), and TUJ1 (yellow), GluN1-Syn colocalization (white) at days 30 and 60 in BPM and NMM conditions. GluN1-Syn colocalization channel was built (white). **C)** GluN1 and synaptophysin colocalization was quantified using thresholded Mander's coefficient, as a measurement of SynNMDARs.

4.4.4 Astrocytes also express NMDARs in BPM and NMM

Astrocytes in the mouse brain can express NMDARs [318]; these respond to NMDA [148] and memantine [318, 319], and they could play a role in AD [320]. To test whether the astrocytes present in NMM and BPM express NMDARs, we performed immunostainings using antibodies against GluN1 and the astrocytic marker S100 β . In cultures differentiated with BPM, almost all cells S100 β + were also GluN1+ (**Figure 20A**). In NMM, only a few S100 β + cells were stained for GluN1. This indicates that astrocytes in BPM cultures express GluN1, while astrocytes in NMM cultures express discrete and more diffuse GluN1. Accordingly, we cannot ensure that the

increase in GluN2A expression noticed in cells differentiated with BPM is exclusively due to neurons and not astrocytes. Further characterization with GluN2A/GluN2B colocalization with S100 β is needed.

At this point, we decided to develop a pure astrocytic culture (iAstrocytes) from the same NPCs and test whether these astrocytes show high levels of GluN1 staining. Following the manufacturer's instructions, NPCs were differentiated into astrocytes using STEMdiff™ Astrocyte Differentiation Kit (Stemcell Technologies) and matured using STEMdiff™ Astrocyte Maturation Kit (Stemcell Technologies). The presence of astrocytes was checked by the expression of astrocytic markers GFAP and S100 β (**Figure 20B**). The culture also contained some sparse TUJ1+ cells (**Figure 20B**) that indicated the presence of neurons. GluN1 staining was found in iAstrocytes, as in the astrocytes from BPM cultures, although GluN1 expression was stronger in those sparse neurons than in iAstrocytes, as expected (**Figure 20C**).



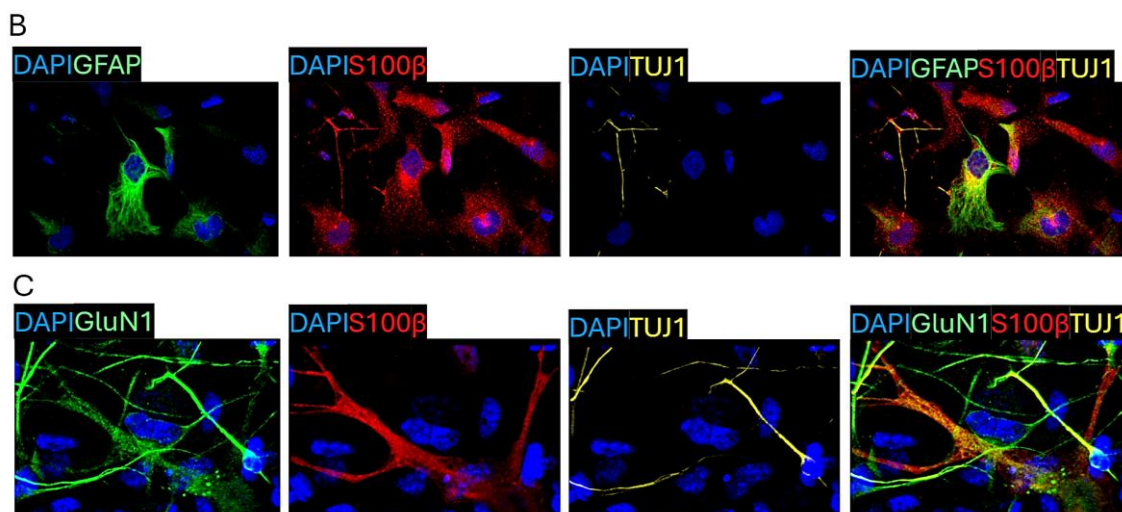


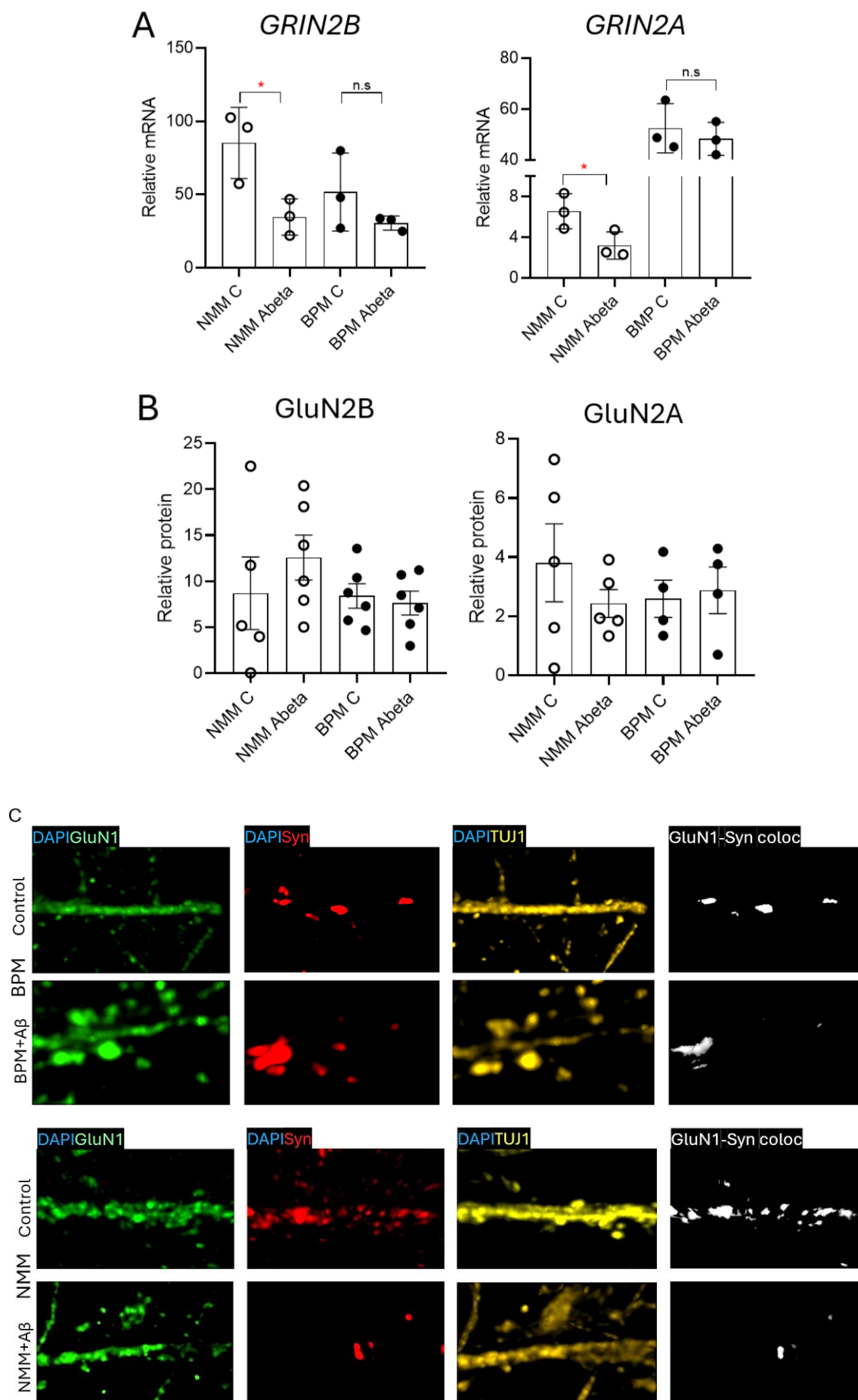
Figure 20. NMDARs are expressed by astrocytes from BPM and by iAstrocytes. A) 63× images of DAPI (blue), S100β (red), GluN1 (green) and TUJ1 (magenta) at day 60 in BPM and NMM conditions. **B)** 63× image of DAPI (blue), GFAP (green), S100β (red) and TUJ1 (yellow) of iAstrocytes. **C)** 63× image of DAPI (blue), GluN1 (green), S100β (red) and TUJ1 (yellow) of iAstrocytes.

4.4.5 Effect of Aβ on GluN2B and GluN2A in iNeurons

A classical approach for studying protein changes in AD-cellular models is to treat the culture with Aβ₄₂ (the more amyloidogenic form of Aβ). Since our data may suggest that the GluN2B-GluN2A switch could occur at day 60 but not earlier, we chose that time point for the Aβ₄₂ treatment. We treated our cultures with 2 μM of Aβ₄₂ for 24 hours.

Interestingly, we observed that Aβ₄₂ induced a decrease in *GRIN2B* and *GRIN2A* mRNA levels in cultures differentiated with NMM ($p = 0.032$; $p = 0.050$, respectively) but not with BPM (**Figure 21A**). However, we did not observe any change at the protein level by western blot (**Figure 21B**).

When we performed GluN1-synaptophysin colocalization analysis to test whether this Aβ₄₂ treatment could modify the proportion of SynNMDARs, we observed that SynNMDARs decreased a $55 \pm 26\%$ ($p = 0.037$) with NMM but did not with BPM ($p = 0.602$) (**Figure 21C, D**).



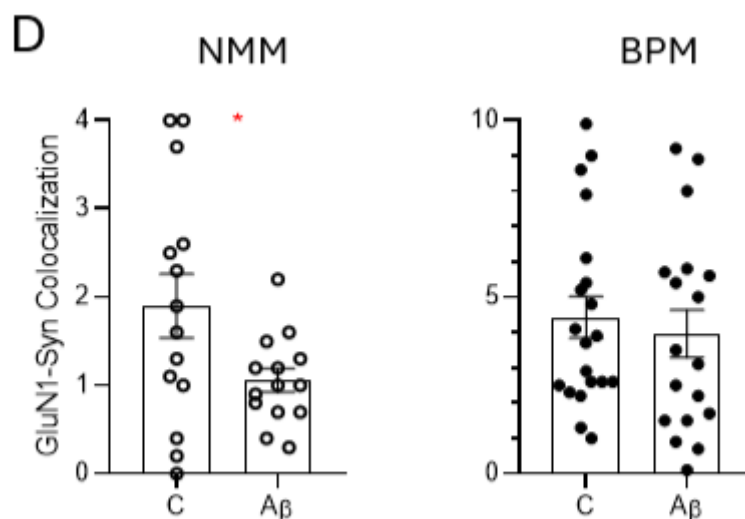


Figure 21. iNeurons differentiated with BPM and NMM and treated with Aβ42. A) *GRIN2B* and *GRIN2A* mRNA levels measured by qPCR of BPM and NMM iNeurons treated with Aβ42 2 μM for 24 hours. **B)** GluN2B and GluN2A protein levels measured by western blot of BPM and NMM iNeurons treated with Aβ42 2 μM for 24 hours. **C)** 63× zoom images of GluN1 (green), Synaptophysin (Syn) (red), TUJ1 (yellow) and GluN1-Syn colocalization (white) at days 30 and 60 in BPM and NMM. **D)** GluN1-Syn colocalization was quantified using thresholded Mander's coefficient, as a measurement of SynNMDARs.

4.5 The synaptic and extrasynaptic proteome of the AD brain

In the final part of this thesis, we aim to gain a broader perspective of the disease. To do so, we intend to uncover the synaptic and extrasynaptic proteome of the AD brain.

4.5.1 Experimental design

We performed our fractionation protocol to obtain SynF and ExsynF from 9 controls (control, male $n = 6$, female $n = 3$; age 58.6 ± 12.6 years) and 9 AD individuals (Braak VI, male $n = 4$, female $n = 5$; age 78.1 ± 6.7 years). These fractions were pooled to reduce variability among individual samples [256, 257]. Each pool contained three fractions, and a total of three pools were prepared for each SynF and ExsynF from control and AD samples (**Figure 22**). All pools were analyzed using label-free shotgun proteomics LC-MS/MS.

Pool	Samples
1	SynF C1
	SynF C2
	SynF C3
2	SynF C4
	SynF C5
	SynF C6
3	SynF C7
	SynF C8
	SynF C9
4	SynF AD10
	SynF AD11
	SynF AD12
5	SynF AD13
	SynF AD14
	SynF AD15
6	SynF AD16
	SynF AD17
	SynF AD18
7	ExsynF C1
	ExsynF C2
	ExsynF C3
8	ExsynF C4
	ExsynF C5

	ExsynF C6
9	ExsynF C7
	ExsynF C8
	ExsynF C9
10	ExsynF AD10
	ExsynF AD11
	ExsynF AD12
11	ExsynF AD13
	ExsynF AD14
	ExsynF AD15
12	ExsynF AD16
	ExsynF AD17
	ExsynF AD18

Figure 22. Experimental design of the proteomic study. A) Experimental design. SynFs and ExsynFs from AD and Control (C) were grouped into categories SynF C, SynF AD, ExsynF C, and ExsynF AD. Each one contained 3 pools, each consisting of 40 µg of three different samples (a total of 120 µg per pool).

A total of 1983 proteins were detected in control SynF, 1980 in the AD ExsynF, 1760 in control ExsynF, and 1697 in the AD ExsynF, after applying a false discovery rate (FDR) of 1%.

Principal Component Analysis (PCA) was applied to all the samples to ensure good reproducibility among samples.

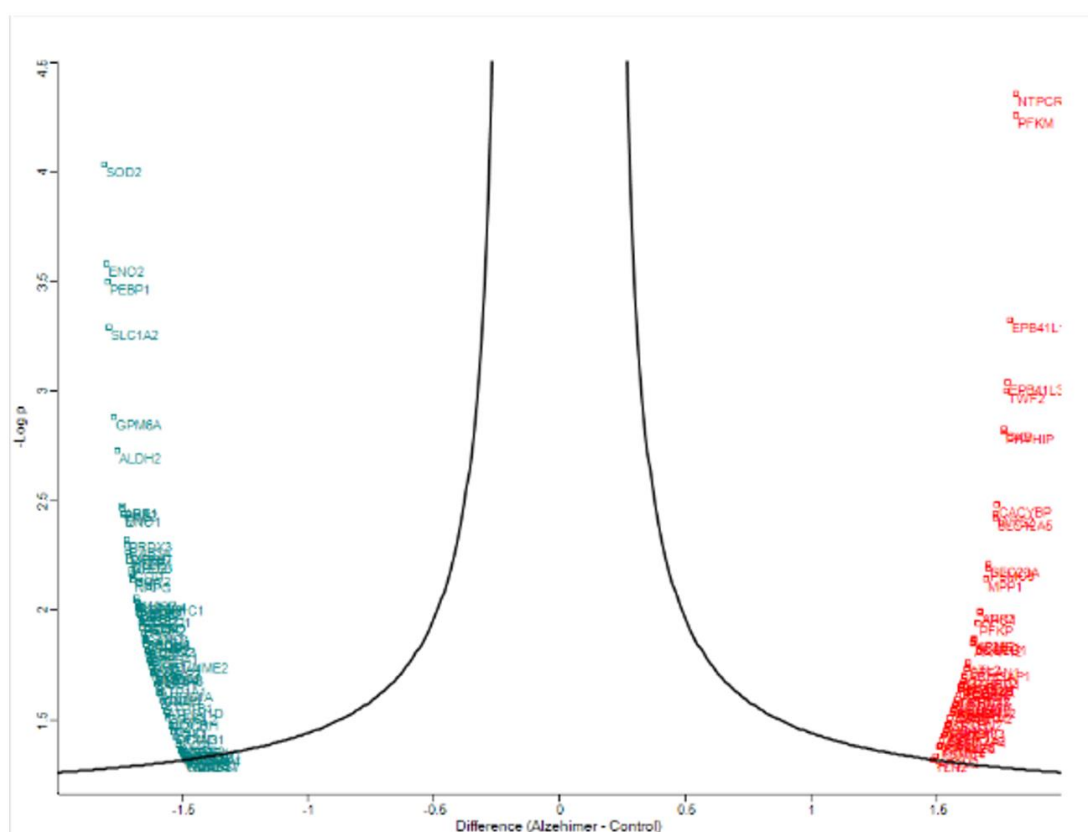
4.5.2 Proteomic analysis: differentially expressed proteins in SynF and ExsynF

The analysis of the differential expression of proteins, which is the outcome of our LC-MS/MS analysis, is complex due to the comparison of multiple samples. This analysis has used a general human-proteomic database from UniProt. In addition, data was analyzed using a brain-specific proteomic database (the keyword “brain” was used to filter the human proteome from UniProt). Protein expression is considered as “under” or “over” expressed regarding the expression in control samples.

As a first approach, a Volcano plot and Heatmap are shown for every experimental group. The interpretation of these graphs is explained in the Methods section.

We first analyze the differentially expressed proteins (DEP) in the AD SynF (**Figure 23**). The volcano plot showed that the most underexpressed protein in the AD SynF was Superoxide dismutase, while the two most overexpressed were Cancer-related nucleoside-triphosphatase and ATP-dependent 6-phosphofructokinase. The heatmap was created through a hierarchical clustering algorithm that confirmed the existence of two clusters of DEP: under and overexpressed, and the stratification of samples, suggesting which two samples are closer to each other.

A

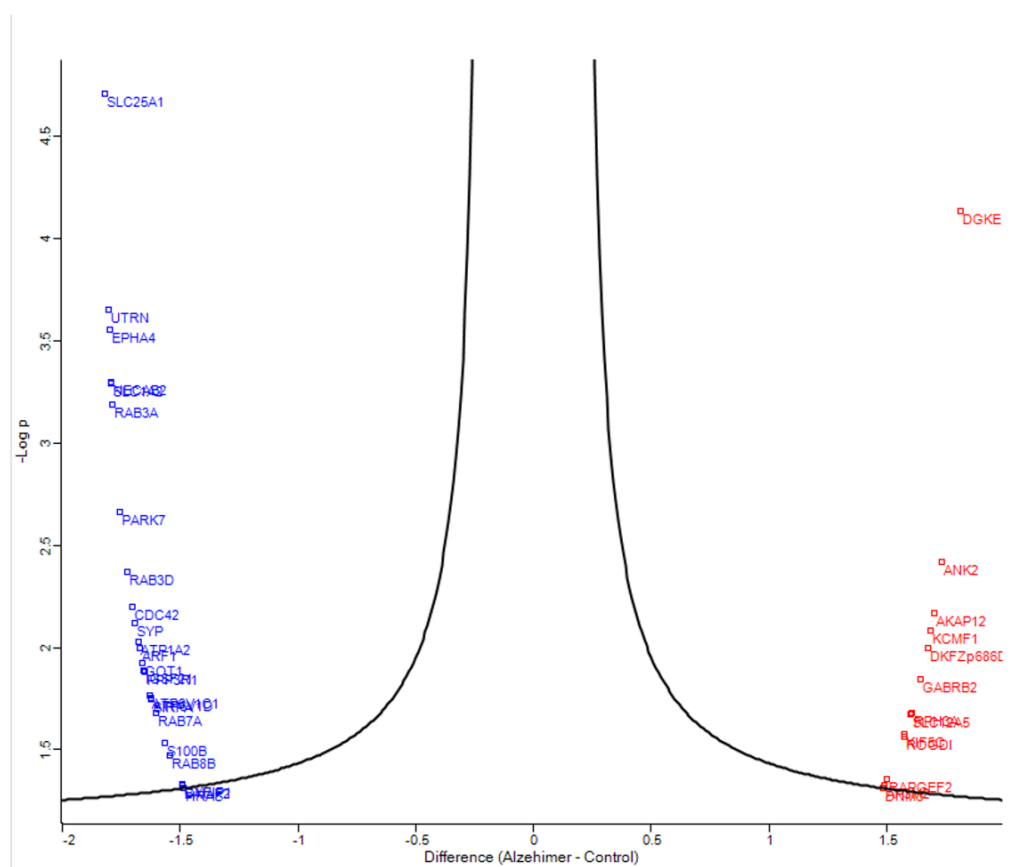


The volcano plot shows the most DEP in the AD SynF. The most underexpressed protein was SOD2, while the two most overexpressed were NTPCR and PFKM. **B)** The heatmap shows two differentiated clusters: green means overexpression, and red underexpression.

87

Hierarchical clustering grouped similar proteins closer to each other in the Y-axis. Two well-differentiated clusters can be seen in the overexpressed proteins in AD. However, in the underexpressed proteins, that clustering was not clear.

A



B

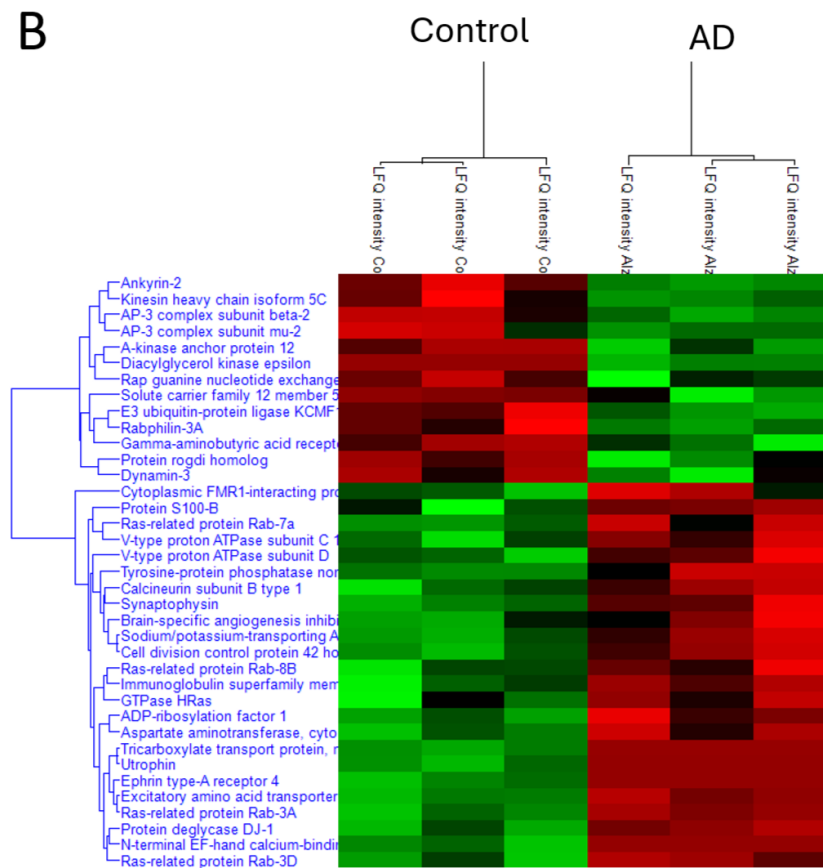
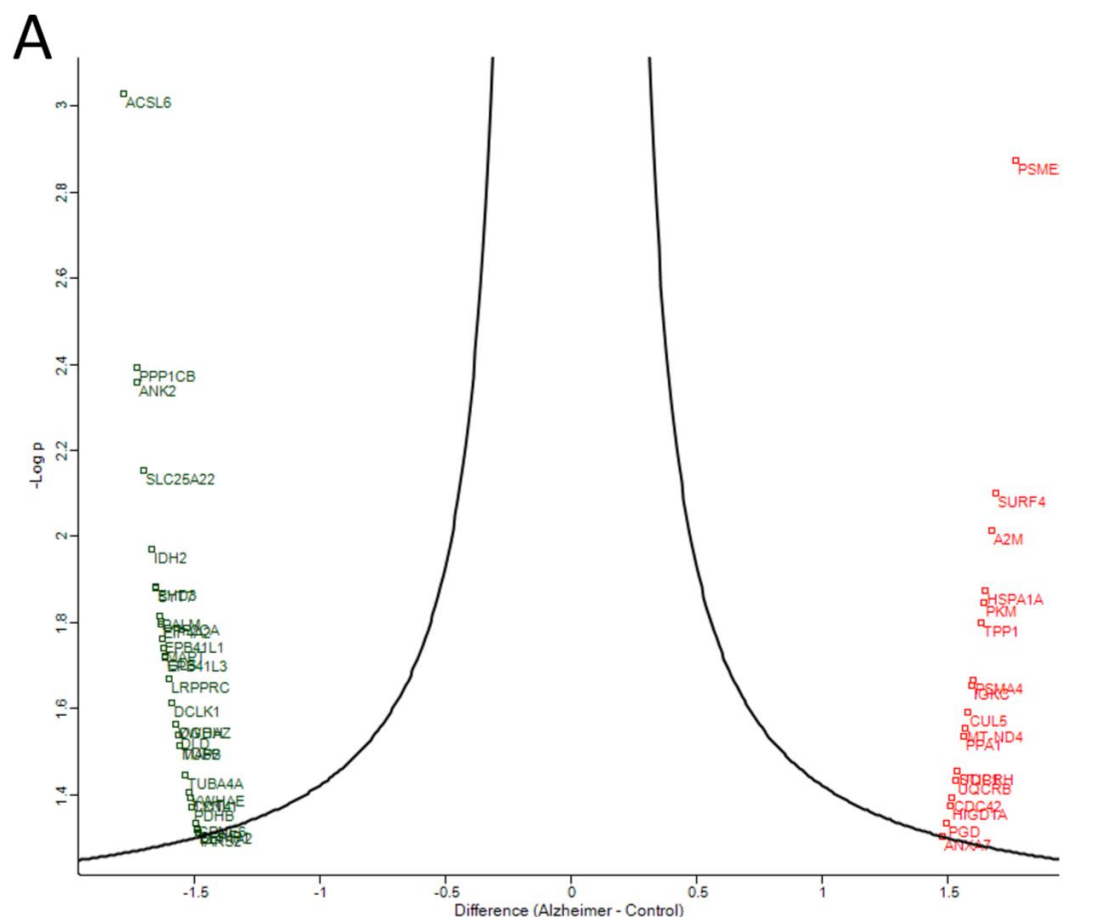


Figure 24. PCA, volcano plot and heatmap of the AD SynF (brain-specific database). A) The volcano blot shows the most DEP in the AD SynF. The most underexpressed protein was SLC25A1, while the most overexpressed was DGKE. **B)** The heatmap shows two differentiated clusters, green means overexpression and red underexpression.

We continue with the same plots applied to the AD ExsynF using the general human proteome database (**Figure 25**). Volcano plot showed that the most underexpressed protein in the AD ExsynF was Long-chain-fatty-acid--CoA ligase 6, while the most overexpressed was Proteasome activator complex subunit 2. The heatmap showed two differentiated clusters of under and overexpressed proteins in control and AD samples. Hierarchical clustering grouped similar proteins closer to each other in the Y-axis. Three well-differentiated clusters can be seen in the overexpressed proteins in AD. However, in the underexpressed proteins, that clustering was not clear.



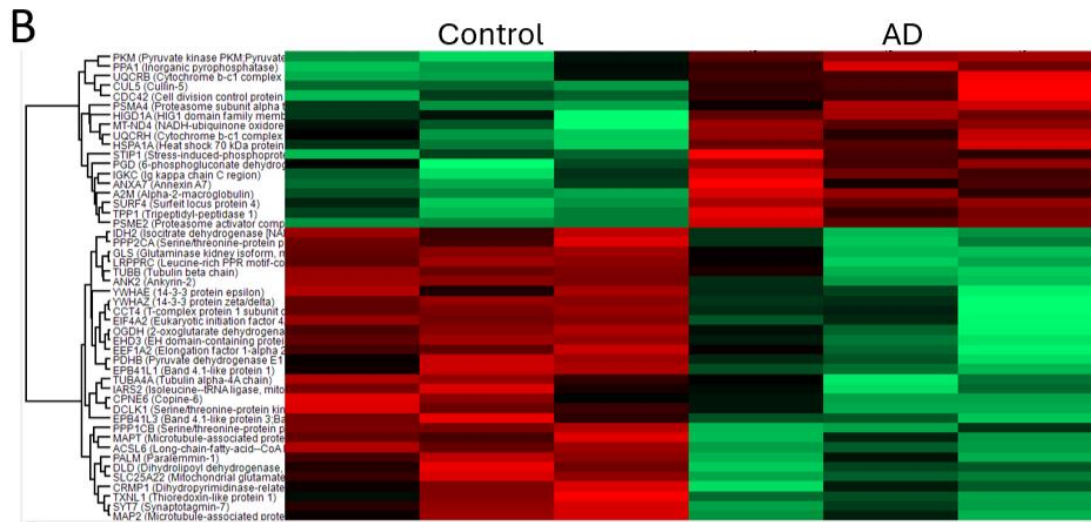


Figure 25. PCA, volcano plot and heatmap of the AD ExsynF (human proteome database). A)

The volcano blot shows the most DEP in the AD SynF. The most underexpressed protein was ACSL6, while the most overexpressed was PSME. **B)** The heatmap shows two differentiated clusters, green means overexpression and red underexpression.

Finally, we compared our ExsynF datasets with the brain-specific database (**Figure 26**). Volcano plot showed that the most underexpressed protein in the AD ExsynF was Synaptotagmin-7, while the most overexpressed was Sodium/potassium/calcium exchanger 2. The heatmap showed two differentiated clusters of under and overexpressed proteins in control and AD samples. Hierarchical clustering grouped similar proteins closer to each other in the Y-axis. Two well-differentiated clusters can be seen in the overexpressed proteins in AD. In the underexpressed proteins, there were three clusters.

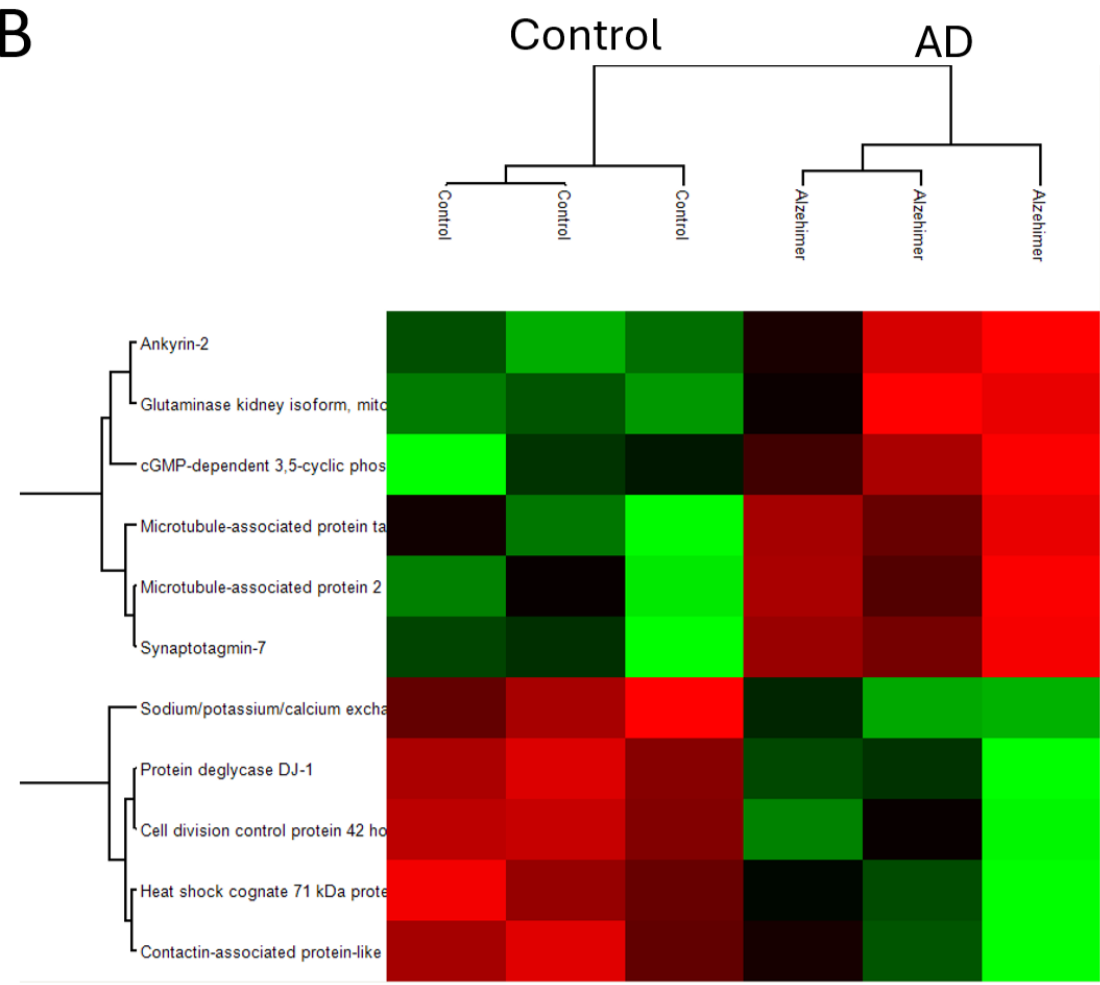
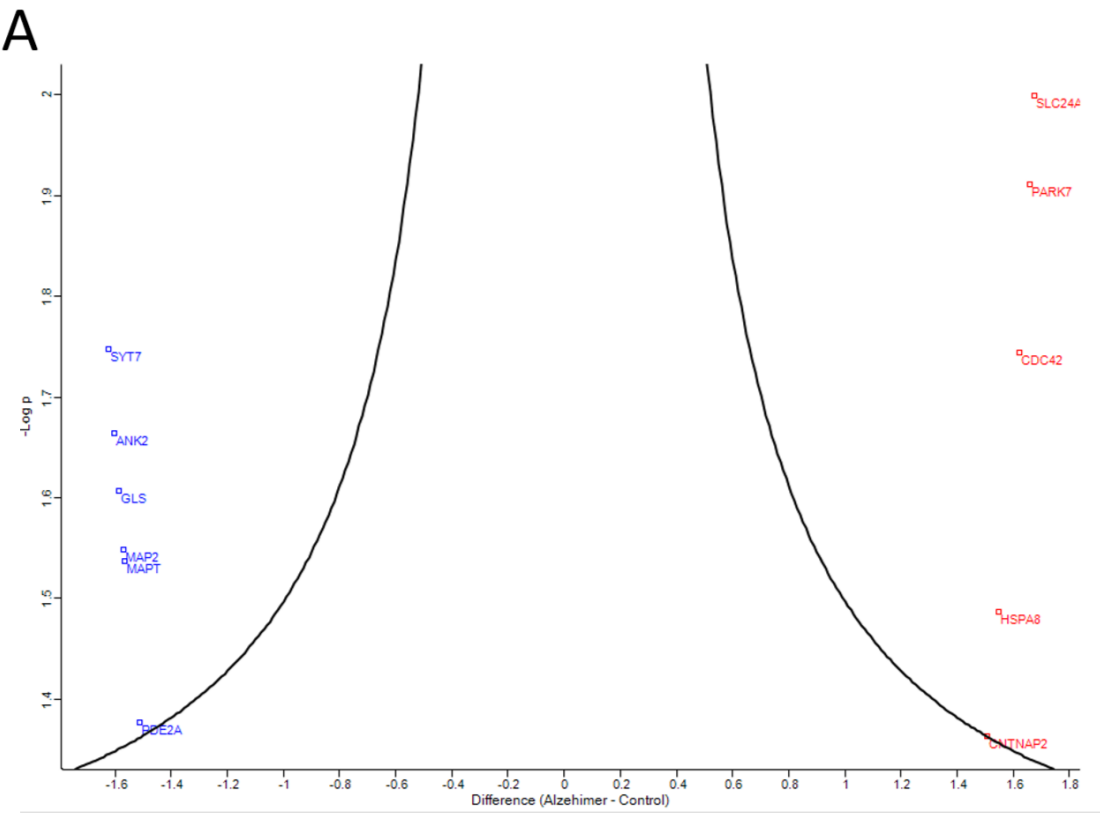


Figure 26. PCA, volcano plot, and heatmap of the AD ExsynF (brain-specific database). A) The volcano blot shows the most DEP in the AD SynF. The most underexpressed protein was SYT7, while the most overexpressed was SLC24A2. **B)** The heatmap shows two differentiated clusters, green means overexpression and red underexpression.

Next, the complete list of DEP in the AD SynF and ExsynF is provided. To make the reading easier, we employed ↓SynF for underexpressed proteins in SynF, ↑SynF for overexpressed proteins in SynF, ↓ExsynF for underexpressed proteins in ExsynF, and ↑ExsynF for overexpressed proteins in ExsynF

List of DEP using the *Homo sapiens* proteomic database

↓SynF	↑SynF	↓ExsynF	↑ExsynF
SOD2	TLN2	MAP2	PSME2
ENO2	AP3M2	EPB41L3	HSPA1A
PEBP1	PSMC4	EPB41L1	TPP1
SLC1A2	OGDH	EEF1A2	HIGD1A
GPM6A	PIP4K2A	ACSL6	SURF4
ALDH2	RANBP6	ANK2	A2M
ARF1	ARFGAP1	MAPT	IGKC
PHB2	GLS	LRPPRC	MT-ND4
MVP	CSNK2A2	PPP1CB	UQCRH
ENO1	LONP1	PPP2CA	PKM
PRDX3	DNM3	CRMP1	UQCRB
RAB3A	C21orf33	DCLK1	ANXA7
PARK7	AUH	TXNL1	PSMA4
MDH1	DCTN1	SYT7	STIP1
HSPE1	SPTBN2	PALM	PGD
ATP5B	AARS	GLS	CDC42
GPD2	RPS6KA2	CPNE6	PPA1
GDI1	CRYZ	TUBB	CUL5

GOT2	OGDHL	DLD	
PHB	CCDC132	PDHB	
NAPG	RPH3A	IDH2	
S100B	TXNRD2	CCT4	
SLC4A4	DECR1	YWHAЕ	
ATP6V1C1	DYNC111	YWHAZ	
CDC42	PTPN23	TUBA4A	
ARPC2	DLST	OGDH	
ECHS1	LRRC47	EIF4A2	
LDHA	ROGDI	SLC25A22	
ABAT	PCBP1	IARS2	
IGSF21	PIN1	EHD3	
ATP5C1	TUBA4A		
ATP5O	SEC22B		
GLUL	SPTBN1		
GOT1	MTHFD1		
PSAP	GABRB2		
PRDX2	ARHGAP1		
VSNL1	SPTAN1		
CAND1	ATL2		
PRDX6	AKAP12		
GLUD1	SUCLG1		
ATP5H	KCMF1		
LDHB	AP3B2		
NDRG2	PFKP		
ATP1A3	XPO1		
CA4	ANK2		
ATP5A1	MPP1		
MIF	PSMC5		
OPA1	SEC23A		
NME1	SLC12A5		
SLC1A4	IARS2		
SYP	CACYBP		

VCP	PHYHIP		
GNB1	CKB		
MCCC2	TWF2		
AK5	EPB41L3		
ARPC4	EPB41L1		
S100A1	PFKM		
SLC1A3	NTPCR		
LARP1			
ATP1A1			
ARPC1A			
ICAM5			
GNAI1			
ATP1B1			
ATP6V1D			
DPYSL2			
SIRPA			
UQCRH			
THY1			
PGK1			
OCIAD1			
SFXN3			
SV2A			
BAIAP2			
ARF4			
PPP3R1			
SKP1			
CORO1C			
LRRC57			
COX5B			
ALDH5A1			
GDI2			
CADM3			
DDAH1			

COX6B1			
NDUFS7			
HRAS			
RAB2A			

Table 5. List of differentially expressed proteins using a general database of the human proteome. The complete proteome of *Homo sapiens* in UniProt dataset was considered. The four columns correspond to the four experimental groups: 87 proteins underexpressed in the AD SynF (\downarrow SynF), 58 overexpressed in the SynF (\uparrow SynF), 30 underexpressed in the ExsynF (\downarrow ExsynF), and 18 overexpressed in the ExsynF (\uparrow ExsynF).

List of DEP using the brain *Homo sapiens* proteomic database

\downarrow SynF	\uparrow SynF	\downarrow ExsynF	\uparrow ExsynF
RAB3D	AP3M2	PDE2A	CNTNAP2
RAB3A	DGKE	SYT7	CDC42
ATP6V1C1	SLC12A5	GLS	HSPA8
S100B	RPH3A	MAPT	PARK7
RAB7A	KIF5C	MAP2	SLC24A2
CDC42	GABRB2	ANK2	
HRAS	ANK2		
SYP	AKAP12		
GOT1	DKFZp686D17136		
SLC1A2	ROGDI		
UTRN	KCMF1		
ATP1A2	DNM3		
SLC25A1	RAPGEF2		
EPHA4			
PPP3R1			
SIRPA			
ARF1			
CYFIP1			
NECAB2			

RAB8B			
IGSF21			
PARK7			
BAIAP2			
ATP6V1D			

Table 6. List of differentially expressed proteins using a brain-specific database of the human proteome. The *Homo sapiens* proteome was filtered in UniProt using the word ‘brain’. The proteins that are only present in this database, but not in the the general human proteome (**Table 5**) are in bold. The four columns correspond to the four experimental groups: 25 proteins underexpressed in the AD SynF (\downarrow SynF), 13 overexpressed in the SynF (\uparrow SynF), 6 underexpressed in the ExsynF (\downarrow ExsynF), and 5 overexpressed in the ExsynF (\uparrow ExsynF).

In the following sections, the enrichment analysis is developed, and its significance and interpretation are explained in the Methods section.

4.5.3 Proteomic analysis: Underexpressed proteins in SynF

A total of 87 proteins were underexpressed in the SynF of the AD brain cortex when the human proteome database was used. The list is available in **Table 5** in section 4.5.2. According to p-value and relative fold change, the most underexpressed proteins in the AD SynF were Superoxide dismutase, Gamma-enolase, Phosphatidylethanolamine-binding protein 1, Excitatory amino acid transporter 2, Neuronal membrane glycoprotein M6-a and Aldehyde dehydrogenase.

4.5.3.1 Enrichment analysis

The enrichment analysis revealed 20 functional clusters. Each cluster is represented in order of statistical significance in Enrichment Ontology Cluster plot (**Figure 27A**). Each cluster was composed of many GO terms. Most GO terms in each cluster were related among them, although some novel GO terms appeared in every cluster. For example, the first cluster for underexpressed proteins in SynF was “purine ribonucleoside triphosphate metabolic process” with a LogP value of -17.96. This first GO term with the highest LogP value is the one represented in the Enrichment Ontology Cluster plot, and many very similar GO terms appeared too in the complete list of the cluster. However, in the same cluster, it also appeared

GO terms such as “Huntington disease”, “Mitochondrial biogenesis” and “Prion disease” with LogP values of -9.46, -9.06 and -7.69, respectively.

An analysis consisting in identifying potentially relevant GO terms for AD pathogenesis but not represented in the Enrichment Ontology Cluster plot reveals that other processes affected are “oxidative phosphorylation”, “regulation of membrane potential”, “amino acid and glucose metabolism”, “glutamatergic synaptic physiology”, “endocytosis”, “VEGFA-VEGFR2 pathway”, “iron uptake and transport”, “insulin secretion”, “signaling by insulin receptor”, “thyroid hormone signaling”, “regulation of autophagy”, “signaling by receptor tyrosine kinases”, “membrane trafficking”, “COPI-dependent Golgi-to-ER retrograde traffic”, and “asparagine N-linked glycosylation”.

4.5.3.3 Proteomic analysis: Underexpressed proteins in SynF (using brain-specific database)

When we relaunched the analysis using the brain-specific database, a total of 25 proteins were underexpressed in the SynF of the AD brain cortex (**Table 6** in section 4.5.2). According to p-value and relative fold change, the most underexpressed proteins in the SynF were Tricarboxylate transport protein, Utrophin, Ephrin type-A receptor 4, N-terminal EF-hand calcium-binding protein 2, Excitatory amino acid transporter 2, Ras-related protein Rab-3A and Protein delicate DJ-1. Of these 25 underexpressed proteins, 8 (33%) were not present in the first list compared against the general proteomic database (marked in bold in **Table 6** in section 4.5.2).

Since network analysis was applied to GO terms and PPI analysis did not provide additional relevant information, we excluded them from the brain-specific database analysis.

4.5.3.3.1 Enrichment analysis (using brain-specific database)

Enrichment analysis revealed 18 functional clusters. Each cluster is represented in order of statistical significance in Enrichment Ontology Cluster plot (**Figure 27B**).

An analysis consisting in identifying potentially relevant GO terms for AD pathogenesis but not represented in the Enrichment Ontology Cluster plot reveals that other processes affected are “release of presynaptic vesicles”, “transport of vesicles”, “synaptic plasticity”, “remodelation of cytoskeleton”, “synaptic structure”, “uptake of glutamate from synaptic cleft”, “exchange of ions” and “calcium binding”.

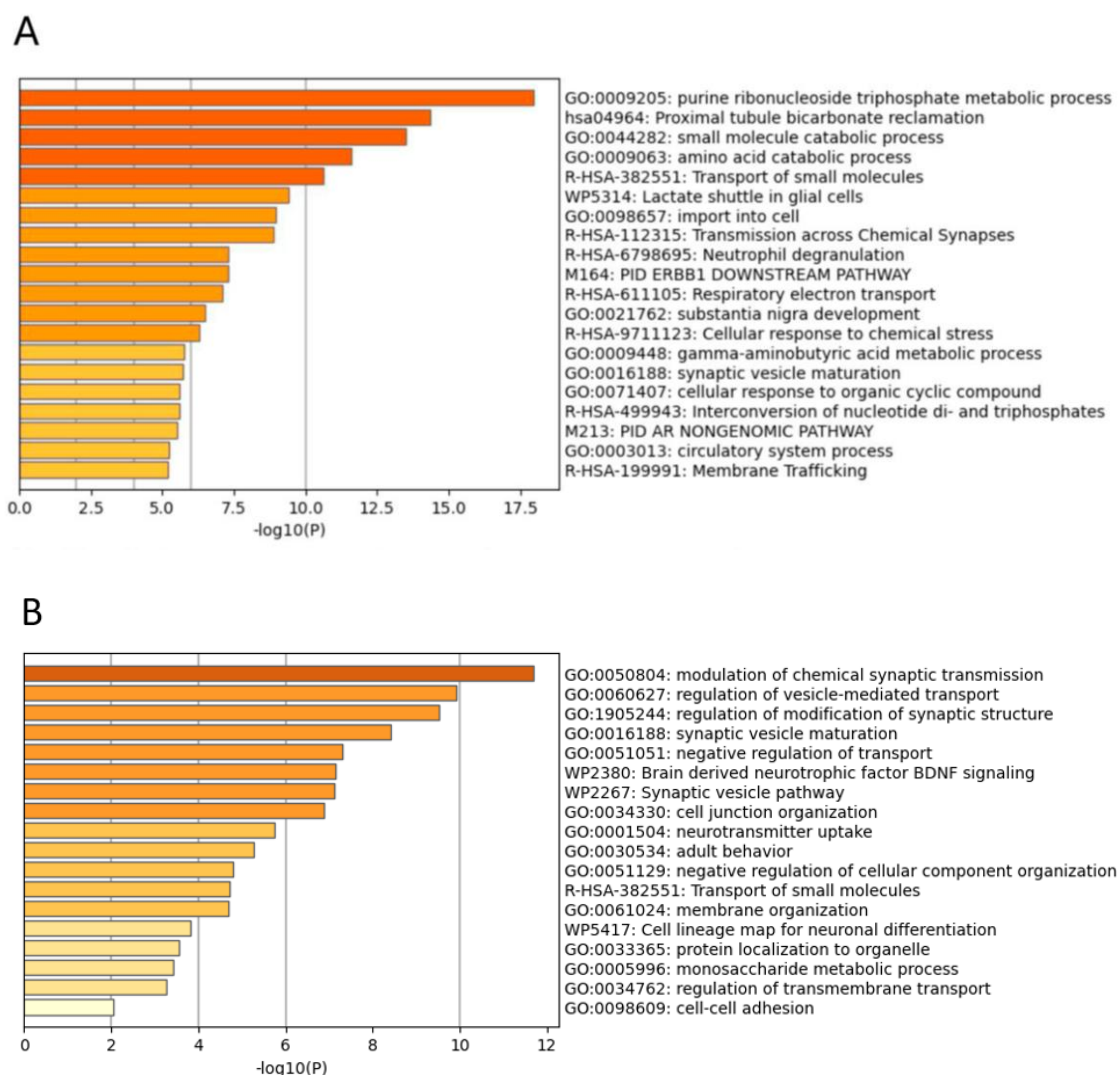


Figure 27. Underexpressed proteins in the AD SynF. A) Enrichment Ontology Cluster plot using human proteome database. **B)** Enrichment Ontology Cluster using brain-specific database.

4.5.4 Proteomic analysis: Overexpressed proteins in SynF

A total of 58 proteins were overexpressed in the SynF of the AD brain cortex when the human proteome database was used. The list is available in **Table 5** in section 4.5.2. According to p-value and relative fold change, the most overexpressed proteins were Cancer-related nucleoside-triphosphatase, ATP-dependent 6-phosphofructokinase, muscle type, Band 4.1-like protein 1, Band 4.1-like protein 3, Twinfilin-2, Creatine kinase B-type, Phytanoyl-CoA hydroxylase-interacting protein, Calcyclin-binding protein, Isoleucine--tRNA ligase and Solute carrier family 12 member 5.

4.5.4.1 Enrichment analysis

The enrichment analysis revealed 17 functional clusters. Each cluster is represented in order of statistical significance in Enrichment Ontology Cluster plot (**Figure 28A**).

An analysis consisting in identifying potentially relevant GO terms for AD pathogenesis but not represented in the Enrichment Ontology Cluster plot reveals that other processes affected are “membrane trafficking” (especially “ER to Golgi anterograde transport”), “cell adhesion” (especially through “L1CAM interactions”), “metabolism of glucose”, “transport of synaptic vesicles”, “synaptic organization”, “Signaling by Rho GTPases”, “MAPK family signaling cascades”, “cell cycle transitions”, “mRNA stability”, “endocytosis”, “phosphorylation” and “mitochondrial protein degradation”.

4.5.4.2 Proteomic analysis: Overexpressed proteins in SynF (using brain-specific database)

When we relaunched the analysis using the brain-specific database, a total of 13 proteins were underexpressed in the SynF of the AD brain cortex (**Table 6** in section 4.5.2). According to p-value and relative fold change, the most underexpressed proteins in the SynF were Diacylglycerol kinase epsilon, Ankyrin-2, A-kinase anchor protein 12, E3 ubiquitin-protein ligase KCMF1, AP-3 complex subunit beta-2 and Gamma-aminobutyric acid receptor subunit beta-2.

Of these 13 underexpressed proteins, 3 (23%) (Diacylglycerol kinase epsilon, Kinesin heavy chain isoform 5C and Rap guanine nucleotide exchange factor 2) were not present in the first list compared against the general proteomic database (marked in bold in **Table 6** in section 4.5.2).

4.5.4.2.1 Enrichment analysis (using brain-specific database)

Enrichment analysis revealed 5 functional clusters. Each cluster is represented in order of statistical significance in Enrichment Ontology Cluster plot (**Figure 28B**).

An analysis consisting in identifying potentially relevant GO terms for AD pathogenesis but not represented in the Enrichment Ontology Cluster plot reveals that other processes affected are “synaptic vesicle transport”, “anterograde axonal transport”, “synaptic signaling”, “cell junction assembly”, “modulation of chemical synaptic transmission” and “neuron projection development”.

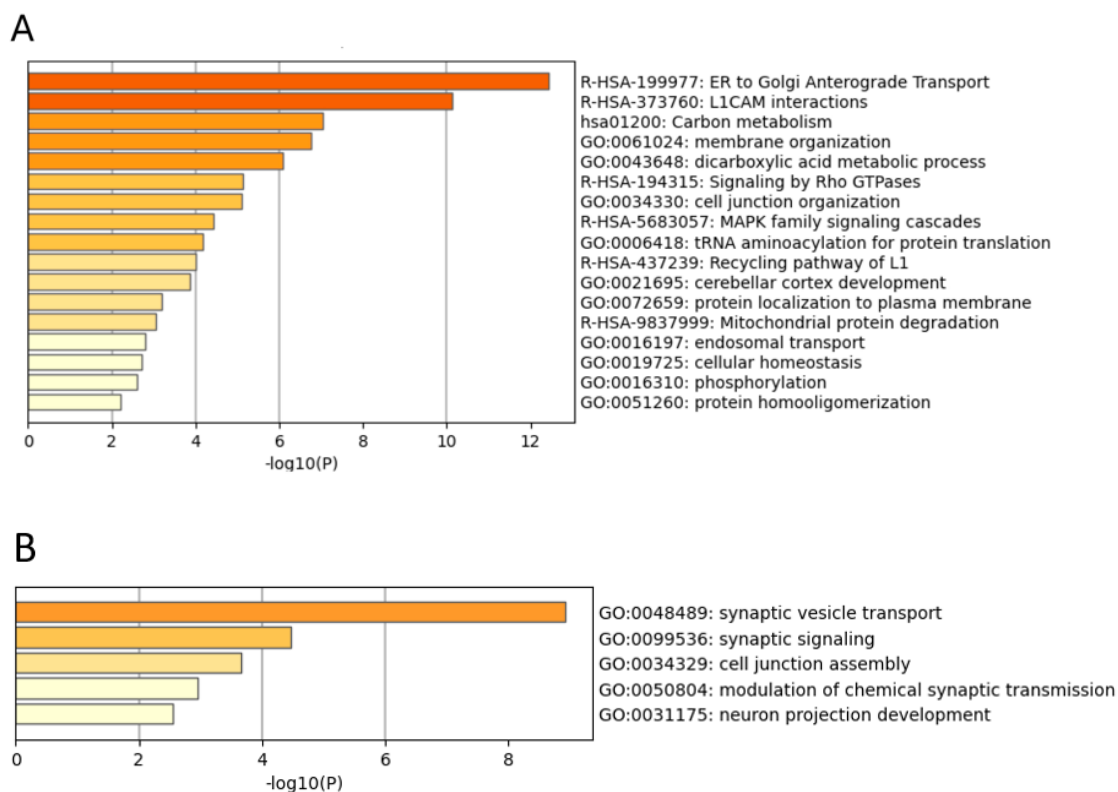


Figure 28. Overexpressed proteins in the AD SynF. A) Enrichment Ontology Cluster plot using human proteome database. **B)** Enrichment Ontology Cluster using brain-specific database.

4.5.5 Proteomic analysis: Underexpressed proteins in ExsynF

A total of 30 proteins were underexpressed in the ExsynF of the AD brain cortex when the human proteome database was used. The list is available in **Table 5**. According to p-value and relative fold change, the most underexpressed proteins were Long-chain-fatty-acid--oA ligase 6, Serine/threonine-protein phosphatase PP1-beta catalytic subunit, Ankyrin-2, Mitochondrial glutamate carrier 1 and Isocitrate dehydrogenase [NADP].

4.5.5.1 Enrichment analysis

Enrichment analysis revealed 16 functional clusters. Each cluster is represented in order of statistical significance in Enrichment Ontology Cluster plot (**Figure 29A**).

An analysis consisting in identifying potentially relevant GO terms for AD pathogenesis but not represented in the Enrichment Ontology Cluster plot reveals that other processes affected are “Mitotic G2-G2/M phases”, “Cell Cycle”, “Long-term potentiation”, “Aerobic respiration and respiratory electron transport”, “MAPK cascade”, “Transmission across Chemical Synapses”, “Protein-protein interactions at synapses”, “protein localization to plasma membrane”, “Translation”, “regulation of intracellular transport”.

4.5.5.2 Proteomic analysis: Underexpressed proteins in ExsynF (using brain-specific database)

A total of 6 proteins were underexpressed in the ExsynF of the AD brain cortex. According to p-value and relative fold change, the proteins are displayed in order: Synaptotagmin-7, Ankyrin-2, Glutaminase kidney isoform, Microtubule-associated protein 2, Microtubule-associated protein tau and cGMP-dependent 3,5-cyclic phosphodiesterase.

Of these 6 underexpressed proteins, 1 (cGMP-dependent 3,5-cyclic phosphodiesterase) was not present in the first list compared against the general proteomic database (marked in bold in **Table 6** in section 4.5.2).

4.5.5.2.1 Enrichment analysis (using brain-specific database)

Enrichment analysis revealed a single cluster: Neuronal System (**Figure 29B**).

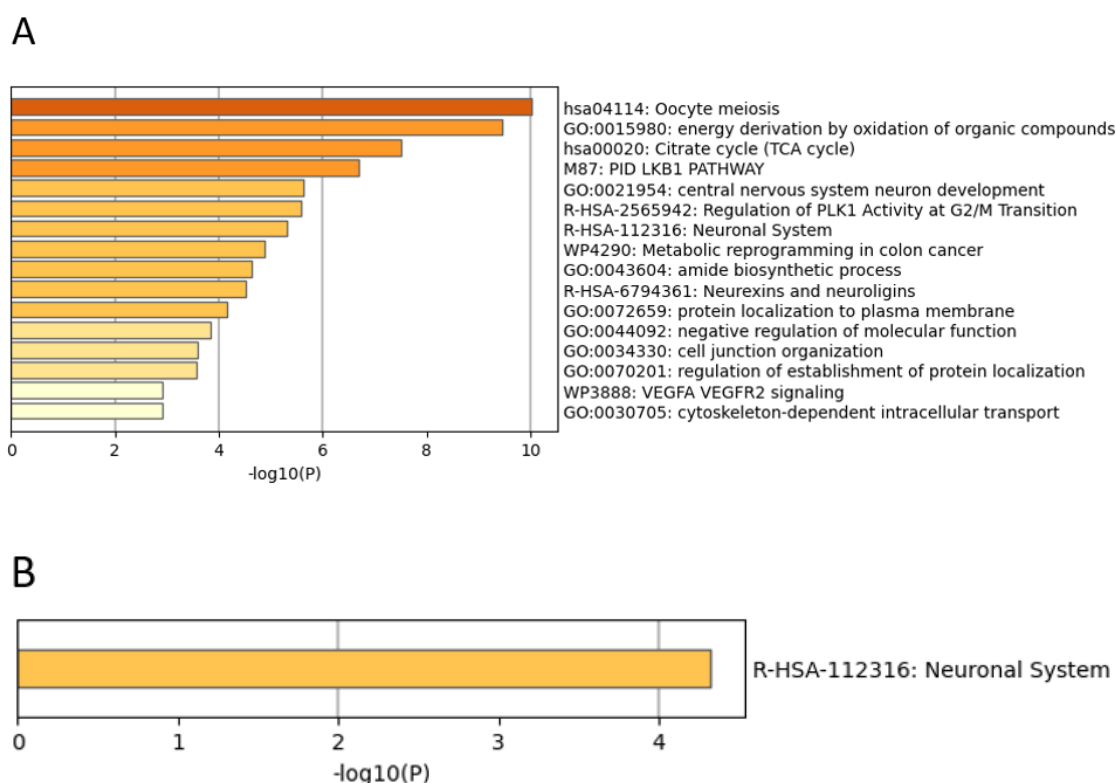


Figure 29. Underexpressed proteins in the AD ExsynF. A) *Enrichment Ontology Cluster using human proteome database. B)* *Enrichment Ontology Cluster using a brain-specific database*

4.5.6 Proteomic analysis: Overexpressed proteins in ExsynF

A total of 18 proteins were overexpressed in the ExsynF of the AD brain cortex (list available in **Table 5** in section 4.5.2). According to p-value and relative fold change, the most overexpressed proteins in the ExsynF were Proteasome activator complex subunit 2, Surfeit locus protein 4,

Alpha-2-macroglobulin, Heat shock 70 kDa protein 1A, Pyruvate kinase and Tripeptidyl-peptidase 1.

4.5.6.1 Enrichment analysis

Enrichment analysis revealed 5 functional clusters. Each cluster is represented in order of statistical significance in the Enrichment Ontology Cluster plot (**Figure 30A**).

An analysis consisting in identifying potentially relevant GO terms for AD pathogenesis but not represented in the Enrichment Ontology Cluster plot reveals that other processes affected are “prion disease”, “oxidative phosphorylation”, “mRNA stability”, “adaptive immune system”, “cellular response to hypoxia”, “VEGFA VEGFR2 signaling” and “mitochondrion organization”.

4.5.6.2 Proteomic analysis: Overexpressed proteins in ExsynF (using brain-specific database)

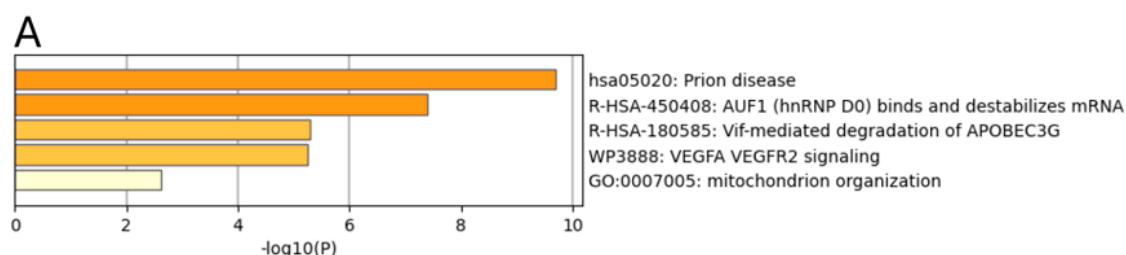
A total of 5 proteins were overexpressed in the ExsynF of the AD brain cortex. According to p-value and relative fold change, the proteins are displayed in order: Sodium/potassium/calcium exchanger 2, Protein deglycase DJ-1, Cell division control protein 42 homolog, Heat shock cognate 71 kDa protein and Contactin-associated protein-like 2.

Of these 5 overexpressed proteins, 4 (except Cell division control protein 42 homolog) were not present in the first list compared against the general proteomic database (marked in bold in **Table 6** in section 4.5.2).

4.5.6.2.1 Enrichment analysis (using brain-specific database)

Enrichment analysis revealed 4 functional clusters. Each cluster is represented in order of statistical significance in the Enrichment Ontology Cluster plot (**Figure 30B**).

An analysis consisting in identifying potentially relevant GO terms for AD pathogenesis but not represented in the Enrichment Ontology Cluster plot reveals that other processes affected are “negative regulation of protein-containing complex assembly”, “import into cell”, “regulation of supramolecular fiber organization”, “positive regulation of cellular component biogenesis”, “behavior” and “brain development”.



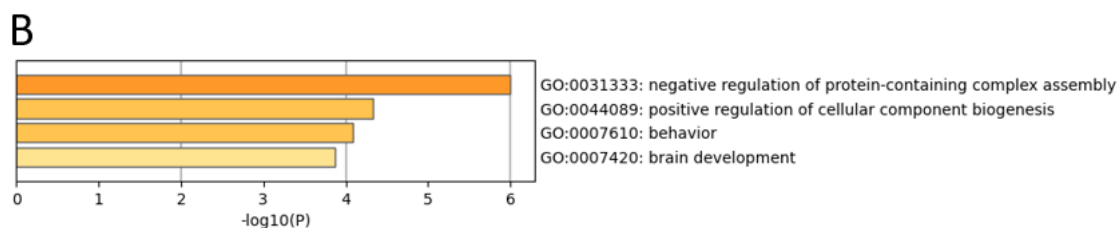


Figure 30. Overexpressed proteins in the AD ExsynF. A) Enrichment Ontology Cluster using human proteome database. **B)** Enrichment Ontology Cluster using brain-specific database.

4.5.7 Comparative analysis between SynF and ExsynF

We realized that many processes that were affected in AD could be grouped into a single category. For example, in the enrichment analysis of underexpressed proteins in SynF, we can find the GO terms “purine ribonucleoside triphosphate metabolic process”, “cellular respiration”, “amino acids metabolism”, “glycolysis” and “gluconeogenesis” among many others. All these GO terms can be gathered under the category *Metabolism* since all these processes are involved in metabolic pathways. Similarly, GO terms such as “Ion channel transport”, “transport of small molecules”, “import into cell”, “endocytosis”, “acidic amino acid transport”, “membrane trafficking” or “ER to Golgi anterograde transport” can be gathered under the category of *Transport*. Hence, to gain a broader perspective and comprehend the overall situation, we have simplified the outcome of the proteomic study following this criterion. The basis for including different GO terms in the same category was the share of DEP and a direct relationship in the Ancestor Chart or Child Terms for the GO term (<https://www.ebi.ac.uk/QuickGO/>).

We ultimately reduced all the GO terms to 16 categories: Metabolism, Transport, Mitochondria, Proteosome/Proteostasis, Neuronal structure, Synaptic physiology, Signaling, Oxidative stress, Immune system, Vascular system, Neuronal adhesion, Prion disease, mRNA stability, Stress response, Cell cycle, and phosphatases.

The aim of this operation was to eliminate redundancy and extract the main biological processes affected, collecting GO terms highly represented and interrelated into a single category. Thus, the analysis left some GO terms out of the analysis that were rarely present, such as Thyroid hormone signaling, Iron uptake, or insulin signaling (these terms will be analyzed in the next section).

Next, we classified whether every one of these 16 categories was present in every experimental group (**Figure 31**).

Category	SynF ↓	SynF ↑	ExsynF ↓	ExsynF ↑
Synaptic physiology	X		X	
Neuronal structure		X	X	
Transport	X	X	X	
Signaling	X	X	X	
Mitochondrial structure	X			
Proteasome/ Proteostasis	X		X	
Prion disease				X
Phosphatases			X	
Neuronal adhesion		X	X	
Phosphatases			X	
Neuronal adhesion		X	X	
Metabolism	X	X	X	X
Vascular system	X		X	X
Oxidative stress	X			
Immune system	X		X	X
mRNA stability			X	X
Cell cycle			X	

Figure 31. Summary table of changes in expression of synaptic and extrasynaptic proteins classified into 16 categories. ↓SynF: Underexpressed in SynF, ↑SynF: overexpressed in SynF, ↓ExsynF: underexpressed in ExsynF, ↑ExsynF: overexpressed in ExsynF.

5. Discussion

This section includes a discussion of the four objectives and, finally, a general discussion that will unify the whole thesis.

5.1 Synaptic and extrasynaptic distribution of NMDA receptors in cortex of AD patients

We described for the first time in the human cortex the distribution of the main four subunits of NMDARs, GluN2B, GluN2A, GluN1, and GluN3A, between synaptic and extrasynaptic membranes. The different nature of these membranes makes it possible to use biochemical fractionation protocols and separate synaptic membranes, defined as the plasma membrane of the PSD, and extrasynaptic membranes, which include spine necks, dendritic shafts, or somas, which are further away from the PSD [321, 322]. We have characterized the distribution of NMDAR subunits, as well as phosphorylation and glycosylation levels in synaptic and extrasynaptic membrane fractions from controls and AD subjects.

We have found that in the human brain, GluN2B, GluN2A, and GluN1 subunits are enriched in synaptic membranes, while GluN3A predominates in extrasynaptic membranes, as previously reported in mouse brains due to lower stabilization at synaptic sites [323]. Early reports established that GluN2B-containing NMDAR are mainly extrasynaptic, while GluN2A-containing NMDAR are mainly synaptic [138, 164, 324]. This led to the notion that extrasynaptic GluN2B-containing NMDARs drive long-term depression and excitotoxicity, while GluN2A-containing NMDARs mediate long-term potentiation (LTP) and survival cell signaling [325]. However, this oversimplified idea was challenged by studies that found that GluN2B and GluN2A subunits are present in both synaptic and extrasynaptic membranes [145], that activation of synaptic and extrasynaptic NMDARs are equally capable of inducing excitotoxicity [326], and that synaptic GluN2A-containing NMDAR are also necessary to induce excitotoxicity [327]. Results may have differed along the studies because of different protocol conditions and lack of pharmacological/biochemical tools to definitively distinguish NMDAR subtypes; additionally, the employment of different neurodevelopmental stages in mice can also contribute to discrepancies in the interpretations [127].

Anyhow, an imbalance between synaptic and extrasynaptic NMDAR activity has been considered a possible pathogenic factor for neurodegenerative diseases and a major contributing factor to glutamatergic dysfunction and pathogenesis in AD [127, 128]. Besides,

different studies have reported lower levels of GluN2B and GluN2A proteins and mRNA expression in hippocampus and entorhinal cortex from AD individuals [187, 189, 190, 193]; although none of them examined the levels of these subunits as we achieved here. Our approach to studying NMDAR subunit distribution in synaptic and extrasynaptic membranes, not feasible using crude membrane preparations, uncovered relevant differences in NMDAR subunit distribution between controls and AD, particularly for GluN2B and at specific neurodegenerative stages related to AD.

At synaptic membranes, the levels of the canonical GluN2B-170 kDa subunit were significantly lower in AD fractions, compared with controls, but higher at extrasynaptic membranes. Similarly, the canonical GluN2A-170 kDa was less abundant in AD synaptic membranes and showed a tendency to increase in extrasynaptic membranes. GluN1 levels were similar at synaptic membranes in controls and AD, but at extrasynaptic membranes, levels were higher in AD. As an exception, GluN3A levels were unchanged in AD. In sum, we find an impaired distribution of NMDAR subunit levels between synaptic and extrasynaptic membranes in AD relative to the control frontal cortex. The shift of NMDARs towards extrasynaptic membranes could be relevant to the excitotoxicity thought to be mediated by extrasynaptic NMDARs. Chronic NMDAR stimulation, lasting for months to years, has been associated with AD with increased levels of extrasynaptic GluN2B-containing NMDARs, which induce enlarged tonic NMDAR currents and excitotoxicity [153]. Remarkably, we have found higher levels of the canonical GluN2B-170 kDa and also of the GluN2B-160 kDa glycoform in Braak V-VI in extrasynaptic membranes. This suggests that excitotoxicity could be facilitated at late stages of AD by GluN2B enrichment in extrasynaptic membranes.

Deglycosylation and lectin binding analysis confirmed that GluN2B, GluN2A, GluN1 and GluN3A are glycosylated in human cortex, and indicated that GluN2B and GluN2A are N-glycosylated. Remarkably, glycoforms of GluN2B and GluN2A with a lower apparent molecular mass (GluN2B-160 kDa and GluN2A-160 kDa) are found exclusively at extrasynaptic membranes in control and AD cases. Changes in protein glycosylation have been reported in AD [328], even in N-linked glycosylation [329] and in specific NMDAR subunits such as GluN2B, GluN2A, and GluN1 [330]. Our lectin binding analysis demonstrated differences in extrasynaptic GluN2B-160 kDa and GluN2A-160 kDa glycoforms between controls and AD, with higher levels at Braak V-VI than in controls. This could be explained because N-glycosylation is a post-translational modification essential for NMDAR subunit surface delivery [288], and altered glycosylation could affect the surface expression [331] and intracellular sorting [332] of GluN2B and GluN2A

subunits. This would lead to increased levels at the extrasynaptic membranes of these glycoforms rather than reflecting enhanced translocation from synaptic membranes.

We have previously described aberrant glycosylation in AD-related proteins, such as APP [333], apoE [334], reelin [335], and acetylcholinesterase [336], as well as changes in glycosylated epitopes [337]. Glycosylation changes in NMDAR subunits could occur early or be associated with neurodegeneration progression in AD, but whether the 160-kDa glycoforms of GluN2B and GluN2A modify NMDAR activity in AD should be determined.

A worth-mentioning possibility is that the increase in ExsynNMDARs does not occur in neurons but in glia. As noted, NMDARs are expressed by astrocytes [318], microglia [150], and oligodendrocytes [149]. Since the membrane of these cells probably resides in the ExsynF (**Figure 1B**), the hypothesis that the increase in ExsynNMDARs is in glia rather than neurons is compatible with the data. In fact, a study found higher levels of GluN1, specifically in astrocytes in the AD human hippocampus [338].

In this study, GluN2B phosphorylation at Tyr1336 was significantly high in extrasynaptic membranes compared to Tyr1472 phosphorylation. Phosphorylation at Tyr1336 and Tyr1472 at synaptic membranes was quantifiable, but at extrasynaptic membranes, phosphorylation at Tyr1472 was particularly low, making quantification difficult in both controls and AD fractions. Tyr1336 GluN2B phosphorylation levels showed consistency in control and AD fractions, which means that, independently of the different relative GluN2B levels in synaptic and extrasynaptic membranes from control and AD samples, the phosphorylation ratio at Tyr1336 remained similar in both conditions. On the contrary, phosphorylation levels of GluN2B at Tyr1472 relative to GluN2B levels were significantly low in AD synaptic membranes, and this suggests a non-proportional decay of phosphorylation of GluN2B respect to the lower GluN2B levels found in AD; and therefore, a specific affectation of synaptic GluN2B Tyr1472 phosphorylation in AD.

It is broadly assumed that Tyr1472 is the major phosphorylation site within GluN2B [133]. GluN2B Tyr1472 phosphorylation activates and stabilizes NMDARs in the synaptic plasma membrane, prevents it from being endocytosed or translocated to non-clustered extrasynaptic membranes, and increases after LTP [133, 137]. Our results suggest that the lesser synaptic Tyr1472 phosphorylation in AD could impair GluN2B retention at synaptic membranes, explaining the higher levels at the extrasynaptic membranes. However, the proportion of the Tyr1472 GluN2B translocated was not sufficient to be measurable, and Tyr1336 GluN2B was the principal subunit in ExsynF. Our study opens the question about the role of synaptic

GluN2B Tyr1336 phosphorylation, which is thought to promote NMDARs anchoring at extrasynaptic membranes [117, 284, 339], and our study points to this. The mechanistic relationship between phosphorylation and glycosylation on GluN2B mislocalization remains to be explored since specific interrelations have been suggested for key AD proteins such as APP [332] and tau [340].

Our analysis of tau and A β transgenic models reproduced only partially the alterations found in AD patients, suggesting that some of the changes in NMDAR subunits observed in human AD brains are likely the consequence of complex or compensatory processes that could require the participation of more than one pathological alteration. However, studies using tau-based mouse models point in the same direction as our data. A shift in the balance from synaptic towards extrasynaptic NMDARs was described in the hippocampus of TauP301S mice at 10 months of age [341], and tau knockout mice do not exhibit changes in NMDAR phosphorylation at Tyr1472 and Tyr1336 [339], suggesting that tau is not related to NMDAR phosphorylation, in agreement with our results. Therefore, the accumulation of phosphorylated tau is relevant to altering NMDAR distribution, but tau could not have any role in NMDAR phosphorylation.

Besides, the amyloid peptide accumulation in APP/PS1 mice seems to affect only GluN1 in the frontal cortex. Studies in the hippocampus report low levels of GluN2B and GluN2A and no changes in GluN1 [342], but also higher levels of GluN2B and phosphorylated GluN2B-Tyr1472 in the extrasynaptic fraction from hippocampal homogenates [343]. Our results suggest that in the frontal cortex of APP/PS1 mice, reduced levels of the mandatory subunit GluN1 in synaptic and extrasynaptic membranes may affect all NMDARs and contribute to the synaptic failure described in this model [344] driven by amyloid pathology.

In conclusion, the alterations in the NMDAR subunits distribution described here could affect essential NMDAR functioning, involved in processes such as synaptic plasticity and memory [137, 345], and consequently, cognitive decline associated with normal aging and AD [346]. The shift to extrasynaptic membranes of GluN2B, GluN2A, and GluN1 could explain the exacerbated NMDA-related excitotoxicity observed in AD.

5.2 NMDA receptor subunits characterization in the CSF of AD

Detecting NMDAR subunits in CSF can be a valuable read-out of brain changes and even a diagnostic tool for certain neurological conditions. Indeed, it has been proposed that changes in synaptic proteins precede neurodegeneration [214]. However, until now, NMDARs have not been explored as a biomarker in CSF despite their association with disease progression. Several synaptic proteins, such as neurogranin, have demonstrated potential as AD CSF biomarkers

[213], most being cytosolic proteins, but others, such as SNAP-25, function as membrane-bound proteins [347]. Here, we described the presence of NMDAR subunits in CSF and the fact that levels of subunits are associated with neuropathological conditions.

Several full-length transmembrane proteins containing a preserved intracellular domain have also been found in CSF. In this regard, our group reported the existence of full-length forms of AD-related transmembrane proteins such as APP [221], BACE1 [222], and ADAM10 [223], also including subunits of membranes multi-pass protein complexes such as presenilin-1 [225]. The full-length ACE2 receptor is also found in human and mouse plasma, co-existing with ectodomain fragments [224, 348]. The mechanisms by which these membrane-bound proteins reached the CSF are unknown (discussed in [349]).

In fact, C-terminal fragments of APP that contain transmembrane and intracellular domains have also been described in CSF [350] and tears [351]. Interestingly, APP-CTF fragments are enriched in brain exosomes [352]. Following such associations, we address the hypothesis that NMDAR subunits are present in CSF associated with membranes. However, we were not able to find evidence of NMDAR enrichment in CSF EVs. It also appeared plausible that in neurodegenerative conditions, neuronal damage leads to the release into the CSF of cellular components, including membrane-resident NMDAR subunits. However, NMDAR subunits are also present in non-disease CSF samples, and depending on the neurodegenerative condition, the relative amount of particular subunits is increased or decreased.

Until we can define the mechanism(s) by which NMDARs reach the CSF, it is difficult to interpret the observed changes. Here, we focused on the full-length forms of the NMDAR subunits and normalized their levels to the mandatory subunit present in all NMDARs, the GluN1. This approach has some limitations. NMDARs could also reach CSF as fragments. For example, GluN2B is present in the brain as a 170 kDa full-length protein but also detectable as 150 kDa and 130 kDa proteolytic fragments, whose origin is thought to be post-mortem degradation [188]. These, or other fragments from other NMDAR subunits, can be associated with neurodegeneration. Once more, fragments of transmembrane receptors, such as ErbB4 [353] and apoER2 [354], have been identified in CSF, and these fragments probably correspond to ectodomain fragments originated by proteolytic processing. Indeed, the *Drosophila* glutamate receptor GluRIIA suffers cleavage [355], and proteolytic processing has also been described for GluN2B [356, 357] *in vivo* or *in vitro*. Therefore, in the future, the characterization of NMDAR subunit fragments should be addressed, particularly to design specialized techniques for the detection of NMDAR subunits in CSF, such as enzyme-linked immunosorbent assays (ELISA) that can discriminate full-length species from fragments.

The C-terminal domains of NMDAR subunits served to bind various proteins regulating synaptic receptor retention and signaling, as well as subunit interaction (reviewed in [115]). Therefore, even if NMDAR is not present in CSF associated with membranes, it is probable that the more stable forms of soluble NMDAR are full-length forms that maintain subunit interactions.

Furthermore, it is commonly assumed that NMDARs are mainly expressed by neurons, but they can also be expressed by other cell types, including glial [149, 150, 318, 358] and endothelial [359] cells. Therefore, it is reasonable to think that brain inflammation could also contribute to releasing NMDAR subunits into the CSF. The main cellular origin of specific NMDAR subunits in CSF is also relevant in defining their potential as a read-out of altered brain mechanisms. In this regard, post-translational modifications such as glycosylation and phosphorylation can serve to characterize NMDAR subunits located at subcellular localization [426], but also with different cellular origins.

Despite limitations, we have demonstrated that GluN3A appeared to increase in the CSF of HD patients, even at asymptomatic stages, and that GluN2A decreases in AD subjects. In both cases, we referred the changes to the levels of the GluN1 subunit, the compulsory subunit present in all NMDAR complexes. A previous report using immunohistochemical analysis of human postmortem brain tissue also reported higher GluN1 levels in the human HD hippocampus than in control patients [360]. Other ratios between GluN3A and GluN2A or GluN2B should be explored to better characterize changes in levels of specific subunits, but in this study, the accessible CSF volume limited our analysis.

Changes in AD CSF, with decreased GluN2A, could reflect a subunit decrease noticed particularly in synapsis. GluN2A subunits are more abundant in synaptic membranes than in extrasynaptic membranes [426]. However, in HD CSF, GluN3A resulted in increased, probably noticing extrasynaptic changes. GluN3A subunits are preferentially located at extrasynaptic sites in humans [426] and mouse brains [285]. Thus, altered CSF NMDAR levels could reflect brain changes related to synapsis but also with extrasynaptic dysfunction.

In conclusion, the detection of NMDAR subunits in the human CSF could be exploited as a diagnostic tool for neurological conditions or, rather, as a stratifying biomarker. Although mechanisms for NMDAR release into CSF remain unclear, their presence in both healthy and diseased samples indicates that specific subunit alterations may correlate with disease progression. For instance, GluN2A decreases in AD, while GluN3A increases in HD, suggesting a correlation with synaptic events. Despite current limitations, further investigation into NMDAR subunit fragments and improved detection methods could enhance their use as biomarkers for neurodegenerative disorders.

5.3 To study the suitability of iNeurons for the study of NMDARs in the context of AD

iPSC-derived neurons (iNeurons) represent a crucial step forward in modeling diseases in a human-relevant manner. It is crucial to study the developmental stages of iNeurons to understand their biological limitations, especially when the interest is modeling an aging-related disease. Key developmental stages in neuronal maturation consist of the replacement of GluN2B by GluN2A, namely, the GluN2B-GluN2A switch [361-363] and the incorporation of NMDARs into the synapse [128]. In this study, we used two commonly used neurodifferentiation protocols, Neural Maintenance Media [271, 296] (NMM) and BrainPhys media (BPM) [272], and compared them at three time points to determine which one achieves a more physiologically relevant maturation of NMDARs, with the final purpose of modulating the NMDAR system with A β treatment.

Classical neurodifferentiations using NMM are time-consuming because it takes longer for neurons to mature and because the preparation of the media is more custom-based, requiring additional ‘hands-on’ work. This is why alternative methods that achieve faster neurodifferentiations are desirable. However, the fastest protocols based on overexpression of neurogenin are not physiologically relevant: these neurons develop synapses composed of AMPA receptors but no NMDARs [364, 365]. Thus, there is a tradeoff between time and economic resources needed to achieve neurodifferentiation and the physiological relevance of the culture obtained.

In this regard, BPM has emerged as a faster protocol to achieve neuronal differentiation [271]. Although the precise mechanisms through which this is achieved are unclear, a reasonable possibility is the presence of astrocytes. Classical protocols incorporate exogenous astrocytes (either human or rodent) to provide a more physiologically relevant environment that supports neural function and differentiation [366-369]. BPM promotes greater spontaneous differentiation to astrocytes, which could explain the accelerated differentiation [271, 273]. However, no study insofar has evaluated whether these two key physiologically relevant processes -the GluN2B-GluN2A switch and incorporation of NMDARs into the synapse - occur differently in NMM and BPM. The outcome of these experiments could help researchers decide which protocol to choose to model a neurodegenerative or neuropsychiatric disease [314].

GluN2B-GluN2A switch

A first characterization through qPCR showed that mRNA levels of neuronal markers *MAP2* and *CAMKII β* displayed identical trends in BPM and NMM, peaking at day 30 and decreasing afterward. *GRIA1*, the subunit of the synaptic AMPAR, and *APP* also showed a peak at day 30 to decrease afterward. However, BPM achieves greater levels of expression and a slower decrease compared to NMM. Higher *APP* levels in BPM than in NMM have been previously reported [271].

The GluN2B-GluN2A switch is widely studied in mice [361-363] and is considered a crucial step in neuronal and synaptic maturation [312]. In mice, the switch occurs in the second post-natal week and requires synaptic activity induced by sensory experience as well as other key regulators, such as the activation of group I metabotropic glutamate receptors [125], the transcriptional downregulation of *GRIN2B* through epigenetic remodeling induced by the transcriptional repressor element 1-silencing transcription factor [370], relative availability of co-agonists glycine and D-serine [104], the protein Reelin [371], EphB signaling [372] and the expression of specific microRNAs [126].

Regarding the mRNA level expression, *GRIN2B* is highly expressed early in development, achieving the greatest expression in the second post-natal week, while *GRIN2A* starts to increase after birth, surpassing *GRIN2B* in adulthood [99, 373]. Importantly, when the switch is studied in mice primary hippocampal neurons, the mRNA levels of *GRIN2A* and *GRIN2B* follow the same dynamics as *in vivo* [126].

The switch is particularly important in the synapse. The so-called 'silent synapses' are populated exclusively by GluN2B. When synaptic activity promoted by sensory input starts, GluN2B leaves the synapse and GluN2A enters, constituting the switch [374]. A possible mechanism supporting this switch could be the availability of the two alternative co-agonists of NMDARs, D-serine and glycine [104]. Replacement of glycine by D-serine at CA3-CA1 synapsis in the first post-natal period promotes a conformational change in the C-terminal region of GluN2B leading to different interaction with PDZ scaffolding partners and subsequently partial removal from the synapse, populating afterward also the extrasynaptic membranes [104].

However, the GluN2B-GluN2A switch has been much less studied in human iNeurons. Neurodifferentiation protocols that achieve a faster differentiation based on neurogenin overexpression achieve active synapses populated by AMPARs but no NMDARs [364, 365] even at day 70 of differentiation. Even if these protocols save time and economic resources, they are not physiologically relevant enough since there is no NMDAR expression, and they are especially undesirable when interested in studying the role of NMDARs in a disorder.

Expression of *GRIN1* [375], *GRIN2A*, and *GRIN2B* [376] have been reported at the mRNA level in iNeurons. A study suggested that GluN2B is the main subunit expressed by iNeurons [377]. They detected GluN2B but not GluN2A by western blot. When they isolated GluN2B and GluN2A currents, they showed that the former was the principal component. However, this study had important limitations since it did not explain the differentiation protocol or media used, which limits an attempt to replicate it. Moreover, differentiation was maintained until day 15, which was too short for synaptic maturation assessment.

The most interesting study [378] in this regard showed a peak of *GRIN2B* and *GRIN2A* mRNA levels at day 57 and a decrease at day 88, although *GRIN2A* decayed less than *GRIN2B*. The authors claimed that this supports the GluN2B-GluN2A switch. In our opinion, *GRIN2A* expression should be maintained, as it happens *in vivo*. In fact, researchers suggested that the increase in expression of *GRIN2A* could be the trigger of the switch [379]. Interestingly, this is the only study besides ours that achieves a peak of expression of *GRIN2A* in iNeurons. To our knowledge, our BPM iNeurons are unique in keeping a high level of *GRIN2A* expression. The handicap of this study is that these iNeurons were obtained through the overexpression of transcription factors, but these are not specified, representing a key limitation for reproducibility.

Many electrophysiology studies support the idea that GluN2A mediates around 10% of NMDA-evoked currents, while GluN2B is the major component [314, 377, 380, 381], supporting that there is no switch.

Although NMDARs are considered predominantly neuronal, they can also be expressed by astrocytes [147, 148]. Thus, we will determine in future experiments whether the increase in GluN2A at the mRNA and protein levels observed in BPM occurs in neurons and/or astrocytes. Specifically, we will isolate GFAP+ and TUJ1+ cells through FACS and independently measure mRNA and protein GluN2A and GluN2B levels in neurons and astrocytes. If our results indicate that the increase in GluN2A occurs in neurons, it will be the first strong evidence for the GluN2B-GluN2A switch in iNeurons. On the contrary, if this increase occurs in astrocytes, it will be worth studying to understand the implications of this phenomenon.

To our knowledge, experiments in which GluN2B and GluN2A levels have been assessed after treatment with A β have not been performed in iNeurons. Interestingly, both GluN2B and GluN2A decreased after the treatment at the mRNA but not at the protein level in NMM but not in BPM. This mismatch between mRNA and protein could be explained by the difficulties in quantifying the immunoreactive bands in the western blot. The band intensities were too low,

and the membranes were too dirty to allow optimal quantification. Given the scarce material, western blots could not be repeated. Future neurodifferentiations and experiments will tackle this issue. Regarding the difference between NMM and BPM, a possibility is that the support that astrocytes give to neurons in BPM protects them from the impact of A β 42. Another possibility is that BPM achieves a neuronal maturation that makes iNeurons less susceptible to A β 42. In future experiments, we will vary the type of treatment (72 instead of 24 hours) to see whether this is enough for NMDARs to be affected in BPM. The last possibility is that neurons in BPM may suffer the A β 42 consequences, but this is masked by the huge amount of astrocytes. That is why we plan to perform FACS and separate neurons from astrocytes after A β 42 treatment and test whether NMDAR levels are affected specifically in BPM neurons but not astrocytes.

Evidence for SynNMDARs

To achieve synaptic maturation, it is necessary to incorporate NMDARs into the synapse, firstly GluN2B. In postnatal days 14-21 in hippocampal slices from mice, two-thirds of NMDARs are in the synapse, while the rest are in extrasynaptic membranes [382]. However, in primary cell cultures, after one week *in vitro*, around 90% of NMDARs are in the extrasynaptic space, and this number reduces to 50% or less after two weeks [128, 138, 156, 311-313]. It is crucial to know this timing because when researchers are interested in modeling neurodegeneration, having immature, embryonic-like instead of mature synapses, is a handicap for translating those results to humans.

To our knowledge, no work has been done to characterize the incorporation of NMDARs into the synapse in iNeurons. Here, immunostaining against Synaptophysin, exclusively expressed in the presynaptic compartment, is a criterion for defining an NMDAR as synaptic (SynNMDAR) when they colocalize. The rest of GluN1 staining is considered ExsynNMDARs. We aimed to compare NMM and BPM and study how the proportion of SynNMDARs changes across time points and after A β 42 treatment.

A previous work relied on electrophysiological data to suggest that GluN2B is the main subunit populating the synapses of iNeurons. This is because GluN2B and GluN2A have different decay time constants [383], and the obtained kinetics fit better into the GluN2B range. However, kinetics may vary on the distance to the synapse for both subunits [384]. Furthermore, there are pharmacological tools, such as the use of MK-801 for inhibiting selectively the SynNMDARs-mediated currents [385-387] and isolating the ExsynNMDARs-mediated, that can be considered as a different approach to address this issue. This pharmacological targeting aimed to

disentangle synaptic from extrasynaptic NMDA-induced currents is missing in the iNeurons research field.

Our data indicates that the GluN1-Synaptophysin colocalization (SynNMDARs) increases from day 30 to day 60 in both NMM and BPM cultures, although *GRIN1* expression decreases at this time point. This suggests a synaptic refinement where mRNA transcripts decrease, but GluN1-containing NMDARs are incorporated into synapses.

In future experiments, we will independently assess GluN2B and GluN2A incorporation into the synapse. Importantly, we are planning to perform electrophysiological studies to isolate SynNMDARs from ExsynNMDARs-mediated currents (blocking SynNMDARs with MK-801) and those GluN2B from GluN2A NMDARs (using the GluN2B specific blocker ifenprodil). In this manner, we will have electrophysiological evidence for the synaptic versus extrasynaptic distribution of NMDARs and the relative GluN2B-GluN2A components of NMDA-elicited currents.

5.4 The synaptic and extrasynaptic proteome of the AD brain

We described for the first time a proteomic study comparing the synaptic and extrasynaptic proteome of the AD versus control brain frontal cortex. Several studies have analyzed the proteome of the cerebral cortex of patients with AD and compared it with that of control patients [258, 388-390]. However, bulk proteomics of whole tissue can mask subtle changes in specific subcellular localizations, such as the synapse [258, 267, 391-393].

Synapse loss is the best correlate of cognitive impairment in AD, better than amyloid or tau deposition [45, 394, 395]. This fact and additional evidence prompted scientists to analyze the specific proteome of the synapse [396, 397], or synaptic proteome. In this experiment, we performed a shotgun proteomics label-free strategy applied to the outcome of a biochemical fractionation protocol that yields a fraction enriched in the postsynaptic density (SynF) and another fraction enriched in neuronal non-synaptic and glial membranes (ExsynF). This allowed us to compare the synaptic and the extrasynaptic proteome of AD vs control.

5.1.1 Validation of differentially expressed proteins in AD

In **Figure 32** there is a summary of the number of DEP using a general and a brain-specific database in the AD SynF and ExsynF.

Database	SynF ↓	SynF ↑	ExsynF ↓	ExsynF ↑
General	87	58	18	30
Brain	25	13	6	5

Figure 32. Number of DEP when using a general and a brain-specific database in the AD SynF and ExsynF. Summary table of the number of DEP using a general and a brain-specific database in the AD SynF and ExsynF. ↓SynF: underexpression in SynF; ↑SynF: overexpression in SynF; ↓ExsynF: underexpression in ExsynF; ↑ExsynF: overexpression in ExsynF.

We have not yet validated the differential expression of any target protein study using an alternative technique, such as western blot or ELISA. We will perform such validations in the near future, but until then, we can validate our results with previous proteomic studies.

Most DEP that are previously reported in the literature change their expression in the same direction that our study indicates. For example, Excitatory amino acid transporter 2, Amino acid transporter, and Prohibitin-2 were underexpressed in the SynF, and they have been reported to be underexpressed in bulk tissue proteomic studies [398, 399]. Rabphilin-3A was overexpressed in the SynF, in accordance with other bulk tissue studies [388]. Regarding the ExsynF, Long-chain-fatty-acid--CoA ligase 6 [400], Serine/threonine-protein phosphatase PP1-beta catalytic subunit [401] and Leucine-rich PPR motif-containing protein [402] have been reported to be underexpressed in the AD brain. Accordingly, we found them underexpressed in the ExsynF.

Remarkably, in those proteins where differential expression have been found in SynF and ExsynF simultaneously, these changes result in opposite directions. For example, Ankyrin-2 is overexpressed in SynF and underexpressed in ExsynF (**Figure 33**). This illustrates the consistency of our data.

Protein	SynF ↓	SynF ↑	ExsynF ↓	ExsynF ↑
ANK2		X	X	
CDC42	X			X
EPB41L1		X	X	
EPB41L3		X	X	
GLS		X	X	
IARS2		X	X	
OGDH		X	X	
TUBA4A		X	X	
UQCRH	X			X

Figure 33. Repeated DEP in AD SynF and ExsynF. Summary table of the number of DEP present in more than one experimental group. ↓SynF: underexpression in SynF; ↑SynF: overexpression in SynF; ↓ExsynF: underexpression in ExsynF; ↑ExsynF: overexpression in ExsynF. ANK2 is Ankyrin-2, CDC42 is Cell division control protein 42 homolog, EPB41L1 and 3 are Band 4.1-like protein 1 and 3, GLS is Glutaminase kidney isoform, IARS2 is Isoleucine--tRNA ligase, OGDH is 2-oxoglutarate dehydrogenase complex component E1, TUBA4A is Tubulin alpha-4A chain and UQCRH is Cytochrome b-c1 complex subunit 6.

5.1.2 Synaptic-related differentially expressed proteins

In this section, we focus on synaptic-related DEP in both SynF and ExsynF, including the function to which they are related (in brackets).

Underexpressed proteins in SynF involved in synaptic physiology include V-type proton ATPase subunit C 1 (maintenance of membrane potential), Cell division control protein 42 homolog (cytoskeleton remodeling), Tyrosine-protein phosphatase non-receptor type substrate 1 (synaptic plasticity) and ADP-ribosylation factor 1 (synaptic plasticity).

Overexpressed proteins in SynF involved in synaptic physiology include Solute carrier family 12 member 5 (maintenance of membrane potential), Rabphilin-3A (synaptic plasticity), and Ankyrin-2 (localization and membrane stabilization of ion transporters and ion channels).

Underexpressed proteins in ExsynF involved in synaptic physiology include Synaptotagmin-7 (involved in synaptic vesicle exocytosis) and Ankyrin-2 (localization and membrane stabilization of ion transporters and ion channels).

Overexpressed proteins in ExsynF involved in synaptic physiology include Sodium/potassium/calcium exchanger 2 (maintenance of membrane potential) and Annexin A7 (involved in synaptic vesicle exocytosis).

From the enrichment analysis, we found that GO terms related to synaptic physiology were highly represented in our datasets, especially in SynF, as expected. We differentiated among 10 categories of synaptic-related GO terms (**Figure 34**).

Category	SynF ↓	SynF ↑	ExsynF ↓	ExsynF ↑
Synaptic plasticity	X		X	
Postsynaptic structure organization	X	X		
Synaptic vesicle cycle	X	X		
Axon guidance	X	X		X
GABAergic synapse	X	X		
Glutamatergic synapse	X	X		
Phosphorylation	X	X	X	
Membrane potential	X		X	
Glutamate uptake	X			
Axonal transport		X		

Figure 34. Summary table of the comparative among GO terms present in the four experimental groups related to the synaptopathy hypothesis and classified into 10 categories. The brain-specific database was used. ↓SynF: Underexpressed in SynF, ↑SynF: overexpressed in SynF, ↓ExsynF: underexpressed in ExsynF, ↑ExsynF: overexpressed in ExsynF.

Several terms directly involved in synaptic physiology, such as synaptic plasticity [388], postsynaptic structure organization [388, 390], synaptic vesicle cycle [262, 388, 403], GABAergic synapse [262, 403], glutamatergic synapse [262, 388, 390, 403, 404], phosphorylation regulation [262, 405], and regulation of membrane potential [262] have been linked to AD in previous proteomic studies. Only one proteomic study found ‘axogenesis’, similar to our Axon guidance GO term [390]. However, many studies have suggested an

implication of the molecular mechanisms involved in axon guidance and regulation in AD [406-408].

From these GO terms, we highlight 1) synaptic plasticity, linked to proteins including Ephrin type-A receptor 4, Tyrosine-protein phosphatase non-receptor type substrate 1, N-terminal EF-hand calcium-binding protein 2, and Synaptophysin; and 2) postsynaptic structure organization, which was linked to proteins including ADP-ribosylation factor 4, Cell division control protein 42 homolog, Utrophin and Brain-specific angiogenesis inhibitor 1-associated protein 2.

Intracellular transport and trafficking of synaptic vesicles and molecules is essential for neuronal function. This group of processes was majorly represented in our datasets. Terms such as Transport of small molecules, endocytosis, exocytosis, synaptic vesicle transport, vesicle-mediated transport in the synapse, Membrane Trafficking, protein localization to plasma membrane, ER to Golgi Anterograde Transport and Golgi-to-ER retrograde transport were highly represented in \downarrow SynF and \uparrow SynF, but not in \downarrow ExsynF and \uparrow ExsynF.

Importantly, when we relaunched the analysis with the brain-specific database, the total number of DEP was reduced. Notwithstanding, new neuron-related proteins appeared. In the case of \downarrow SynF, 8 new proteins appeared; in the case of \uparrow SynF, only 3. In \downarrow ExsynF, it was only 1, and in \uparrow ExsynF, 4 new proteins were identified. As expected, DEP and GO terms related to synaptic physiology were more abundant in SynF than in ExsynF (**Figure 34**). At the same time, ExsynF was more enriched with GO terms related to transport, signaling, mitochondria, and metabolism.

5.1.3 Mitochondria-related differentially expressed proteins

Mitochondrial proteins and mitochondrial GO-related terms are highly represented in our datasets. This may seem oddly at first sight since our starting material is biochemical fractions enriched in either synaptic or extrasynaptic membranes. However, images taken with electron microscopes of fractions enriched in synaptosomes obtained with protocols similar to ours show that small mitochondria remain in the synaptic compartment after the fractionation [397]. Moreover, other proteomic studies have linked synaptic and mitochondrial modules, and it is common for synaptic modules to include a variety of mitochondrial-metabolic proteins [409]. The origin of these mitochondrial proteins found in our SynF and ExsynF could be either from mitovesicles (double-membraned EVs containing multiple mitochondrial proteins) [410] or synaptic mitochondria. Mitochondria are present in the pre-synaptic compartment [411,

412], where they provide energy for exocytosis of synaptic vesicles, and in the postsynaptic space, where a high energy amount is needed to build postsynaptic potentials and perform synaptic plasticity events [412, 413].

We will now analyze which percentage of DEP in every experimental group (\downarrow SynF, \uparrow SynF, \downarrow ExsynF, and \uparrow ExsynF) have mitochondrial origin. To stratify our data, we created six functional categories for mitochondrial proteins, performing a very similar process to that of section 4.5.7 *Comparison between SynF and ExsynF*. These were: subunits of ATP synthase, proteins involved in catabolism/Krebs cycle, proteins involved in mitochondrial structural/integrity, proteins involved in oxidative stress, proteins involved in the electron transport chain, and proteins involved in other functions, such as GABA metabolism or the proteasome system.

In \downarrow SynF, we detected that 28 out of 87 (32%) of all DEP are mitochondrial. Among the mitochondrial proteins, there were 5 subunits of ATP synthase (17%), 8 proteins involved in catabolism and/or Krebs cycle (28%), 3 proteins involved in mitochondrial structural integrity (10%), 2 proteins involved in oxidative stress (7%), 4 proteins involved in the electron transport chain (14%) and 6 proteins involved in other functions such as GABA metabolism (21%). The same operation is repeated for the other experimental groups and is represented in **Figure 35**.

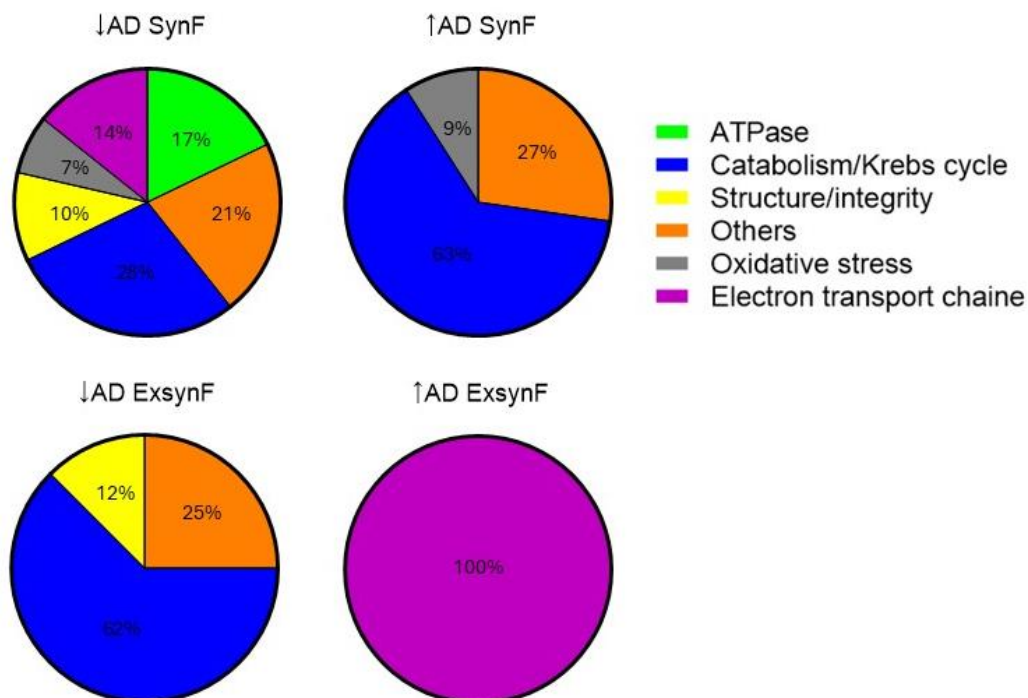


Figure 35. Schematic illustration of mitochondrial proteins found in the four experimental groups. The mitochondrial proteins found in the four experimental groups (\downarrow SynF, \uparrow SynF, \downarrow ExsynF and \uparrow ExsynF) were classified into six functional categories: ATPase subunit (green), Catabolism/Krebs cycle (blue), Mitochondrial structure/Integrity (yellow), Oxidative stress (grey), Electron transport chain (purple) and Others (orange). Data are represented as a pie chart including the percentage that every functional category represented.

The affection of mitochondria has been linked to late rather than early stages of AD [388]. Different studies have seen a dysregulation of mitochondrial physiology [258, 262, 390, 404], including a meta-analysis that found oxidative phosphorylation to be a common dysregulated pathway [403]. Interestingly, a study found that aging did not impair mitochondrial function, suggesting that it is a feature specific to AD [404]. Another study that performed label-free proteomics in a synaptosome preparation (included both pre and postsynaptic terminals) found oxidative phosphorylation to be upregulated in one brain area (BA17) but downregulated in another (BA1/42) [397] (in accordance with another study [409]). This mismatch could be explained by the specific affection of lesions such as amyloid plaques and NFT in each brain area [388]. Another possible explanation is the relative density of different cell types in each brain area [409].

5.1.4 Metabolism-related differentially expressed proteins

On the other hand, most of the DEP found in our experimental groups are involved in metabolism in one way or another. We detected four main categories related to different types of metabolism: nucleotides, amino acids, sugars, and RNA (mRNA and tRNA stability) (**Figure 36**).

Sugar metabolism was dramatically altered in our samples in accordance with previous proteomic studies. The dysfunction of sugar metabolism in AD is a well-established concept [414, 415]. Interestingly, the Krebs cycle was particularly affected in \downarrow ExsynF, reported to be related to late-stage AD [388, 390, 404].

Metabolism of nucleotides was the only type of metabolism altered in the four groups, indicating that it is dramatically impaired in AD. Interestingly, nucleotide metabolism is not commonly reported in proteomics studies of the AD brain, although there is an exception that performed label-free proteomics of the AD left prefrontal cortex [262]. Only one study has specifically addressed nucleotide metabolism in AD [416]. They showed that pathways for

pyrimidine nucleotide synthesis are altered in the brains of AD patients. Since nucleotide metabolism is crucial for cell biology, and its role in AD is almost completely unexplored, it is an interesting field to explore in future studies.

Like ours, many proteomic studies have obtained data suggesting an impairment of RNA metabolism [262]. A study showed that proteins related to RNA metabolism changed in the AD brain when the first symptoms appeared [417]. Specifically, a study saw that proteins related to RNA metabolism increased in the insoluble fraction of the AD brain, where amyloid plaques and NFT accumulate, suggesting a direct connection to the main lesions of the disease [409]. Importantly, proteins related to RNA metabolism were specifically affected in AD but not in healthy age-matched individuals [404].

Type of metabolism affected	SynF ↓	SynF ↑	ExsynF ↓	ExsynF ↑
Nucleotides	X	X	X	X
Amino acids	X	X	X	
Sugars	X	X	X	
RNA		X	X	X

Figure 36. Summary table of the types of metabolism affected. Summary table containing which are the four main categories of metabolism that are affected -nucleotides, amino acids, sugar metabolism and RNA- and which experimental group (↓SynF, ↑SynF, ↓ExsynF and ↑ExsynF) is affected by which category.

5.1.3 Limitations

We expected to find changes in GluN1, GluN2B, and GluN2A levels in our proteomic study, but they did not change. We found NMDAR subunits GluN1, GluN2B, and GluN2A with an FDR of 1% in the proteome of the SynF but not in the ExsynF. However, statistical analysis showed no differential expression between AD and control individuals.

Technical biases inherent to the use of LC-MS/MS may mask potential differences. First, label-free shotgun proteomics is not the best choice to follow the differential expression of a target protein. For that purpose, targeted proteomics is the right choice, where the protein of interest is labeled with radioisotopes, and a calibration line is used for highly precise quantification [418]. Second, LC-MS/MS is that it is not the most suitable technique to study membrane proteins. This is because membrane proteins possess hydrophobic residues that do not get trypsinized [419, 420]. Moreover, NMDARs, like other membrane proteins, may not be as

abundant as other proteins in SynF and ExsynF [420]. Together, this could give rise to a peptide mixture in which membrane proteins are underrepresented. This may explain why we did not find differentially expressed synaptic proteins previously reported by western blot of brain extracts, such as NMDARs [189], PSD95 [421], or AMPAR [388, 422]. A possibility to overcome these limitations in future experiments would be the use of the so-called SP3 method, which allows the use of harsh detergents to solubilize, rather than the urea-based methods followed in this experiment [423].

5.5 General discussion

In this thesis, we have characterized in a multidimensional view the involvement of NMDARs in AD. We designed and successfully used a biochemical protocol to isolate synaptic and extrasynaptic membranes from human frozen brain tissue. We dug into a crucial question about the subcellular distribution of NMDARs in the AD human brain, and we discovered that an imbalance exists between synaptic and extrasynaptic membranes. We showed lower levels of NMDARs in the synapse but higher levels in the extrasynaptic membranes. This likely contributes to synaptic failure and excitotoxicity observed in the brains of patients with AD. Furthermore, we describe novel GluN2A and GluN2B glycoforms exclusive of extrasynaptic membranes and that these subunits have anomalous N-glycosylation in AD.

Importantly, amyloidosis and tauopathy animal models failed to recapitulate findings in humans, highlighting the complexity of the disease and the need for studying human brain tissue and human-relevant models.

A block of the thesis is, in fact, destined to explore how to achieve a human-relevant system to model the role of NMDARs in AD. To do so, we differentiated iPSC cells into iNeurons utilizing two neurodifferentiation protocols and evaluated two fundamental mechanisms for NMDAR maturation in each one. We described that NMDARs incorporate into the synapse in both protocols at day 60 with respect to day 30, a sign of synaptic maturation. Remarkably, we shed some light on the GluN2B-GluN2A switch, a crucial developmental process needed for a synapse to mature and, consequently, needed to have an appropriate model for neurodegenerative diseases such as AD. We demonstrate that astrocytes present in these cultures, especially in BPM, also express NMDARs. Intrigued by this fact, we developed a pure astrocytic culture and discovered that they express NMDARs as well. This paves the way for future studies addressing the role of astrocytic-NMDARs in AD.

Furthermore, we described NMDARs as being present in human CSF for the first time and that GluN2A levels are lower in AD CSF. A possible continuation of this research is to investigate the mechanism behind the presence of NMDARs in the CSF. It would be interesting to explore in iNeurons whether there is a mechanism for the exocytosis of NMDARs to the media and why there is a reduction of GluN2A, but not GluN2B, in the CSF.

Finally, we embrace label-free shotgun proteomics to uncover the synaptic and extrasynaptic proteome in the AD human brain, a strategy that has not been previously performed and that allowed us to gain insight into the differential proteome of these two subcellular localizations.

One of the most relevant results of this thesis is the high levels of ExsynNMDARs in the AD brain with respect to controls. In Section 5.1 it has been discussed some mechanisms that could underlie this increase in levels, such as lateral diffusion, impaired endocytosis, or failure in synaptic delivery due to anomalous N-glycosylation. Interestingly, impaired endocytosis, intracellular transport of proteins, glycosylation, and transport to plasma membrane were recurrent GO terms in our datasets, which supports the idea that these processes are affected by AD. All these mechanisms could be explored in iNeurons. Furthermore, the BPM protocol offers a good opportunity to test the participation of glia in the population of ExsynNMDARs due to the high number of astrocytes in these cultures.

Insights from the proteomic study help us to hypothesize additional mechanisms responsible for the increase in ExsynNMDARs in the AD brain related to cytoskeletal stabilization. CRMP1 is a protein that regulates F-actin depolymerization and is associated with synaptic plasticity mechanisms [424, 425]. *crmp1* KO mice present higher ExsynNMDAR levels than control mice and increased levels of phosphorylated tau, a hallmark of AD. Interestingly, we have found CRMP1 underexpressed in the AD ExsynF. Additionally, other proteins related to cytoskeletal stabilization were underexpressed in the AD SynF, such as Cell division control protein 42 homolog, Cytoplasmic FMR1-interacting protein 1, and Brain-specific angiogenesis inhibitor 1-associated protein 2. These data support a model in which destabilization of the cytoskeletal structure of the dendritic spine could lead to the exit of SynNMDARs to extrasynaptic membranes. The protocol for differentiation and maturation of iNeurons designed in this thesis, which incorporates NMDARs into synapses on day 60, is presented as a good model for testing this hypothesis.

The thesis pursues a translational objective. The results obtained here have the potential to explore 1) targeted therapies aimed to restore the NMDAR imbalance found in the AD brain, 2) the usefulness of measuring NMDARs in CSF as a diagnostic tool or to stratify patients with

neurodegenerative diseases, 3) the use of patient-derived iNeurons to gain insight into fundamental AD biology and ultimately pursue personalized medicine, and 4) to discover new proteins and biological processes affected in AD.

Taken together, these findings underscore the importance of NMDARs as key modulators of AD and provide a framework for future research aimed at slowing the progression of this devastating disease.

6. Conclusions

Conclusions in English:

1. The biochemical fractionation developed here is suitable for studying synaptic and extrasynaptic membranes from frozen human brain samples.
2. NMDAR subunits GluN2A and GluN2B levels are lower in the synaptic fraction but higher in the extrasynaptic fraction of AD cortex.
3. A new 160 kDa glycoform of GluN2A and GluN2B is discovered exclusively in the extrasynaptic fraction.
4. N-glycosylation is altered in extrasynaptic GluN2A and GluN2B in the AD cortex.
5. According to our data, animal models for amyloidosis and tauopathy recapitulate only partially some features of AD.
6. NMDARs are present in CSF.
7. GluN2A levels are lower in the AD CSF, and GluN3A levels are higher in the HD CSF.
8. Both NMM and BPM iNeurons increase synaptic NMDARs with maturation.
9. Only iNeurons from BPM show signs compatible with the GluN2B-GluN2A switch, although further research at the synapse level is needed.
10. A β decreases *GRIN2A* and *GRIN2B* expression and decreases synaptic NMDARs in NMM but not BPM.

Conclusiones en español:

1. La fraccionación bioquímica desarrollada aquí es adecuada para estudiar las membranas sinápticas y extrasinápticas a partir de muestras de cerebro humano congelado.
2. Los niveles de las subunidades GluN2A y GluN2B de los NMDAR son más bajos en la fracción sináptica, pero más altos en la fracción extrasináptica de la corteza con EA.
3. Se descubre una nueva glicoforma de 160 kDa de GluN2A y GluN2B exclusivamente en la fracción extrasináptica.
4. La N-glicosilación está alterada en las subunidades extrasinápticas GluN2A y GluN2B en la corteza con EA.
5. Según nuestros datos, los modelos animales para la amiloidosis y tauopatía solo recapitulan parcialmente algunas características de la EA.
6. Los NMDAR están presentes en el líquido cefalorraquídeo (CSF).

7. Los niveles de GluN2A son más bajos en el CSF de pacientes con EA, y los niveles de GluN3A son más altos en el CSF de pacientes con EH.
8. Tanto las iNeurons en NMM como en BPM aumentan los NMDAR sinápticos con la maduración.
9. Solo las iNeurons de BPM muestran signos compatibles con el cambio de GluN2B a GluN2A, aunque se necesita más investigación a nivel sináptico.
10. El A β disminuye la expresión de GRIN2A y GRIN2B y reduce los NMDAR sinápticos en NMM, pero no en BPM.

7. References

1. Blennow, K., M.J. de Leon, and H. Zetterberg, *Alzheimer's disease*. Lancet, 2006. **368**(9533): p. 387-403.
2. Winblad, B., et al., *Defeating Alzheimer's disease and other dementias: a priority for European science and society*. Lancet Neurol, 2016. **15**(5): p. 455-532.
3. Qiu, C., M. Kivipelto, and E. von Strauss, *Epidemiology of Alzheimer's disease: occurrence, determinants, and strategies toward intervention*. Dialogues Clin Neurosci, 2009. **11**(2): p. 111-28.
4. Zhang, X.X., et al., *The Epidemiology of Alzheimer's Disease Modifiable Risk Factors and Prevention*. J Prev Alzheimers Dis, 2021. **8**(3): p. 313-321.
5. Gustavsson, A., et al., *Predictors of costs of care in Alzheimer's disease: a multinational sample of 1222 patients*. Alzheimers Dement, 2011. **7**(3): p. 318-27.
6. Wimo, A., et al., *The worldwide economic impact of dementia 2010*. Alzheimers Dement, 2013. **9**(1): p. 1-11.e3.
7. Wong, W., *Economic burden of Alzheimer disease and managed care considerations*. Am J Manag Care, 2020. **26**(8 Suppl): p. S177-S183.
8. world health, o., *FIRST WHO MINISTERIAL CONFERENCE ON GLOBAL ACTION AGAINST DEMENTIA: 16-17 MARCH 2015, GENEVA, SWITZERLAND MEETING REPORT*. 2015: World Health Organization.
9. Rizzuto, D., et al., *Dementia after age 75: survival in different severity stages and years of life lost*. Curr Alzheimer Res, 2012. **9**(7): p. 795-800.
10. Steele, C., et al., *Psychiatric symptoms and nursing home placement of patients with Alzheimer's disease*. Am J Psychiatry, 1990. **147**(8): p. 1049-51.
11. Mirra, S.S., et al., *The Consortium to Establish a Registry for Alzheimer's Disease (CERAD). Part II. Standardization of the neuropathologic assessment of Alzheimer's disease*. Neurology, 1991. **41**(4): p. 479-86.
12. Murayama, S. and Y. Saito, *Neuropathological diagnostic criteria for Alzheimer's disease*. Neuropathology, 2004. **24**(3): p. 254-60.
13. Braak, H. and E. Braak, *Neuropathological staging of Alzheimer-related changes*. Acta Neuropathol, 1991. **82**(4): p. 239-59.
14. Braak, H., et al., *Staging of Alzheimer disease-associated neurofibrillary pathology using paraffin sections and immunocytochemistry*. Acta Neuropathol, 2006. **112**(4): p. 389-404.
15. Hampel, H., et al., *The amyloid- β pathway in Alzheimer's disease: a plain language summary*. Neurodegener Dis Manag, 2023. **13**(3): p. 141-149.
16. Thal, D.R., et al., *Phases of A beta-deposition in the human brain and its relevance for the development of AD*. Neurology, 2002. **58**(12): p. 1791-800.
17. Medeiros, R., D. Baglietto-Vargas, and F.M. LaFerla, *The role of tau in Alzheimer's disease and related disorders*. CNS Neurosci Ther, 2011. **17**(5): p. 514-24.
18. Braak, H. and K. Del Tredici, *The preclinical phase of the pathological process underlying sporadic Alzheimer's disease*. Brain, 2015. **138**(Pt 10): p. 2814-33.
19. Vogel, J.W., et al., *Spread of pathological tau proteins through communicating neurons in human Alzheimer's disease*. Nat Commun, 2020. **11**(1): p. 2612.
20. Xia, C., et al., *Association of In Vivo [18F]AV-1451 Tau PET Imaging Results With Cortical Atrophy and Symptoms in Typical and Atypical Alzheimer Disease*. JAMA Neurol, 2017. **74**(4): p. 427-436.
21. Lane, C.A., J. Hardy, and J.M. Schott, *Alzheimer's disease*. Eur J Neurol, 2018. **25**(1): p. 59-70.
22. Loy, C.T., et al., *Genetics of dementia*. Lancet, 2014. **383**(9919): p. 828-40.

23. Sepulveda-Falla, D., M. Glatzel, and F. Lopera, *Phenotypic profile of early-onset familial Alzheimer's disease caused by presenilin-1 E280A mutation*. J Alzheimers Dis, 2012. **32**(1): p. 1-12.
24. Mendez, M.F., *Early-onset Alzheimer Disease and Its Variants*. Continuum (Minneapolis), 2019. **25**(1): p. 34-51.
25. Misra, A., S.S. Chakrabarti, and I.S. Gambhir, *New genetic players in late-onset Alzheimer's disease: Findings of genome-wide association studies*. Indian J Med Res, 2018. **148**(2): p. 135-144.
26. Zimmerman, S.C., et al., *Association of Genetic Variants Linked to Late-Onset Alzheimer Disease With Cognitive Test Performance by Midlife*. JAMA Netw Open, 2022. **5**(4): p. e225491.
27. Andrews, S.J., et al., *The complex genetic architecture of Alzheimer's disease: novel insights and future directions*. EBioMedicine, 2023. **90**: p. 104511.
28. Guest, P.C. and SpringerLink, *Reviews on Biomarker Studies in Psychiatric and Neurodegenerative Disorders*. 1st 2019. ed. Proteomics, Metabolomics, Interactomics and Systems Biology 1118. 2019, Cham: Springer International Publishing : Imprint: Springer.
29. Corder, E.H., et al., *Gene dose of apolipoprotein E type 4 allele and the risk of Alzheimer's disease in late onset families*. Science, 1993. **261**(5123): p. 921-3.
30. Yamazaki, Y., et al., *Apolipoprotein E and Alzheimer disease: pathobiology and targeting strategies*. Nat Rev Neurol, 2019. **15**(9): p. 501-518.
31. Fortea, J., et al., *APOE4 homozygosity represents a distinct genetic form of Alzheimer's disease*. Nat Med, 2024.
32. Elliott, D.A., G.M. Halliday, and B. Garner, *Apolipoprotein-E forms dimers in human frontal cortex and hippocampus*. BMC Neurosci, 2010. **11**: p. 23.
33. Rebeck, G.W., *The role of APOE on lipid homeostasis and inflammation in normal brains*. J Lipid Res, 2017. **58**(8): p. 1493-1499.
34. Kanekiyo, T., H. Xu, and G. Bu, *ApoE and A β in Alzheimer's disease: accidental encounters or partners?* Neuron, 2014. **81**(4): p. 740-54.
35. Husain, M.A., B. Laurent, and M. Plourde, *APOE and Alzheimer's Disease: From Lipid Transport to Physiopathology and Therapeutics*. Front Neurosci, 2021. **15**: p. 630502.
36. Karran, E. and B. De Strooper, *The amyloid cascade hypothesis: are we poised for success or failure?* J Neurochem, 2016. **139** Suppl 2: p. 237-252.
37. Hardy, J.A. and G.A. Higgins, *Alzheimer's disease: the amyloid cascade hypothesis*. Science, 1992. **256**(5054): p. 184-5.
38. Wildsmith, K.R., et al., *Evidence for impaired amyloid β clearance in Alzheimer's disease*. Alzheimers Res Ther, 2013. **5**(4): p. 33.
39. Karran, E. and B. De Strooper, *The amyloid hypothesis in Alzheimer disease: new insights from new therapeutics*. Nat Rev Drug Discov, 2022. **21**(4): p. 306-318.
40. Lakatos, I., *The methodology of scientific research programmes*. His Philosophical papers v 1. 1978, Cambridge ; New York: Cambridge University Press. viii, 250 p.
41. Selkoe, D.J., *Alzheimer's disease is a synaptic failure*. Science, 2002. **298**(5594): p. 789-91.
42. Meftah, S. and J. Gan, *Alzheimer's disease as a synaptopathy: Evidence for dysfunction of synapses during disease progression*. Front Synaptic Neurosci, 2023. **15**: p. 1129036.
43. Sheng, M., B.L. Sabatini, and T.C. Südhof, *Synapses and Alzheimer's disease*. Cold Spring Harb Perspect Biol, 2012. **4**(5).
44. DeKosky, S.T. and S.W. Scheff, *Synapse loss in frontal cortex biopsies in Alzheimer's disease: correlation with cognitive severity*. Ann Neurol, 1990. **27**(5): p. 457-64.
45. Terry, R.D., et al., *Physical basis of cognitive alterations in Alzheimer's disease: synapse loss is the major correlate of cognitive impairment*. Ann Neurol, 1991. **30**(4): p. 572-80.

46. Tzioras, M., et al., *Synaptic degeneration in Alzheimer disease*. Nat Rev Neurol, 2023. **19**(1): p. 19-38.
47. Chen, Y., A.K.Y. Fu, and N.Y. Ip, *Synaptic dysfunction in Alzheimer's disease: Mechanisms and therapeutic strategies*. Pharmacol Ther, 2019. **195**: p. 186-198.
48. Harris, S.S., et al., *Tipping the Scales: Peptide-Dependent Dysregulation of Neural Circuit Dynamics in Alzheimer's Disease*. Neuron, 2020. **107**(3): p. 417-435.
49. Scaduto, P., et al., *Functional excitatory to inhibitory synaptic imbalance and loss of cognitive performance in people with Alzheimer's disease neuropathologic change*. Acta Neuropathol, 2023. **145**(3): p. 303-324.
50. Peng, L., I. Bestard-Lorigados, and W. Song, *The synapse as a treatment avenue for Alzheimer's Disease*. Mol Psychiatry, 2022. **27**(7): p. 2940-2949.
51. Jackson, J., et al., *Targeting the Synapse in Alzheimer's Disease*. Front Neurosci, 2019. **13**: p. 735.
52. Wilkinson, D., *A review of the effects of memantine on clinical progression in Alzheimer's disease*. Int J Geriatr Psychiatry, 2012. **27**(8): p. 769-76.
53. Chen, H.S., et al., *Open-channel block of N-methyl-D-aspartate (NMDA) responses by memantine: therapeutic advantage against NMDA receptor-mediated neurotoxicity*. J Neurosci, 1992. **12**(11): p. 4427-36.
54. Moreta, M.P., et al., *Efficacy of Acetylcholinesterase Inhibitors on Cognitive Function in Alzheimer's Disease. Review of Reviews*. Biomedicines, 2021. **9**(11).
55. Swerdlow, R.H., J.M. Burns, and S.M. Khan, *The Alzheimer's disease mitochondrial cascade hypothesis: progress and perspectives*. Biochim Biophys Acta, 2014. **1842**(8): p. 1219-31.
56. Parker, W.D., C.M. Filley, and J.K. Parks, *Cytochrome oxidase deficiency in Alzheimer's disease*. Neurology, 1990. **40**(8): p. 1302-3.
57. Hirai, K., et al., *Mitochondrial abnormalities in Alzheimer's disease*. J Neurosci, 2001. **21**(9): p. 3017-23.
58. Webster, M.T., et al., *The effects of perturbed energy metabolism on the processing of amyloid precursor protein in PC12 cells*. J Neural Transm (Vienna), 1998. **105**(8-9): p. 839-53.
59. Gabuzda, D., et al., *Inhibition of energy metabolism alters the processing of amyloid precursor protein and induces a potentially amyloidogenic derivative*. J Biol Chem, 1994. **269**(18): p. 13623-8.
60. Wallace, D.C., *Mitochondrial genetics: a paradigm for aging and degenerative diseases?* Science, 1992. **256**(5057): p. 628-32.
61. Lin, M.T., et al., *High aggregate burden of somatic mtDNA point mutations in aging and Alzheimer's disease brain*. Hum Mol Genet, 2002. **11**(2): p. 133-45.
62. Ashleigh, T., R.H. Swerdlow, and M.F. Beal, *The role of mitochondrial dysfunction in Alzheimer's disease pathogenesis*. Alzheimers Dement, 2023. **19**(1): p. 333-342.
63. Yassine, H.N., et al., *Nutritional metabolism and cerebral bioenergetics in Alzheimer's disease and related dementias*. Alzheimers Dement, 2023. **19**(3): p. 1041-1066.
64. Small, S.A. and K. Duff, *Linking Abeta and tau in late-onset Alzheimer's disease: a dual pathway hypothesis*. Neuron, 2008. **60**(4): p. 534-42.
65. Hoyer, S., *Abnormalities of glucose metabolism in Alzheimer's disease*. Ann N Y Acad Sci, 1991. **640**: p. 53-8.
66. Morgen, K. and L. Frölich, *The metabolism hypothesis of Alzheimer's disease: from the concept of central insulin resistance and associated consequences to insulin therapy*. J Neural Transm (Vienna), 2015. **122**(4): p. 499-504.
67. de la Torre, J.C., *Is Alzheimer's disease a neurodegenerative or a vascular disorder? Data, dogma, and dialectics*. Lancet Neurol, 2004. **3**(3): p. 184-90.
68. Sagare, A.P., R.D. Bell, and B.V. Zlokovic, *Neurovascular dysfunction and faulty amyloid β -peptide clearance in Alzheimer disease*. Cold Spring Harb Perspect Med, 2012. **2**(10).

69. Marchesi, V.T., *Alzheimer's dementia begins as a disease of small blood vessels, damaged by oxidative-induced inflammation and dysregulated amyloid metabolism: implications for early detection and therapy*. FASEB J, 2011. **25**(1): p. 5-13.
70. Kumar-Singh, S., et al., *Dense-core plaques in Tg2576 and PSAPP mouse models of Alzheimer's disease are centered on vessel walls*. Am J Pathol, 2005. **167**(2): p. 527-43.
71. Walsh, D.M. and D.J. Selkoe, *A beta oligomers - a decade of discovery*. J Neurochem, 2007. **101**(5): p. 1172-84.
72. Heneka, M.T., et al., *Neuroinflammation in Alzheimer's disease*. Lancet Neurol, 2015. **14**(4): p. 388-405.
73. Leng, F. and P. Edison, *Neuroinflammation and microglial activation in Alzheimer disease: where do we go from here?* Nat Rev Neurol, 2021. **17**(3): p. 157-172.
74. Thakur, S., et al., *Neuroinflammation in Alzheimer's Disease: Current Progress in Molecular Signaling and Therapeutics*. Inflammation, 2023. **46**(1): p. 1-17.
75. Wang, C., et al., *The effects of microglia-associated neuroinflammation on Alzheimer's disease*. Front Immunol, 2023. **14**: p. 1117172.
76. Kinney, J.W., et al., *Inflammation as a central mechanism in Alzheimer's disease*. Alzheimers Dement (N Y), 2018. **4**: p. 575-590.
77. Li, R., X. Wang, and P. He, *The most prevalent rare coding variants of TREM2 conferring risk of Alzheimer's disease: A systematic review and meta-analysis*. Exp Ther Med, 2021. **21**(4): p. 347.
78. Griciuc, A. and R.E. Tanzi, *The role of innate immune genes in Alzheimer's disease*. Curr Opin Neurol, 2021. **34**(2): p. 228-236.
79. Takatori, S., et al., *Genetic Risk Factors for Alzheimer Disease: Emerging Roles of Microglia in Disease Pathomechanisms*. Adv Exp Med Biol, 2019. **1118**: p. 83-116.
80. Eef, H., E. Hogervorst, and ProQuest, *Hormones, cognition, and dementia : state of the art and emergent therapeutic strategies*. 1st ed. Cambridge medicine. 2009, Cambridge ; New York: Cambridge University Press.
81. Sumien, N., et al., *Neurodegenerative Disease: Roles for Sex, Hormones, and Oxidative Stress*. Endocrinology, 2021. **162**(11).
82. Xiong, J., et al., *FSH and ApoE4 contribute to Alzheimer's disease-like pathogenesis via C/EBP β / δ -secretase in female mice*. Nat Commun, 2023. **14**(1): p. 6577.
83. Xiong, J., et al., *FSH blockade improves cognition in mice with Alzheimer's disease*. Nature, 2022. **603**(7901): p. 470-476.
84. Valencia-Olvera, A.C., et al., *Role of estrogen in women's Alzheimer's disease risk as modified by APOE*. J Neuroendocrinol, 2023. **35**(2): p. e13209.
85. Hogervorst, E., et al., *Low free testosterone is an independent risk factor for Alzheimer's disease*. Exp Gerontol, 2004. **39**(11-12): p. 1633-9.
86. Escamilla, S. and F. Salas-Lucia, *Thyroid Hormone and Alzheimer's: Bridging Epidemiology to Mechanism*. Endocrinology, 2024.
87. Quinlan, P., et al., *Altered thyroid hormone profile in patients with Alzheimer's disease*. Psychoneuroendocrinology, 2020. **121**: p. 104844.
88. Figueroa, P.B.S., et al., *Association between thyroid function and Alzheimer's disease: A systematic review*. Metab Brain Dis, 2021. **36**(7): p. 1523-1543.
89. Li, Z. and J. Liu, *Thyroid dysfunction and Alzheimer's disease, a vicious circle*. Front Endocrinol (Lausanne), 2024. **15**: p. 1354372.
90. Accorroni, A., et al., *Thyroid hormone levels in the cerebrospinal fluid correlate with disease severity in euthyroid patients with Alzheimer's disease*. Endocrine, 2017. **55**(3): p. 981-984.
91. Davis, J.D., et al., *Thyroid hormone levels in the prefrontal cortex of post-mortem brains of Alzheimer's disease patients*. Curr Aging Sci, 2008. **1**(3): p. 175-81.

92. Paoletti, P., C. Bellone, and Q. Zhou, *NMDA receptor subunit diversity: impact on receptor properties, synaptic plasticity and disease*. Nat Rev Neurosci, 2013. **14**(6): p. 383-400.
93. Sanz-Clemente, A., R.A. Nicoll, and K.W. Roche, *Diversity in NMDA Receptor Composition*. The Neuroscientist, 2013. **19**(1): p. 62-75.
94. Sanz-Clemente, A., R.A. Nicoll, and K.W. Roche, *Diversity in NMDA receptor composition: many regulators, many consequences*. Neuroscientist, 2013. **19**(1): p. 62-75.
95. Al-Hallaq, R.A., et al., *NMDA di-heteromeric receptor populations and associated proteins in rat hippocampus*. J Neurosci, 2007. **27**(31): p. 8334-43.
96. Rauner, C. and G. Köhr, *Triheteromeric NR1/NR2A/NR2B receptors constitute the major N-methyl-D-aspartate receptor population in adult hippocampal synapses*. J Biol Chem, 2011. **286**(9): p. 7558-66.
97. Pérez-Otaño, I., R.S. Larsen, and J.F. Wesseling, *Emerging roles of GluN3-containing NMDA receptors in the CNS*. Nat Rev Neurosci, 2016. **17**(10): p. 623-35.
98. Farrant, M., et al., *NMDA-receptor channel diversity in the developing cerebellum*. Nature, 1994. **368**(6469): p. 335-9.
99. Monyer, H., et al., *Developmental and regional expression in the rat brain and functional properties of four NMDA receptors*. Neuron, 1994. **12**(3): p. 529-40.
100. Paoletti, P., *Molecular basis of NMDA receptor functional diversity*. Eur J Neurosci, 2011. **33**(8): p. 1351-65.
101. Labrie, V. and J.C. Roder, *The involvement of the NMDA receptor D-serine/glycine site in the pathophysiology and treatment of schizophrenia*. Neurosci Biobehav Rev, 2010. **34**(3): p. 351-72.
102. Zhang, Y., et al., *Dysfunction of NMDA receptors in Alzheimer's disease*. Neurol Sci, 2016. **37**(7): p. 1039-47.
103. Henson, M.A., et al., *Influence of the NR3A subunit on NMDA receptor functions*. Prog Neurobiol, 2010. **91**(1): p. 23-37.
104. Ferreira, J.S., et al., *Co-agonists differentially tune GluN2B-NMDA receptor trafficking at hippocampal synapses*. Elife, 2017. **6**.
105. Herz, J. and Y. Chen, *Reelin, lipoprotein receptors and synaptic plasticity*. Nat Rev Neurosci, 2006. **7**(11): p. 850-9.
106. Chen, Y., et al., *ApoE4 reduces glutamate receptor function and synaptic plasticity by selectively impairing ApoE receptor recycling*. Proc Natl Acad Sci U S A, 2010. **107**(26): p. 12011-6.
107. Ishchenko, Y., M.G. Carrizales, and A.J. Koleske, *Regulation of the NMDA receptor by its cytoplasmic domains: (How) is the tail wagging the dog?* Neuropharmacology, 2021. **195**: p. 108634.
108. Groveman, B.R., et al., *The regulation of N-methyl-D-aspartate receptors by Src kinase*. FEBS J, 2012. **279**(1): p. 20-8.
109. Wang, Y., et al., *Cross talk between PI3K-AKT-GSK-3 β and PP2A pathways determines tau hyperphosphorylation*. Neurobiol Aging, 2015. **36**(1): p. 188-200.
110. Hunt, D.L. and P.E. Castillo, *Synaptic plasticity of NMDA receptors: mechanisms and functional implications*. Curr Opin Neurobiol, 2012. **22**(3): p. 496-508.
111. Morris, R.G., *NMDA receptors and memory encoding*. Neuropharmacology, 2013. **74**: p. 32-40.
112. Tsien, J.Z., P.T. Huerta, and S. Tonegawa, *The essential role of hippocampal CA1 NMDA receptor-dependent synaptic plasticity in spatial memory*. Cell, 1996. **87**(7): p. 1327-38.
113. Li, F. and J.Z. Tsien, *Memory and the NMDA receptors*. N Engl J Med, 2009. **361**(3): p. 302-3.
114. Sanhueza, M., et al., *Role of the CaMKII/NMDA receptor complex in the maintenance of synaptic strength*. J Neurosci, 2011. **31**(25): p. 9170-8.

115. Gardoni, F. and M. Di Luca, *Protein-protein interactions at the NMDA receptor complex: From synaptic retention to synaptonuclear protein messengers*. Neuropharmacology, 2021. **190**: p. 108551.
116. Dieterich, D.C., et al., *Caldendrin-Jacob: a protein liaison that couples NMDA receptor signalling to the nucleus*. PLoS Biol, 2008. **6**(2): p. e34.
117. Hardingham, G.E., Y. Fukunaga, and H. Bading, *Extrasynaptic NMDARs oppose synaptic NMDARs by triggering CREB shut-off and cell death pathways*. Nat Neurosci, 2002. **5**(5): p. 405-14.
118. Karpova, A., et al., *Encoding and transducing the synaptic or extrasynaptic origin of NMDA receptor signals to the nucleus*. Cell, 2013. **152**(5): p. 1119-33.
119. Shrimall, S., N.A. Cherepanova, and R. Gilmore, *Cotranslational and posttranslational N-glycosylation of proteins in the endoplasmic reticulum*. Semin Cell Dev Biol, 2015. **41**: p. 71-8.
120. Storey, G.P., X. Opitz-Araya, and A. Barria, *Molecular determinants controlling NMDA receptor synaptic incorporation*. J Neurosci, 2011. **31**(17): p. 6311-6.
121. Lichnerova, K., et al., *Two N-glycosylation Sites in the GluN1 Subunit Are Essential for Releasing N-methyl-D-aspartate (NMDA) Receptors from the Endoplasmic Reticulum*. J Biol Chem, 2015. **290**(30): p. 18379-90.
122. Huh, K.H. and R.J. Wenthold, *Turnover analysis of glutamate receptors identifies a rapidly degraded pool of the N-methyl-D-aspartate receptor subunit, NR1, in cultured cerebellar granule cells*. J Biol Chem, 1999. **274**(1): p. 151-7.
123. Bellone, C. and R.A. Nicoll, *Rapid bidirectional switching of synaptic NMDA receptors*. Neuron, 2007. **55**(5): p. 779-85.
124. Sanz-Clemente, A., et al., *Casein kinase 2 regulates the NR2 subunit composition of synaptic NMDA receptors*. Neuron, 2010. **67**(6): p. 984-96.
125. Matta, J.A., et al., *mGluR5 and NMDA receptors drive the experience- and activity-dependent NMDA receptor NR2B to NR2A subunit switch*. Neuron, 2011. **70**(2): p. 339-51.
126. Corbel, C., et al., *Developmental attenuation of N-methyl-D-aspartate receptor subunit expression by microRNAs*. Neural Dev, 2015. **10**: p. 20.
127. Parsons, M.P. and L.A. Raymond, *Extrasynaptic NMDA receptor involvement in central nervous system disorders*. Neuron, 2014. **82**(2): p. 279-93.
128. Gladding, C.M. and L.A. Raymond, *Mechanisms underlying NMDA receptor synaptic/extrasynaptic distribution and function*. Mol Cell Neurosci, 2011. **48**(4): p. 308-20.
129. Williams, J.M., et al., *Differential trafficking of AMPA and NMDA receptors during long-term potentiation in awake adult animals*. J Neurosci, 2007. **27**(51): p. 14171-8.
130. Grosshans, D.R., et al., *LTP leads to rapid surface expression of NMDA but not AMPA receptors in adult rat CA1*. Nat Neurosci, 2002. **5**(1): p. 27-33.
131. Chen, B.S. and K.W. Roche, *Regulation of NMDA receptors by phosphorylation*. Neuropharmacology, 2007. **53**(3): p. 362-8.
132. Khan, R., D. Kulasiri, and S. Samarasinghe, *Functional repertoire of protein kinases and phosphatases in synaptic plasticity and associated neurological disorders*. Neural Regen Res, 2021. **16**(6): p. 1150-1157.
133. Nakazawa, T., et al., *Characterization of Fyn-mediated tyrosine phosphorylation sites on GluR epsilon 2 (NR2B) subunit of the N-methyl-D-aspartate receptor*. J Biol Chem, 2001. **276**(1): p. 693-9.
134. Rostas, J.A., et al., *Enhanced tyrosine phosphorylation of the 2B subunit of the N-methyl-D-aspartate receptor in long-term potentiation*. Proc Natl Acad Sci U S A, 1996. **93**(19): p. 10452-6.
135. Takasu, M.A., et al., *Modulation of NMDA receptor-dependent calcium influx and gene expression through EphB receptors*. Science, 2002. **295**(5554): p. 491-5.

136. Lavezzari, G., et al., *Differential binding of the AP-2 adaptor complex and PSD-95 to the C-terminus of the NMDA receptor subunit NR2B regulates surface expression*. Neuropharmacology, 2003. **45**(6): p. 729-37.
137. Prybylowski, K., et al., *The synaptic localization of NR2B-containing NMDA receptors is controlled by interactions with PDZ proteins and AP-2*. Neuron, 2005. **47**(6): p. 845-57.
138. Groc, L., et al., *NMDA receptor surface mobility depends on NR2A-2B subunits*. Proc Natl Acad Sci U S A, 2006. **103**(49): p. 18769-74.
139. Erreger, K., et al., *Subunit-specific gating controls rat NR1/NR2A and NR1/NR2B NMDA channel kinetics and synaptic signalling profiles*. J Physiol, 2005. **563**(Pt 2): p. 345-58.
140. Vicini, S., et al., *Functional and pharmacological differences between recombinant N-methyl-D-aspartate receptors*. J Neurophysiol, 1998. **79**(2): p. 555-66.
141. Gray, J.A., et al., *Distinct modes of AMPA receptor suppression at developing synapses by GluN2A and GluN2B: single-cell NMDA receptor subunit deletion in vivo*. Neuron, 2011. **71**(6): p. 1085-101.
142. Raïch, I., et al., *Dual Role of NMDAR Containing NR2A and NR2B Subunits in Alzheimer's Disease*. Int J Mol Sci, 2024. **25**(9).
143. Thomas, C.G., A.J. Miller, and G.L. Westbrook, *Synaptic and extrasynaptic NMDA receptor NR2 subunits in cultured hippocampal neurons*. J Neurophysiol, 2006. **95**(3): p. 1727-34.
144. Petralia, R.S., et al., *Organization of NMDA receptors at extrasynaptic locations*. Neuroscience, 2010. **167**(1): p. 68-87.
145. Petralia, R.S., *Distribution of extrasynaptic NMDA receptors on neurons*. ScientificWorldJournal, 2012. **2012**: p. 267120.
146. Yan, J., et al., *Coupling of NMDA receptors and TRPM4 guides discovery of unconventional neuroprotectants*. Science, 2020. **370**(6513).
147. Skowrońska, K., et al., *NMDA Receptors in Astrocytes: In Search for Roles in Neurotransmission and Astrocytic Homeostasis*. Int J Mol Sci, 2019. **20**(2).
148. Kirchhoff, F., *Analysis of Functional NMDA Receptors in Astrocytes*. Methods Mol Biol, 2017. **1677**: p. 241-251.
149. Káradóttir, R., et al., *NMDA receptors are expressed in oligodendrocytes and activated in ischaemia*. Nature, 2005. **438**(7071): p. 1162-6.
150. Raghunatha, P., et al., *Microglial NMDA receptors drive pro-inflammatory responses via PARP-1/TRMP2 signaling*. Glia, 2020. **68**(7): p. 1421-1434.
151. Booker, S.A. and D.J.A. Wyllie, *NMDA receptor function in inhibitory neurons*. Neuropharmacology, 2021. **196**: p. 108609.
152. Banerjee, A., et al., *Roles of Presynaptic NMDA Receptors in Neurotransmission and Plasticity*. Trends Neurosci, 2016. **39**(1): p. 26-39.
153. Papouin, T. and S.H. Oliet, *Organization, control and function of extrasynaptic NMDA receptors*. Philos Trans R Soc Lond B Biol Sci, 2014. **369**(1654): p. 20130601.
154. Chen, X., et al., *Organization of the core structure of the postsynaptic density*. Proc Natl Acad Sci U S A, 2008. **105**(11): p. 4453-8.
155. Hardingham, G.E. and H. Bading, *Synaptic versus extrasynaptic NMDA receptor signalling: implications for neurodegenerative disorders*. Nat Rev Neurosci, 2010. **11**(10): p. 682-96.
156. Ivanov, A., et al., *Opposing role of synaptic and extrasynaptic NMDA receptors in regulation of the extracellular signal-regulated kinases (ERK) activity in cultured rat hippocampal neurons*. J Physiol, 2006. **572**(Pt 3): p. 789-98.
157. Lau, D. and H. Bading, *Synaptic activity-mediated suppression of p53 and induction of nuclear calcium-regulated neuroprotective genes promote survival through inhibition of mitochondrial permeability transition*. J Neurosci, 2009. **29**(14): p. 4420-9.
158. Léveillé, F., et al., *Suppression of the intrinsic apoptosis pathway by synaptic activity*. J Neurosci, 2010. **30**(7): p. 2623-35.

159. Röncke, R., et al., *Early neuronal dysfunction by amyloid β oligomers depends on activation of NR2B-containing NMDA receptors*. *Neurobiol Aging*, 2011. **32**(12): p. 2219-28.
160. Dick, O. and H. Bading, *Synaptic activity and nuclear calcium signaling protect hippocampal neurons from death signal-associated nuclear translocation of FoxO3a induced by extrasynaptic N-methyl-D-aspartate receptors*. *J Biol Chem*, 2010. **285**(25): p. 19354-61.
161. Vanhoutte, P. and H. Bading, *Opposing roles of synaptic and extrasynaptic NMDA receptors in neuronal calcium signalling and BDNF gene regulation*. *Curr Opin Neurobiol*, 2003. **13**(3): p. 366-71.
162. Liu, Y., et al., *NMDA receptor subunits have differential roles in mediating excitotoxic neuronal death both in vitro and in vivo*. *J Neurosci*, 2007. **27**(11): p. 2846-57.
163. Papadia, S., et al., *Synaptic NMDA receptor activity boosts intrinsic antioxidant defenses*. *Nat Neurosci*, 2008. **11**(4): p. 476-87.
164. Martel, M.A., D.J. Wyllie, and G.E. Hardingham, *In developing hippocampal neurons, NR2B-containing N-methyl-D-aspartate receptors (NMDARs) can mediate signaling to neuronal survival and synaptic potentiation, as well as neuronal death*. *Neuroscience*, 2009. **158**(1): p. 334-43.
165. von Engelhardt, J., et al., *Excitotoxicity in vitro by NR2A- and NR2B-containing NMDA receptors*. *Neuropharmacology*, 2007. **53**(1): p. 10-7.
166. Yu, S.P., et al., *Extrasynaptic NMDA receptors in acute and chronic excitotoxicity: implications for preventive treatments of ischemic stroke and late-onset Alzheimer's disease*. *Mol Neurodegener*, 2023. **18**(1): p. 43.
167. Bading, H., *Therapeutic targeting of the pathological triad of extrasynaptic NMDA receptor signaling in neurodegenerations*. *Journal of Experimental Medicine*, 2017. **214**(3): p. 569-578.
168. Carles, A., et al., *Targeting*. *Int J Mol Sci*, 2024. **25**(7).
169. Masliah, E., et al., *Deficient glutamate transport is associated with neurodegeneration in Alzheimer's disease*. *Ann Neurol*, 1996. **40**(5): p. 759-66.
170. Jacob, C.P., et al., *Alterations in expression of glutamatergic transporters and receptors in sporadic Alzheimer's disease*. *J Alzheimers Dis*, 2007. **11**(1): p. 97-116.
171. Scott, H.A., et al., *Glutamate transporter variants reduce glutamate uptake in Alzheimer's disease*. *Neurobiol Aging*, 2011. **32**(3): p. 553.e1-11.
172. Xia, P., et al., *Memantine preferentially blocks extrasynaptic over synaptic NMDA receptor currents in hippocampal autapses*. *J Neurosci*, 2010. **30**(33): p. 11246-50.
173. Wu, Y.N. and S.W. Johnson, *Memantine selectively blocks extrasynaptic NMDA receptors in rat substantia nigra dopamine neurons*. *Brain Res*, 2015. **1603**: p. 1-7.
174. Léveillé, F., et al., *Neuronal viability is controlled by a functional relation between synaptic and extrasynaptic NMDA receptors*. *FASEB J*, 2008. **22**(12): p. 4258-71.
175. Folch, J., et al., *Memantine for the Treatment of Dementia: A Review on its Current and Future Applications*. *J Alzheimers Dis*, 2018. **62**(3): p. 1223-1240.
176. Parsons, C.G., et al., *Memantine and cholinesterase inhibitors: complementary mechanisms in the treatment of Alzheimer's disease*. *Neurotox Res*, 2013. **24**(3): p. 358-69.
177. Karimi Tari, P., et al., *Memantine: Updating a rare success story in pro-cognitive therapeutics*. *Neuropharmacology*, 2024. **244**: p. 109737.
178. Armada-Moreira, A., et al., *Going the Extra (Synaptic) Mile: Excitotoxicity as the Road Toward Neurodegenerative Diseases*. *Front Cell Neurosci*, 2020. **14**: p. 90.
179. Liu, J., et al., *The Role of NMDA Receptors in Alzheimer's Disease*. *Front Neurosci*, 2019. **13**: p. 43.

180. Liu, W., et al., *The role of N-methyl-D-aspartate glutamate receptors in Alzheimer's disease: From pathophysiology to therapeutic approaches*. Prog Neurobiol, 2023. **231**: p. 102534.
181. Talantova, M., et al., *A β induces astrocytic glutamate release, extrasynaptic NMDA receptor activation, and synaptic loss*. Proc Natl Acad Sci U S A, 2013. **110**(27): p. E2518-27.
182. Bordji, K., et al., *Activation of extrasynaptic, but not synaptic, NMDA receptors modifies amyloid precursor protein expression pattern and increases amyloid- β production*. J Neurosci, 2010. **30**(47): p. 15927-42.
183. Marshall, C.A., et al., *Inhibition of CK2 mitigates Alzheimer's tau pathology by preventing NR2B synaptic mislocalization*. Acta Neuropathol Commun, 2022. **10**(1): p. 30.
184. Sun, X.Y., et al., *Extrasynaptic NMDA receptor-induced tau overexpression mediates neuronal death through suppressing survival signaling ERK phosphorylation*. Cell Death Dis, 2016. **7**(11): p. e2449.
185. Xu, C.S., et al., *Overactivation of NR2B-containing NMDA receptors through entorhinal-hippocampal connection initiates accumulation of hyperphosphorylated tau in rat hippocampus after transient middle cerebral artery occlusion*. J Neurochem, 2015. **134**(3): p. 566-77.
186. Hoey, S.E., R.J. Williams, and M.S. Perkinson, *Synaptic NMDA receptor activation stimulates alpha-secretase amyloid precursor protein processing and inhibits amyloid-beta production*. J Neurosci, 2009. **29**(14): p. 4442-60.
187. Mishizen-Eberz, A.J., et al., *Biochemical and molecular studies of NMDA receptor subunits NR1/2A/2B in hippocampal subregions throughout progression of Alzheimer's disease pathology*. Neurobiol Dis, 2004. **15**(1): p. 80-92.
188. Wang, Y., et al., *Effects of post-mortem delay on subunits of ionotropic glutamate receptors in human brain*. Brain Res Mol Brain Res, 2000. **80**(2): p. 123-31.
189. Hynd, M.R., H.L. Scott, and P.R. Dodd, *Differential expression of N-methyl-D-aspartate receptor NR2 isoforms in Alzheimer's disease*. J Neurochem, 2004. **90**(4): p. 913-9.
190. Sze, C., et al., *N-Methyl-D-aspartate receptor subunit proteins and their phosphorylation status are altered selectively in Alzheimer's disease*. J Neurol Sci, 2001. **182**(2): p. 151-9.
191. Ortiz-Sanz, C., et al., *Amyloid β / PKC-dependent alterations in NMDA receptor composition are detected in early stages of Alzheimer's disease*. Cell Death Dis, 2022. **13**(3): p. 253.
192. Kravitz, E., I. Gaisler-Salomon, and A. Biegon, *Hippocampal glutamate NMDA receptor loss tracks progression in Alzheimer's disease: quantitative autoradiography in postmortem human brain*. PLoS One, 2013. **8**(11): p. e81244.
193. Bi, H. and C.I. Sze, *N-methyl-D-aspartate receptor subunit NR2A and NR2B messenger RNA levels are altered in the hippocampus and entorhinal cortex in Alzheimer's disease*. J Neurol Sci, 2002. **200**(1-2): p. 11-8.
194. Hynd, M.R., H.L. Scott, and P.R. Dodd, *Glutamate(NMDA) receptor NR1 subunit mRNA expression in Alzheimer's disease*. J Neurochem, 2001. **78**(1): p. 175-82.
195. Lau, S.F., et al., *Single-nucleus transcriptome analysis reveals dysregulation of angiogenic endothelial cells and neuroprotective glia in Alzheimer's disease*. Proc Natl Acad Sci U S A, 2020. **117**(41): p. 25800-25809.
196. Das, S., et al., *Distinct transcriptomic responses to A β plaques, neurofibrillary tangles, and APOE in Alzheimer's disease*. Alzheimers Dement, 2024. **20**(1): p. 74-90.
197. Mathys, H., et al., *Single-cell transcriptomic analysis of Alzheimer's disease*. Nature, 2019. **570**(7761): p. 332-337.

198. Qian, Z., et al., *Large-Scale Integration of Single-Cell RNA-Seq Data Reveals Astrocyte Diversity and Transcriptomic Modules across Six Central Nervous System Disorders*. *Biomolecules*, 2023. **13**(4).
199. Sperling, R.A., et al., *Toward defining the preclinical stages of Alzheimer's disease: recommendations from the National Institute on Aging-Alzheimer's Association workgroups on diagnostic guidelines for Alzheimer's disease*. *Alzheimers Dement*, 2011. **7**(3): p. 280-92.
200. Molinuevo, J.L., et al., *Current state of Alzheimer's fluid biomarkers*. *Acta Neuropathol*, 2018. **136**(6): p. 821-853.
201. Márquez, F. and M.A. Yassa, *Neuroimaging Biomarkers for Alzheimer's Disease*. *Mol Neurodegener*, 2019. **14**(1): p. 21.
202. Hampel, H., et al., *Perspective on future role of biological markers in clinical therapy trials of Alzheimer's disease: a long-range point of view beyond 2020*. *Biochem Pharmacol*, 2014. **88**(4): p. 426-49.
203. Smets, N.G., et al., *Cerebrospinal fluid turnover as a driver of brain clearance*. *NMR Biomed*, 2024. **37**(7): p. e5029.
204. Blennow, K., et al., *Clinical utility of cerebrospinal fluid biomarkers in the diagnosis of early Alzheimer's disease*. *Alzheimers Dement*, 2015. **11**(1): p. 58-69.
205. Andreasen, N., et al., *Cerebrospinal fluid tau and Abeta42 as predictors of development of Alzheimer's disease in patients with mild cognitive impairment*. *Neurosci Lett*, 1999. **273**(1): p. 5-8.
206. Hansson, O., et al., *Association between CSF biomarkers and incipient Alzheimer's disease in patients with mild cognitive impairment: a follow-up study*. *Lancet Neurol*, 2006. **5**(3): p. 228-34.
207. Visser, P.J., et al., *Prevalence and prognostic value of CSF markers of Alzheimer's disease pathology in patients with subjective cognitive impairment or mild cognitive impairment in the DESCRIPA study: a prospective cohort study*. *Lancet Neurol*, 2009. **8**(7): p. 619-27.
208. Shaw, L.M., et al., *Cerebrospinal fluid biomarker signature in Alzheimer's disease neuroimaging initiative subjects*. *Ann Neurol*, 2009. **65**(4): p. 403-13.
209. Mattsson, N., et al., *CSF biomarkers and incipient Alzheimer disease in patients with mild cognitive impairment*. *JAMA*, 2009. **302**(4): p. 385-93.
210. Dubois, B., et al., *Research criteria for the diagnosis of Alzheimer's disease: revising the NINCDS-ADRDA criteria*. *Lancet Neurol*, 2007. **6**(8): p. 734-46.
211. Albert, M.S., et al., *The diagnosis of mild cognitive impairment due to Alzheimer's disease: recommendations from the National Institute on Aging-Alzheimer's Association workgroups on diagnostic guidelines for Alzheimer's disease*. *Alzheimers Dement*, 2011. **7**(3): p. 270-9.
212. McKhann, G.M., et al., *The diagnosis of dementia due to Alzheimer's disease: recommendations from the National Institute on Aging-Alzheimer's Association workgroups on diagnostic guidelines for Alzheimer's disease*. *Alzheimers Dement*, 2011. **7**(3): p. 263-9.
213. Blennow, K. and H. Zetterberg, *Biomarkers for Alzheimer's disease: current status and prospects for the future*. *J Intern Med*, 2018. **284**(6): p. 643-663.
214. Lleó, A., et al., *Changes in Synaptic Proteins Precede Neurodegeneration Markers in Preclinical Alzheimer's Disease Cerebrospinal Fluid*. *Mol Cell Proteomics*, 2019. **18**(3): p. 546-560.
215. Guo, Y., et al., *Multiplex cerebrospinal fluid proteomics identifies biomarkers for diagnosis and prediction of Alzheimer's disease*. *Nat Hum Behav*, 2024.
216. Dong, R., et al., *CSF metabolites associated with biomarkers of Alzheimer's disease pathology*. *Front Aging Neurosci*, 2023. **15**: p. 1214932.

217. Piccio, L., et al., *Cerebrospinal fluid soluble TREM2 is higher in Alzheimer disease and associated with mutation status*. *Acta Neuropathol*, 2016. **131**(6): p. 925-33.
218. Suárez-Calvet, M., et al., *sTREM2 cerebrospinal fluid levels are a potential biomarker for microglia activity in early-stage Alzheimer's disease and associate with neuronal injury markers*. *EMBO Mol Med*, 2016. **8**(5): p. 466-76.
219. Masliah, E., et al., *Altered expression of synaptic proteins occurs early during progression of Alzheimer's disease*. *Neurology*, 2001. **56**(1): p. 127-9.
220. Brinkmalm, A., et al., *SNAP-25 is a promising novel cerebrospinal fluid biomarker for synapse degeneration in Alzheimer's disease*. *Mol Neurodegener*, 2014. **9**: p. 53.
221. Cuchillo-Ibañez, I., et al., *Heteromers of amyloid precursor protein in cerebrospinal fluid*. *Mol Neurodegener*, 2015. **10**: p. 2.
222. Lopez-Font, I., et al., *Characterization of Cerebrospinal Fluid BACE1 Species*. *Mol Neurobiol*, 2019. **56**(12): p. 8603-8616.
223. Sogorb-Esteve, A., et al., *Levels of ADAM10 are reduced in Alzheimer's disease CSF*. *J Neuroinflammation*, 2018. **15**(1): p. 213.
224. García-Ayllón, M.S., et al., *Plasma ACE2 species are differentially altered in COVID-19 patients*. *FASEB J*, 2021. **35**(8): p. e21745.
225. García-Ayllón, M.S., et al., *CSF Presenilin-1 complexes are increased in Alzheimer's disease*. *Acta Neuropathol Commun*, 2013. **1**: p. 46.
226. Dalmau, J., et al., *Anti-NMDA-receptor encephalitis: case series and analysis of the effects of antibodies*. *Lancet Neurol*, 2008. **7**(12): p. 1091-8.
227. Hughes, E.G., et al., *Cellular and synaptic mechanisms of anti-NMDA receptor encephalitis*. *J Neurosci*, 2010. **30**(17): p. 5866-75.
228. Chen, Z.Y. and Y. Zhang, *Animal models of Alzheimer's disease: Applications, evaluation, and perspectives*. *Zool Res*, 2022. **43**(6): p. 1026-1040.
229. Shea, Y.F., et al., *A systematic review of familial Alzheimer's disease: Differences in presentation of clinical features among three mutated genes and potential ethnic differences*. *J Formos Med Assoc*, 2016. **115**(2): p. 67-75.
230. Drummond, E. and T. Wisniewski, *Alzheimer's disease: experimental models and reality*. *Acta Neuropathol*, 2017. **133**(2): p. 155-175.
231. Games, D., et al., *Alzheimer-type neuropathology in transgenic mice overexpressing V717F beta-amyloid precursor protein*. *Nature*, 1995. **373**(6514): p. 523-7.
232. Hsiao, K., et al., *Correlative memory deficits, Abeta elevation, and amyloid plaques in transgenic mice*. *Science*, 1996. **274**(5284): p. 99-102.
233. Allen, B., et al., *Abundant tau filaments and nonapoptotic neurodegeneration in transgenic mice expressing human P301S tau protein*. *J Neurosci*, 2002. **22**(21): p. 9340-51.
234. Yokoyama, M., et al., *Mouse Models of Alzheimer's Disease*. *Front Mol Neurosci*, 2022. **15**: p. 912995.
235. Kamat, P.K. and C. Nath, *Okadaic acid: a tool to study regulatory mechanisms for neurodegeneration and regeneration in Alzheimer's disease*. *Neural Regen Res*, 2015. **10**(3): p. 365-7.
236. Saito, T., et al., *Single App knock-in mouse models of Alzheimer's disease*. *Nat Neurosci*, 2014. **17**(5): p. 661-3.
237. Zhao, J., et al., *APOE4 exacerbates synapse loss and neurodegeneration in Alzheimer's disease patient iPSC-derived cerebral organoids*. *Nat Commun*, 2020. **11**(1): p. 5540.
238. Barak, M., et al., *Human iPSC-Derived Neural Models for Studying Alzheimer's Disease: from Neural Stem Cells to Cerebral Organoids*. *Stem Cell Rev Rep*, 2022. **18**(2): p. 792-820.
239. Marei, H.E., M.U.A. Khan, and A. Hasan, *Potential use of iPSCs for disease modeling, drug screening, and cell-based therapy for Alzheimer's disease*. *Cell Mol Biol Lett*, 2023. **28**(1): p. 98.

240. Cerneckis, J., H. Cai, and Y. Shi, *Induced pluripotent stem cells (iPSCs): molecular mechanisms of induction and applications*. Signal Transduct Target Ther, 2024. **9**(1): p. 112.
241. Takahashi, K. and S. Yamanaka, *Induction of pluripotent stem cells from mouse embryonic and adult fibroblast cultures by defined factors*. Cell, 2006. **126**(4): p. 663-76.
242. Ochalek, A., et al., *Neurons derived from sporadic Alzheimer's disease iPSCs reveal elevated TAU hyperphosphorylation, increased amyloid levels, and GSK3B activation*. Alzheimers Res Ther, 2017. **9**(1): p. 90.
243. Oakley, D.H., et al., *β -Amyloid species production and tau phosphorylation in iPSC-neurons with reference to neuropathologically characterized matched donor brains*. J Neuropathol Exp Neurol, 2024.
244. Voulgaris, D., P. Nikolakopoulou, and A. Herland, *Generation of Human iPSC-Derived Astrocytes with a mature star-shaped phenotype for CNS modeling*. Stem Cell Rev Rep, 2022. **18**(7): p. 2494-2512.
245. Ramaswami, G., et al., *Transcriptional characterization of iPSC-derived microglia as a model for therapeutic development in neurodegeneration*. Sci Rep, 2024. **14**(1): p. 2153.
246. Cerneckis, J., G. Bu, and Y. Shi, *Pushing the boundaries of brain organoids to study Alzheimer's disease*. Trends Mol Med, 2023. **29**(8): p. 659-672.
247. Hu, N.W., et al., *Extracellular Forms of A β and Tau from iPSC Models of Alzheimer's Disease Disrupt Synaptic Plasticity*. Cell Rep, 2018. **23**(7): p. 1932-1938.
248. Meyer, K., et al., *REST and Neural Gene Network Dysregulation in iPSC Models of Alzheimer's Disease*. Cell Rep, 2019. **26**(5): p. 1112-1127.e9.
249. Oksanen, M., et al., *PSEN1 Mutant iPSC-Derived Model Reveals Severe Astrocyte Pathology in Alzheimer's Disease*. Stem Cell Reports, 2017. **9**(6): p. 1885-1897.
250. Raska, J., et al., *Generation of six human iPSC lines from patients with a familial Alzheimer's disease (n = 3) and sex- and age-matched healthy controls (n = 3)*. Stem Cell Res, 2021. **53**: p. 102379.
251. Riemens, R.J.M., G. Kenis, and T. van den Beucken, *Human-induced pluripotent stem cells as a model for studying sporadic Alzheimer's disease*. Neurobiol Learn Mem, 2020. **175**: p. 107318.
252. Verheijen, M.C.T., et al., *iPSC-derived cortical neurons to study sporadic Alzheimer disease: A transcriptome comparison with post-mortem brain samples*. Toxicol Lett, 2022. **356**: p. 89-99.
253. Rowland, H.A., N.M. Hooper, and K.A.B. Kellett, *Modelling Sporadic Alzheimer's Disease Using Induced Pluripotent Stem Cells*. Neurochem Res, 2018. **43**(12): p. 2179-2198.
254. Cohen, B.M. and K.C. Sonntag, *Identifying the earliest-occurring clinically targetable precursors of late-onset Alzheimer's disease*. EBioMedicine, 2024. **106**: p. 105238.
255. Morris, R., K.A. Black, and E.J. Stollar, *Uncovering protein function: from classification to complexes*. Essays Biochem, 2022. **66**(3): p. 255-285.
256. Ren, A.H., E.P. Diamandis, and V. Kulasingam, *Uncovering the Depths of the Human Proteome: Antibody-based Technologies for Ultrasensitive Multiplexed Protein Detection and Quantification*. Mol Cell Proteomics, 2021. **20**: p. 100155.
257. Nilsson, T., et al., *Mass spectrometry in high-throughput proteomics: ready for the big time*. Nat Methods, 2010. **7**(9): p. 681-5.
258. Bai, B., et al., *Proteomic landscape of Alzheimer's Disease: novel insights into pathogenesis and biomarker discovery*. Mol Neurodegener, 2021. **16**(1): p. 55.
259. Cui, M., C. Cheng, and L. Zhang, *High-throughput proteomics: a methodological mini-review*. Lab Invest, 2022. **102**(11): p. 1170-1181.
260. Wilhelm, M., et al., *Mass-spectrometry-based draft of the human proteome*. Nature, 2014. **509**(7502): p. 582-7.

261. Wingo, A.P., et al., *Integrating human brain proteomes with genome-wide association data implicates new proteins in Alzheimer's disease pathogenesis*. Nat Genet, 2021. **53**(2): p. 143-146.
262. Montero-Calle, A., et al., *Proteomics analysis of prefrontal cortex of Alzheimer's disease patients revealed dysregulated proteins in the disease and novel proteins associated with amyloid- β pathology*. Cell Mol Life Sci, 2023. **80**(6): p. 141.
263. Navarro-Lérida, I., M. Sánchez-Álvarez, and M. Del Pozo, *Post-Translational Modification and Subcellular Compartmentalization: Emerging Concepts on the Regulation and Physiopathological Relevance of RhoGTPases*. Cells, 2021. **10**(8).
264. Millar, A.H., et al., *The Scope, Functions, and Dynamics of Posttranslational Protein Modifications*. Annu Rev Plant Biol, 2019. **70**: p. 119-151.
265. Huang, Q., et al., *Human proteins with target sites of multiple post-translational modification types are more prone to be involved in disease*. J Proteome Res, 2014. **13**(6): p. 2735-48.
266. Mirzaei, H., M. Carrasco, and SpringerLink, *Modern Proteomics – Sample Preparation, Analysis and Practical Applications*. 1st 2016. ed. Advances in Experimental Medicine and Biology 919. 2016, Cham: Springer International Publishing : Imprint: Springer.
267. Kandigian, S.E., et al., *Proteomic characterization of post-mortem human brain tissue following ultracentrifugation-based subcellular fractionation*. Brain Commun, 2022. **4**(3): p. fcac103.
268. Bayés, À., et al., *Human post-mortem synapse proteome integrity screening for proteomic studies of postsynaptic complexes*. Mol Brain, 2014. **7**: p. 88.
269. Schobel, S.A., et al., *Motor, cognitive, and functional declines contribute to a single progressive factor in early HD*. Neurology, 2017. **89**(24): p. 2495-2502.
270. Zhang, Y., et al., *Indexing disease progression at study entry with individuals at-risk for Huntington disease*. Am J Med Genet B Neuropsychiatr Genet, 2011. **156B**(7): p. 751-63.
271. Satir, T.M., et al., *Accelerated neuronal and synaptic maturation by BrainPhys medium increases A β secretion and alters A β peptide ratios from iPSC-derived cortical neurons*. Sci Rep, 2020. **10**(1): p. 601.
272. Jackson, T.C., et al., *BrainPhys® increases neurofilament levels in CNS cultures, and facilitates investigation of axonal damage after a mechanical stretch-injury in vitro*. Exp Neurol, 2018. **300**: p. 232-246.
273. Bardy, C., et al., *Neuronal medium that supports basic synaptic functions and activity of human neurons in vitro*. Proc Natl Acad Sci U S A, 2015. **112**(20): p. E2725-34.
274. Yoshiyama, Y., et al., *Synapse loss and microglial activation precede tangles in a P301S tauopathy mouse model*. Neuron, 2007. **53**(3): p. 337-51.
275. Takeuchi, H., et al., *P301S mutant human tau transgenic mice manifest early symptoms of human tauopathies with dementia and altered sensorimotor gating*. PLoS One, 2011. **6**(6): p. e21050.
276. Das, S., et al., *Increased NMDA current and spine density in mice lacking the NMDA receptor subunit NR3A*. Nature, 1998. **393**(6683): p. 377-81.
277. Stuenkel, A., et al., *Induction of α -synuclein aggregate formation by CSF exosomes from patients with Parkinson's disease and dementia with Lewy bodies*. Brain, 2016. **139**(Pt 2): p. 481-94.
278. Li, W., *Volcano plots in analyzing differential expressions with mRNA microarrays*. J Bioinform Comput Biol, 2012. **10**(6): p. 1231003.
279. Cui, X. and G.A. Churchill, *Statistical tests for differential expression in cDNA microarray experiments*. Genome Biol, 2003. **4**(4): p. 210.
280. Key, M., *A tutorial in displaying mass spectrometry-based proteomic data using heat maps*. BMC Bioinformatics, 2012. **13 Suppl 16**(Suppl 16): p. S10.

281. Bessarabova, M., et al., *Knowledge-based analysis of proteomics data*. BMC Bioinformatics, 2012. **13 Suppl 16**(Suppl 16): p. S13.
282. Jiang, X., et al., *Developmental localization of NMDA receptors, Src and MAP kinases in mouse brain*. Neurosci Lett, 2011. **503**(3): p. 215-9.
283. Lundgren, J.L., et al., *Proximity ligation assay reveals both pre- and postsynaptic localization of the APP-processing enzymes ADAM10 and BACE1 in rat and human adult brain*. BMC Neurosci, 2020. **21**(1): p. 6.
284. Goebel-Goody, S.M., et al., *Phospho-regulation of synaptic and extrasynaptic N-methyl-D-aspartate receptors in adult hippocampal slices*. Neuroscience, 2009. **158**(4): p. 1446-59.
285. Pérez-Otaño, I., et al., *Endocytosis and synaptic removal of NR3A-containing NMDA receptors by PACSIN1/syndapin1*. Nat Neurosci, 2006. **9**(5): p. 611-21.
286. Wee, K.S., et al., *Ontogenic Profile and Synaptic Distribution of GluN3 Proteins in the Rat Brain and Hippocampal Neurons*. Neurochem Res, 2016. **41**(1-2): p. 290-7.
287. Kaniakova, M., et al., *Biochemical and electrophysiological characterization of N-glycans on NMDA receptor subunits*. J Neurochem, 2016. **138**(4): p. 546-56.
288. Horak, M., et al., *The Extracellular Domains of GluN Subunits Play an Essential Role in Processing NMDA Receptors in the ER*. Front Neurosci, 2021. **15**: p. 603715.
289. Verhaeghe, R., et al., *No evidence for cognitive decline or neurodegeneration in strain-matched Grin3a knockout mice*. Alzheimers Dement, 2023. **19**(9): p. 4264-4266.
290. Borchelt, D.R., et al., *Accelerated amyloid deposition in the brains of transgenic mice coexpressing mutant presenilin 1 and amyloid precursor proteins*. Neuron, 1997. **19**(4): p. 939-45.
291. Jankowsky, J.L., et al., *Mutant presenilins specifically elevate the levels of the 42 residue beta-amyloid peptide in vivo: evidence for augmentation of a 42-specific gamma secretase*. Hum Mol Genet, 2004. **13**(2): p. 159-70.
292. Sanchez-Mut, J.V., et al., *PM20D1 is a quantitative trait locus associated with Alzheimer's disease*. Nat Med, 2018. **24**(5): p. 598-603.
293. Jeppesen, D.K., et al., *Reassessment of Exosome Composition*. Cell, 2019. **177**(2): p. 428-445.e18.
294. Gleichman, A.J., et al., *Anti-NMDA receptor encephalitis antibody binding is dependent on amino acid identity of a small region within the GluN1 amino terminal domain*. J Neurosci, 2012. **32**(32): p. 11082-94.
295. Marco, S., et al., *Suppressing aberrant GluN3A expression rescues synaptic and behavioral impairments in Huntington's disease models*. Nat Med, 2013. **19**(8): p. 1030-8.
296. Shi, Y., P. Kirwan, and F.J. Livesey, *Directed differentiation of human pluripotent stem cells to cerebral cortex neurons and neural networks*. Nat Protoc, 2012. **7**(10): p. 1836-46.
297. Menezes, J.R. and M.B. Luskin, *Expression of neuron-specific tubulin defines a novel population in the proliferative layers of the developing telencephalon*. J Neurosci, 1994. **14**(9): p. 5399-416.
298. Zhang, J. and J. Jiao, *Molecular Biomarkers for Embryonic and Adult Neural Stem Cell and Neurogenesis*. Biomed Res Int, 2015. **2015**: p. 727542.
299. Yang, Z. and K.K. Wang, *Glial fibrillary acidic protein: from intermediate filament assembly and gliosis to neurobiomarker*. Trends Neurosci, 2015. **38**(6): p. 364-74.
300. Jurga, A.M., et al., *Beyond the GFAP-Astrocyte Protein Markers in the Brain*. Biomolecules, 2021. **11**(9).
301. Miranda-Negrón, Y. and J.E. García-Arrarás, *Radial glia and radial glia-like cells: Their role in neurogenesis and regeneration*. Front Neurosci, 2022. **16**: p. 1006037.

302. Docampo-Seara, A., et al., *Expression of radial glial markers (GFAP, BLBP and GS) during telencephalic development in the catshark (Scyliorhinus canicula)*. Brain Struct Funct, 2019. **224**(1): p. 33-56.
303. Diotel, N., et al., *Common and Distinct Features of Adult Neurogenesis and Regeneration in the Telencephalon of Zebrafish and Mammals*. Front Neurosci, 2020. **14**: p. 568930.
304. Englund, C., et al., *Pax6, Tbr2, and Tbr1 are expressed sequentially by radial glia, intermediate progenitor cells, and postmitotic neurons in developing neocortex*. J Neurosci, 2005. **25**(1): p. 247-51.
305. Götz, M., A. Stoykova, and P. Gruss, *Pax6 controls radial glia differentiation in the cerebral cortex*. Neuron, 1998. **21**(5): p. 1031-44.
306. Warren, N., et al., *The transcription factor, Pax6, is required for cell proliferation and differentiation in the developing cerebral cortex*. Cereb Cortex, 1999. **9**(6): p. 627-35.
307. Zhang, Z., et al., *The Appropriate Marker for Astrocytes: Comparing the Distribution and Expression of Three Astrocytic Markers in Different Mouse Cerebral Regions*. Biomed Res Int, 2019. **2019**: p. 9605265.
308. Miller, R.H. and M.C. Raff, *Fibrous and protoplasmic astrocytes are biochemically and developmentally distinct*. J Neurosci, 1984. **4**(2): p. 585-92.
309. Emsley, J.G. and J.D. Macklis, *Astroglial heterogeneity closely reflects the neuronal-defined anatomy of the adult murine CNS*. Neuron Glia Biol, 2006. **2**(3): p. 175-86.
310. Raponi, E., et al., *S100B expression defines a state in which GFAP-expressing cells lose their neural stem cell potential and acquire a more mature developmental stage*. Glia, 2007. **55**(2): p. 165-77.
311. Rosenmund, C., A. Feltz, and G.L. Westbrook, *Synaptic NMDA receptor channels have a low open probability*. J Neurosci, 1995. **15**(4): p. 2788-95.
312. Tovar, K.R. and G.L. Westbrook, *The incorporation of NMDA receptors with a distinct subunit composition at nascent hippocampal synapses in vitro*. J Neurosci, 1999. **19**(10): p. 4180-8.
313. Tovar, K.R. and G.L. Westbrook, *Mobile NMDA receptors at hippocampal synapses*. Neuron, 2002. **34**(2): p. 255-64.
314. Zhang, W., et al., *Targeting NMDA receptors in neuropsychiatric disorders by drug screening on human neurons derived from pluripotent stem cells*. Transl Psychiatry, 2022. **12**(1): p. 243.
315. Escamilla, S., J. Sáez-Valero, and I. Cuchillo-Ibáñez, *NMDARs in Alzheimer's Disease: Between Synaptic and Extrasynaptic Membranes*. Int J Mol Sci, 2024. **25**(18).
316. Snyder, E.M., et al., *Regulation of NMDA receptor trafficking by amyloid-beta*. Nat Neurosci, 2005. **8**(8): p. 1051-8.
317. Li, S., et al., *Soluble A β oligomers inhibit long-term potentiation through a mechanism involving excessive activation of extrasynaptic NR2B-containing NMDA receptors*. J Neurosci, 2011. **31**(18): p. 6627-38.
318. Lee, M.C., et al., *Characterisation of the expression of NMDA receptors in human astrocytes*. PLoS One, 2010. **5**(11): p. e14123.
319. Torrez, V.R., et al., *Memantine mediates astrocytic activity in response to excitotoxicity induced by PP2A inhibition*. Neurosci Lett, 2019. **696**: p. 179-183.
320. Wu, H.M., et al., *Novel neuroprotective mechanisms of memantine: increase in neurotrophic factor release from astroglia and anti-inflammation by preventing microglial activation*. Neuropsychopharmacology, 2009. **34**(10): p. 2344-57.
321. Yanamandra, K., et al., *Anti-tau antibodies that block tau aggregate seeding in vitro markedly decrease pathology and improve cognition in vivo*. Neuron, 2013. **80**(2): p. 402-414.
322. Zhou, X., et al., *Extrasynaptic NMDA Receptor in Excitotoxicity: Function Revisited*. Neuroscientist, 2015. **21**(4): p. 337-44.

323. González-González, I.M., et al., *GluN3A subunit tunes NMDA receptor synaptic trafficking and content during postnatal brain development*. Cell Rep, 2023. **42**(5): p. 112477.
324. Sanz-Clemente, A., et al., *Activated CaMKII couples GluN2B and casein kinase 2 to control synaptic NMDA receptors*. Cell Rep, 2013. **3**(3): p. 607-14.
325. Lai, T.W., W.C. Shyu, and Y.T. Wang, *Stroke intervention pathways: NMDA receptors and beyond*. Trends Mol Med, 2011. **17**(5): p. 266-75.
326. Sattler, R., et al., *Distinct roles of synaptic and extrasynaptic NMDA receptors in excitotoxicity*. J Neurosci, 2000. **20**(1): p. 22-33.
327. Huang, Y.A., et al., *ApoE2, ApoE3, and ApoE4 Differentially Stimulate APP Transcription and A β Secretion*. Cell, 2017. **168**(3): p. 427-441.e21.
328. Schedin-Weiss, S., B. Winblad, and L.O. Tjernberg, *The role of protein glycosylation in Alzheimer disease*. FEBS J, 2014. **281**(1): p. 46-62.
329. Conroy, L.R., et al., *Emerging roles of N-linked glycosylation in brain physiology and disorders*. Trends Endocrinol Metab, 2021. **32**(12): p. 980-993.
330. Zhang, Q., et al., *Human brain glycoform coregulation network and glycan modification alterations in Alzheimer's disease*. Sci Adv, 2024. **10**(14): p. eadk6911.
331. Bieberich, E., *Synthesis, Processing, and Function of N-Glycans in N-Glycoproteins*. Adv Neurobiol, 2023. **29**: p. 65-93.
332. Song, X.J., et al., *Phosphorylation and Glycosylation of Amyloid- β Protein Precursor: The Relationship to Trafficking and Cleavage in Alzheimer's Disease*. J Alzheimers Dis, 2021. **84**(3): p. 937-957.
333. Boix, C.P., et al., *Amyloid precursor protein glycosylation is altered in the brain of patients with Alzheimer's disease*. Alzheimers Res Ther, 2020. **12**(1): p. 96.
334. Lennol, M.P., et al., *Apolipoprotein E imbalance in the cerebrospinal fluid of Alzheimer's disease patients*. Alzheimers Res Ther, 2022. **14**(1): p. 161.
335. Botella-López, A., et al., *Reelin expression and glycosylation patterns are altered in Alzheimer's disease*. Proc Natl Acad Sci U S A, 2006. **103**(14): p. 5573-8.
336. Sáez-Valero, J., et al., *Glycosylation of acetylcholinesterase as diagnostic marker for Alzheimer's disease*. Lancet, 1997. **350**(9082): p. 929.
337. García-Ayllón, M.S., et al., *HNK-1 Carrier Glycoproteins Are Decreased in the Alzheimer's Disease Brain*. Mol Neurobiol, 2017. **54**(1): p. 188-199.
338. Yeung, J.H.Y., et al., *Glutamatergic receptor expression changes in the Alzheimer's disease hippocampus and entorhinal cortex*. Brain Pathol, 2021. **31**(6): p. e13005.
339. Pallas-Bazarra, N., et al., *Tau is required for the function of extrasynaptic NMDA receptors*. Sci Rep, 2019. **9**(1): p. 9116.
340. Gong, C.X., et al., *Impaired brain glucose metabolism leads to Alzheimer neurofibrillary degeneration through a decrease in tau O-GlcNAcylation*. J Alzheimers Dis, 2006. **9**(1): p. 1-12.
341. Alfaro-Ruiz, R., et al., *Different modes of synaptic and extrasynaptic NMDA receptor alteration in the hippocampus of P301S tau transgenic mice*. Brain Pathol, 2023. **33**(1): p. e13115.
342. Xu, L., et al., *Deficits in N-Methyl-D-Aspartate Receptor Function and Synaptic Plasticity in Hippocampal CA1 in APP/PS1 Mouse Model of Alzheimer's Disease*. Front Aging Neurosci, 2021. **13**: p. 772980.
343. He, R.B., et al., *Ceftriaxone improves impairments in synaptic plasticity and cognitive behavior in APP/PS1 mouse model of Alzheimer's disease by inhibiting extrasynaptic NMDAR-STEP*. J Neurochem, 2023. **166**(2): p. 215-232.
344. Rammes, G., et al., *Involvement of GluN2B subunit containing N-methyl-d-aspartate (NMDA) receptors in mediating the acute and chronic synaptotoxic effects of oligomeric amyloid-beta (A β) in murine models of Alzheimer's disease (AD)*. Neuropharmacology, 2017. **123**: p. 100-115.

345. Salter, M.W. and G.M. Pitcher, *Dysregulated Src upregulation of NMDA receptor activity: a common link in chronic pain and schizophrenia*. FEBS J, 2012. **279**(1): p. 2-11.
346. Waters, E.M., et al., *Effects of estrogen and aging on synaptic morphology and distribution of phosphorylated Tyr1472 NR2B in the female rat hippocampus*. Neurobiol Aging, 2019. **73**: p. 200-210.
347. Kádková, A., J. Radecke, and J.B. Sørensen, *The SNAP-25 Protein Family*. Neuroscience, 2019. **420**: p. 50-71.
348. Lennol, M.P., et al., *Serum angiotensin-converting enzyme 2 as a potential biomarker for SARS-CoV-2 infection and vaccine efficacy*. Front Immunol, 2022. **13**: p. 1001951.
349. Lopez-Font, I., et al., *Transmembrane Amyloid-Related Proteins in CSF as Potential Biomarkers for Alzheimer's Disease*. Front Neurol, 2015. **6**: p. 125.
350. García-Ayllón, M.S., et al., *C-terminal fragments of the amyloid precursor protein in cerebrospinal fluid as potential biomarkers for Alzheimer disease*. Sci Rep, 2017. **7**(1): p. 2477.
351. Gharbiya, M., et al., *Beta-Amyloid Peptide in Tears: An Early Diagnostic Marker of Alzheimer's Disease Correlated with Choroidal Thickness*. Int J Mol Sci, 2023. **24**(3).
352. Pérez-González, R., et al., *Extracellular vesicles: where the amyloid precursor protein carboxyl-terminal fragments accumulate and amyloid- β oligomerizes*. FASEB J, 2020. **34**(9): p. 12922-12931.
353. Lopez-Font, I., et al., *Decreased circulating ErbB4 ectodomain fragments as a read-out of impaired signaling function in amyotrophic lateral sclerosis*. Neurobiol Dis, 2019. **124**: p. 428-438.
354. Lopez-Font, I., et al., *CSF-ApoER2 fragments as a read-out of reelin signaling: Distinct patterns in sporadic and autosomal-dominant Alzheimer disease*. Clin Chim Acta, 2019. **490**: p. 6-11.
355. Metwally, E., et al., *Calcium-Activated Calpain Specifically Cleaves Glutamate Receptor IIA But Not IIB at the*. J Neurosci, 2019. **39**(15): p. 2776-2791.
356. Ng, K.S., et al., *Cleavage of the NR2B subunit amino terminus of N-methyl-D-aspartate (NMDA) receptor by tissue plasminogen activator: identification of the cleavage site and characterization of ifenprodil and glycine affinities on truncated NMDA receptor*. J Biol Chem, 2012. **287**(30): p. 25520-9.
357. Wu, H.Y., et al., *Fyn-mediated phosphorylation of NR2B Tyr-1336 controls calpain-mediated NR2B cleavage in neurons and heterologous systems*. J Biol Chem, 2007. **282**(28): p. 20075-87.
358. Wu, C.C., et al., *NMDA receptor inhibitor MK801 alleviated pro-inflammatory polarization of BV-2 microglia cells*. Eur J Pharmacol, 2023. **955**: p. 175927.
359. Kim, K.S., et al., *Activation of NMDA receptors in brain endothelial cells increases transcellular permeability*. Fluids Barriers CNS, 2022. **19**(1): p. 70.
360. Fourie, C., et al., *Differential Changes in Postsynaptic Density Proteins in Postmortem Huntington's Disease and Parkinson's Disease Human Brains*. J Neurodegener Dis, 2014. **2014**: p. 938530.
361. Barria, A. and R. Malinow, *Subunit-specific NMDA receptor trafficking to synapses*. Neuron, 2002. **35**(2): p. 345-53.
362. Flint, A.C., et al., *NR2A subunit expression shortens NMDA receptor synaptic currents in developing neocortex*. J Neurosci, 1997. **17**(7): p. 2469-76.
363. Sheng, M., et al., *Changing subunit composition of heteromeric NMDA receptors during development of rat cortex*. Nature, 1994. **368**(6467): p. 144-7.
364. Lam, R.S., et al., *Functional Maturation of Human Stem Cell-Derived Neurons in Long-Term Cultures*. PLoS One, 2017. **12**(1): p. e0169506.
365. Zhang, Y., et al., *Rapid single-step induction of functional neurons from human pluripotent stem cells*. Neuron, 2013. **78**(5): p. 785-98.

366. Supakul, S., et al., *Mutual interaction of neurons and astrocytes derived from iPSCs with APP V717L mutation developed the astrocytic phenotypes of Alzheimer's disease*. Inflamm Regen, 2024. **44**(1): p. 8.
367. Klapper, S.D., et al., *Astrocyte lineage cells are essential for functional neuronal differentiation and synapse maturation in human iPSC-derived neural networks*. Glia, 2019. **67**(10): p. 1893-1909.
368. Hedegaard, A., et al., *Pro-maturational Effects of Human iPSC-Derived Cortical Astrocytes upon iPSC-Derived Cortical Neurons*. Stem Cell Reports, 2020. **15**(1): p. 38-51.
369. Tang, X., et al., *Astroglial cells regulate the developmental timeline of human neurons differentiated from induced pluripotent stem cells*. Stem Cell Res, 2013. **11**(2): p. 743-57.
370. Rodenas-Ruano, A., et al., *REST-dependent epigenetic remodeling promotes the developmental switch in synaptic NMDA receptors*. Nat Neurosci, 2012. **15**(10): p. 1382-90.
371. Groc, L., et al., *NMDA receptor surface trafficking and synaptic subunit composition are developmentally regulated by the extracellular matrix protein Reelin*. J Neurosci, 2007. **27**(38): p. 10165-75.
372. Nolt, M.J., et al., *EphB controls NMDA receptor function and synaptic targeting in a subunit-specific manner*. J Neurosci, 2011. **31**(14): p. 5353-64.
373. Barth, A.L. and R.C. Malenka, *NMDAR EPSC kinetics do not regulate the critical period for LTP at thalamocortical synapses*. Nat Neurosci, 2001. **4**(3): p. 235-6.
374. Yashiro, K. and B.D. Philpot, *Regulation of NMDA receptor subunit expression and its implications for LTD, LTP, and metaplasticity*. Neuropharmacology, 2008. **55**(7): p. 1081-94.
375. Frega, M., et al., *Neuronal network dysfunction in a model for Kleefstra syndrome mediated by enhanced NMDAR signaling*. Nat Commun, 2019. **10**(1): p. 4928.
376. Zaslavsky, K., et al., *SHANK2 mutations associated with autism spectrum disorder cause hyperconnectivity of human neurons*. Nat Neurosci, 2019. **22**(4): p. 556-564.
377. Neagoe, I., et al., *The GluN2B subunit represents a major functional determinant of NMDA receptors in human induced pluripotent stem cell-derived cortical neurons*. Stem Cell Res, 2018. **28**: p. 105-114.
378. Lin, W., et al., *Dendritic spine formation and synapse maturation in transcription factor-induced human iPSC-derived neurons*. iScience, 2023. **26**(4): p. 106285.
379. McKay, S., et al., *The Developmental Shift of NMDA Receptor Composition Proceeds Independently of GluN2 Subunit-Specific GluN2 C-Terminal Sequences*. Cell Rep, 2018. **25**(4): p. 841-851.e4.
380. Zhang, W.B., et al., *Fyn Kinase regulates GluN2B subunit-dominant NMDA receptors in human induced pluripotent stem cell-derived neurons*. Sci Rep, 2016. **6**: p. 23837.
381. Rzechorzek, N.M., et al., *Hypothermic Preconditioning Reverses Tau Ontogenesis in Human Cortical Neurons and is Mimicked by Protein Phosphatase 2A Inhibition*. EBioMedicine, 2016. **3**: p. 141-154.
382. Harris, A.Z. and D.L. Pettit, *Extrasynaptic and synaptic NMDA receptors form stable and uniform pools in rat hippocampal slices*. J Physiol, 2007. **584**(Pt 2): p. 509-19.
383. Tovar, K.R., M.J. McGinley, and G.L. Westbrook, *Triheteromeric NMDA receptors at hippocampal synapses*. J Neurosci, 2013. **33**(21): p. 9150-60.
384. Santucci, D.M. and S. Raghavachari, *The effects of NR2 subunit-dependent NMDA receptor kinetics on synaptic transmission and CaMKII activation*. PLoS Comput Biol, 2008. **4**(10): p. e1000208.
385. Coan, E.J., W. Saywood, and G.L. Collingridge, *MK-801 blocks NMDA receptor-mediated synaptic transmission and long term potentiation in rat hippocampal slices*. Neurosci Lett, 1987. **80**(1): p. 111-4.

386. McKay, S., et al., *Recovery of NMDA receptor currents from MK-801 blockade is accelerated by Mg²⁺ and memantine under conditions of agonist exposure*. *Neuropharmacology*, 2013. **74**: p. 119-25.
387. Bengtson, C.P., O. Dick, and H. Bading, *A quantitative method to assess extrasynaptic NMDA receptor function in the protective effect of synaptic activity against neurotoxicity*. *BMC Neurosci*, 2008. **9**: p. 11.
388. Askenazi, M., et al., *Compilation of reported protein changes in the brain in Alzheimer's disease*. *Nat Commun*, 2023. **14**(1): p. 4466.
389. Seifar, F., et al., *Large-scale Deep Proteomic Analysis in Alzheimer's Disease Brain Regions Across Race and Ethnicity*. *bioRxiv*, 2024.
390. Johnson, E.C.B., et al., *Large-scale deep multi-layer analysis of Alzheimer's disease brain reveals strong proteomic disease-related changes not observed at the RNA level*. *Nat Neurosci*, 2022. **25**(2): p. 213-225.
391. Carlyle, B.C., et al., *Synaptic proteins associated with cognitive performance and neuropathology in older humans revealed by multiplexed fractionated proteomics*. *Neurobiol Aging*, 2021. **105**: p. 99-114.
392. Sathe, G., et al., *Quantitative Proteomic Profiling of Cerebrospinal Fluid to Identify Candidate Biomarkers for Alzheimer's Disease*. *Proteomics Clin Appl*, 2019. **13**(4): p. e1800105.
393. Higginbotham, L., et al., *Integrated proteomics reveals brain-based cerebrospinal fluid biomarkers in asymptomatic and symptomatic Alzheimer's disease*. *Sci Adv*, 2020. **6**(43).
394. Griffiths, J. and S.G.N. Grant, *Synapse pathology in Alzheimer's disease*. *Semin Cell Dev Biol*, 2023. **139**: p. 13-23.
395. DeKosky, S.T., S.W. Scheff, and S.D. Styren, *Structural correlates of cognition in dementia: quantification and assessment of synapse change*. *Neurodegeneration*, 1996. **5**(4): p. 417-21.
396. Chang, R.Y., et al., *The synaptic proteome in Alzheimer's disease*. *Alzheimers Dement*, 2013. **9**(5): p. 499-511.
397. Hesse, R., et al., *Comparative profiling of the synaptic proteome from Alzheimer's disease patients with focus on the APOE genotype*. *Acta Neuropathol Commun*, 2019. **7**(1): p. 214.
398. Hoshi, A., et al., *Altered expression of glutamate transporter-1 and water channel protein aquaporin-4 in human temporal cortex with Alzheimer's disease*. *Neuropathol Appl Neurobiol*, 2018. **44**(6): p. 628-638.
399. Lachén-Montes, M., et al., *Olfactory bulb neuroproteomics reveals a chronological perturbation of survival routes and a disruption of prohibitin complex during Alzheimer's disease progression*. *Sci Rep*, 2017. **7**(1): p. 9115.
400. Li, M.D., et al., *Integrated multi-cohort transcriptional meta-analysis of neurodegenerative diseases*. *Acta Neuropathol Commun*, 2014. **2**: p. 93.
401. Li, M., et al., *Dysregulated gene-associated biomarkers for Alzheimer's disease and aging*. *Transl Neurosci*, 2021. **12**(1): p. 83-95.
402. Bennett, J.P. and P.M. Keeney, *Alzheimer's and Parkinson's brain tissues have reduced expression of genes for mtDNA OXPHOS Proteins, mitobiogenesis regulator PGC-1 α protein and mtRNA stabilizing protein LRPPRC (LRP130)*. *Mitochondrion*, 2020. **53**: p. 154-157.
403. Haytural, H., et al., *Insights into the changes in the proteome of Alzheimer disease elucidated by a meta-analysis*. *Sci Data*, 2021. **8**(1): p. 312.
404. Johnson, E.C.B., et al., *Large-scale proteomic analysis of Alzheimer's disease brain and cerebrospinal fluid reveals early changes in energy metabolism associated with microglia and astrocyte activation*. *Nat Med*, 2020. **26**(5): p. 769-780.

405. Morshed, N., et al., *Quantitative phosphoproteomics uncovers dysregulated kinase networks in Alzheimer's disease*. Nat Aging, 2021. **1**(6): p. 550-565.
406. Zhang, L., et al., *Roles and Mechanisms of Axon-Guidance Molecules in Alzheimer's Disease*. Mol Neurobiol, 2021. **58**(7): p. 3290-3307.
407. Dan, L. and Z. Zhang, *Alzheimer's disease: an axonal injury disease?* Front Aging Neurosci, 2023. **15**: p. 1264448.
408. Blazquez-Llorca, L., et al., *High plasticity of axonal pathology in Alzheimer's disease mouse models*. Acta Neuropathol Commun, 2017. **5**(1): p. 14.
409. Rayaprolu, S., et al., *Systems-based proteomics to resolve the biology of Alzheimer's disease beyond amyloid and tau*. Neuropsychopharmacology, 2021. **46**(1): p. 98-115.
410. D'Acunzo, P., et al., *Mitovesicles are a novel population of extracellular vesicles of mitochondrial origin altered in Down syndrome*. Sci Adv, 2021. **7**(7).
411. Pekkurnaz, G. and X. Wang, *Mitochondrial heterogeneity and homeostasis through the lens of a neuron*. Nat Metab, 2022. **4**(7): p. 802-812.
412. Rangaraju, V., M. Lauterbach, and E.M. Schuman, *Spatially Stable Mitochondrial Compartments Fuel Local Translation during Plasticity*. Cell, 2019. **176**(1-2): p. 73-84.e15.
413. Freeman, D.W., et al., *Mitochondria in hippocampal presynaptic and postsynaptic compartments differ in size as well as intensity*. Matters (Zur), 2017. **2017**.
414. Butterfield, D.A. and B. Halliwell, *Oxidative stress, dysfunctional glucose metabolism and Alzheimer disease*. Nat Rev Neurosci, 2019. **20**(3): p. 148-160.
415. Minhas, P.S., et al., *Restoring hippocampal glucose metabolism rescues cognition across Alzheimer's disease pathologies*. Science, 2024. **385**(6711): p. eabm6131.
416. Pesini, A., et al., *Brain pyrimidine nucleotide synthesis and Alzheimer disease*. Aging (Albany NY), 2019. **11**(19): p. 8433-8462.
417. Johnson, E.C.B., et al., *Deep proteomic network analysis of Alzheimer's disease brain reveals alterations in RNA binding proteins and RNA splicing associated with disease*. Mol Neurodegener, 2018. **13**(1): p. 52.
418. Borràs, E. and E. Sabidó, *What is targeted proteomics? A concise revision of targeted acquisition and targeted data analysis in mass spectrometry*. Proteomics, 2017. **17**(17-18).
419. Schey, K.L., A.C. Grey, and J.J. Nicklay, *Mass spectrometry of membrane proteins: a focus on aquaporins*. Biochemistry, 2013. **52**(22): p. 3807-17.
420. Alfonso-Garrido, J., E. Garcia-Calvo, and J.L. Luque-Garcia, *Sample preparation strategies for improving the identification of membrane proteins by mass spectrometry*. Anal Bioanal Chem, 2015. **407**(17): p. 4893-905.
421. Proctor, D.T., E.J. Coulson, and P.R. Dodd, *Reduction in post-synaptic scaffolding PSD-95 and SAP-102 protein levels in the Alzheimer inferior temporal cortex is correlated with disease pathology*. J Alzheimers Dis, 2010. **21**(3): p. 795-811.
422. Zhang, Y., et al., *Amyloid- β Induces AMPA Receptor Ubiquitination and Degradation in Primary Neurons and Human Brains of Alzheimer's Disease*. J Alzheimers Dis, 2018. **62**(4): p. 1789-1801.
423. Hughes, C.S., et al., *Single-pot, solid-phase-enhanced sample preparation for proteomics experiments*. Nat Protoc, 2019. **14**(1): p. 68-85.
424. Nakamura, F., et al., *Amino- and carboxyl-terminal domains of Filamin-A interact with CRMP1 to mediate Sema3A signalling*. Nat Commun, 2014. **5**: p. 5325.
425. Quach, T.T., et al., *Collapsin Response Mediator Proteins: Novel Targets for Alzheimer's Disease*. J Alzheimers Dis, 2020. **77**(3): p. 949-960.

8. Annex

RESEARCH ARTICLE

Synaptic and extrasynaptic distribution of NMDA receptors in the cortex of Alzheimer's disease patients

Sergio Escamilla^{1,2,3} | Raquel Badillos^{2,4,5} | Joan X. Comella^{2,4,5,6} | Montse Solé^{2,4,5} | Isabel Pérez-Otaño¹ | Jose V. Sánchez Mut¹ | Javier Sáez-Valero^{1,2,3} | Inmaculada Cuchillo-Ibáñez^{1,2,3} ¹Instituto de Neurociencias, Universidad Miguel Hernández-Consejo Superior de Investigaciones Científicas (UMH-CSIC), Sant Joan d'Alacant, Spain²Centro de Investigación Biomédica en Red sobre Enfermedades Neurodegenerativas (Ciberned), Madrid, Spain³Instituto de Investigación Sanitaria y Biomédica de Alicante (Isabial), Alicante, Spain⁴Departament de Bioquímica i Biologia Molecular, School of Medicine, Universitat Autònoma de Barcelona (UAB), Bellaterra (Barcelona), Spain⁵Institut de Neurociències, Universitat Autònoma de Barcelona (UAB), Bellaterra (Barcelona), Spain⁶Institut de Recerca Sant Joan de Déu, Hospital Sant Joan de Déu, Esplugues de Llobregat, Spain

Correspondence

Inmaculada Cuchillo-Ibáñez and Javier Sáez-Valero, Instituto de Neurociencias, Universidad Miguel Hernández-Consejo Superior de Investigaciones Científicas (UMH-CSIC), 03550 Sant Joan d'Alacant, Spain.
Email: icuchillo@umh.es and j.saez@umh.es

Funding information

Fondo de Investigaciones Sanitarias, co-funded by the Fondo Europeo de Desarrollo Regional, FEDER "Investing in your future, Grant/Award Number: PI22/01329; Direcció General de Ciència i Investigació, Generalitat Valenciana, Grant/Award Number: AICO/2021/308; Centro de Excelencia Severo Ochoa, Agencia Estatal de Investigación, Grant/Award Number: CEX2021-001165-S; Instituto de Investigación Sanitaria y Biomédica de Alicante (Isabial); Programa Investigo, Conselleria de Innovación, Universidades, Investigación y Sociedad Digital, Generalitat Valenciana, Grant/Award Number: INVEST-2023-157; CIBERNED (Instituto de Salud Carlos III)

Abstract

BACKGROUND: Synaptic and extrasynaptic distribution of N-methyl-D-aspartate receptors (NMDARs) has not been addressed in the brain from Alzheimer's disease (AD) subjects, despite their contribution to neurodegeneration.**METHODS:** We have developed a protocol to isolate synaptic and extrasynaptic membranes from controls and AD frontal cortex. We characterized the distribution of the NMDAR subunits GluN2B, GluN2A, GluN1, and GluN3A, as well as post-translational modifications, such as phosphorylation and glycosylation.**RESULTS:** Lower levels of synaptic GluN2B and GluN2A were found in AD fractions, while extrasynaptic GluN2B and GluN1 levels were significantly higher; GluN3A distribution remained unaffected in AD. We also identified different glycoforms of GluN2B and GluN2A in extrasynaptic membranes. Synaptic Tyr1472 GluN2B phosphorylation was significantly lower in AD fractions.**DISCUSSION:** Reduction of synaptic NMDAR subunits, particularly for GluN2B, is likely to contribute to synaptic transmission failure in AD. Additionally, the increment of extrasynaptic NMDAR subunits could favor the activation of excitotoxicity in AD.

KEYWORDS

Alzheimer's disease, extrasynaptic, GluN1, GluN2A, GluN2B, GluN3A, human, NMDA, Tyr1336, Tyr1472

This is an open access article under the terms of the [Creative Commons Attribution-NonCommercial-NoDerivs](https://creativecommons.org/licenses/by-nc-nd/4.0/) License, which permits use and distribution in any medium, provided the original work is properly cited, the use is non-commercial and no modifications or adaptations are made.© 2024 The Author(s). *Alzheimer's & Dementia* published by Wiley Periodicals LLC on behalf of Alzheimer's Association.

Highlights

- New protocol to isolate synaptic and extrasynaptic membranes from the human cortex.
- Low GluN2B and GluN2A levels in Alzheimer's disease (AD) synaptic membranes.
- High GluN2B and GluN1 levels in AD extrasynaptic membranes.
- Specific glycoforms of extrasynaptic GluN2B and GluN2A.
- Low phosphorylation at Tyr1472 in synaptic GluN2B in AD.

1 | BACKGROUND

N-Methyl-D-aspartate receptors (NMDARs), cation channels gated by the neurotransmitter glutamate, are essential mediators of synaptic transmission and many forms of synaptic plasticity.¹ NMDARs displays unique properties that depend on their subunit composition, but few studies have employed human brain tissues to examine their distribution.¹ Furthermore, the characterization of NMDAR diversity under neuropathological conditions such as Alzheimer's disease (AD) has not been fully addressed in human tissue, despite the fact that memantine, a drug that binds weakly to the ion channel, is used in AD therapy.²

Functional NMDARs are tetramers composed of different subunits, GluN1, GluN2(A-D), and GluN3(A-B). Endogenous NMDARs are di-heteromers composed of two obligatory GluN1 subunits and two GluN2 or GluN3 subunits, which finally assemble as a dimer of dimers³ although NMDARs are also able to assemble as tri-heteromers.⁴ In the brains of adult mice and adult human together with GluN1, the main subunits are GluN2A and GluN2B,^{1,5} which have a large N-terminal extracellular domain that contains the binding sites for glutamate and co-agonists D-serine or glycine, necessary for the effective activation of NMDARs.⁶ The NMDAR intracellular domains interact with the intracellular post-synaptic density protein-95 (PSD-95) adaptor protein,⁷ and the C-terminal of ApoER2, a receptor that binds apolipoprotein E (apoE) and reelin.^{8,9} Additionally, NMDAR subunit ectodomains are robustly glycosylated, as N-glycosylation is required for the efficient surface expression of NMDAR in neurons (reviewed in Ref.¹⁰).

The trafficking and synaptic expression of NMDARs are also tightly regulated by Src a family of protein tyrosine kinases, including Fyn, via direct phosphorylation in tyrosines located within the long intracellular C-terminal domains of GluN2 subunits.¹¹ Three major tyrosines in the GluN2B C-terminal tail have been identified by site-directed mutagenesis as Fyn phosphorylation sites: Tyr1472, Tyr1336, and Tyr1252. Phosphorylation of GluN2B at Tyr1472¹² strengthens the interaction between NMDARs and PSD-95 and prevents their binding to the endocytic adaptor AP2, enhancing the synaptic clustering and activity of GluN2B-containing NMDARs.¹³ Tyr1472 phosphorylation and GluN2B interaction with PSD-95 stabilize NMDAR in the synaptic plasma membrane and prevent it from being endocytosed or translocated to extrasynaptic membranes. GluN2B is also

phosphorylated at Tyr1336 by Fyn, an event that has been associated with enrichment of GluN2B-containing receptors in extrasynaptic membranes^{14,15} and low colocalization with PSD-95.¹⁶ The role of Tyr1252 phosphorylation is yet unknown.

Synaptic NMDARs are directly involved in excitatory neurotransmission, plasticity, and pro-survival activity, whereas stimulation of extrasynaptic NMDARs causes a loss of mitochondrial membrane potential, an early marker for glutamate-induced neuronal damage, and cell death.¹⁴ Chronic activation of extrasynaptic GluN2B and GluN2A-containing NMDARs leads to excitotoxicity, while the GluN3A subunit is considered preventive against excitotoxicity.^{17,18}

Sustained NMDAR hyperactivity and Ca²⁺ dysregulation lasting from months to years is likely related to AD development.¹⁹ In this context, two key proteins for the pathophysiology of the disease, tau, a microtubule-associated protein, and amyloid- β , A β , the principal component of senile plaques, have been associated with NMDAR impairment. Dysregulated tau phosphorylation negatively affects synaptic NMDAR-glutamatergic signaling (reviewed in Ref.²⁰). A β causes NMDAR dysregulation by loss of Ca²⁺ homeostasis, which is related to early cognitive deficits, and both A β oligomers and NMDAR impairment contribute to synaptic dysfunction in AD.²¹⁻²³

This study is the first to characterize the levels of GluN2B, GluN2A, GluN1, and GluN3A subunits in the brain of AD subjects, discriminating between synaptic and extrasynaptic membranes and addressing post-translational modifications, specifically phosphorylation, and glycosylation. Analyzing frontal cortices from AD patients and brain cortices from two mice models of AD, Tau301S, and APP/PS1, we now report changes in the distribution of NMDAR subunits between synaptic and extrasynaptic fractions.

2 | METHODS

2.1 | Human brain samples

This study was approved by the ethics committee of both, the Universidad Miguel Hernández de Elche and the Departamento de Salud de Alicante – Hospital General (Spain), and it was carried out in accordance with the WMA Declaration of Helsinki. Brain samples (frontal cortex, Brodmann area 8) and data from patients included in this study were provided by the Biobank HUB-ICO-IDIBELL (PT20/00171),

integrated into the ISC-III Biobanks and Biomodels Platform and they were processed following standard operating procedures with the appropriate approval of the Ethics and Scientific Committees. Cases with AD-related pathology were considered those showing neurofibrillary tangles (NFT) and/or senile plaques with the distribution established by Braak and Braak at the *post mortem* neuropathological examination.²⁴ These were categorized as Braak stages I–II, $n = 8$, 1 female/7 males, 63 ± 5 years; Braak stages III–IV, $n = 9$, 4 females/5 males, 78 ± 7 years; and Braak stages V–VI, $n = 8$, 3 females/5 males, 76 ± 6 years. Taking together from Braak I–VI $n = 25$, 8 females/17 males, 72 ± 9 years. Cases at stages I, II, and III did not have cognitive impairment; three cases at stage IV had moderate cognitive impairment, and cases at stages V and VI all suffered dementia. Special care was taken not to include cases with combined pathologies to avoid bias in the pathological series. Non-demented subjects, $n = 14$, 4 females/10 males, 56 ± 10 years. The mean *post mortem* interval of the tissue was 7.1 h in all cases, with no significant difference between the subgroups. See Table S1 for summarized details.

2.2 | Mice

The APP/PS1 mouse model of AD initiates A β deposits, astrogliosis and learning deficits at 6 months of age, all of which increase with age. In this study APP/PS1 mice of 12 months of age were used ($n = 22$, all males). The TauP301S mouse model of tauopathy accumulate pTau/Tau at 6 months of age in the hippocampus, but until 9 months, when these mice were used, they do not show a decrease in PSD95 and GluR2, and an increase in GFAP, that indicates hippocampal pathology (n male = 13, n female = 17).

2.3 | Subcellular fractionation protocol

Human frozen frontal cortices were cut into pieces (100 mg) trying to avoid white matter and excess of vascular tissue. When the protocol was performed in mouse brain tissue, whole frontal cortices were used (~20 mg). Each piece was homogenized in 100 μ L for human samples or 200 μ L for mouse samples of homogenization buffer (ice-cold sucrose buffer containing 0.32 M sucrose, 10 mM Tris-HCl (pH 7.4), 1 mM Na₃VO₄, 1 mM NaF, 1 mM HEPES, 1 mM ethylenediaminetetraacetic acid (EDTA), 1 mM EGTA, protease, and phosphatase inhibitors) in a 1.5 mL eppendorf using a Heidolf homogenizer (10 strokes). The subsequent centrifugations were all performed at 4°C. Cortical homogenates (Ho) were centrifuged at 1000 \times g for 10 min to obtain a nuclear-free supernatant (S1) and a pellet (P1) containing the nucleus. Further centrifugation of S1 at 10,000 \times g for 15 min resulted in a supernatant that contained cell cytosol and microsomes (S2) and a pellet (P2) of plasma membranes. P2 was incubated with homogenization buffer containing 1% TX-100 (w/v) for 20 min in rotation at 4°C and then centrifuged at 32,000 \times g for 20 min. The supernatant fraction collected contained extrasynaptic membranes, which include non-synaptic membranes and presynaptic membranes (extrasynaptic

RESEARCH IN CONTEXT

1. **Systematic review:** Unbalanced N-methyl-D-aspartate receptor (NMDAR) distribution in synaptic and extrasynaptic membranes is crucial for Alzheimer's disease (AD). Most evidence accumulated on this topic is based on transgenic models and does not discriminate between synaptic and extrasynaptic membranes. We include these publications and those performed in synaptosomes from the human brain.
2. **Interpretation:** The value of our study lies in the first characterization of NMDAR subunit distribution in the human cortex from controls and AD subjects, with special emphasis on the description of extrasynaptic NMDAR subunits.
3. **Future directions:** Additional studies could address the following questions: (A) We have identified specific glycoforms of GluN2B and GluN2A in extrasynaptic membranes. Further investigation is needed to know whether these subunits are functional and contribute to excitotoxic mechanisms. (B) Some authors point to a decrease of GluN3A subunit in AD, but we observed no changes in its distribution. More studies are needed to clarify its role in AD.

fraction, ExsynF); the pellet fraction, containing the insoluble fraction, was solubilized in RIPA buffer. This pellet was mainly composed of post-synaptic densities and therefore, post-synaptic membranes (synaptic fraction, SynF). Finally, ultracentrifugation at 100,000 \times g for 1 h of S2 fraction made it possible to discriminate microsomal (solubilized in RIPA buffer, P3) and cytosolic fractions (S3).

2.4 | Western blotting

Brain fractions were run on sodium dodecyl sulfate-polyacrylamide gel electrophoresis (SDS-PAGE) (7.5% Tris-glycine) after boiling at 98°C for 5 min in 6 \times Laemmli sample buffer. Proteins were transferred by electrophoresis to nitrocellulose membranes for 1 h at 100 V. Primary antibodies were used against GluN2B C-terminal (mouse, 1:800, Invitrogen MA1-2014), GluN2A C-terminal (rabbit, 1:800, Invitrogen A6473), phospho-Tyr1472-GluN2B (rabbit, 1:800, Phosphosolutions, p1516-1472), phospho-Tyr1336-GluN2B (rabbit, 1:800, Phosphosolutions p1516-1336), GluN1 N-terminal (guinea pig, 1:1000, Alomone AGP-046), GluN3A -Ct (rabbit, 1:1000, Millipore 07-356), PSD-95 (goat, 1:1500, Abcam ab12093), synaptophysin (mouse, 1:1000, Proteintech 60191-1-Ig), CaMKII α (rabbit, 1:1000, Proteintech 20666-1-AP), TGN46 (rabbit, 1:1000, Proteintech AB10597396), GFAP (mouse, 1:1000, Thermofischer MA5-12023), EEA1 (mouse: 1:1000, Hybridoma Bank PCR-P-EEA1-1F8) and finally

α -tubulin (1:4000, Sigma-Aldrich), as a loading control. Primary antibody binding was visualized with fluorescent secondary antibodies (IRDye, 1: 10000, Bioss), and images were acquired using an Odyssey CLx Infrared Imaging system (LI-COR Biosciences GmbH).

2.5 | Immunoprecipitation assays

Brain extracts (100 μ g in 500 μ L phosphate buffered saline [PBS]) were incubated on a roller overnight at 4°C with Protein A Sepharose CL-4B (100 μ L, Cytiva 17078001) coupled with antibodies against GluN2B N-terminal (rabbit, 15 μ L, Alomone AGC-003), GluN2B N-terminal (mouse, 10 μ L, NeuroMab 75-097 Clone N59/20), GluN2A N-terminal (mouse, 10 μ L, Hybridoma Bank N327/95), or GluN1 N-terminal (mouse, 10 μ L, Hybridoma Bank N308/48). The same number of beads without coupled antibody was used as a negative control. The input, bound, and unbound fractions were analyzed by Western blotting using antibodies against the GluN2B C-terminal (Invitrogen MA1-2014), GluN2A C-terminal (Invitrogen A6473) and GluN1 N-terminal (Alomone AGP-046).

2.6 | Enzymatic deglycosylation assays

Enzymatic deglycosylation was performed using an Agilent Enzymatic Deglycosylation Kit (Agilent Technologies, GK80110) following the manufacturer's instructions. Briefly, 100 μ g of control or AD brain extract (SynF or ExsynF) was mixed with 10 μ L incubation buffer and 2.5 μ L denaturing buffer (both provided by the kit) and heated at 100°C for 5 min. Then, samples were cooled down to room temperature and 2.5 μ L of detergent (15% w/v, NP-40) was added while mixing gently. Sialidase (1 μ L), O-glycanase (1 μ L), or N-glycanase (1 μ L) enzymes were added to the samples and then heated at 37°C for 3 h.

2.7 | Lectin binding assays

SynF and ExsynF samples (50 μ g) were incubated overnight at 4°C with lectins immobilized in agarose beads (100 μ L), either Con A lectin (from *Canavalia ensiformis*; Sigma) or wheat germ agglutinin (WGA) lectin (from *Triticum vulgaris*, Sigma). After centrifugation at 3000 \times g for 1 min, the supernatant containing the unbound fraction was analyzed by Western blot. The proportion of unbound protein was calculated with respect to the total input.

2.8 | Statistical analysis

The distribution of data was tested for normality using a D'Agostino-Pearson test. Analysis of variance (ANOVA) was used for parametric variables and the Kruskal-Wallis test for non-parametric variables for comparison between groups. A Student's *t*-test for parametric variables and a Mann-Whitney *U* test for non-parametric variables

were employed for comparison between two groups and for determining *p* values. For unpaired Student's *t*-test, a Welch's correction was employed in data with different standard deviations. Correlations were performed by Pearson correlation coefficients for parametric distributions and Spearman correlation coefficients for non-parametric distributions. The results are presented as the means \pm SEM, and all the analyses were performed using GraphPad Prism (version 7; GraphPad Software, Inc). *p*-Value < 0.05 was considered significant.

3 | RESULTS

3.1 | SynF and ExsynF in human cortex

We have designed and validated an effective fractionation protocol to obtain synaptic and extrasynaptic membranes from frozen human cortex. This protocol is based on previous methods reported by other groups, designed for mouse fresh brains.^{15,25} We have modified specific parameters such as Triton X-100 concentration, the use of acetone, and incubation times in key steps. In our protocol, cortical brain pieces were first homogenized as specified in Methods section and in Figure 1A, to obtain a supernatant that contained cell cytosol and microsomes (S2) and a P2 fraction of plasma membranes. P2 was incubated with 1% (w/v) Triton X-100 and centrifuged to get a supernatant fraction containing extrasynaptic membranes, which includes non-synaptic membranes and presynaptic membranes (extrasynaptic fraction, ExsynF); the pellet fraction was solubilized in RIPA buffer to collect post-synaptic membranes (synaptic fraction, SynF). Ultracentrifugation of S2 fraction was used to discriminate microsomal (P3) from cytosolic fractions (S3).

To validate this fractionation protocol in frontal cortices from controls and AD samples, synaptic and non-synaptic markers were assayed by Western blot (Figure 1B). PSD-95, a post-synaptic density protein, was mainly present in P2 and SynF, the fractions containing synaptic membranes. Synaptophysin, a presynaptic protein, was mainly observed in P2 and ExsynF, the fractions containing extrasynaptic membranes, but also at the cytosolic fraction (S2). The astrocytic glial fibrillary acidic protein (GFAP), a marker for glial cells, was mainly present at S2 and ExsynF. Non-synaptic-related proteins, as the early endosome-associated protein (EEA1) and the trans-Golgi network integral membrane protein 2 (detected with the TGN46 antibody) were enriched in S3 and P3 respectively, and not detected in SynF. Therefore, our protocol showed a high efficiency in discriminating cell compartments and specifically, synaptic and extrasynaptic membranes.

Since our goal was to characterize the synaptic and extrasynaptic distribution of NMDARs in the human cortex, it was compulsory to ensure the integrity and preservation of the *post mortem* samples prior to analysis. For this purpose, we estimated the Human Synapse Proteome Integrity Ratio or "HUSPIR index",²⁶ which measures the ratio of proteolytic fragments of the NMDAR subunit GluN2B in SynF by immunoblots (Figure 1C). In human brain samples, particularly at synaptic membranes, GluN2B is present as a ~170 kDa full-length protein, but also detectable as ~150 and ~130 kDa species.

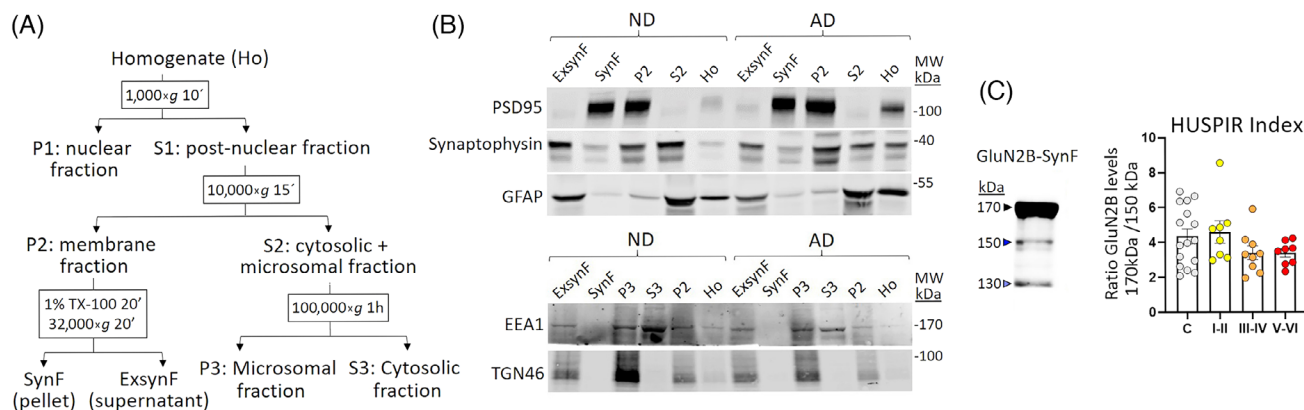


FIGURE 1 Validation of the fractionation protocol in human *post mortem* cortex. (A) Scheme of the fractionation procedure indicating the centrifugation steps and the fractions resulting from each one. P: pellet. S: supernatant. In brief, cortical homogenates (Ho) were centrifuged at 1000×g to obtain a nuclear-free supernatant (S1) and a pellet (P1) containing the nucleus. Centrifugation at 10,000×g of S1 resolved a supernatant that contained cell cytosol and microsomes (S2) and a pellet (P2) of plasma membranes. P2 was incubated with 1% (w/v) Triton X-100 and centrifuged at 32,000×g to obtain a supernatant fraction collected contained extrasynaptic membranes (ExsynF); the pellet fraction was solubilized in RIPA buffer to obtain the post-synaptic membranes (synaptic fraction, SynF). Ultracentrifugation at 100,000×g of S2 fraction served to obtain microsomal (P3) and cytosolic fractions (S3). (B) Western blot of different fractions from the fractionation protocol revealed with antibodies against synaptic-related proteins (PSD-95, synaptophysin), astroglial cells (glial fibrillary acidic protein [GFAP]) and no synaptic proteins associated to early endosome-associated protein (EEA1) and to Golgi apparatus (TGN46), in control and AD samples. (C) Representative Western blot of the N-methyl-D-aspartate receptor (NMDAR) subunit GluN2B, revealed with an antibody against the C-terminal of GluN2B, of a synaptic fraction from a control sample and the quantification of the HUSPIR index for all samples (controls $n = 16$, Braak I–II $n = 8$, Braak III–IV $n = 9$ and Braak V–VI $n = 8$).

These two shorter bands correspond to proteolytic fragments which increase during *post mortem* degradation.²⁷ A GluN2B full-length-170 kDa/fragment-150 kDa ratio, or HUSPIR index, above 1 indicates good synaptic structure integrity, which is more commonly found in *post mortem* cortical regions with respect to non-cortical regions.²⁶ The HUSPIR index of our brain cortical samples averaged 3.85 ± 1.5 (controls: 4.19 ± 0.4 ; AD: 3.65 ± 0.25 , $p = 0.29$; no differences were found when comparing AD samples sub-grouped by Braak stages). This index indicates a high synaptic structural integrity and an optimal quality for biochemical analysis of our control and AD samples. Samples with a HUSPIR index ≤ 1 were removed from the study.

3.2 | SynF and ExsynF characterization of NMDAR subunits

The evaluation of NMDAR subunits distribution in SynF and ExsynF was performed by Western blot to make the discrimination of these two fractions possible. When equal amounts of SynF and ExsynF (10 μ g) were loaded, it was clearly observed that NMDAR subunits were more abundant in synaptic membranes. To allow a quantitative analysis of fewer abundant extrasynaptic NMDAR subunits, we used a five times higher concentration (50 μ g) of ExsynF in all subsequent Western blots.

We first characterized the expression of NMDAR subunits in brain cortices from controls in S2 (50 μ g; containing the cytosol and therefore predictably low levels), P2 (10 μ g), SynF (10 μ g) and ExsynF (50 μ g, Figure 2A). GluN2B and GluN2A full-length subunits were present at SynF with the expected ~ 170 kDa molecular mass. At ExsynF, GluN2B

and GluN2A immunoreactivity showed an additional ~ 160 kDa band. GluN1 and GluN3 were observed as a 120 and 130 kDa bands respectively, both with the same apparent molecular mass in SynF and ExsynF. Remarkably, GluN3A seemed to be an exception with respect to the rest of NMDAR subunits, as it was more abundant at extrasynaptic membranes, as reported by other groups in mouse brain.^{28,29} To confirm the identity of GluN2B, GluN2A, and GluN1, in SynF and ExsynF, we performed immunoprecipitations to pull down the NMDAR subunits, resolving with alternative antibodies that verified the identity of the bands (Figure 2B). To verify the identity of the GluN3A band we employed mice lacking GluN3A (*Grin3a*^{−/−}). The absence of the GluN3A-130 kDa band in *Grin3a*^{−/−} brain extracts, but not in those from the wild-type, validated the identity of the GluN3A subunit (Figure 2C).

3.3 | Identification of GluN2B and GluN2A glycoforms

We aimed to understand why GluN2B and GluN2A subunits appeared as two distinct species in extrasynaptic membranes. NMDAR subunits are post-translationally modified by glycosylation, an adjustment key for their function and sorting.^{10,30,31} Therefore, we hypothesized that extrasynaptic GluN2B-160 kDa and GluN2A-160 kDa could represent different glycoforms of the synaptic subunits. To test this, we performed an enzymatic deglycosylation assay in control and AD samples. Enzymatic deglycosylation (N-glycanase + sialidase + O-glycanase) of synaptic membranes induced a change in the electrophoretic mobility of GluN2A and GluN2B as a result of the removal of sugars.

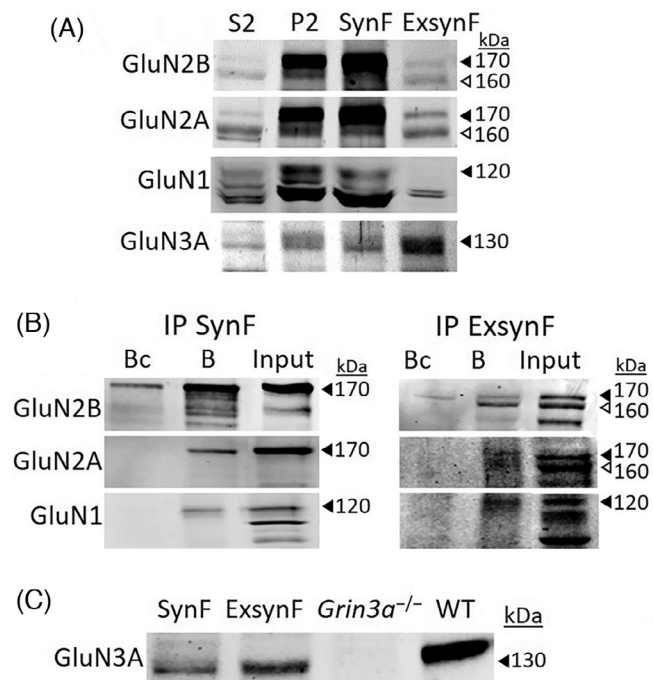


FIGURE 2 Characterization of N-methyl-D-aspartate receptor (NMDAR) subunits in SynF and ExsynF. (A) Representative blots of the NMDAR subunits GluN2B, GluN2A, GluN1, and GluN3A from different fractions of the fractionation protocol (50 μ g for S2 and extrasynaptic membranes [ExsynF]; 10 μ g for P2 and synaptic fraction [SynF]). Black arrowheads indicate bands corresponding to ~170 kDa GluN2B, ~170 kDa GluN2A, ~120 kDa GluN1 and ~130 kDa GluN3A in each blot. White arrowheads indicate ~160 kDa bands of GluN2B and GluN2A. (B) Immunoprecipitations (IP) of SynF and ExsynF of control samples. IP of GluN2B (antibody GluN2B N-terminal, rabbit, 10 μ L, Alomone AGC-003); revealed with antibody against GluN2B C-terminal (mouse, 1:800, Invitrogen MA1-2014). IP of GluN2A (antibody GluN2A N-terminal, mouse, 100 μ L supernatant, HybridomaBank N327/95) revealed with antibody against GluN2A C-terminal (rabbit, 1:800, Invitrogen A6473). IP of GluN1 (antibody GluN1 N-terminal, guinea pig, 10 μ L, Alomone AGP-046) revealed with antibody against GluN1 N-terminal (mouse, 30 μ L supernatant, HybridomaBank, N308/48). Bc, bound from control IP (IgG); B, bound fraction from the IP; Input, SynF or ExsynF. (C) Western blot of brain homogenates from a wild-type mouse (WT), a mouse lacking GluN3A (*Grin3a*^{-/-}) and from control human samples (SynF and ExsynF) revealed with GluN3A -Ct (rabbit, 1:1000, Millipore 07-356).

Remarkably, it was only in the presence of N-glycanase when the mobility of these subunits was affected, which suggests that their glycosylation was mainly due to N-glycosylation. In ExsynF, the N-deglycosylation simplified the 170 and 160 kDa bands of GluN2B and GluN2A to a single immunoreactive band, the 160 kDa band (Figure 3A). This indicated that GluN2B and GluN2A are expressed as two different glycoforms. The 170 kDa form would be predominantly found at synaptic membranes and correspond to fully glycosylated subunits, which are likely to be mature forms that harbor N-linked sugars. The 160 kDa glycoform would be almost exclusively at extrasynaptic membranes and could represent different glycoforms of synaptic GluN2B and GluN2A. When N-deglycosylation was performed in AD

fractions, the NMDAR subunits exhibited similar migration change as in controls, in both SynF and ExsynF (Figure 3B).

3.4 | Tyr1336 is the main site for GluN2B phosphorylation

GluN2B-170 kDa phosphorylation at Tyr1472 and Tyr1336 was analyzed in SynF and ExsynF to evaluate whether there is a preferential phosphorylation site associated with each membrane fraction (Figure 4A). In SynF from control and AD cases (Braak stage V–VI), GluN2B was phosphorylated at Tyr1472 and Tyr1336, showing higher levels of the last. Interestingly, phosphorylation at Tyr1472 was identified only in synaptic membranes and was almost undetectable in extrasynaptic membranes (Figure 4B). This indicated that GluN2B is phosphorylated at Tyr1472 almost exclusively at synapses, while phosphorylation at Tyr1336 occurs in synaptic and extrasynaptic membranes.

3.5 | Synaptic and extrasynaptic distribution of NMDAR subunits in control and AD cortex

We next compared NMDAR subunit levels in control and AD cases sub-grouped by different Braak stages of neurodegeneration related to AD. Quantitative infra-red Western blotting has a greater linear range of detection than the more widely used chemiluminescent technique; however, due to the large differences in the levels of NMDAR subunits between membrane fractions, we analyzed P2, SynF, and ExsynF samples in separate blots to make the analysis feasible and more reproducible. We observed the same banding pattern in synaptic membranes and extrasynaptic membranes for all the NMDAR subunits when comparing control and AD samples (Figure 5A). Quantification (Figure 5B) revealed that P2 fractions expressed significantly lower levels of GluN2B in AD than control tissues when pooling all Braak stages ($58.2 \pm 37.0\%$; $p = 0.0009$) and in each independent stage, except for Braak III–IV, that showed a tendency to decrease ($67.0 \pm 25.6\%$; $p = 0.072$). Similarly, GluN2A levels were significantly lower in AD when pooling all Braak stages ($57.2 \pm 53.7\%$; $p = 0.0006$) and in Braak III–IV ($56.1 \pm 9.3\%$; $p = 0.020$). GluN1 levels were significantly lower in AD than in controls when taking all Braak stages into account ($80.3 \pm 25.2\%$; $p = 0.039$), and in Braak V–VI ($69.36 \pm 22.8\%$; $p = 0.041$). As previously reported,³² GluN3A levels did not change between control and AD fractions. Since SynF contributes more to P2 signal than ExsynF, synaptic membrane levels of NMDAR subunits mirrored the decrease observed in P2. Both GluN2B and GluN2A levels were significantly lower in all Braak stages overall relative to controls ($67.3 \pm 43.0\%$, $p = 0.022$; $63.2 \pm 44.5\%$, $p = 0.017$, respectively), and in Braak III–IV and V–VI stages for GluN2A ($54.4 \pm 33.4\%$, $p = 0.043$; $55.6 \pm 34.9\%$, $p = 0.050$ respectively). GluN1 and GluN3A levels did not change in AD in overall or individual Braak stages relative to controls.

Interestingly, NMDAR subunit levels in extrasynaptic membranes displayed an opposite trend to those observed in synaptic

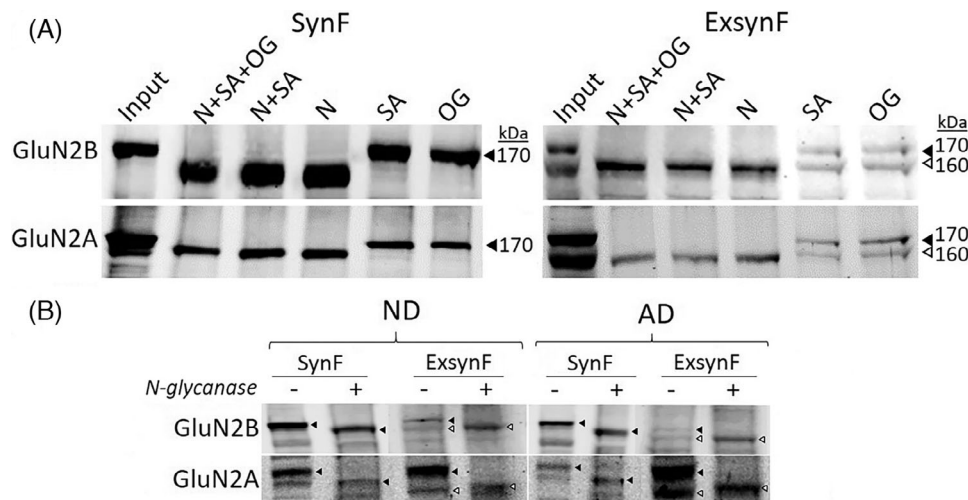


FIGURE 3 Glycosylation of N-methyl-D-aspartate receptor (NMDAR) subunits. (A) Enzymatic deglycosylation of synaptic fraction (SynF) and extrasynaptic membranes (ExsynF) (3B) with N-glycanase (N), sialidase (SA), O-glycanase (OG), or a combination of them in control samples, revealed with antibodies against GluN2B C-terminal (Invitrogen MA1-2014) and GluN2A C-terminal (Invitrogen A6473). Black arrowheads indicate bands corresponding to ~170 kDa GluN2B and ~170 kDa GluN2A. White arrowheads indicate ~160 kDa bands of GluN2B and GluN2A. (B) NMDAR subunits in SynF and ExsynF fractions from control and AD cases, after N-deglycosilation (+) or in unprocessed samples (-), revealed with antibodies against the C-terminal of GluN2B and GluN2A.

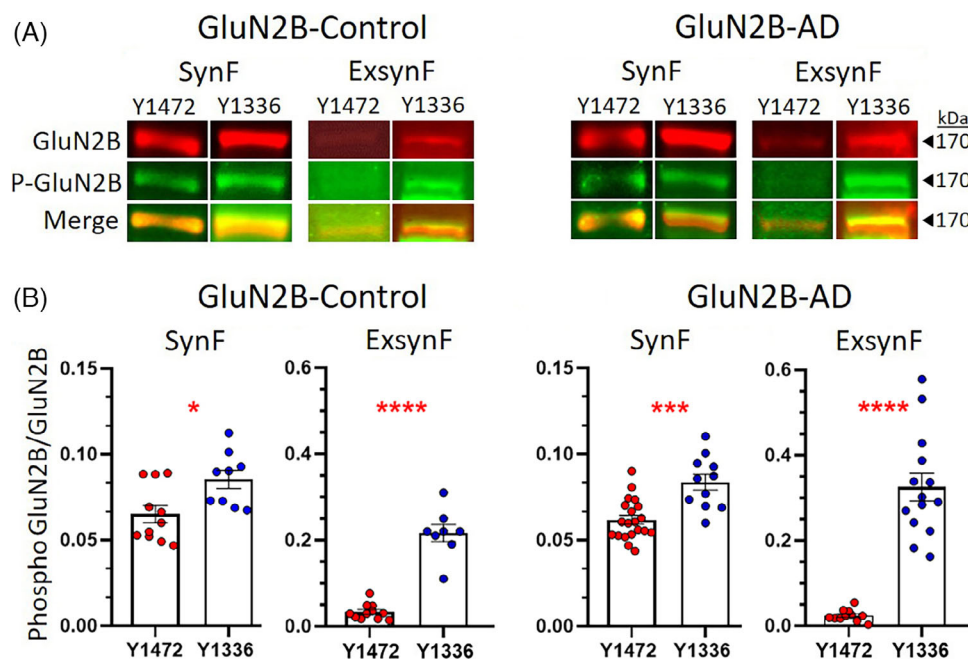


FIGURE 4 Comparison of GluN2B phosphorylation in synaptic fraction (SynF) and extrasynaptic membranes (ExsynF) between control and Alzheimer's disease (AD) cases. (A) Representative blots and (B) quantification of GluN2B (total protein resolved with mouse C-terminal antibody MA1-2014) and GluN2B phosphorylation (P-GluN2B) at Tyr1472 (rabbit antibody p1516-1472) and at Tyr1336 (rabbit antibody p1516-1336) in synaptic and extrasynaptic GluN2B-170 kDa from control and AD samples (Braak V–VI). The fluorescence of the secondary antibodies (IRDye 680RD goat anti-mouse, red; IRDye 800CW goat anti-rabbit, green) was detected with the Odyssey CLx Infrared Imaging system (LI-COR); merge fluorescence shows co-localization (yellow). Ratio of phosphorylated GluN2B respect to total GluN2B levels are plotted. Cases control SynF $n = 9–11$; control ExsynF $n = 8–11$; AD SynF $n = 11–20$; AD ExsynF $n = 11–14$. Observe the different Y scale for ExsynF graphs. * $p < 0.05$, ** $p < 0.001$ with respect to control, t -test.

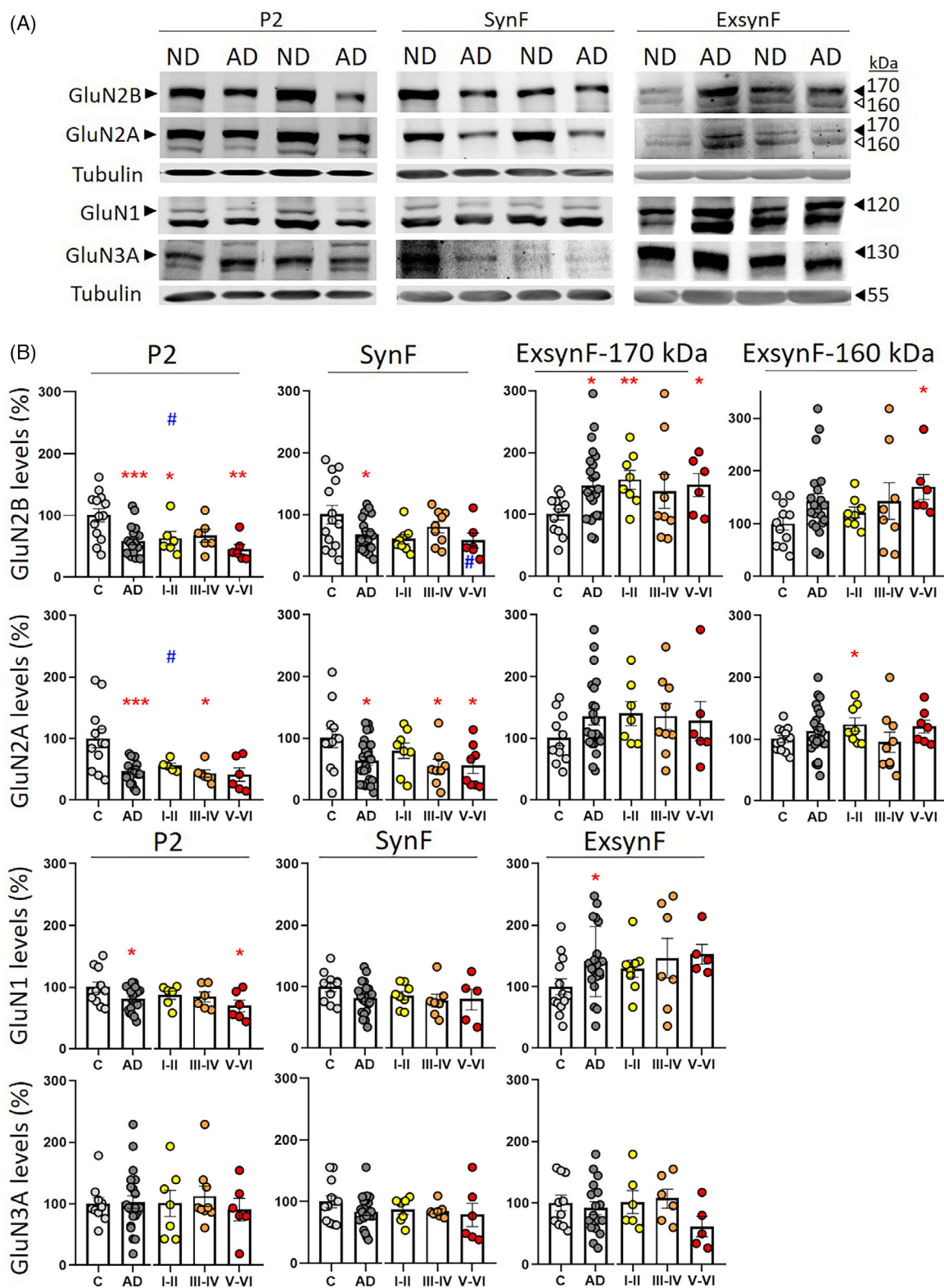


FIGURE 5 Distribution of N-methyl-D-aspartate receptor (NMDAR) subunits in membrane-containing fractions from control and Alzheimer's disease (AD) cases. (A) Representative Western blots of NMDAR subunits in membrane fraction (P2, 10 μ g), synaptic fraction (SynF, 10 μ g) and extrasynaptic fractions (ExsynF, 50 μ g) from control and AD samples (Braak V–VI). Tubulin was used to normalize quantifications. (B) Quantification of NMDAR subunits levels at different Braak stages and all Braak stages together (AD: Braak stages I–VI) expressed as percentage respect to controls. GluN2B-170 kDa and GluN2A-170 kDa levels were measured in P2, SynF and ExsynF; GluN2B-160 kDa and GluN2A-160 kDa were measured in ExsynF only. * $p < 0.05$, ** $p < 0.01$, *** $p < 0.001$ respect to control, t -test; # $p < 0.01$ analysis of variance (ANOVA) one-way comparing control and all Braak stages. Cases control P2 $n = 10$ –13; control SynF $n = 10$ –14; control ExsynF $n = 10$ –12; AD P2 $n = 18$ –22; AD SynF $n = 21$ –24; AD ExsynF AD $n = 17$ –24.

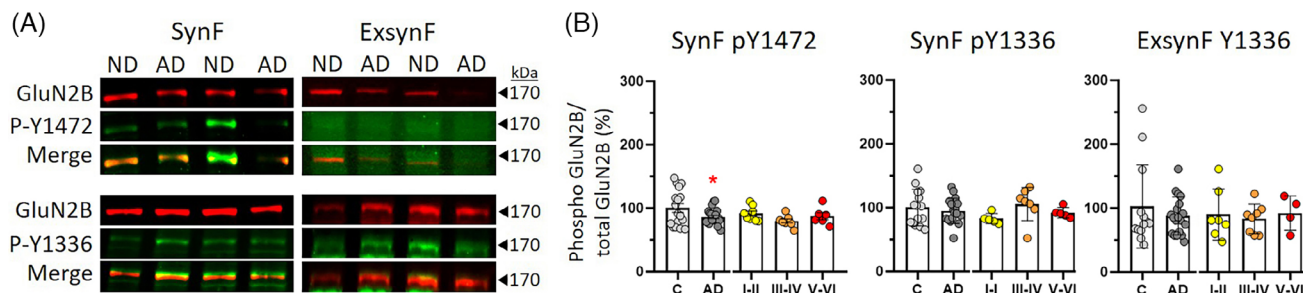


FIGURE 6 GluN2B phosphorylation from control and Alzheimer's disease (AD) cases comparing synaptic fraction (SynF) and extrasynaptic membranes (ExsynF). (A) Representative Western blots of GluN2B, phospho GluN2B Tyr 1472, and phospho GluN2B Tyr 1336 in SynF and ExsynF of controls and AD (Braak V–VI) samples. (B) Quantification of GluN2B-170 kDa phosphorylation at SynF (phospho Tyr1472, phospho Tyr1336) and at ExsynF (phospho Tyr1336). Levels of phosphorylated GluN2B were normalized to total GluN2B and estimated as in Figure 4. * $p < 0.05$ AD v control, t -test. Cases control SynF $n = 15–17$; control ExsynF $n = 13$; AD SynF $n = 17–22$; AD ExsynF $n = 19$.

membranes, suggesting a subcellular redistribution in AD cases (Figure 5B). Extrasynaptic GluN2B-170 kDa levels were higher in AD overall ($146.5 \pm 55.6\%$; $p = 0.016$) and in most individual Braak stages compared to controls. Notably, the glycoform GluN2B-160 kDa displayed higher levels only at Braak V–VI ($169.5 \pm 58.0\%$; $p = 0.010$). Extrasynaptic GluN2A-170 kDa levels showed a tendency to be higher overall in AD than controls ($134.8 \pm 56.8\%$; $p = 0.098$), and the 160 kDa glycoform was significantly more abundant in Braak stages I–II compared with controls ($123.5 \pm 30.8\%$; $p = 0.050$), and a tendency in Braak stage V–VI ($120.4 \pm 27.7\%$; $p = 0.076$). Extrasynaptic GluN1 was significantly higher in overall AD ($137.3 \pm 49.9\%$; $p = 0.039$). Remarkably, GluN3A, the unique NMDAR subunit that is more abundant in ExsynF membranes than in SynF, did not show any change in ExsynF from AD tissues.

To confirm that changes in NMDAR subunits levels were related to the pathology of each group rather than to the age, we performed correlations in controls and at each Braak stage. No association between age and the levels of any NMDAR subunit was found in P2 and SynF in control or Braak stages. In ExsynF, a positive correlation was found in Braak V–VI for GluN2A ($p = 0.037$, *Pearson*) and GluN2B-160 kDa ($p = 0.008$, *Pearson*). This indicated that the higher levels of these subunits were found in the oldest subjects at the late stages of the pathology. In control ExsynF GluN2A-160 kDa and control and Braak I–II stage ExsynF GluN3A, levels correlated with age ($p = 0.0358$; positive correlation, *Pearson*; $p = 0.050$, negative correlation, *Pearson*; $p = 0.037$, negative correlation, respectively) although it did not seem to affect quantification (see Figure 5). We also analyzed the correlation between NMDAR subunit levels and the gender of the individuals, but no association was found in any group. There was no correlation between age and GluN2B phosphorylation at either Tyr1472 or Tyr1336 in any group.

3.6 | Low Tyr1472 phosphorylation at synaptic GluN2B in AD cortex

We then examined the phosphorylation pattern of GluN2B-170 kDa between controls and different Braak stages of AD (Figure 6A). The

only significant difference was an overall lower GluN2B phosphorylation at Tyr1472 in SynF of AD tissue relative to controls ($88.1 \pm 15.3\%$; $p = 0.043$); phosphorylation at Tyr1336 remained unchanged. In ExsynF, no changes were observed between control and AD fractions in Tyr1336 phosphorylation (Figure 6B). Phosphorylation at Tyr1472 was too weak to be evaluated in ExsynF, as mentioned before. This finding suggests that the stabilization of GluN2B at synapses could be compromised in AD due to low levels of Tyr1472 phosphorylation.

3.7 | N-glycosylation is altered in extrasynaptic GluN2B and GluN2A in AD cortex

Modifications of N-glycosylation have been reported in AD for many glycoproteins; consequently, we evaluated whether the glycosylation of NMDAR subunits is affected. To this end, SynF and ExsynF from controls and AD samples (Braak V–VI) were incubated with lectins, which bind to specific carbohydrates linked to protein residues. We employed two agarose-immobilized lectins, Con A (binds mannose/glucose) and WGA (binds N-acetyl-D-glucosamine and sialic acid residues), that previously have demonstrated a saccharide-specificity and high affinity for NMDAR subunits.³¹ After incubation, the levels of unbound glycoforms were determined by Western blot (Figure 7A) and quantified for each lectin. The unbound fractions of GluN2B-170 kDa and GluN2A-170 kDa were measured only in SynF, as the affinities of either Con A or WGA lectins for these subunits were so high in ExsynF that it made it difficult to quantify the unbound fraction, due to its weakness in the immunoblot. In SynF the percentages of GluN2B, GluN2A, and GluN1 unbound to lectins showed no differences among controls and AD (Figure 7B). Likewise, ExsynF GluN1 unbound fraction to ConA and WGA was similar in controls and AD. GluN3A affinity for Con A and WGA lectins was so high in SynF and ExsynF from both control and AD samples that the unbound fraction was quite weak; therefore, it was not quantified either. Statistical differences were found only in the ExsynF GluN2B-160 kDa and GluN2A-160 kDa, both with lower unbound percentages to Con A in AD fractions with respect to controls, indicating a higher affinity for this lectin. This suggests a specific AD-related alteration in the glycosylation of these extrasynaptic GluN2B and GluN2A glycoforms.

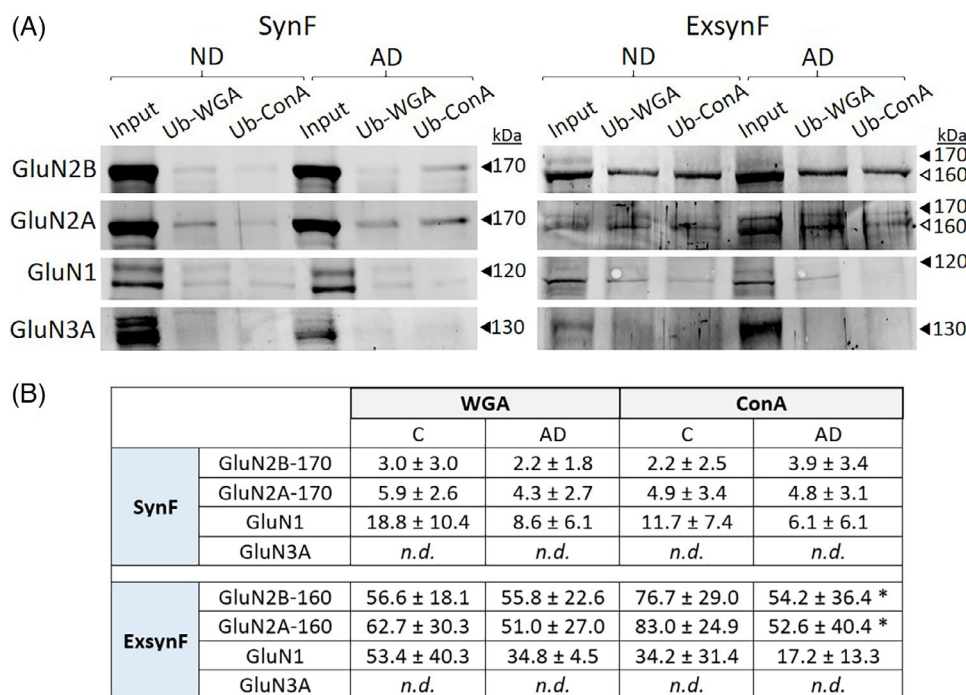


FIGURE 7 N-Methyl-D-aspartate receptor (NMDAR) subunits interaction with N-glycan lectins. (A) Representative Western blots for GluN2B, GluN2A, GluN1, and GluN3A of unbound and inputs of synaptic fraction (SynF) and extrasynaptic membranes (ExsynF) fractions after incubation with wheat germ agglutinin (WGA) and Con A lectins, from control and Braak stage V–VI samples. (B) Quantification of SynF and ExsynF unbound fraction to WGA or Con A lectins from control and AD samples, with respect to the input fraction (SynF or ExsynF respectively) expressed as percentage (%). Data represent SynF GluN2B-170 kDa, SynF GluN2A-170 kDa, SynF GluN1, ExsynF GluN2B-160 kDa, ExsynF GluN2A-160 kDa, and ExsynF GluN1. Values represent percentage unbound ± standard deviation. Control SynF $n = 5$, controls ExsynF $n = 7$; Braak V–VI SynF $n = 6$, Braak V–VI ExsynF $n = 7$. *nd*, not determined.

3.8 | NMDAR subunits distribution in mice models

Finally, we used two mouse models to determine whether dysfunction in AD key proteins, tau and APP, could be related to changes in NMDAR subunits distribution among synaptic and extrasynaptic membranes. The same fractionation protocol was used, yielding a high discrimination among cytosolic, synaptic, and extrasynaptic fractions (Figure 8A). In all immunoblots, mouse NMDAR subunits were identified at similar molecular mass than in human samples, but ExsynF GluN2B and GluN2A were resolved as a unique band. The first transgenic line used, TauP301S is a tauopathy model that expresses the human P301S mutant tau protein and is characterized by neurofibrillary pathology and neurological manifestations.³³ At 9 months of age, a decrease was observed in SynF GluN2B ($62.3 \pm 27.6\%$; $p = 0.009$), SynF GluN1 ($62.2 \pm 27.6\%$; $p = 0.009$), and ExsynF GluN3A levels ($62.2 \pm 31.3\%$; $p = 0.014$) when compared with those in wild-type mice (Figure 8B, C). This resembles somehow what occurs in AD samples and suggests that tau phosphorylation could be involved in GluN2B/GluN1 and GluN3A/GluN1 retention at their main synaptic locations. A second transgenic model, the APP/PS1 mouse,³⁴ develops amyloid plaques pathology, astrogliosis, and learning deficits starting at 7 months of age.^{35,36} In this model, at 12 months of age only GluN1 levels were affected, in both SynF ($33.2 \pm 4.3\%$; $p = 0.0317$) and ExsynF ($57.3 \pm 24.6\%$; $p = 0.003$), compared with wild-type con-

trols (Figure 8B, D). In any of these mouse models, phosphorylation of GluN2B was affected, suggesting that Fyn kinase activity may not been altered in these transgenic mice.

4 | DISCUSSION

For the first time, we have described the distribution of the main four NMDAR subunits -GluN2B, GluN2A, GluN1, and GluN3A- between synaptic and extrasynaptic membranes in the human cortex. The different nature of these membranes makes it possible to use biochemical fractionation protocols and separate synaptic membranes, defined as plasma membrane of the post-synaptic density, and extrasynaptic membranes, which include spine necks, dendritic shafts, or somas, which are further away from the post-synaptic density.^{37,38} We have characterized the distribution of NMDAR subunits, as well as the phosphorylation, and glycosylation levels in membrane fractions from controls and AD subjects.

We have found that in the human brain, GluN2B, GluN2A, and GluN1 subunits are enriched in synaptic membranes, while GluN3A predominates in extrasynaptic membranes, as previously reported in mouse brains due to lower stabilization at synaptic sites.³⁹ Early reports established that GluN2B-containing NMDAR is mainly extrasynaptic, while GluN2A-containing NMDAR is mainly synaptic.^{40,41} This

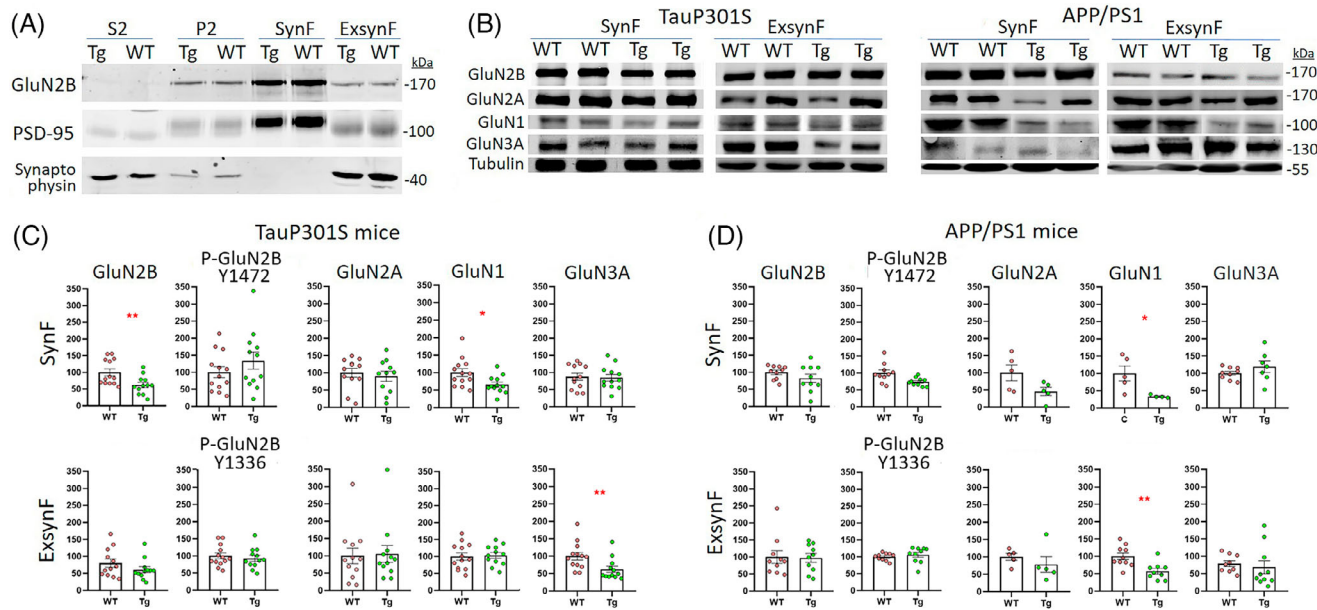


FIGURE 8 N-Methyl-D-aspartate receptor (NMDAR) subunit levels and GluN2B phosphorylation in Alzheimer's disease (AD) mouse models TauP301S and APP/PS1. (A) The fractionation protocol in wild-type mice (WT) and transgenic mice (Tg) cortex was the same as that described for human samples in Figure 1. Representative Western blot of S2, P2, synaptic fraction (SynF), and extrasynaptic membranes (ExsynF) fractions from WT and TauP301S mice (Tg) developed with antibodies against GluN2B, post-synaptic density95 (PSD95), synaptophysin, and glial fibrillary astrocytic protein (GFAP); similar patterns were obtained for APP/PS1 mice (not shown). (B) Representative Western blots of NMDAR subunits in SynF and ExsynF from WT and TauP301S mice (Tg); and from WT and APP/PS1 mice (Tg), as indicated. (C) Quantification of GluN2B, Tyr1472 phosphorylation of GluN2B (P-GluN2B Tyr1472), Tyr1336 phosphorylation of GluN2B (P-GluN2B Tyr1472), GluN2A, GluN1, and GluN3A levels in SynF and ExsynF from WT and TauP301S mice (Tg). WT SynF $n = 6-13$, WT ExsynF $n = 12-13$, Tg SynF $n = 6-12$, Tg ExsynF $n = 12$. (D) Quantification of GluN2B, Tyr1472 phosphorylation of GluN2B (P-GluN2B Tyr1472), Tyr1336 phosphorylation of GluN2B (P-GluN2B Tyr1472), GluN2A, GluN1, and GluN3A levels in SynF and ExsynF from WT and APP/PS1 mice (Tg). WT SynF $n = 5-10$, WT ExsynF $n = 5-10$, Tg SynF $n = 5-10$, Tg ExsynF $n = 5-10$. ** $p < 0.01$ respect to WT.

led to the notion that extrasynaptic GluN2B-containing NMDAR drives long-term depression and excitotoxicity, while GluN2A-containing NMDAR mediates for long-term potentiation (LTP) and survival cell signaling.⁴² However, this oversimplified idea was challenged by studies that found that GluN2B and GluN2A subunits are present in both synaptic and extrasynaptic membranes.⁴³ Furthermore, activation of synaptic and extrasynaptic NMDARs is equally capable of inducing excitotoxicity,⁴⁴ and synaptic GluN2A-containing NMDAR is also necessary to induce excitotoxicity.⁴⁵ Results may have differed along the studies because of different protocol conditions and lack of pharmacological/biochemical tools to definitively distinguish NMDAR subtypes; additionally, the employment of different neurodevelopmental stages in mice can also contribute to discrepancies in the interpretations.⁴⁶

Despite discrepancies, an imbalance between synaptic and extrasynaptic NMDAR activity has been considered as a possible pathogenic factor for neurodegenerative diseases, and a major contributing factor to glutamatergic dysfunction and pathogenesis in AD.^{46,47} Our approach to study NMDAR subunits distribution in synaptic and extrasynaptic membranes, while not feasible using crude membrane preparations, uncovered relevant differences between controls and AD, particularly for GluN2B, and at specific neurodegenerative stages related to AD.

At synaptic membranes, the levels of the canonical GluN2B-170 kDa subunit were significantly lower in AD fractions compared with controls; but higher at extrasynaptic membranes. Similarly, the canonical GluN2A-170 kDa was less abundant in AD synaptic membranes and showed a tendency to increase in extrasynaptic membranes. GluN1 levels were similar at synaptic membranes in controls and AD, but at extrasynaptic membranes, levels were higher in AD. As an exception, GluN3A levels were unchanged in AD. In sum, we find an impaired distribution of NMDAR subunits levels between synaptic and extrasynaptic membranes in AD relative to control frontal cortex. The shift of NMDARs toward extrasynaptic membranes could be relevant to the excitotoxicity that is thought to be mediated by extrasynaptic NMDARs. Chronic NMDAR stimulation lasting for months to years has been associated with AD with increased levels of extrasynaptic GluN2B-containing NMDARs, which induce enlarged tonic NMDAR currents and excitotoxicity.^{48,49} Remarkably, we have found higher levels of the canonical GluN2B-170 kDa and also of the GluN2B-160 kDa glycoform in Braak V-VI in extrasynaptic membranes. This suggests that excitotoxicity could be facilitated at the late stages of AD by GluN2B enrichment in extrasynaptic membranes.

Differences in NMDAR subunits expression have been observed in AD with respect to the control at different regions of the *post mortem* human cortex. Transcriptomic analysis has revealed that the

expression of GluN1 gene, *GRIN1*, is the most affected in the AD brain. *GRIN1* is downregulated in the temporal cortex and superior temporal gyrus^{50,51} from AD individuals. Interestingly, in the prefrontal cortex *GRIN1* expression is modulated through AD progression, being upregulated at early-AD pathology with respect to control, and downregulated at late-AD pathology regarding early-AD pathology.⁵² Other studies have not found changes in *GRIN1* expression in the frontal and prefrontal cortex,^{50,53} or when transcriptomic analysis is performed in astrocytes.⁵⁴ Overall, these studies suggest that the low GluN1 protein levels observed in AD extrasynaptic membranes could be attributed to downregulation of *GRIN1* expression. Moreover, some studies report downregulation of *GRIN2B* and *GRIN2A* mRNA and protein levels in the hippocampus, and in the temporal entorhinal cortex from AD individuals.^{51,55–58} In our study, GluN2B and GluN2A protein levels were lower in AD synaptic membranes and higher in extrasynaptic membranes. This suggests that the more dynamic transcriptional modifications, a key factor in regulating trafficking and sorting of these subunits to the membrane, would be responsible for the altered GluN2B and GluN2A distribution in AD, rather than due to transcriptional changes.

Deglycosylation and lectin binding analysis confirmed that GluN2B, GluN2A, GluN1, and GluN3A are glycosylated in human cortices, and indicated that GluN2B and GluN2A are N-glycosylated. N-Glycosylation is a complex process that involves numerous enzymes. It is a highly regulated mechanism that includes many sequential steps controlled by the ordered actions of a variety of glycosyltransferases, glycosidases, and other regulators in the endoplasmic reticulum and Golgi compartments.⁵⁹ It is not known which glucosyltransferases participate in GluN2A/B glycosylation; however, glycosylation is essential for NMDAR-dependent electric currents^{30,60} and correct intracellular sorting. Glycosylation of Asn675 in GluN2B has been identified as a requirement for trafficking NMDARs to synapses in an activity-independent manner.⁶¹

Remarkably, glycoforms of GluN2B and GluN2A with a lower apparent molecular mass (GluN2B-160 kDa and GluN2A-160 kDa) are found exclusively at extrasynaptic membranes in control and AD cases. Changes in protein glycosylation have been reported in AD,⁶² even in N-linked glycosylation,⁶³ and in specific NMDAR subunits such as GluN2B, GluN2A, and GluN1.⁶⁴ Our lectin binding analysis demonstrated differences in extrasynaptic GluN2B-160 kDa and GluN2A-160 kDa glycoforms between controls and AD, with higher levels at Braak V–VI than in controls. This could be explained because N-glycosylation is a post-translational modification essential for NMDAR subunit surface delivery,¹⁰ and altered glycosylation could affect the surface expression⁶⁵ and intracellular sorting⁶⁶ of GluN2B and GluN2A subunits. This would lead to increased levels at the extrasynaptic membranes of these glycoforms, rather than reflecting enhanced translocation from synaptic membranes.

We have previously described aberrant glycosylation in AD-related proteins, such as APP,⁶⁷ apoE,⁶⁸ reelin,⁶⁹ and acetylcholinesterase,⁷⁰ as well as changes in glycosylated epitopes.⁷¹ Glycosylation changes in NMDAR subunits could occur early or be associated with neurodegeneration progression in AD, but whether the 160-kDa glycoforms

of GluN2B and GluN2A modify NMDAR activity in AD should be determined.

In this study, GluN2B phosphorylation at Tyr1336 was significantly high in extrasynaptic membranes compared to Tyr1472 phosphorylation. At synaptic membranes, phosphorylation at Tyr1336 and Tyr1472 were quantifiable, but at extrasynaptic membranes phosphorylation at Tyr1472 was particularly low, making quantification difficult in both controls and AD fractions. Tyr1336 GluN2B phosphorylation levels showed consistency in control and AD fractions, which means that, independently of the different relative GluN2B levels in synaptic and extrasynaptic membranes from control and AD samples, the phosphorylation ratio at Tyr1336 remained similar in both conditions. On the contrary, phosphorylation levels of GluN2B at Tyr1472 relative to GluN2B levels were significantly low in AD synaptic membranes; and this suggests a non-proportional decay of phosphorylation of GluN2B with respect to the lower GluN2B levels found in AD and, therefore, a specific affectation of synaptic GluN2B Tyr1472 phosphorylation in AD.

It is broadly assumed that Tyr1472 is the major phosphorylation site within GluN2B.⁷² GluN2B Tyr1472 phosphorylation activates and stabilizes NMDAR in synaptic plasma membrane, which prevents it from being endocytosed or translocated to non-clustered extrasynaptic membranes, and increases after LTP.^{7,72} Our results suggest that the lesser synaptic Tyr1472 phosphorylation in AD could impair GluN2B retention at synaptic membranes, therefore explaining the higher levels at the extrasynaptic membranes. However, the proportion of the Tyr1472 GluN2B translocated was not sufficient to be measurable, and Tyr1336 GluN2B was the principal subunit in ExsynF. Our study raises questions about the role of synaptic GluN2B Tyr1336 phosphorylation, which is thought to promote NMDAR anchoring at extrasynaptic membranes,^{14–16} as also indicated by our findings.

Glycosylation and phosphorylation are processes mostly studied separately; therefore, the relation between them is not fully understood. Specific interrelations have been suggested for key AD proteins such as APP⁶⁶ and tau.⁷³ However, the mechanistic relationship between glycosylation and phosphorylation on GluN2B mislocalization remains to be explored.

Our analysis of tau and A β transgenic models only partially reproduced the alterations found in AD patients, suggesting that some of the changes in NMDAR subunits observed in human AD brains are likely to be the consequence of complex or compensatory processes that could require the participation of more than one pathological alteration. However, studies using tau-based mouse models point in the same direction as our data. A shift in the balance from synaptic toward extrasynaptic NMDARs was described in the hippocampus of TauP301S mice at 10 months of age,⁷⁴ and tau knockout mice do not exhibit changes in NMDAR phosphorylation at Tyr1472 and Tyr1336,¹⁶ suggesting that tau is not related to NMDAR phosphorylation, in agreement with our results. Therefore, the accumulation of phosphorylated tau is relevant to alter NMDAR distribution, but tau may not have a role in NMDAR phosphorylation. Furthermore, the amyloid peptide accumulation that occurs in APP/PS1 mice seems to affect only GluN1 in the frontal cortex, in agreement with

transcriptomic studies in the *post mortem* human brain.^{50–52} However, studies in the hippocampus report low levels of GluN2B and GluN2A, and no changes in GluN1,⁷⁵ but also higher levels of GluN2B and phosphorylated GluN2B-Tyr1472 in the extrasynaptic fraction from hippocampal homogenates.⁷⁶ Our results suggest that, in the frontal cortex from APP/PS1 mice, reduced levels of the obligatory subunit GluN1 in synaptic and extrasynaptic membranes may affect all NMDARs, and contribute to the synaptic failure described in this model⁷⁷ driven by amyloid-beta.

In conclusion, the alterations in the NMDAR subunits distribution described here could affect essential NMDAR functions involved in processes such as synaptic plasticity and memory.^{7,78,79} Consequently, the aforementioned alterations may contribute to the cognitive decline associated with normal aging and AD.⁸⁰ The shift to extrasynaptic membranes of GluN2B, GluN2A and GluN1, could explain the exacerbated NMDA-related excitotoxicity observed in AD.

ACKNOWLEDGMENTS

We particularly want to acknowledge patients and Biobank HUB-ICO-IDIBELL (PT20/00171) integrated in the ISCIII Biobanks and Biomodels Platform and Xarxa Banc de Tumors de Catalunya (XBTC) for their collaboration. This work was supported by grants from the Fondo de Investigaciones Sanitarias (PI22/01329, co-funded by the Fondo Europeo de Desarrollo Regional, FEDER “Investing in your future”), CIBERNED (Instituto de Salud Carlos III, Spain), and from the Direcció General de Ciència i Investigació, Generalitat Valenciana (AICO/2021/308). Sergio Escamilla is supported by a PFIS fellowship from the ISC-III, Centro de Excelencia Severo Ochoa, Agencia Estatal de Investigación (CEX2021-001165-S), Instituto de Investigación Sanitaria y Biomédica de Alicante (Isabial), and Programa Investigo, Conselleria de Innovación, Universidades, Investigación y Sociedad Digital, Generalitat Valenciana (INVEST-2023-157).

CONFLICT OF INTEREST STATEMENT

The authors declare no conflicts of interest. Author disclosures are available in the [Supporting information](#).

CONSENT STATEMENT

Consent was not necessary.

ORCID

Inmaculada Cuchillo-Ibáñez  <https://orcid.org/0000-0002-3689-5518>

REFERENCES

- Paoletti P, Bellone C, Zhou Q. NMDA receptor subunit diversity: impact on receptor properties, synaptic plasticity and disease. *Nat Rev Neurosci*. 2013;14(6):383–400. doi:10.1038/NRN3504
- Reisberg B, Doody R, Stöffler A, Schmitt F, Ferris S, Möbius HJ. Memantine in moderate-to-severe Alzheimer's disease. *N Engl J Med*. 2003;348(14):1333–1341. doi:10.1056/NEJMOA013128
- Paoletti P. Molecular basis of NMDA receptor functional diversity. *Eur J Neurosci*. 2011;33(8):1351–1365. doi:10.1111/J.1460-9568.2011.07628.X
- Sanz-Clemente A, Nicoll RA, Roche KW. Diversity in NMDA receptor composition: many regulators, many consequences. *Neuroscientist*. 2013;19(1):62–75. doi:10.1177/1073858411435129
- Pegasiou CM, Zolnourian A, Gomez-Nicola D, et al. Age-dependent changes in synaptic NMDA receptor composition in adult human cortical neurons. *Cereb Cortex*. 2020;30(7):4246–4256. doi:10.1093/CERCOR/BHAA052
- Wang R, Reddy PH. Role of glutamate and NMDA receptors in Alzheimer's disease. *J Alzheimers Dis*. 2017;57(4):1041–1048. doi:10.3233/JAD-160763
- Prybylowski K, Chang K, Sans N, Kan L, Vicini S, Wenthold RJ. The synaptic localization of NR2B-containing NMDA receptors is controlled by interactions with PDZ proteins and AP-2. *Neuron*. 2005;47(6):845–857. doi:10.1016/J.NEURON.2005.08.016
- Herz J, Chen Y, Reelin, lipoprotein receptors and synaptic plasticity. *Nat Rev Neurosci*. 2006;7(11):850–859. doi:10.1038/nrn2009
- Cuchillo-Ibáñez I, Balmaceda V, Mata-Balaguer T, Lopez-Font I, Sáez-Valero J. Reelin in Alzheimer's disease, increased levels but impaired signaling: when more is less. *J Alzheimer's Dis*. 2016;52(2):403–416. doi:10.3233/JAD-151193
- Horak M, Barackova P, Langore E, Netolicky J, Rivas-Ramirez P, Rehakova K. The extracellular domains of GluN subunits play an essential role in processing NMDA receptors in the ER. *Front Neurosci*. 2021;15:603715. doi:10.3389/FNINS.2021.603715
- Trepanier CH, Jackson MF, MacDonald JF. Regulation of NMDA receptors by the tyrosine kinase Fyn. *FEBS J*. 2012;279(1):12–19. doi:10.1111/J.1742-4658.2011.08391.X
- Tezuka T, Umemori H, Akiyama T, Nakanishi S, Yamamoto T. PSD-95 promotes Fyn-mediated tyrosine phosphorylation of the N-methyl-D-aspartate receptor subunit NR2A. *Proc Natl Acad Sci U S A*. 1999;96(2):435–440. doi:10.1073/PNAS.96.2.435
- Grovesman BR, Feng S, Fang XQ, et al. The regulation of N-methyl-D-aspartate receptors by Src kinase. *FEBS J*. 2012;279(1):20–28. doi:10.1111/j.1742-4658.2011.08413.x
- Hardingham GE, Fukunaga Y, Bading H. Extrasynaptic NMDARs oppose synaptic NMDARs by triggering CREB shut-off and cell death pathways. *Nat Neurosci*. 2002;5(5):405–414. doi:10.1038/nn835
- Goebel-Goody SM, Davies KD, Alvestad Linger RM, Freund RK, Browning MD. Phospho-regulation of synaptic and extrasynaptic N-methyl-D-aspartate receptors in adult hippocampal slices. *Neuroscience*. 2009;158(4):1446–1459. doi:10.1016/j.neuroscience.2008.11.006
- Pallas-Bazarra N, Draffin J, Cuadros R, Antonio Esteban J, Avila J. Tau is required for the function of extrasynaptic NMDA receptors. *Sci Rep*. 2019;9(1):9116. doi:10.1038/s41598-019-45547-8
- Marco S, Giral A, Petrovic MM, et al. Suppressing aberrant GluN3A expression rescues synaptic and behavioral impairments in Huntington's disease models. *Nat Med*. 2013;19(8):1030–1038. doi:10.1038/NM.3246
- Yan J, Peter Bengtson C, Buchthal B, Hagenston AM, Bading H. Coupling of NMDA receptors and TRPM4 guides discovery of unconventional neuroprotectants. *Science*. 2020;370(6513):eaay3302. doi:10.1126/SCIENCE.AAY3302
- Yu SP, Jiang MQ, Shim SS, Pourkhodad S, Wei L. Extrasynaptic NMDA receptors in acute and chronic excitotoxicity: implications for preventive treatments of ischemic stroke and late-onset Alzheimer's disease. *Mol Neurodegener*. 2023;18(1):43. doi:10.1186/S13024-023-00636-1
- Italia M, Ferrari E, Diluca M, Gardoni F. NMDA and AMPA receptors at synapses: novel targets for tau and α -synuclein proteinopathies. *Biomedicines*. 2022;10(7):1550. doi:10.3390/BIMEDICINES10071550
- Roselli F, Tirard M, Lu J, et al. Soluble beta-amyloid1-40 induces NMDA-dependent degradation of postsynaptic density-95 at

- glutamatergic synapses. *J Neurosci*. 2005;25(48):11061-11070. doi:[10.1523/JNEUROSCI.3034-05.2005](https://doi.org/10.1523/JNEUROSCI.3034-05.2005)
22. Chang L, Zhang Y, Liu J, et al. Differential regulation of N-methyl-D-aspartate receptor subunits is an early event in the actions of soluble amyloid- β (1-40) oligomers on hippocampal neurons. *J Alzheimers Dis*. 2016;51(1):197-212. doi:[10.3233/JAD-150942](https://doi.org/10.3233/JAD-150942)
23. Li Y, Chang L, Song Y, et al. Astrocytic GluN2A and GluN2B oppose the synaptotoxic effects of amyloid- β 1-40 in hippocampal cells. *J Alzheimers Dis*. 2016;54(1):135-148. doi:[10.3233/JAD-160297](https://doi.org/10.3233/JAD-160297)
24. Braak H, Alafuzoff I, Arzberger T, Kretschmar H, Del Tredici K. Staging of Alzheimer disease-associated neurofibrillary pathology using paraffin sections and immunocytochemistry. *Acta Neuropathol*. 2006;112(4):389-404. doi:[10.1007/s00401-006-0127-z](https://doi.org/10.1007/s00401-006-0127-z)
25. Jiang X, Knox R, Pathipati P, Ferriero D. Developmental localization of NMDA receptors, Src and MAP kinases in mouse brain. *Neurosci Lett*. 2011;503(3):215-219. doi:[10.1016/j.neulet.2011.08.039](https://doi.org/10.1016/j.neulet.2011.08.039)
26. Bayés À, Collins MO, Galtrey CM, et al. Human post-mortem synapse proteome integrity screening for proteomic studies of postsynaptic complexes. *Mol Brain*. 2014;7(1):88. doi:[10.1186/S13041-014-0088-4](https://doi.org/10.1186/S13041-014-0088-4)
27. Wang Y, TesFaye E, Yasuda RP, Mash DC, Armstrong DM, Wolfe BB. Effects of post-mortem delay on subunits of ionotropic glutamate receptors in human brain. *Mol Brain Res*. 2000;80(2):123-131. doi:[10.1016/S0169-328X\(00\)00111-X](https://doi.org/10.1016/S0169-328X(00)00111-X)
28. Pérez-Otaño I, Luján R, Tavalin SJ, et al. Endocytosis and synaptic removal of NR3A-containing NMDA receptors by PAC-SIN1/syndapin1. *Nat Neurosci*. 2006;9(5):611-621. doi:[10.1038/nn1680](https://doi.org/10.1038/nn1680)
29. Wee KSL, Tan FCK, Cheong YP, Khanna S, Low CM. Ontogenic profile and synaptic distribution of GluN3 proteins in the rat brain and hippocampal neurons. *Neurochem Res*. 2016;41(1-2):290-297. doi:[10.1007/S11064-015-1794-8](https://doi.org/10.1007/S11064-015-1794-8)
30. Lichnerova K, Kaniakova M, Park SP, et al. Two N-glycosylation sites in the GluN1 subunit are essential for releasing N-methyl-d-aspartate (NMDA) receptors from the endoplasmic reticulum. *J Biol Chem*. 2015;290(30):18379-18390. doi:[10.1074/JBC.M115.656546](https://doi.org/10.1074/JBC.M115.656546)
31. Kaniakova M, Lichnerova K, Skrenkova K, Vyklicky L, Horak M. Biochemical and electrophysiological characterization of N-glycans on NMDA receptor subunits. *J Neurochem*. 2016;138(4):546-556. doi:[10.1111/JNC.13679](https://doi.org/10.1111/JNC.13679)
32. Verhaeghe R, Elia-Zudaire O, Escamilla S, Sáez-Valero J, Pérez-Otaño I. No evidence for cognitive decline or neurodegeneration in strain-matched Grin3a knockout mice. *Alzheimers Dement*. 2023;19(9):4264-4266. doi:[10.1002/ALZ.13375](https://doi.org/10.1002/ALZ.13375)
33. Allen B, Ingram E, Takao M, et al. Abundant tau filaments and non-apoptotic neurodegeneration in transgenic mice expressing human P301S tau protein. *J Neurosci*. 2002;22(21):9340-9351. doi:[10.1523/JNEUROSCI.22-21-09340.2002](https://doi.org/10.1523/JNEUROSCI.22-21-09340.2002)
34. Borchelt DR, Ratovitski T, Van Lare J, et al. Accelerated amyloid deposition in the brains of transgenic mice coexpressing mutant presenilin 1 and amyloid precursor proteins. *Neuron*. 1997;19(4):939-945. doi:[10.1016/S0896-6273\(00\)80974-5](https://doi.org/10.1016/S0896-6273(00)80974-5)
35. Jankowsky JL, Fadale DJ, Anderson J, et al. Mutant presenilins specifically elevate the levels of the 42 residue beta-amyloid peptide in vivo: evidence for augmentation of a 42-specific gamma secretase. *Hum Mol Genet*. 2004;13(2):159-170. doi:[10.1093/HMG/DDH019](https://doi.org/10.1093/HMG/DDH019)
36. Sanchez-Mut J V., Heyn H, Silva BA, et al. PM20D1 is a quantitative trait locus associated with Alzheimer's disease. *Nat Med*. 2018;24(5):598-603. doi:[10.1038/S41591-018-0013-Y](https://doi.org/10.1038/S41591-018-0013-Y)
37. Zhou X, Chen Z, Yun W, Ren J, Li C, Wang H. Extrasynaptic NMDA receptor in excitotoxicity: function revisited. *Neuroscientist*. 2015;21(4):337-344. doi:[10.1177/1073858414548724](https://doi.org/10.1177/1073858414548724)
38. Yanamandra K, Kfoury N, Jiang H, et al. Anti-tau antibodies that block tau aggregate seeding invitro markedly decrease pathology and improve cognition in vivo. *Neuron*. 2013;80(2):402-414. doi:[10.1016/j.neuron.2013.07.046](https://doi.org/10.1016/j.neuron.2013.07.046)
39. González-González IM, Gray JA, Ferreira J, et al. GluN3A subunit tunes NMDA receptor synaptic trafficking and content during post-natal brain development. *Cell Rep*. 2023;42(5):112477. doi:[10.1016/J.CELREP.2023.112477](https://doi.org/10.1016/J.CELREP.2023.112477)
40. Groc L, Heine M, Cousins SL, et al. NMDA receptor surface mobility depends on NR2A-2B subunits. *Proc Natl Acad Sci U S A*. 2006;103(49):18769-18774. doi:[10.1073/PNAS.0605238103](https://doi.org/10.1073/PNAS.0605238103)
41. Martel MA, Wyllie DJ, Hardingham GE. In developing hippocampal neurons, NR2B-containing N-methyl-d-aspartate receptors (NMDARs) can mediate signaling to neuronal survival and synaptic potentiation, as well as neuronal death. *Neuroscience*. 2009;158(1):334-343. doi:[10.1016/j.neuroscience.2008.01.080](https://doi.org/10.1016/j.neuroscience.2008.01.080)
42. Lai TW, Shyu WC, Wang YT. Stroke intervention pathways: NMDA receptors and beyond. *Trends Mol Med*. 2011;17(5):266-275. doi:[10.1016/J.MOLMED.2010.12.008](https://doi.org/10.1016/J.MOLMED.2010.12.008)
43. Petralia RS. Distribution of extrasynaptic NMDA receptors on neurons. *ScientificWorldJournal*. 2012;2012:267120. doi:[10.1100/2012/267120](https://doi.org/10.1100/2012/267120)
44. Sattler R, Xiong Z, Lu WY, MacDonald JF, Tymianski M. Distinct roles of synaptic and extrasynaptic NMDA receptors in excitotoxicity. *J Neurosci*. 2000;20(1):22. doi:[10.1523/JNEUROSCI.20-01-00022.2000](https://doi.org/10.1523/JNEUROSCI.20-01-00022.2000)
45. Huang YWA, Zhou B, Wernig M, Südhof TC. ApoE2, ApoE3, and ApoE4 differentially stimulate APP transcription and $\alpha\beta$ secretion. *Cell*. 2017;168(3):427-441.e21. doi:[10.1016/j.cell.2016.12.044](https://doi.org/10.1016/j.cell.2016.12.044)
46. Parsons MP, Raymond LA. Extrasynaptic NMDA receptor involvement in central nervous system disorders. *Neuron*. 2014;82(2):279-293. doi:[10.1016/J.NEURON.2014.03.030](https://doi.org/10.1016/J.NEURON.2014.03.030)
47. Gladding CM, Raymond LA. Mechanisms underlying NMDA receptor synaptic/extrasynaptic distribution and function. *Mol Cell Neurosci*. 2011;48(4):308-320. doi:[10.1016/J.MCN.2011.05.001](https://doi.org/10.1016/J.MCN.2011.05.001)
48. Papouin T, Oliet SHR. Organization, control and function of extrasynaptic NMDA receptors. *Philos Trans R Soc B Biol Sci*. 2014;369(1654):20130601. doi:[10.1098/RSTB.2013.0601](https://doi.org/10.1098/RSTB.2013.0601)
49. Nakanishi N, Tu S, Shin Y, et al. Neuroprotection by the NR3A subunit of the NMDA receptor. *J Neurosci*. 2009;29(16):5260. doi:[10.1523/JNEUROSCI.1067-09.2009](https://doi.org/10.1523/JNEUROSCI.1067-09.2009)
50. Lau SF, Cao H, Fu AKY, Ip NY. Single-nucleus transcriptome analysis reveals dysregulation of angiogenic endothelial cells and neuroprotective glia in Alzheimer's disease. *Proc Natl Acad Sci U S A*. 2020;117(41):25800-25809. doi:[10.1073/PNAS.2008762117/-DCSUPPLEMENTAL](https://doi.org/10.1073/PNAS.2008762117/-DCSUPPLEMENTAL)
51. Das S, Li Z, Wachter A, et al. Distinct transcriptomic responses to $\alpha\beta$ plaques, neurofibrillary tangles, and APOE in Alzheimer's disease. *Alzheimers Dement*. 2024;20(1):74-90. doi:[10.1002/alz.13387](https://doi.org/10.1002/alz.13387)
52. Mathys H, Davila-Velderrain J, Peng Z, et al. Single-cell transcriptomic analysis of Alzheimer's disease. *Nature*. 2019;570(7761):332-337. doi:[10.1038/S41586-019-1195-2](https://doi.org/10.1038/S41586-019-1195-2)
53. Bossers K, Wirz KTS, Meerhoff GF, et al. Concerted changes in transcripts in the prefrontal cortex precede neuropathology in Alzheimer's disease. *Brain*. 2010;133(Pt 12):3699-3723. doi:[10.1093/BRAIN/AWQ258](https://doi.org/10.1093/BRAIN/AWQ258)
54. Qian Z, Qin J, Lai Y, Zhang C, Zhang X. Large-scale integration of single-cell RNA-Seq data reveals astrocyte diversity and transcriptomic modules across six central nervous system disorders. *Biomolecules*. 2023;13(4):692. doi:[10.3390/B13040692](https://doi.org/10.3390/B13040692)
55. Sze CI, Bi H, Kleinschmidt-DeMasters BK, Filley CM, Martin LJ. N-Methyl-D-aspartate receptor subunit proteins and their phosphorylation status are altered selectively in Alzheimer's disease. *J Neurol Sci*. 2001;182(2):151-159. doi:[10.1016/S0022-510X\(00\)00467-6](https://doi.org/10.1016/S0022-510X(00)00467-6)
56. Bi H, Sze CI. N-methyl-D-aspartate receptor subunit NR2A and NR2B messenger RNA levels are altered in the hippocampus and

- entorhinal cortex in Alzheimer's disease. *J Neurol Sci.* 2002;200(1-2):11-18. doi:10.1016/S0022-510X(02)00087-4
57. Mishizen-Eberz AJ, Rissman RA, Carter TL, Ikonovic MD, Wolfe BB, Armstrong DM. Biochemical and molecular studies of NMDA receptor subunits NR1/2A/2B in hippocampal subregions throughout progression of Alzheimer's disease pathology. *Neurobiol Dis.* 2004;15(1):80-92. doi:10.1016/j.nbd.2003.09.016
 58. Hynd MR, Scott HL, Dodd PR. Differential expression of N-methyl-D-aspartate receptor NR2 isoforms in Alzheimer's disease. *J Neurochem.* 2004;90(4):913-919. doi:10.1111/J.1471-4159.2004.02548.X
 59. Zhang Q, Ma C, Chin LS, Pan S, Li L. Human brain glycoform coregulation network and glycan modification alterations in Alzheimer's disease. *Sci Adv.* 2024;10(14):eadk6911. doi:10.1126/SCIADV.ADK6911
 60. Kaniakova M, Lichnerova K, Skrenkova K, Vyklicky L, Horak M. Biochemical and electrophysiological characterization of N-glycans on NMDA receptor subunits. *J Neurochem.* 2016;546-556. doi:10.1111/jnc.13679
 61. Storey GP, Opitz-Araya X, Barria A. Molecular determinants controlling NMDA receptor synaptic incorporation. *J Neurosci.* 2011;31(17):6311-6316. doi:10.1523/JNEUROSCI.5553-10.2011
 62. Schedin-Weiss S, Winblad B, Tjernberg LO. The role of protein glycosylation in Alzheimer disease. *FEBS J.* 2014;281(1):46-62. doi:10.1111/FEBS.12590
 63. Conroy LR, Hawkinson TR, Young LEA, Gentry MS, Sun RC. Emerging roles of N-linked glycosylation in brain physiology and disorders. *Trends Endocrinol Metab.* 2021;32(12):980-993. doi:10.1016/J.TEM.2021.09.006
 64. Zhang Q, Ma C, Chin L-S, Pan S, Li L. Human brain glycoform coregulation network and glycan modification alterations in Alzheimer's disease. *bioRxiv [Preprint].* 2023;2023.11.13.566889. doi:10.1101/2023.11.13.566889
 65. Bieberich E. Synthesis, processing, and function of N-glycans in N-glycoproteins. *Adv Neurobiol.* 2023;29:65-93. doi:10.1007/978-3-031-12390-0_3
 66. Song XJ, Zhou HY, Sun YY, Huang HC. Phosphorylation and glycosylation of amyloid- β protein precursor: the relationship to trafficking and cleavage in Alzheimer's disease. *J Alzheimers Dis.* 2021;84(3):937-957. doi:10.3233/JAD-210337
 67. Boix CP, Lopez-Font I, Cuchillo-Ibañez I, Sáez-Valero J. Amyloid precursor protein glycosylation is altered in the brain of patients with Alzheimer's disease. *Alzheimers Res Ther.* 2020;12(1):96. doi:10.1186/S13195-020-00664-9
 68. Lennol MP, Sánchez-Domínguez I, Cuchillo-Ibañez I, et al. Apolipoprotein E imbalance in the cerebrospinal fluid of Alzheimer's disease patients. *Alzheimer's Res Ther.* 2022;14(1):161. doi:10.1186/s13195-022-01108-2
 69. Botella-López A, Burgaya F, Gavín R, et al. Reelin expression and glycosylation patterns are altered in Alzheimer's disease. *Proc Natl Acad Sci U S A.* 2006;103(14):5573-5578. doi:10.1073/pnas.0601279103
 70. Sáez-Valero J, Sberna G, McLean CA, Masters CL, Small DH. Glycosylation of acetylcholinesterase as diagnostic marker for Alzheimer's disease. *Lancet (London, England).* 1997;350(9082):929. doi:10.1016/S0140-6736(97)24039-0
 71. García-Ayllón MS, Botella-López A, Cuchillo-Ibañez I, et al. HNK-1 carrier glycoproteins are decreased in the Alzheimer's disease brain. *Mol Neurobiol.* 2017;54(1):188-199. doi:10.1007/s12035-015-9644-x
 72. Nakazawa T, Komai S, Tezuka T, et al. Characterization of Fyn-mediated tyrosine phosphorylation sites on GluR epsilon 2 (NR2B) subunit of the N-methyl-D-aspartate receptor. *J Biol Chem.* 2001;276(1):693-699. doi:10.1074/JBC.M008085200
 73. Gong CX, Liu F, Grundke-Iqbal I, Iqbal K. Impaired brain glucose metabolism leads to Alzheimer neurofibrillary degeneration through a decrease in tau O-GlcNAcylation. *J Alzheimers Dis.* 2006;9(1):1-12. doi:10.3233/JAD-2006-9101
 74. Alfaro-Ruiz R, Aguado C, Martín-Belmonte A, et al. Different modes of synaptic and extrasynaptic NMDA receptor alteration in the hippocampus of P301S tau transgenic mice. *Brain Pathol.* 2023;33(1):e13115. doi:10.1111/bpa.13115
 75. Xu L, Zhou Y, Hu L, et al. Deficits in N-methyl-D-aspartate receptor function and synaptic plasticity in hippocampal CA1 in APP/PS1 mouse model of Alzheimer's disease. *Front Aging Neurosci.* 2021;13:772980. doi:10.3389/FNAGI.2021.772980
 76. He RB, Li L, Liu LZ, et al. Ceftriaxone improves impairments in synaptic plasticity and cognitive behavior in APP/PS1 mouse model of Alzheimer's disease by inhibiting extrasynaptic NMDAR-STEP61 signaling. *J Neurochem.* 2023;166(2):215-232. doi:10.1111/JNC.15874
 77. Rammes G, Mattusch C, Wulff M, et al. Involvement of GluN2B subunit containing N-methyl-d-aspartate (NMDA) receptors in mediating the acute and chronic synaptotoxic effects of oligomeric amyloid-beta (A β) in murine models of Alzheimer's disease (AD). *Neuropharmacology.* 2017;123:100-115. doi:10.1016/J.NEUROPHARM.2017.02.003
 78. Salter MW, Pitcher GM. Dysregulated Src upregulation of NMDA receptor activity: a common link in chronic pain and schizophrenia. *FEBS J.* 2012;279(1):2-11. doi:10.1111/J.1742-4658.2011.08390.X
 79. Barki-Harrington L, Elkobi A, Tzabary T, Rosenblum K. Tyrosine phosphorylation of the 2B subunit of the NMDA receptor is necessary for taste memory formation. *J Neurosci.* 2009;29(29):9219-9226. doi:10.1523/JNEUROSCI.5667-08.2009
 80. Waters EM, Mazid S, Dodos M, et al. Effects of estrogen and aging on synaptic morphology and distribution of phosphorylated Tyr1472 NR2B in the female rat hippocampus. *Neurobiol Aging.* 2019;73:200-210. doi:10.1016/J.NEUROBIOLAGING.2018.09.025

SUPPORTING INFORMATION


Additional supporting information can be found online in the Supporting Information section at the end of this article.

How to cite this article: Escamilla S, Badillos R, Comella JX, et al. Synaptic and extrasynaptic distribution of NMDA receptors in the cortex of Alzheimer's disease patients. *Alzheimer's Dement.* 2024;1-15.
<https://doi.org/10.1002/alz.14125>



Review

NMDARs in Alzheimer's Disease: Between Synaptic and Extrasynaptic Membranes

Sergio Escamilla ^{1,2,3,*}, Javier Sáez-Valero ^{1,2,3}  and Inmaculada Cuchillo-Ibáñez ^{1,2,3,*}

¹ Instituto de Neurociencias, Universidad Miguel Hernández-Consejo Superior de Investigaciones Científicas (UMH-CSIC), 03550 Sant Joan d'Alacant, Spain; j.saez@umh.es

² Centro de Investigación Biomédica en Red Enfermedades Neurodegenerativas (CIBERNED), 03550 Sant Joan d'Alacant, Spain

³ Instituto de Investigación Sanitaria y Biomédica de Alicante (ISABIAL), 03010 Alicante, Spain

* Correspondence: sescamilla@umh.es (S.E.); icuchillo@umh.es (I.C.-I.)

Abstract: N-methyl-D-aspartate receptors (NMDARs) are glutamate receptors with key roles in synaptic communication and plasticity. The activation of synaptic NMDARs initiates plasticity and stimulates cell survival. In contrast, the activation of extrasynaptic NMDARs can promote cell death underlying a potential mechanism of neurodegeneration occurring in Alzheimer's disease (AD). The distribution of synaptic versus extrasynaptic NMDARs has emerged as an important parameter contributing to neuronal dysfunction in neurodegenerative diseases including AD. Here, we review the concept of extrasynaptic NMDARs, as this population is present in numerous neuronal cell membranes but also in the membranes of various non-neuronal cells. Previous evidence regarding the membranal distribution of synaptic versus extrasynaptic NMDRs in relation to AD mice models and in the brains of AD patients will also be reviewed.

Keywords: NMDAR; GluN2B; GluN2A; GluN1; excitotoxicity; extrasynaptic NMDAR; Alzheimer's disease



Citation: Escamilla, S.; Sáez-Valero, J.; Cuchillo-Ibáñez, I. NMDARs in Alzheimer's Disease: Between Synaptic and Extrasynaptic Membranes. *Int. J. Mol. Sci.* **2024**, *25*, 10220. <https://doi.org/10.3390/ijms251810220>

Academic Editor: Alberto Pérez-Mediavilla

Received: 2 September 2024

Revised: 16 September 2024

Accepted: 19 September 2024

Published: 23 September 2024



Copyright: © 2024 by the authors. Licensee MDPI, Basel, Switzerland. This article is an open access article distributed under the terms and conditions of the Creative Commons Attribution (CC BY) license (<https://creativecommons.org/licenses/by/4.0/>).

1. Structure, Function, and Subcellular Localization of NMDARs

N-methyl-D-aspartate receptors (NMDARs) are glutamate-binding calcium-gating channels involved in learning and memory processes [1–3]. NMDARs form tetrameric complexes assembled with two compulsory GluN1 subunits and two homomeric or heteromeric GluN2 (2A–2D) or GluN3 (3A–3B) subunits [4–6]. The four GluN2 subunits are major determinants of the heterogeneity of NMDAR function [4]. NMDARs are present in the whole central nervous system (CNS), with the highest densities in cortical and hippocampal structures [7,8]. The expression of NMDAR subunits, especially GluN2B, varies across different brain areas [9]. NMDAR density follows a gradient matching the cortical hierarchy, with neurons involved in more complex functions expressing more NMDARs [10]. The function of native NMDARs depends on their channel properties, abundance, and subcellular distribution between synaptic and extrasynaptic membranes [5,11]. This distribution defines their chemical micro-environment, its activation mode (tonic vs. phasic), and its interaction with different intracellular signaling molecules [12].

To fulfill their biological roles, most NMDARs are located at synaptic membranes, within the postsynaptic density (PSD) in neurons, being defined as synaptic NMDARs (SynNMDARs) [12]; however, NMDARs can also be located outside the synapses at a lower density than SynNMDARs [13], thus being defined as extrasynaptic NMDARs (ExsynNMDARs). This criterion usually includes those NMDARs in the perisynaptic space, such as the dendritic spine neck and places further from synapses in the dendritic shaft, the soma, or the axon [11–14]. Relying on morphological criteria, receptors are considered extrasynaptic when located at 100 nm or more from the PSD [12].

SynNMDARs and ExsynNMDARs display distinct roles in signaling pathways and gene regulation. SynNMDARs are important for LTP and prosurvival signaling [15]. Their activation produces phosphorylation and activation of the extracellular signal-regulated kinase (ERK) [16], phosphorylation of cAMP response element-binding protein (CREB) and neuroprotective effects [17]. On the other hand, the activation of ExsynNMDARs triggers the opposite mechanisms, as de novo long-term depression (LTD) [18,19], ERK dephosphorylation and inactivation, and shutting off of the CREB pathway. Pathological activation of ExsynNMDARs drives neuronal death through a process called excitotoxicity [17]. This process acts through mechanisms such as synapto-nuclear communication [20,21] and inversion of mitochondrial potential [22–24] and results in altered calcium influx [22,25,26].

In the adult human and mouse cortex, the most abundant subunits, along with GluN1, are GluN2A, GluN2B [4,27], and GluN3A, GluN3A being expressed more during the post-natal period [6,28]. GluN2A and GluN2B have different kinetics and biochemical properties [29,30] and different protein partners [31]. GluN2B is thought to be more mobile across membrane localizations than GluN2A [32]. Still, both GluN2A and GluN2B are present in synaptic and extrasynaptic membranes [13,33–35], with a complex and dynamic interplay between these two subcellular localizations. Furthermore, the presence of the GluN2A subunit increases NMDAR stability at synapses [15,22,32]. The consensus is that GluN2A and GluN2B are mainly synaptic [34], while GluN3A is mainly associated with the perisynaptic site of the PSD [28,36]. Remarkably, extrasynaptic GluN2A and GluN2B are related to excitotoxicity [35,37–39]. Therefore, changes in the distribution of NMDAR subunits can affect synaptic stability and play a role in various neurodegenerative diseases [40].

2. How to Distinguish SynNMDARs and ExsynNMDARs

Approaches to analyzing the synaptic/extrasynaptic distribution of NMDARs are based on imaging analysis, electrophysiological studies using pharmacologic tools, and biochemical fractionation. Imaging tools such as electron micrographs and confocal or high-resolution microscopy identify SynNMDARs when they colocalize with a protein present in the PSD, typically PSD95 [41,42], or with the presynaptic proteins synaptophysin or synapsin 1 [43,44]. Specific pharmacological drugs distinguish synaptic and extrasynaptic NMDARs based on their capacity to block preferentially one over the other. For instance, MK-801 blocks SynNMDARs preferentially [17,45], while memantine blocks ExsynNMDARs preferentially [46,47]. Other drugs act on specific subunits, such as ifenprodil, that block GluN2B preferentially [44,48], and this is useful in electrophysiological characterization.

Biochemical fractionation protocols can isolate SynNMDARs and ExsynNMDARs based on the differential solubility of the plasma membranes where they are located. The PSD-containing membranes are very dense and contain a meshwork of proteins linking synaptic receptors to signaling molecules and the cytoskeleton [49]. Consequently, these membranes are insoluble in solutions with low detergent concentrations and generate a pellet after centrifugation, mainly composed of the PSD, and thus, it is considered the synaptic fraction. Conversely, those plasmatic membranes not attached to the PSD are highly soluble in detergent solutions and remain in the supernatant after centrifugation, representing the extrasynaptic fraction [50,51]. Different biochemical fractionation protocols exist for PSD isolation [52–55], mainly designed and tested for fresh mice brains.

The Conception of ExsynNMDARs

SynNMDARs are primarily found in the postsynaptic membranes of glutamatergic excitatory neurons. However, they have also been identified in inhibitory GABAergic interneurons in mice [56–60]. In contrast, the term “ExsynNMDARs” is ambiguous and not well established. Typically, ExsynNMDARs refer to neuronal NMDARs located in the plasma membrane outside the PSD, dendritic shaft, and soma. This category may also encompass presynaptic NMDARs, which have distinct synaptic transmission and plasticity

functions, although their function is less explored [14,59,61]. This raises concerns about grouping specific NMDARs located within and outside of synapses under the blanket term of ExsynNMDARs (Figure 1).

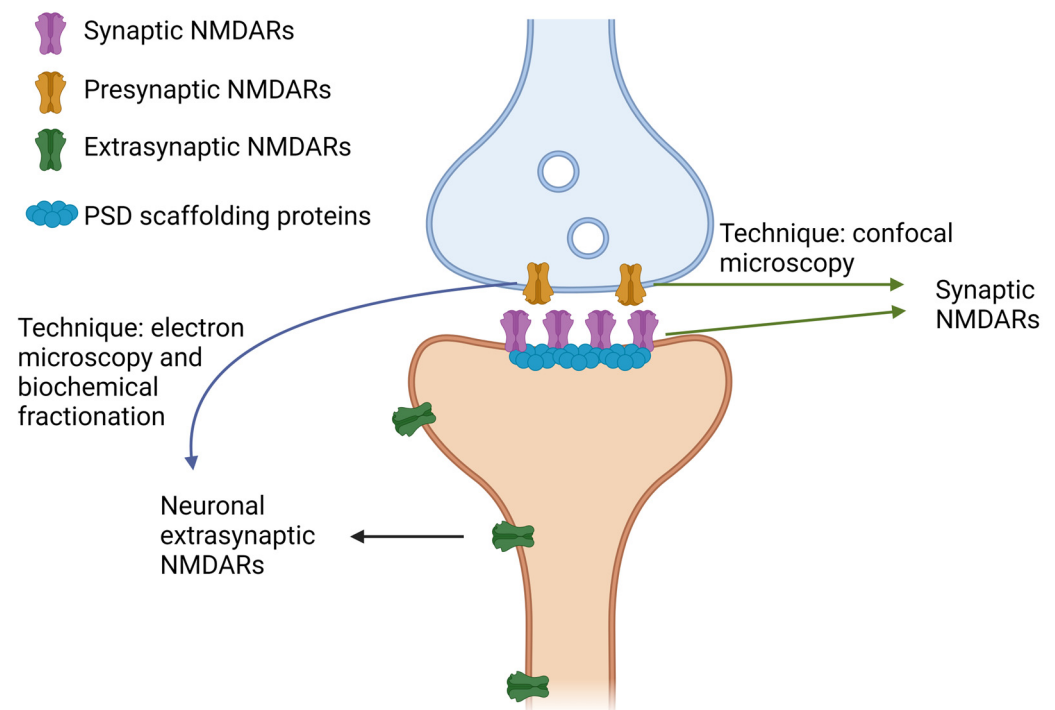


Figure 1. Classification of neuronal NMDARs as synaptic or extrasynaptic according to the technique of choice. Schematic illustration of a glutamatergic synapse, including the pre (blue)- and postsynaptic (orange) terminals. Different populations of NMDARs are represented: (1) presynaptic, (2) those located in the PSD, and (3) extrasynaptic. Synaptic NMDARs include those in the PSD and the presynaptic ones when the technique of choice is confocal microscopy, especially when the synaptic marker is a presynaptic protein, such as synaptophysin and syntaxin 1. However, when the technique is biochemical fractionation, presynaptic NMDARs will reside in the extrasynaptic fraction, and the synaptic fraction will be composed mainly of the PSD. In addition, electron microscopy allows us to distinguish pre- from postsynaptic terminals and, thus, presynaptic NMDARs and those in the PSD. Created in [BioRender.com](#).

Overall, neuronal ExsynNMDARs may have specific functions that differ from synaptic NMDARs. ExsynNMDARs may be in extrasynaptic membranes because they are in transit, either being stored temporarily or actively moving to synapses from exocytosis sites or synapses to sites of endocytosis [62,63]. However, they could reside permanently in extrasynaptic membranes organized in supramolecular structures like their synaptic counterparts. Most of these extrasynaptic sites are points of contact with adjacent processes, including glia, axons, synaptic terminals, and dendrites [13,64].

Furthermore, it is important to note that ExsynNMDARs may also refer to non-neuronal NMDARs, expressed by astrocytes [65–67], microglia [68–70], oligodendrocytes [71], and endothelial cells [72,73].

In immunofluorescence studies, “synaptic NMDARs” refer to the population of NMDARs in the PSD that typically colocalizes with PSD95 [41,74,75]. However, other postsynaptic markers such as Homer [28,76–79] or Shank [77] are also used. Another typical criterion for defining SynNMDARs is the colocalization with a presynaptic marker, usually synaptophysin [43,44], which would include presynaptic NMDARs as SynNMDARs. To standardize the protocol for measuring synaptic and extrasynaptic NMDARs, the best approach to identify SynNMDARs would likely be to use a combination of pre- and post-

synaptic markers [34,80], since both pre- and postsynaptic terminals are needed to build a synapse.

It is not always clear whether ExsynNMDARs are free or part of protein complexes. Some candidates associated with neuronal ExsynNMDARs are protein phosphatase 1 (PP1) [74], adhesion proteins such as cadherin and catenin [13], the C-terminus of GIPC (G α -interacting protein) [81], or membrane-associated guanylate kinases (MAGUKs) [11] such as SAP102 [62,82] or SAP97 [83]. These proteins may not be exclusively confined to a single membrane compartment (synaptic or extrasynaptic), making it challenging to distinguish between synaptic and extrasynaptic NMDARs [13,82,83]. In this line, PSD95, essentially postsynaptic, was found by immunofluorescence and electron-microscopy immunogold images in extrasynaptic membranes in clusters containing NMDARs [13]. This suggests that neuronal NMDARs attached to PSD95 could not be considered exclusively as SynNMDARs, and some overestimation of this population could occur when using imaging techniques.

When immunofluorescence is the technique of choice, the type of biological sample determines the necessary precautions to prevent mixing NMDARs from different cell types. In pure neuronal cultures, neuronal ExsynNMDARs will be those that do not colocalize with synaptic markers since there are no other cell types. However, in cultures containing non-neuronal cells (e.g., mixed neuronal and astrocytic cultures), brain tissue slices, or brain organoids, ExsynNMDARs will correspond to different populations. NMDARs that do not colocalize with synaptic markers but do with neuron-specific cytoskeletal markers, such as class III beta-tubulin (TUB1) or MAP2, will correspond to neuronal ExsynNMDARs, whereas NMDARs that colocalize with markers, such as GFAP or S100 β (astrocytes) or iba1 (microglia), will correspond to non-neuronal ExsynNMDARs (astrocytic and microglial NMDARs, respectively) (Figure 2). When biochemical fractionation is the technique of choice and a piece of brain is the starting material, the extrasynaptic fraction will contain NMDARs from different cell types besides neurons, such as astrocytes, microglia, oligodendrocytes, and endothelial cells [84].

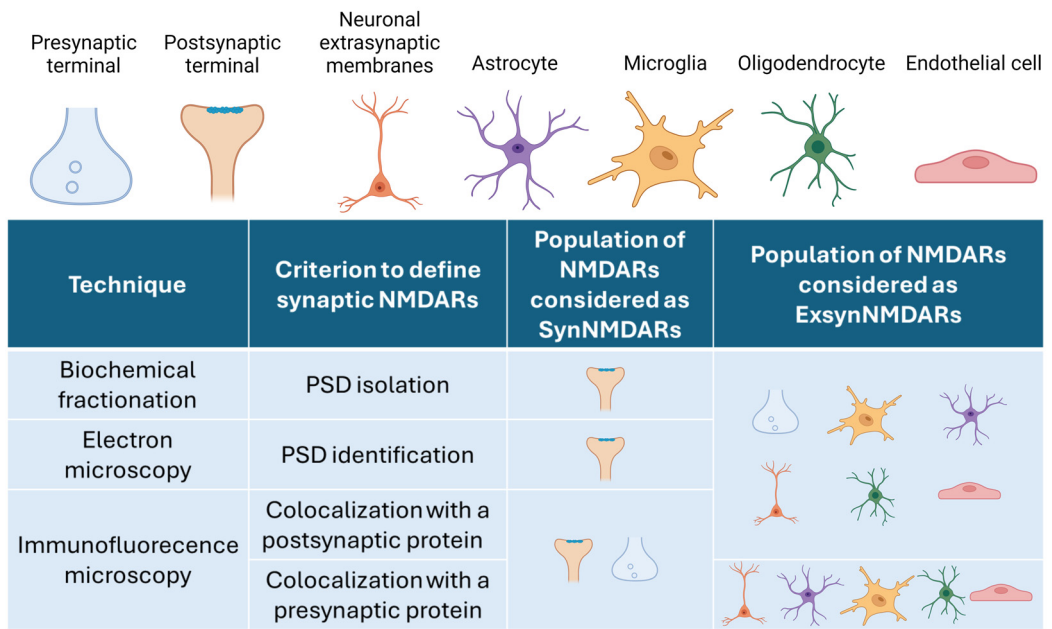


Figure 2. Classification of NMDARs as synaptic or extrasynaptic according to the technique of choice and cell type. The schematic table contains columns for the technique of choice, the criterion to define an NMDAR as synaptic, and which NMDAR populations will be considered as SynNMDARs or ExsynNMDARs attending to subcellular localization or cell type origin. Created in [BioRender.com](#).

Finally, specific blockers such as MK-801 and memantine are used to discriminate the activity of neuronal SynNMDARs and ExsynNMDARs, but these drugs also block ExsynNMDARs from astrocytes [65,85,86] and microglia [68,69,86,87], highlighting the

need for precise characterization of the ExsynNMDAR populations. Electron-microscopy images can discriminate between presynaptic and postsynaptic NMDARs. This technique has shown the presence of presynaptic NMDARs at rat cortical presynaptic terminals, where immunostaining was sparse and substantially less intense than postsynaptic staining [61]. Cellular fractionation is another tool for isolating presynaptic from postsynaptic NMDARs [84].

When the sample includes different cell types, such as those in brain slices, cerebral organoids, and in vitro co-cultures, it is important to consider that NMDARs are expressed not only by neurons but also by astrocytes, microglia, oligodendrocytes, and endothelial cells. Depending on the technique of choice, the NMDARs considered synaptic or extrasynaptic will differ. Biochemical fractionation will isolate the PSD. Thus, SynNMDARs will be those in the PSD, and the ExsynNMDARs will be the rest. Electron microscopy allows the identification of the PSD. Thus, it will be able to consider the NMDARs in the PSD, the presynaptic and the extrasynaptic NMDARs independently. Immunofluorescence-microscopy criteria rely on the colocalization of NMDARs with either synaptic or extrasynaptic proteins. The most used postsynaptic marker is PSD95, which is considered to reside exclusively in the PSD (even though it has been argued that PSD95 could also be present in extrasynaptic membranes [13]). However, the pre- and postsynaptic terminals are so close to each other that they will colocalize, meaning that immunostaining from presynaptic NMDARs and those NMDARs in the PSD will be mixed, being both populations will be considered as SynNMDARs. When the choice is a presynaptic marker (usually synaptophysin or syn-taxin1), the result will be similar, since NMDARs will colocalize with those in the PSD and presynaptic NMDARs.

3. NMDAR Distribution in Alzheimer's Disease

It is assumed that an imbalance between SynNMDAR and ExsynNMDAR activation could be part of the etiology of neurodegenerative diseases such as AD [36,88–90], where the homeostasis of glutamate is dysregulated [91–93]. However, there is relatively little information about alterations in the distribution of NMDARs in synaptic and extrasynaptic membranes in the brains of individuals with AD. One of the few drugs used in AD therapy, memantine, is an open-channel blocker of ExsynNMDARs [46,47,94,95]. Memantine is currently used in combination with acetylcholinesterase inhibitors [96], and despite the clinical effects being controversial still [97], the data in preclinical studies suggest that it has a positive impact on improving AD brain neuropathology [98].

Chronic activation of ExsynNMDARs could be a contributing effector of AD [36,99–101]. In vitro and in vivo studies suggest an excessive release of glutamate from astrocytes in AD activates ExsynNMDARs in neurons [102]. Moreover, the activation of ExsynNMDARs increases the production of the β -amyloid peptide (A β) [103] and increases the expression [41,104,105] and phosphorylation [102] of tau, the main hallmarks of AD. In this context, it has been reported that pharmacological inhibition of GluN2B ameliorates tau pathology [104–106]. On the contrary, stimulation of SynNMDARs increases the non-amyloidogenic processing of APP by α -secretase, thus decreasing the release of A β [107].

AD is usually modeled in vitro and in vivo using transgenic mice over-expressing human APP or by adding A β peptides [41,43,108], but tau pathology can also be modeled [109,110]. Tau is a cytoskeleton protein mainly present in the axon but also in the dendritic compartment [111]. Several studies show a relation between tau and NMDARs through the stabilization of NMDARs at the PSD [112] and, more specifically, regulating ExsynNMDAR lateral diffusion. However, the possible alteration in the NMDAR distribution in tau models of AD has not been fully explored. We will independently review the impact of these two pathological mechanisms on the distribution of SynNMDARs and ExsynNMDARs.

3.1. Distribution of SynNMDARs and ExsynNMDARs in Animal Models of AD

3.1.1. Distribution of SynNMDARs and ExsynNMDARs in Tauopathy Mice Models

Levels of ExsynNMDAR subunits have been analyzed in the AD mice model expressing P301S, a human mutant tau that leads to the widespread neurofibrillary tangles of phospho-tau, resembling the neurofibrillary tangles found in the brains of patients with AD. In these mice, the subcellular localization of GluN1 has been analyzed using electron micrographs of the hippocampus [113]. In this study, synaptic GluN1 in excitatory synapses and interneuron dendrites was significantly reduced in P301S mice, while extrasynaptic GluN1 increased in interneuron dendrites, with respect to wild-type mice. This differential distribution of synaptic versus extrasynaptic NMDARs supports the notion that the progressive accumulation of phospho-tau is associated with changes in NMDAR distribution since these alterations are observed at 10 months old when pathology is present, but not at 3 months old. In agreement, our recent analysis of NMDAR subunit distribution in this AD model, using a subcellular fractionation protocol, also resulted in lower levels of synaptic GluN1 and GluN2B and also lower levels of extrasynaptic GluN3A, with respect to those in wild-type mice [84].

In another model of tauopathy, the rTg4510 mouse, which also expresses P301L human tau associated with FTDP-17 [114], the authors of a study reported that human tau and mutant P301L tau are enriched in dendritic spines of rTg4510 compared to control mice. In parallel, the synaptic expression of GluN1 and GluN2/3 was lower in rTgP301L mice.

These studies with tau mice models indicate that tau phosphorylation can play a role in NMDAR distribution, probably through tau mislocalization to dendritic spines, rich in F-actin [115], and lead to an impaired intracellular sorting and trafficking of synaptic proteins [116], including NMDARs.

Accordingly, it has been hypothesized that tau hyperphosphorylation could lead to increased levels of NMDARs in the extrasynaptic membranes. In a recent study, researchers reached these conclusions by using *crmp1* KO mice [117]. CRMP1 is a protein that regulates F-actin depolymerization and is associated with synaptic plasticity mechanisms [118,119]. To identify NMDAR distribution, they used a fractionation protocol with PSD95 as a synaptic marker. They found in the *crmp1* KO mice increased ExsynNMDAR subunit levels, accompanied by increased levels of phosphorylated tau, and claimed that CRMP1 and tau malfunction could lead to F-actin depolymerization in the dendritic spine and concomitant increase in ExsynNMDARs.

The effect of tau on NMDAR distribution was also tested in tau-KO mice [120]. The authors of a study analyzed, by immunohistochemistry, the association of GluN2B-Y1336 phosphorylation (phosphorylation that has been associated mainly with extrasynaptic localization [121]) with extrasynaptic GluN2B subunits. They observed that the absence of tau leads to a decrease in functional ExsynNMDARs in the hippocampus and proposed that tau is involved in NMDAR trafficking through actin depolymerization in the spine [122] as a possible mechanism that regulates NMDAR lateral diffusion.

In the same line of evidence, in mice primary hippocampal neurons treated with tau derived from the brains of patients with AD, GluN2B was translocated from the synapse to extrasynaptic membranes, identified by imaging colocalization with PSD95 or by biochemical fractionation [41]. Authors pointed out that, in these cultures, tau derived from AD was able to increase Casein Kinase 2 (CK2), which phosphorylates GluN2B in serine 1480, detaching this subunit from PSD95. This enhances the probability of GluN2B of leaving the synapse by either lateral diffusion or by endocytosis [75,80]. Interestingly, the levels of CK2 are increased in the hippocampus of patients with AD [123] but not in other tauopathies.

Together, these data indicate that the tauopathy that develops in the brains of individuals with AD could promote the translocation of NMDAR subunits from the synaptic to the extrasynaptic membranes.

3.1.2. Distribution of SynNMDARs and ExsynNMDARs in A β -Treated Cultures and Mice Models

A β is related to spine loss by reducing SynNMDAR levels [124]. A pioneering study in cultured cortical neurons showed that A β enhances the activity of the phosphatase STEP61, which dephosphorylates GluN2B at Tyr1472, inducing its endocytosis through clathrin adaptor proteins [43], while extrasynaptic and total NMDARs levels remained unchanged. In agreement, in mice hippocampal slices, a combination of current blockage by MK-801, biochemical fractionation, and confocal colocalization with synapsin determined that prolonged exposure to soluble A β oligomers (hours), but not brief exposure (minutes), decreases synaptic GluN2B while extrasynaptic GluN2B remains unaffected [44].

Most of the *in vitro* studies that evaluate A β effects on NMDAR levels in murine hippocampal or cortical cultures do not discriminate between SynNMDARs and ExsynNMDARs and, instead, evaluate NMDAR total levels or the surface expression of NMDAR subunits. These studies describe that A β reduces the surface expression of GluN1 and GluN2B [48,53,125,126], although the total levels do not change, and causes a reduction in the number of GluN2A-positive dendritic spines [127]. Similarly, in rat entorhinal cortex slices, 3 h of exposure to A β decreases GluN2B and GluN2A total protein levels and GluN2B mRNA levels, but no changes were observed in GluN1 [128].

The discrepancy between the results obtained regarding NMDAR subunit levels when reported as being associated with membranes and those of the total levels could be explained by the population of NMDARs residing in intracellular pools. In cerebellar granule cells, the majority of unassembled GluN1 subunits are located in the endoplasmic reticulum [129]. This could mask possible reductions in GluN1 in synaptic and extrasynaptic membranes precisely when levels are measured in total cell extracts without any fractionation protocol to distinguish them or in immunofluorescence assays in permeabilization conditions.

Other studies have also evaluated NMDAR levels in the brain of the APP/PS1 AD mice model [109,110], which develops amyloid plaques and shows AD-like cognitive impairment. Reduced levels of GluN2B alone or with GluN1 have been observed in these models in the synaptic fraction obtained by biochemical fractionation of the hippocampus [53,126]. Indeed, when a fractionation protocol is employed to isolate synaptic and extrasynaptic membranes, low levels of synaptic GluN2B and high levels of extrasynaptic GluN2B have been described in the hippocampus of these AD mice [52]. In our recent study, we observed low levels of GluN1 in synaptic and extrasynaptic membranes in the cortices of APP/PS1 mice [84], which are likely affecting all NMDARs and, therefore, contributing to the synaptic failure described in this model [130] driven by A β .

3.2. NMDAR Subunit Levels in the Brain of Individuals with AD

Firstly, it is essential to note that the methodological approaches to studying the NMDARs in the human post-mortem brain are hindered by preanalytical confounding factors, such as freeze/thaw cycles [131] and the post-mortem intervals (PMI) of the samples. It is well established that NMDAR subunits are vulnerable to PMI-associated degradation in different degrees. Indeed, the GluN1 subunit protein is unaffected by post-mortem delays up to 18 h, while GluN2A and GluN2B subunit proteins show significant degradation with shortened PMI [132,133].

Currently, brain banks aim to reduce PMI to just a few hours. However, overall rRNA and mRNA stability are maintained for up to 60 h post-mortem [131,134], without apparent correlation with pH changes due to tissue acidification [34], although specific mRNAs may be selectively degraded [35]. Synaptosomes isolated from frozen human brain retain respiratory activity and the ability to release neurotransmitters and appear to be morphologically indistinguishable from those from fresh tissues, even with a PMI of 24 h [135]. On the other hand, dephosphorylation may occur on some proteins in less than 1 min, which is a significant problem even in animal experiments [36].

Ideally, the effect of PMI should be individually addressed for each assay condition, but this may not be practical in many experiments. To address degradations, protocols for estimating NMDAR degradation have been proposed [133,136] to allow researchers to discard brain samples with high synaptic degradation [132]. For example, the HUMAN Synapse Proteome Integrity Ratio or “HUSPIR index” aims to evaluate the integrity and preservation of the post-mortem samples prior to analyses, and to obtain this, this index measures the ratio of two proteolytic fragments of GluN2B in synaptic fractions by immunoblots [136].

Studies of NMDAR expression in human samples are few in comparison with those in mice models. In the human cortex, the evaluation of NMDAR levels has been approached by transcriptional techniques and by measuring total protein levels from brain extracts without the capacity to distinguish SynNMDARs from ExsynNMDARs. Techniques that allow us to distinguish them, such as subcellular fractionation, are quite scarce.

3.2.1. Regional NMDAR Transcript Levels in the Brain of Individuals with AD

Studies that have evaluated NMDAR subunit expression using RT-qPCR report reduced mRNA levels of GluN1, GluN2A, and GluN2B in the hippocampus, temporal cortex, entorhinal cortex, and cingulate cortex from individuals with AD and report no alterations in less vulnerable regions, such as the occipital cortex or cerebellum [132,137–139]. Novel transcriptomic technologies, such as single-cell transcriptomics, have focused the analysis on the expression of *GRIN1*, the gene that codifies the compulsory NMDAR subunit GluN1. *GRIN1* is downregulated in the temporal cortex of individuals with AD [134,140]. In the prefrontal cortex, *GRIN1* expression is modulated through AD progression, being upregulated at the beginning of the disease, but is eventually downregulated with respect to controls [141]. Other studies do not find any change in the expression of *GRIN1* in the frontal or prefrontal cortex [134,142] nor when *GRIN1* was assessed in astrocytes [143]. Transcriptomic expressions of other NMDAR subunits, *GRIN2A*, *GRIN2B*, and *GRIN3A*, are downregulated in the temporal cortex of individuals with AD [140].

3.2.2. Total Protein Levels of NMDAR Subunits in the Brain of Patients with AD

The expression of NMDAR subunits at the protein level measured by immunoblots closely follows the expression at the transcript level. Accordingly, levels of GluN1, GluN2B, and GluN2A are reduced in extracts from AD-susceptible regions such as the hippocampus, entorhinal cortex, frontal cortex, or cingulate cortex from individuals with AD with respect to controls [132,133,138,144], but no changes are reported in less susceptible regions, such as the occipital cortex or the caudate [144]. However, some studies have found increased levels of GluN2A in the hippocampus at moderate stages of AD [132], and increased GluN2B levels in the prefrontal cortex at the earliest stages of the disease [145]. The employment of quantitative in vitro autoradiography with the specific NMDAR antagonist [³H]MK-801 [146], which allows the quantification of global levels of NMDARs, also shows lower levels of the receptor in the hippocampus and entorhinal cortex but not in the basal ganglia in individuals with AD.

In summary, most of the previous reports concluded that total protein and transcript levels of NMDAR subunits decrease in susceptible brain areas in AD. Interestingly, high levels of GluN1 and GluN2A were recently described [147] using confocal microscopy in the astrocytes of the hippocampus of individuals with AD (Braak stage IV–VI) but not in neurons.

This result highlights that the levels of NMDARs could change in the AD brain in different compartments of neurons and other cell types. In this regard, little is known about what functions NMDARs perform in non-neuronal cells (reviewed here for astrocytes [67,148], oligodendrocytes [149,150], microglia [70,151], and non-neuronal cells in general [152], respectively). Overall, this suggests that changes in the levels of NMDARs from different populations are likely contributing to different manifestations associated with AD progression.

3.2.3. NMDAR Subunits Protein Levels in Synaptic and Extrasynaptic Membranes

Studies performed in animal models and primary cell cultures led to the idea that GluN2A populates mainly the synaptic membranes, while GluN2B is mostly extrasynaptic [5,32,37,153]. Thus, the activation of GluN2A would lead to LTP and pro-survival signaling, while GluN2B would be responsible for LTD and excitotoxicity [154]. However, this oversimplified model was rapidly challenged by two main experimental outcomes. First, both GluN2A and GluN2B subunits populate synaptic and extrasynaptic membranes [34]. And second, both subunits participate in excitotoxicity [35,155].

Overall, these results may vary due to differences in experimental conditions. The use of different neurodevelopmental stages and the absence of pharmacological tools to definitively distinguish NMDAR subtypes may account for the conflicting outcomes [88]. The “age” of cultured neurons is another critical factor. After one week of culture, around 90% of NMDARs are in the extrasynaptic membranes, while this number reduces to 50% or less after two weeks in vitro [11]. These conflicting results strengthen the need for studies performed on the human brain.

In this regard, subcellular fractionation methods permit the isolation, purification, and/or enrichment of specific cellular compartments from complex tissue samples [156–160] that allow unique insights, resulting in them being more informative than the assessment of total protein levels. In a recent study, we optimized the fractionation protocol of post-mortem human brain cortex [84], allowing us to describe for the first time the distribution of the main four NMDAR subunits—GluN2B, GluN2A, GluN1, and GluN3A—between synaptic and extrasynaptic membranes in the human frontal cortex. An analysis of the total levels of NMDAR subunits on crude membrane fractions from AD cortex displayed, in good agreement with previous studies, decreased levels of GluN1, GluN2B, and GluN2A, with unchanged GluN3A levels, with respect to controls. Our analysis of the synaptic membranes demonstrated that GluN2B and GluN2A levels were lower in AD than in controls. More interestingly, when we quantified the extrasynaptic membrane levels of GluN2B and GluN1, these were higher in AD, and GluN2A showed a similar trend. Remarkably, we found two different glycoforms of GluN2B and GluN2A in the extrasynaptic membrane that turned out to be increased in an AD brain. Our study uncovered the NMDAR distribution in an AD cortex, showing a reduction in NMDARs in synaptic membranes and an increase in extrasynaptic membranes. The shift to extrasynaptic membranes of GluN2B, GluN2A, and GluN1 reported could explain the exacerbated NMDAR-related excitotoxicity observed in AD (Figure 3).

Several studies suggest that SynNMDARs are lower in the AD brain while ExsynNMDARs are increased. Possible explanations for the decrease in SynNMDARs include endocytosis and posterior degradation or lateral diffusion. The increase in ExsynNMDARs can be explained by the translocation of NMDARs from the PSD to extrasynaptic membranes, impaired delivery of NMDARs to the PSD, and increased expression of NMDARs by non-neuronal cell types, such as astrocytes. Created in [BioRender.com](https://www.biorender.com).

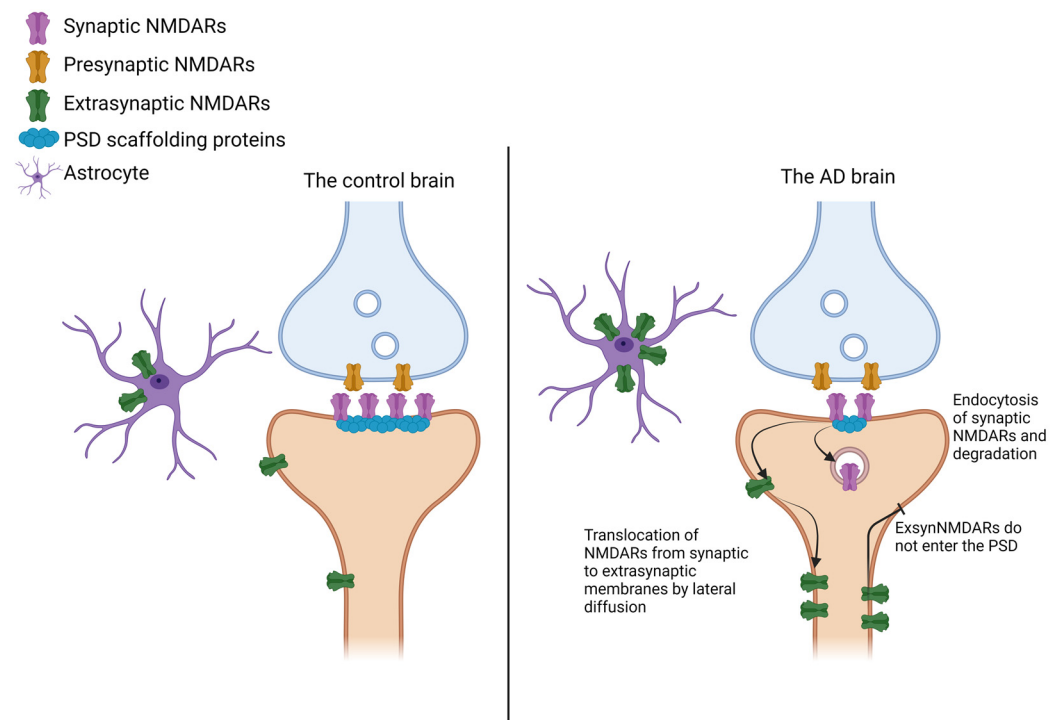


Figure 3. Model of altered levels of NMDARs in the AD brain.

4. Conclusions

The distribution of synaptic versus extrasynaptic NMDARs has emerged as an important parameter that contributes to neuronal dysfunction in neurodegenerative diseases such as AD [11,88]. Protein hallmarks of AD pathology, tau, and beta-amyloid peptide contribute to the imbalance by promoting SynNMDAR endocytosis [43,44] and increasing ExsynNMDARs [52]. Overall, studies in AD mice models and in the human brain from individuals with AD indicate that SynNMDAR levels are reduced while ExsynNMDAR levels increase with respect to controls (Tables 1 and 2). Whereas the activation of SynNMDARs is neuroprotective [17,22], the activation of ExsynNMDARs has neurotoxic effects linked to neuronal death. Consequently, any alteration in the number and density of NMDARs could contribute to the synaptic and memory deficits that are associated with AD. Consequently, distinguishing synaptic from extrasynaptic NMDARs is particularly important for defining therapeutic approaches.

ExsynNMDARs include a broader population of receptors than those included in the term SynNMDAR. Proper criteria are necessary to characterize ExsynNMDARs since neuronal and non-neuronal cells express ExsynNMDARs, and an imprecise identification can arise if it is assumed that most of the ExsynNMDARs are exclusively neuronal. Subcellular fractionation protocols allow us to isolate NMDARs from the PSD (synaptic fraction) from those outside the PSD (extrasynaptic fraction). While the NMDARs in the synaptic fraction are well defined, the NMDARs in the extrasynaptic fraction are a mix of presynaptic, neuronal extrasynaptic, and non-neuronal. However, no further assessments are usually performed to gain insight in this regard. Furthermore, a technique as common as immunofluorescence in neuronal cultures can identify “synaptic NMDARs” without discriminating those located in the post- and presynaptic membranes unless higher-resolution techniques are utilized [158], such as 3D reconstructions of isolated spines [61]. Therefore, a correct identification of ExsynNMDARs is necessary since their role is not yet fully understood.

Table 1. Summary of studies assessing synaptic and extrasynaptic NMDAR subunit protein and mRNA levels in human models. N/A: non-applicable.

mRNA Levels								
Reference	Year	Technique	Brain Area	Sample Size (AD Braak Stage)	Levels with Respect to Control			Cell Type (When Specified)
					GRIN1	GRIN2A	GRIN2B	
[139]	2001	qPCR	Temporal and cingulate cortex	10 (no Braak specified)	Down	N/A	N/A	
[138]	2004	qPCR	Hippocampus, anterior cingulate gyrus, and superior temporal cortex	10 (no Braak specified)	Down	Down	Down	
[132]	2004	qPCR	Hippocampus	10 (I–II); 10 (III–IV); 10 (V–VI)	Down	No change	Down	
[137]	2002	qPCR	Hippocampus	10 (no Braak specified)		Down	Down	
[142]	2010	Microarray	Prefrontal cortex	14 (I–II); 14 (III–IV); 14 (V–VI)		Down		
[141]	2019	snRNAseq	Prefrontal cortex	10 (I–II); 21 (III–IV); 17 (V–VI)	Up at early stages but down at late stages	Down	No change	Excitatory neurons
[140]	2024	RNAseq	Superior temporal gyrus	10 (V–VI)	No change	No change	No change	
[134]	2020	RNAseq	Prefrontal cortex	12 (IV–VI)		Up	Up	Endothelial cells
					Down	Down		Oligodendrocytes
Total Protein Levels								
Reference	Year	Technique	Brain Area	Sample Size (AD Braak Stage)	Levels with Respect to Control			Cell Type (When Specified)
					GluN1	GluN2A	GluN2B	
[138]	2004	WB	Hippocampus, anterior cingulate gyrus, and superior temporal cortex	10 (no Braak specified)		Down	Down	
[132]	2004	WB	Hippocampus		Down	Up (in early stage)	Down	

Table 1. Cont.

[146]	2013	Quantitative autoradiography	Hippocampus	23 (IV–VI)	General NMDAR reduction	General NMDAR reduction	General NMDAR reduction	
[144]	2001	WB	Entorhinal cx	6 (III–VI)	No change	Down	Down	
			Hippocampus		Down	No change	Down	
			Caudate		No change	No change	No change	
			Occipital cortex		No change	No change	No change	
[147]	2021	Quantitative confocal microscopy	Hippocampus	8 (IV–VI)	Up	Up		General and specifically in astrocytes
[133]	2000	WB	Hippocampus	6 (no Braak specified)	Down	No change	Down	
			Frontal cx		Down	Down	Down	
			Entorhinal cx		No change	No change	No change	

Table 2. Summary of studies assessing synaptic and extrasynaptic NMDAR subunit protein and mRNA levels in mice AD models. An asterisk means an additional explanation in the ‘Other findings’ column.

Tauopathy Mice Models										
Reference	Year	Technique	Criterion SynNMDAR	Criterion ExsynNMDAR	Model/Cell Culture Treatment	NMDARs Levels Respect to WT or Control			Observations	Other Findings
						SynNMDAR	ExsynNMDAR	Total NMDAR		
[120]	2019	Microscopy	Y1472-GluN3B	Y1336-GluN3B	tau KO mice	No change	No change	No change	Hippocampus	tau KO lacks ExsynNMDAR currents
[112]	2010	Biochemical	Solubility in SDS	Solubility in pH 8	tau KO mice	Down	Up	No change	Hippocampus	

Table 2. Cont.

[113]	2023	SDS-FRL	(Self-developed semi-automatic software) Dendritic spines were considered as such if (1) they emerged from a dendritic shaft or (2) they opposed an axon terminal recognized by the presence of synaptic vesicles on their cross-fractured portions	Non-specific background labeling was measured on E-face structures surrounding the measured P-faces (specific staining surrounding spines)	Tg P301S mice	No change *	Up **		* In excitatory neurons, decreased SynNMDARs but unaltered ExsynGluN1	** Specifically in interneuron dendrites of the stratum oriens
[41]	2022	Microscopy	Colocalization with PSD95	The rest	Neurons treated with tau from AD brain tau for 7 days	Down	Up	Down	Mouse cultured hippocampal neurons	
Amyloidosis Mice Models										
Reference	Year	Technique	Criterion Syn NMDAR	Criterion ExsynNMDAR	Treatment/ Model	NMDARs Level Respect to WT or Control			Observations	Other Findings
						SynNMDAR	ExsynNMDAR	Total NMDAR		
[43]	2005	Microscopy	Colocalization with synapsin	No colocalization with synapsin	Cultured cortical neurons treated with Aβ 1 h	Down GluN1	Suggests redistribution to extrasynaptic membranes			Detect reduced GluN1 in surface levels but no changes in total levels. Suggests redistribution to extrasynaptic membranes.

Table 2. Cont.

		Biotinylation				No change	Reduced surface expression of GluN2B and GluN1, no change in total levels
[44]	2011	Biochemical	Triton soluble fraction	Triton insoluble fraction	Mice slices treated with Aβ -> fractionation	Down GluN2B	No change
		Microscopy	Colocalization with synapsin	No colocalization with synapsin	Cultured hippocampal neurons + Aβ	Down GluN2B	No change
[52]	2023	Biochemical	Triton insolubility	Triton solubility	APP/PS1 mouse	Down GluN2B	Up GluN2B

In the clinic, NMDARs are currently the targets of numerous programs for finding new drugs for AD or other diseases of the CNS [161,162]. The correct discrimination among all the types of NMDARs present in the brain will benefit the research for specific drugs, to help cure these diseases.

Author Contributions: Conceptualization, S.E. and I.C.-I.; writing—original draft preparation, S.E.; writing—review and editing, S.E., I.C.-I. and J.S.-V.; supervision, I.C.-I. and J.S.-V.; funding acquisition, I.C.-I. and J.S.-V. All authors have read and agreed to the published version of the manuscript.

Funding: This research was funded by Fondo de Investigaciones Sanitarias (PI22-01329, co-funded by the Fondo Europeo de Desarrollo Regional, FEDER “Investing in your future”), CIBERNED (Instituto de Salud Carlos III, Spain), ISABIAL (Instituto de Investigación Sanitaria y Biomédica de Alicante), and the Direcció General de Ciència i Investigació, Generalitat Valenciana (AICO/2021/308). We acknowledge financial support from the Spanish Ministerio de Ciencia, Innovación y Universidades, Agencia Estatal de Investigación, through the “Severo Ochoa” Programme for Centres of Excellence in R&D (CEX2021-001165-S). Sergio Escamilla is funded by the Instituto Carlos III de Madrid (PFIS fellowship).

Conflicts of Interest: The authors declare no conflicts of interest. The funders had no role in the design of the study; in the collection, analyses, or interpretation of data; in the writing of the manuscript; or in the decision to publish the results.

References

- Morris, R.G. NMDA receptors and memory encoding. *Neuropharmacology* **2013**, *74*, 32–40. [\[CrossRef\]](#) [\[PubMed\]](#)
- Tsien, J.Z.; Huerta, P.T.; Tonegawa, S. The essential role of hippocampal CA1 NMDA receptor-dependent synaptic plasticity in spatial memory. *Cell* **1996**, *87*, 1327–1338. [\[CrossRef\]](#) [\[PubMed\]](#)
- Li, F.; Tsien, J.Z. Memory and the NMDA receptors. *N. Engl. J. Med.* **2009**, *361*, 302–303. [\[CrossRef\]](#)
- Paoletti, P.; Bellone, C.; Zhou, Q. NMDA receptor subunit diversity: Impact on receptor properties, synaptic plasticity and disease. *Nat. Rev. Neurosci.* **2013**, *14*, 383–400. [\[CrossRef\]](#)
- Sanz-Clemente, A.; Nicoll, R.A.; Roche, K.W. Diversity in NMDA receptor composition: Many regulators, many consequences. *Neuroscientist* **2013**, *19*, 62–75. [\[CrossRef\]](#) [\[PubMed\]](#)
- Pérez-Otaño, I.; Larsen, R.S.; Wesseling, J.F. Emerging roles of GluN3-containing NMDA receptors in the CNS. *Nat. Rev. Neurosci.* **2016**, *17*, 623–635. [\[CrossRef\]](#)
- Dingledine, R.; Borges, K.; Bowie, D.; Traynelis, S.F. The glutamate receptor ion channels. *Pharmacol. Rev.* **1999**, *51*, 7–61.
- Volianskis, A.; France, G.; Jensen, M.S.; Bortolotto, Z.A.; Jane, D.E.; Collingridge, G.L. Long-term potentiation and the role of N-methyl-D-aspartate receptors. *Brain Res.* **2015**, *1621*, 5–16. [\[CrossRef\]](#) [\[PubMed\]](#)
- Wang, X.J. Macroscopic gradients of synaptic excitation and inhibition in the neocortex. *Nat. Rev. Neurosci.* **2020**, *21*, 169–178. [\[CrossRef\]](#)
- Froudust-Walsh, S.; Xu, T.; Niu, M.; Rapan, L.; Zhao, L.; Margulies, D.S.; Zilles, K.; Wang, X.J.; Palomero-Gallagher, N. Gradients of neurotransmitter receptor expression in the macaque cortex. *Nat. Neurosci.* **2023**, *26*, 1281–1294. [\[CrossRef\]](#)
- Gladding, C.M.; Raymond, L.A. Mechanisms underlying NMDA receptor synaptic/extrasynaptic distribution and function. *Mol. Cell Neurosci.* **2011**, *48*, 308–320. [\[CrossRef\]](#) [\[PubMed\]](#)
- Papouin, T.; Oliet, S.H. Organization, control and function of extrasynaptic NMDA receptors. *Philos. Trans. R. Soc. Lond. B Biol. Sci.* **2014**, *369*, 20130601. [\[CrossRef\]](#) [\[PubMed\]](#)
- Petralia, R.S.; Wang, Y.X.; Hua, F.; Yi, Z.; Zhou, A.; Ge, L.; Stephenson, F.A.; Wenthold, R.J. Organization of NMDA receptors at extrasynaptic locations. *Neuroscience* **2010**, *167*, 68–87. [\[CrossRef\]](#) [\[PubMed\]](#)
- Banerjee, A.; Larsen, R.S.; Philpot, B.D.; Paulsen, O. Roles of Presynaptic NMDA Receptors in Neurotransmission and Plasticity. *Trends Neurosci.* **2016**, *39*, 26–39. [\[CrossRef\]](#)
- Franchini, L.; Stanic, J.; Ponzoni, L.; Mellone, M.; Carrano, N.; Musardo, S.; Zianni, E.; Olivero, G.; Marcello, E.; Pittaluga, A.; et al. Linking NMDA Receptor Synaptic Retention to Synaptic Plasticity and Cognition. *iScience* **2019**, *19*, 927–939. [\[CrossRef\]](#)
- Ivanov, A.; Pellegrino, C.; Rama, S.; Dumalska, I.; Salyha, Y.; Ben-Ari, Y.; Medina, I. Opposing role of synaptic and extrasynaptic NMDA receptors in regulation of the extracellular signal-regulated kinases (ERK) activity in cultured rat hippocampal neurons. *J. Physiol.* **2006**, *572*, 789–798. [\[CrossRef\]](#)
- Hardingham, G.E.; Fukunaga, Y.; Bading, H. Extrasynaptic NMDARs oppose synaptic NMDARs by triggering CREB shut-off and cell death pathways. *Nat. Neurosci.* **2002**, *5*, 405–414. [\[CrossRef\]](#) [\[PubMed\]](#)
- Massey, P.V.; Johnson, B.E.; Moulton, P.R.; Auberson, Y.P.; Brown, M.W.; Molnar, E.; Collingridge, G.L.; Bashir, Z.I. Differential roles of NR2A and NR2B-containing NMDA receptors in cortical long-term potentiation and long-term depression. *J. Neurosci.* **2004**, *24*, 7821–7828. [\[CrossRef\]](#)

19. Lu, W.; Man, H.; Ju, W.; Trimble, W.S.; MacDonald, J.F.; Wang, Y.T. Activation of synaptic NMDA receptors induces membrane insertion of new AMPA receptors and LTP in cultured hippocampal neurons. *Neuron* **2001**, *29*, 243–254. [\[CrossRef\]](#)
20. Karpova, A.; Mikhaylova, M.; Bera, S.; Bär, J.; Reddy, P.P.; Behnisch, T.; Rankovic, V.; Spilker, C.; Bethge, P.; Sahin, J.; et al. Encoding and transducing the synaptic or extrasynaptic origin of NMDA receptor signals to the nucleus. *Cell* **2013**, *152*, 1119–1133. [\[CrossRef\]](#)
21. Röncke, R.; Mikhaylova, M.; Röncke, S.; Meinhardt, J.; Schröder, U.H.; Fändrich, M.; Reiser, G.; Kreutz, M.R.; Reymann, K.G. Early neuronal dysfunction by amyloid β oligomers depends on activation of NR2B-containing NMDA receptors. *Neurobiol. Aging* **2011**, *32*, 2219–2228. [\[CrossRef\]](#) [\[PubMed\]](#)
22. Hardingham, G.E.; Bading, H. Synaptic versus extrasynaptic NMDA receptor signalling: Implications for neurodegenerative disorders. *Nat. Rev. Neurosci.* **2010**, *11*, 682–696. [\[CrossRef\]](#) [\[PubMed\]](#)
23. Lau, D.; Bading, H. Synaptic activity-mediated suppression of p53 and induction of nuclear calcium-regulated neuroprotective genes promote survival through inhibition of mitochondrial permeability transition. *J. Neurosci.* **2009**, *29*, 4420–4429. [\[CrossRef\]](#) [\[PubMed\]](#)
24. Léveillé, F.; Papadia, S.; Fricker, M.; Bell, K.F.; Soriano, F.X.; Martel, M.A.; Puddifoot, C.; Habel, M.; Wyllie, D.J.; Ikonomidou, C.; et al. Suppression of the intrinsic apoptosis pathway by synaptic activity. *J. Neurosci.* **2010**, *30*, 2623–2635. [\[CrossRef\]](#)
25. Dick, O.; Bading, H. Synaptic activity and nuclear calcium signaling protect hippocampal neurons from death signal-associated nuclear translocation of FoxO3a induced by extrasynaptic N-methyl-D-aspartate receptors. *J. Biol. Chem.* **2010**, *285*, 19354–19361. [\[CrossRef\]](#)
26. Vanhoutte, P.; Bading, H. Opposing roles of synaptic and extrasynaptic NMDA receptors in neuronal calcium signalling and BDNF gene regulation. *Curr. Opin. Neurobiol.* **2003**, *13*, 366–371. [\[CrossRef\]](#)
27. Pegasiou, C.M.; Zolnourian, A.; Gomez-Nicola, D.; Deinhardt, K.; Nicoll, J.A.R.; Ahmed, A.I.; Vajramani, G.; Grundy, P.; Verhoog, M.B.; Mansvelder, H.D.; et al. Age-Dependent Changes in Synaptic NMDA Receptor Composition in Adult Human Cortical Neurons. *Cereb. Cortex* **2020**, *30*, 4246–4256. [\[CrossRef\]](#)
28. González-González, I.M.; Gray, J.A.; Ferreira, J.; Conde-Dusman, M.J.; Bouchet, D.; Perez-Otaño, I.; Groc, L. GluN3A subunit tunes NMDA receptor synaptic trafficking and content during postnatal brain development. *Cell Rep.* **2023**, *42*, 112477. [\[CrossRef\]](#) [\[PubMed\]](#)
29. Erreger, K.; Dravid, S.M.; Banke, T.G.; Wyllie, D.J.; Traynelis, S.F. Subunit-specific gating controls rat NR1/NR2A and NR1/NR2B NMDA channel kinetics and synaptic signalling profiles. *J. Physiol.* **2005**, *563*, 345–358. [\[CrossRef\]](#)
30. Gray, J.A.; Shi, Y.; Usui, H.; During, M.J.; Sakimura, K.; Nicoll, R.A. Distinct modes of AMPA receptor suppression at developing synapses by GluN2A and GluN2B: Single-cell NMDA receptor subunit deletion in vivo. *Neuron* **2011**, *71*, 1085–1101. [\[CrossRef\]](#)
31. Gardoni, F.; Di Luca, M. Protein-protein interactions at the NMDA receptor complex: From synaptic retention to synaptonuclear protein messengers. *Neuropharmacology* **2021**, *190*, 108551. [\[CrossRef\]](#) [\[PubMed\]](#)
32. Groc, L.; Heine, M.; Cousins, S.L.; Stephenson, F.A.; Lounis, B.; Cognet, L.; Choquet, D. NMDA receptor surface mobility depends on NR2A-2B subunits. *Proc. Natl. Acad. Sci. USA* **2006**, *103*, 18769–18774. [\[CrossRef\]](#) [\[PubMed\]](#)
33. Thomas, C.G.; Miller, A.J.; Westbrook, G.L. Synaptic and extrasynaptic NMDA receptor NR2 subunits in cultured hippocampal neurons. *J. Neurophysiol.* **2006**, *95*, 1727–1734. [\[CrossRef\]](#) [\[PubMed\]](#)
34. Petralia, R.S. Distribution of extrasynaptic NMDA receptors on neurons. *Sci. World J.* **2012**, *2012*, 267120. [\[CrossRef\]](#)
35. Yan, J.; Bengtson, C.P.; Buchthal, B.; Hagenston, A.M.; Bading, H. Coupling of NMDA receptors and TRPM4 guides discovery of unconventional neuroprotectants. *Science* **2020**, *370*, eaay3302. [\[CrossRef\]](#)
36. Yu, S.P.; Jiang, M.Q.; Shim, S.S.; Pourkhodad, S.; Wei, L. Extrasynaptic NMDA receptors in acute and chronic excitotoxicity: Implications for preventive treatments of ischemic stroke and late-onset Alzheimer's disease. *Mol. Neurodegener.* **2023**, *18*, 43. [\[CrossRef\]](#) [\[PubMed\]](#)
37. Martel, M.A.; Wyllie, D.J.; Hardingham, G.E. In developing hippocampal neurons, NR2B-containing N-methyl-D-aspartate receptors (NMDARs) can mediate signaling to neuronal survival and synaptic potentiation, as well as neuronal death. *Neuroscience* **2009**, *158*, 334–343. [\[CrossRef\]](#)
38. Papadia, S.; Soriano, F.X.; Léveillé, F.; Martel, M.A.; Dakin, K.A.; Hansen, H.H.; Kaindl, A.; Siffringer, M.; Fowler, J.; Stefovská, V.; et al. Synaptic NMDA receptor activity boosts intrinsic antioxidant defenses. *Nat. Neurosci.* **2008**, *11*, 476–487. [\[CrossRef\]](#)
39. von Engelhardt, J.; Coserea, I.; Pawlak, V.; Fuchs, E.C.; Köhr, G.; Seeburg, P.H.; Monyer, H. Excitotoxicity in vitro by NR2A- and NR2B-containing NMDA receptors. *Neuropharmacology* **2007**, *53*, 10–17. [\[CrossRef\]](#)
40. Crawley, O.; Conde-Dusman, M.J.; Pérez-Otaño, I. GluN3A NMDA receptor subunits: More enigmatic than ever? *J. Physiol.* **2022**, *600*, 261–276. [\[CrossRef\]](#)
41. Marshall, C.A.; McBride, J.D.; Changolkar, L.; Riddle, D.M.; Trojanowski, J.Q.; Lee, V.M. Inhibition of CK2 mitigates Alzheimer's tau pathology by preventing NR2B synaptic mislocalization. *Acta Neuropathol. Commun.* **2022**, *10*, 30. [\[CrossRef\]](#) [\[PubMed\]](#)
42. Hoover, B.R.; Reed, M.N.; Su, J.; Penrod, R.D.; Kotilinek, L.A.; Grant, M.K.; Pitstick, R.; Carlson, G.A.; Lanier, L.M.; Yuan, L.L.; et al. Tau mislocalization to dendritic spines mediates synaptic dysfunction independently of neurodegeneration. *Neuron* **2010**, *68*, 1067–1081. [\[CrossRef\]](#) [\[PubMed\]](#)
43. Snyder, E.M.; Nong, Y.; Almeida, C.G.; Paul, S.; Moran, T.; Choi, E.Y.; Nairn, A.C.; Salter, M.W.; Lombroso, P.J.; Gouras, G.K.; et al. Regulation of NMDA receptor trafficking by amyloid-beta. *Nat. Neurosci.* **2005**, *8*, 1051–1058. [\[CrossRef\]](#) [\[PubMed\]](#)

44. Li, S.; Jin, M.; Koeglsperger, T.; Shepardson, N.E.; Shankar, G.M.; Selkoe, D.J. Soluble A β oligomers inhibit long-term potentiation through a mechanism involving excessive activation of extrasynaptic NR2B-containing NMDA receptors. *J. Neurosci.* **2011**, *31*, 6627–6638. [\[CrossRef\]](#) [\[PubMed\]](#)
45. McKay, S.; Bengtson, C.P.; Bading, H.; Wyllie, D.J.; Hardingham, G.E. Recovery of NMDA receptor currents from MK-801 blockade is accelerated by Mg²⁺ and memantine under conditions of agonist exposure. *Neuropharmacology* **2013**, *74*, 119–125. [\[CrossRef\]](#)
46. Xia, P.; Chen, H.S.; Zhang, D.; Lipton, S.A. Memantine preferentially blocks extrasynaptic over synaptic NMDA receptor currents in hippocampal autapses. *J. Neurosci.* **2010**, *30*, 11246–11250. [\[CrossRef\]](#)
47. Wu, Y.N.; Johnson, S.W. Memantine selectively blocks extrasynaptic NMDA receptors in rat substantia nigra dopamine neurons. *Brain Res.* **2015**, *1603*, 1–7. [\[CrossRef\]](#)
48. Lacor, P.N.; Buniel, M.C.; Furlow, P.W.; Clemente, A.S.; Velasco, P.T.; Wood, M.; Viola, K.L.; Klein, W.L. Abeta oligomer-induced aberrations in synapse composition, shape, and density provide a molecular basis for loss of connectivity in Alzheimer's disease. *J. Neurosci.* **2007**, *27*, 796–807. [\[CrossRef\]](#)
49. Boeckers, T.M. The postsynaptic density. *Cell Tissue Res.* **2006**, *326*, 409–422. [\[CrossRef\]](#)
50. Dosemeci, A.; Tao-Cheng, J.H.; Vinade, L.; Jaffe, H. Preparation of postsynaptic density fraction from hippocampal slices and proteomic analysis. *Biochem. Biophys. Res. Commun.* **2006**, *339*, 687–694. [\[CrossRef\]](#)
51. Matas, E.; John Francis William, D.; Toro, C.T. Abnormal expression of post-synaptic proteins in prefrontal cortex of patients with schizophrenia. *Neurosci. Lett.* **2021**, *745*, 135629. [\[CrossRef\]](#) [\[PubMed\]](#)
52. He, R.B.; Li, L.; Liu, L.Z.; Ma, Y.J.; Fan, S.J.; Liu, L.R.; Li, W.B.; Xian, X.H. Ceftriaxone improves impairments in synaptic plasticity and cognitive behavior in APP/PS1 mouse model of Alzheimer's disease by inhibiting extrasynaptic NMDAR-STEP. *J. Neurochem.* **2023**, *166*, 215–232. [\[CrossRef\]](#) [\[PubMed\]](#)
53. Dewachter, I.; Filipkowski, R.K.; Priller, C.; Ris, L.; Neyton, J.; Croes, S.; Terwel, D.; Gysemans, M.; Devijver, H.; Borghgraef, P.; et al. Deregulation of NMDA-receptor function and down-stream signaling in APP[V717I] transgenic mice. *Neurobiol. Aging* **2009**, *30*, 241–256. [\[CrossRef\]](#) [\[PubMed\]](#)
54. Jiang, X.; Knox, R.; Pathipati, P.; Ferriero, D. Developmental localization of NMDA receptors, Src and MAP kinases in mouse brain. *Neurosci. Lett.* **2011**, *503*, 215–219. [\[CrossRef\]](#)
55. Pérez-Otaño, I.; Luján, R.; Tavalin, S.J.; Plomann, M.; Modregger, J.; Liu, X.B.; Jones, E.G.; Heinemann, S.F.; Lo, D.C.; Ehlers, M.D. Endocytosis and synaptic removal of NR3A-containing NMDA receptors by PACSIN1/syndapin1. *Nat. Neurosci.* **2006**, *9*, 611–621. [\[CrossRef\]](#)
56. De Marco García, N.V.; Karayannis, T.; Fishell, G. Neuronal activity is required for the development of specific cortical interneuron subtypes. *Nature* **2011**, *472*, 351–355. [\[CrossRef\]](#)
57. Moreau, A.W.; Kullmann, D.M. NMDA receptor-dependent function and plasticity in inhibitory circuits. *Neuropharmacology* **2013**, *74*, 23–31. [\[CrossRef\]](#)
58. Booker, S.A.; Wyllie, D.J.A. NMDA receptor function in inhibitory neurons. *Neuropharmacology* **2021**, *196*, 108609. [\[CrossRef\]](#)
59. Zhang, L.; Qin, Z.; Sharmin, F.; Lin, W.; Ricke, K.M.; Zasloff, M.A.; Stewart, A.F.R.; Chen, H.H. Tyrosine phosphatase PTP1B impairs presynaptic NMDA receptor-mediated plasticity in a mouse model of Alzheimer's disease. *Neurobiol. Dis.* **2021**, *156*, 105402. [\[CrossRef\]](#)
60. Nyíri, G.; Stephenson, F.A.; Freund, T.F.; Somogyi, P. Large variability in synaptic N-methyl-D-aspartate receptor density on interneurons and a comparison with pyramidal-cell spines in the rat hippocampus. *Neuroscience* **2003**, *119*, 347–363. [\[CrossRef\]](#)
61. Corlew, R.; Brasier, D.J.; Feldman, D.E.; Philpot, B.D. Presynaptic NMDA receptors: Newly appreciated roles in cortical synaptic function and plasticity. *Neuroscientist* **2008**, *14*, 609–625. [\[CrossRef\]](#) [\[PubMed\]](#)
62. Groc, L.; Bard, L.; Choquet, D. Surface trafficking of N-methyl-D-aspartate receptors: Physiological and pathological perspectives. *Neuroscience* **2009**, *158*, 4–18. [\[CrossRef\]](#) [\[PubMed\]](#)
63. Bard, L.; Groc, L. Glutamate receptor dynamics and protein interaction: Lessons from the NMDA receptor. *Mol. Cell Neurosci.* **2011**, *48*, 298–307. [\[CrossRef\]](#)
64. Kharazia, V.N.; Weinberg, R.J. Immunogold localization of AMPA and NMDA receptors in somatic sensory cortex of albino rat. *J. Comp. Neurol.* **1999**, *412*, 292–302. [\[CrossRef\]](#)
65. Lee, M.C.; Ting, K.K.; Adams, S.; Brew, B.J.; Chung, R.; Guillemin, G.J. Characterisation of the expression of NMDA receptors in human astrocytes. *PLoS ONE* **2010**, *5*, e14123. [\[CrossRef\]](#) [\[PubMed\]](#)
66. Kirchhoff, F. Analysis of Functional NMDA Receptors in Astrocytes. *Methods Mol. Biol.* **2017**, *1677*, 241–251. [\[CrossRef\]](#)
67. Skowrońska, K.; Obara-Michlewska, M.; Zielińska, M.; Albrecht, J. NMDA Receptors in Astrocytes: In Search for Roles in Neurotransmission and Astrocytic Homeostasis. *Int. J. Mol. Sci.* **2019**, *20*, 309. [\[CrossRef\]](#)
68. Thomas, D.M.; Kuhn, D.M. MK-801 and dextromethorphan block microglial activation and protect against methamphetamine-induced neurotoxicity. *Brain Res.* **2005**, *1050*, 190–198. [\[CrossRef\]](#)
69. Wu, C.C.; Tzeng, C.Y.; Chang, C.Y.; Wang, J.D.; Chen, Y.F.; Chen, W.Y.; Kuan, Y.H.; Liao, S.L.; Wang, W.Y.; Chen, C.J. NMDA receptor inhibitor MK801 alleviated pro-inflammatory polarization of BV-2 microglia cells. *Eur. J. Pharmacol.* **2023**, *955*, 175927. [\[CrossRef\]](#)
70. Raghunatha, P.; Vosoughi, A.; Kauppinen, T.M.; Jackson, M.F. Microglial NMDA receptors drive pro-inflammatory responses via PARP-1/TRMP2 signaling. *Glia* **2020**, *68*, 1421–1434. [\[CrossRef\]](#)

71. Káradóttir, R.; Cavelier, P.; Bergersen, L.H.; Attwell, D. NMDA receptors are expressed in oligodendrocytes and activated in ischaemia. *Nature* **2005**, *438*, 1162–1166. [\[CrossRef\]](#) [\[PubMed\]](#)
72. Krizbai, I.A.; Deli, M.A.; Pestenác, A.; Siklós, L.; Szabó, C.A.; András, I.; Joó, F. Expression of glutamate receptors on cultured cerebral endothelial cells. *J. Neurosci. Res.* **1998**, *54*, 814–819. [\[CrossRef\]](#)
73. Kim, K.S.; Jeon, M.T.; Kim, E.S.; Lee, C.H.; Kim, D.G. Activation of NMDA receptors in brain endothelial cells increases transcellular permeability. *Fluids Barriers CNS* **2022**, *19*, 70. [\[CrossRef\]](#) [\[PubMed\]](#)
74. Chiu, A.M.; Wang, J.; Fiske, M.P.; Hubalkova, P.; Barse, L.; Gray, J.A.; Sanz-Clemente, A. NMDAR-Activated PP1 Dephosphorylates GluN2B to Modulate NMDAR Synaptic Content. *Cell Rep.* **2019**, *28*, 332–341.E5. [\[CrossRef\]](#)
75. Sanz-Clemente, A.; Matta, J.A.; Isaac, J.T.; Roche, K.W. Casein kinase 2 regulates the NR2 subunit composition of synaptic NMDA receptors. *Neuron* **2010**, *67*, 984–996. [\[CrossRef\]](#)
76. Jamet, Z.; Mergaux, C.; Meras, M.; Bouchet, D.; Villega, F.; Kreye, J.; Prüss, H.; Groc, L. NMDA receptor autoantibodies primarily impair the extrasynaptic compartment. *Brain* **2024**, *147*, 2745–2760. [\[CrossRef\]](#) [\[PubMed\]](#)
77. Dupuis, J.P.; Ladépêche, L.; Seth, H.; Bard, L.; Varela, J.; Mikasova, L.; Bouchet, D.; Rogemond, V.; Honnorat, J.; Hanse, E.; et al. Surface dynamics of GluN2B-NMDA receptors controls plasticity of maturing glutamate synapses. *EMBO J.* **2014**, *33*, 842–861. [\[CrossRef\]](#)
78. Ferreira, J.S.; Papouin, T.; Ladépêche, L.; Yao, A.; Langlais, V.C.; Bouchet, D.; Dulong, J.; Mothet, J.P.; Sacchi, S.; Pollegioni, L.; et al. Co-agonists differentially tune GluN2B-NMDA receptor trafficking at hippocampal synapses. *Elife* **2017**, *6*, e25492. [\[CrossRef\]](#)
79. Mikasova, L.; Xiong, H.; Kerkhofs, A.; Bouchet, D.; Krugers, H.J.; Groc, L. Stress hormone rapidly tunes synaptic NMDA receptor through membrane dynamics and mineralocorticoid signalling. *Sci. Rep.* **2017**, *7*, 8053. [\[CrossRef\]](#)
80. Sanz-Clemente, A.; Gray, J.A.; Ogilvie, K.A.; Nicoll, R.A.; Roche, K.W. Activated CaMKII couples GluN2B and casein kinase 2 to control synaptic NMDA receptors. *Cell Rep.* **2013**, *3*, 607–614. [\[CrossRef\]](#)
81. Yi, Z.; Petralia, R.S.; Fu, Z.; Swanwick, C.C.; Wang, Y.X.; Prybylowski, K.; Sans, N.; Vicini, S.; Wenthold, R.J. The role of the PDZ protein GIPC in regulating NMDA receptor trafficking. *J. Neurosci.* **2007**, *27*, 11663–11675. [\[CrossRef\]](#) [\[PubMed\]](#)
82. Allison, D.W.; Gelfand, V.I.; Spector, I.; Craig, A.M. Role of actin in anchoring postsynaptic receptors in cultured hippocampal neurons: Differential attachment of NMDA versus AMPA receptors. *J. Neurosci.* **1998**, *18*, 2423–2436. [\[CrossRef\]](#) [\[PubMed\]](#)
83. Li, D.; Specht, C.G.; Waites, C.L.; Butler-Munro, C.; Leal-Ortiz, S.; Foote, J.W.; Genoux, D.; Garner, C.C.; Montgomery, J.M. SAP97 directs NMDA receptor spine targeting and synaptic plasticity. *J. Physiol.* **2011**, *589*, 4491–4510. [\[CrossRef\]](#)
84. Escamilla, S.; Sáez-Valero, J.; Cuchillo-Ibáñez, I. Synaptic and extrasynaptic distribution of NMDA receptors in cortex of Alzheimer's disease patients. *Alzheimer's Dement.* **2024**, *in press*. [\[CrossRef\]](#)
85. Torrez, V.R.; Zimmer, E.R.; Kalinine, E.; Haas, C.B.; Zenki, K.C.; Muller, A.P.; Souza, D.O.; Portela, L.V. Memantine mediates astrocytic activity in response to excitotoxicity induced by PP2A inhibition. *Neurosci. Lett.* **2019**, *696*, 179–183. [\[CrossRef\]](#)
86. Wu, H.M.; Tzeng, N.S.; Qian, L.; Wei, S.J.; Hu, X.; Chen, S.H.; Rawls, S.M.; Flood, P.; Hong, J.S.; Lu, R.B. Novel neuroprotective mechanisms of memantine: Increase in neurotrophic factor release from astroglia and anti-inflammation by preventing microglial activation. *Neuropsychopharmacology* **2009**, *34*, 2344–2357. [\[CrossRef\]](#)
87. Murakawa-Hirachi, T.; Mizoguchi, Y.; Ohgidani, M.; Haraguchi, Y.; Monji, A. Effect of memantine, an anti-Alzheimer's drug, on rodent microglial cells in vitro. *Sci. Rep.* **2021**, *11*, 6151. [\[CrossRef\]](#)
88. Parsons, M.P.; Raymond, L.A. Extrasynaptic NMDA receptor involvement in central nervous system disorders. *Neuron* **2014**, *82*, 279–293. [\[CrossRef\]](#)
89. Bading, H. Therapeutic targeting of the pathological triad of extrasynaptic NMDA receptor signaling in neurodegenerations. *J. Exp. Med.* **2017**, *214*, 569–578. [\[CrossRef\]](#) [\[PubMed\]](#)
90. Carles, A.; Freysson, A.; Perin-Dureau, F.; Rubinstenn, G.; Maurice, T. Targeting. *Int. J. Mol. Sci.* **2024**, *25*, 3733. [\[CrossRef\]](#)
91. Masliah, E.; Alford, M.; DeTeresa, R.; Mallory, M.; Hansen, L. Deficient glutamate transport is associated with neurodegeneration in Alzheimer's disease. *Ann. Neurol.* **1996**, *40*, 759–766. [\[CrossRef\]](#)
92. Jacob, C.P.; Koutsilieri, E.; Bartl, J.; Neuen-Jacob, E.; Arzberger, T.; Zander, N.; Ravid, R.; Roggendorf, W.; Riederer, P.; Grünblatt, E. Alterations in expression of glutamatergic transporters and receptors in sporadic Alzheimer's disease. *J. Alzheimer's Dis.* **2007**, *11*, 97–116. [\[CrossRef\]](#) [\[PubMed\]](#)
93. Scott, H.A.; Gebhardt, F.M.; Mitrovic, A.D.; Vandenberg, R.J.; Dodd, P.R. Glutamate transporter variants reduce glutamate uptake in Alzheimer's disease. *Neurobiol. Aging* **2011**, *32*, 553.e1–553.e11. [\[CrossRef\]](#) [\[PubMed\]](#)
94. Lévillé, F.; El Gaamouch, F.; Gouix, E.; Lecocq, M.; Lobner, D.; Nicole, O.; Buisson, A. Neuronal viability is controlled by a functional relation between synaptic and extrasynaptic NMDA receptors. *FASEB J.* **2008**, *22*, 4258–4271. [\[CrossRef\]](#)
95. Folch, J.; Busquets, O.; Ettchet, M.; Sánchez-López, E.; Castro-Torres, R.D.; Verdager, E.; Garcia, M.L.; Olloquequi, J.; Casadesús, G.; Beas-Zarate, C.; et al. Memantine for the Treatment of Dementia: A Review on its Current and Future Applications. *J. Alzheimer's Dis.* **2018**, *62*, 1223–1240. [\[CrossRef\]](#)
96. Parsons, C.G.; Danyasz, W.; Dekundy, A.; Pulte, I. Memantine and cholinesterase inhibitors: Complementary mechanisms in the treatment of Alzheimer's disease. *Neurotox. Res.* **2013**, *24*, 358–369. [\[CrossRef\]](#) [\[PubMed\]](#)
97. Wilkinson, D. A review of the effects of memantine on clinical progression in Alzheimer's disease. *Int. J. Geriatr. Psychiatry* **2012**, *27*, 769–776. [\[CrossRef\]](#)
98. Karimi Tari, P.; Parsons, C.G.; Collingridge, G.L.; Rammes, G. Memantine: Updating a rare success story in pro-cognitive therapeutics. *Neuropharmacology* **2024**, *244*, 109737. [\[CrossRef\]](#)

99. Armada-Moreira, A.; Gomes, J.I.; Pina, C.C.; Savchak, O.K.; Gonçalves-Ribeiro, J.; Rei, N.; Pinto, S.; Morais, T.P.; Martins, R.S.; Ribeiro, F.F.; et al. Going the Extra (Synaptic) Mile: Excitotoxicity as the Road Toward Neurodegenerative Diseases. *Front. Cell. Neurosci.* **2020**, *14*, 90. [\[CrossRef\]](#) [\[PubMed\]](#)
100. Liu, J.; Chang, L.; Song, Y.; Li, H.; Wu, Y. The Role of NMDA Receptors in Alzheimer's Disease. *Front. Neurosci.* **2019**, *13*, 43. [\[CrossRef\]](#)
101. Liu, W.; Li, Y.; Zhao, T.; Gong, M.; Wang, X.; Zhang, Y.; Xu, L.; Li, W.; Jia, J. The role of N-methyl-D-aspartate glutamate receptors in Alzheimer's disease: From pathophysiology to therapeutic approaches. *Prog. Neurobiol.* **2023**, *231*, 102534. [\[CrossRef\]](#)
102. Talantova, M.; Sanz-Blasco, S.; Zhang, X.; Xia, P.; Akhtar, M.W.; Okamoto, S.; Dziewczapolski, G.; Nakamura, T.; Cao, G.; Pratt, A.E.; et al. A β induces astrocytic glutamate release, extrasynaptic NMDA receptor activation, and synaptic loss. *Proc. Natl. Acad. Sci. USA* **2013**, *110*, E2518–E2527. [\[CrossRef\]](#) [\[PubMed\]](#)
103. Bordji, K.; Becerril-Ortega, J.; Nicole, O.; Buisson, A. Activation of extrasynaptic, but not synaptic, NMDA receptors modifies amyloid precursor protein expression pattern and increases amyloid- β production. *J. Neurosci.* **2010**, *30*, 15927–15942. [\[CrossRef\]](#) [\[PubMed\]](#)
104. Sun, X.Y.; Tuo, Q.Z.; Liuyang, Z.Y.; Xie, A.J.; Feng, X.L.; Yan, X.; Qiu, M.; Li, S.; Wang, X.L.; Cao, F.Y.; et al. Extrasynaptic NMDA receptor-induced tau overexpression mediates neuronal death through suppressing survival signaling ERK phosphorylation. *Cell Death Dis.* **2016**, *7*, e2449. [\[CrossRef\]](#) [\[PubMed\]](#)
105. Xu, C.S.; Liu, A.C.; Chen, J.; Pan, Z.Y.; Wan, Q.; Li, Z.Q.; Wang, Z.F. Overactivation of NR2B-containing NMDA receptors through entorhinal-hippocampal connection initiates accumulation of hyperphosphorylated tau in rat hippocampus after transient middle cerebral artery occlusion. *J. Neurochem.* **2015**, *134*, 566–577. [\[CrossRef\]](#)
106. Amadoro, G.; Ciotti, M.T.; Costanzi, M.; Cestari, V.; Calissano, P.; Canu, N. NMDA receptor mediates tau-induced neurotoxicity by calpain and ERK/MAPK activation. *Proc. Natl. Acad. Sci. USA* **2006**, *103*, 2892–2897. [\[CrossRef\]](#) [\[PubMed\]](#)
107. Hoey, S.E.; Williams, R.J.; Perkinson, M.S. Synaptic NMDA receptor activation stimulates alpha-secretase amyloid precursor protein processing and inhibits amyloid-beta production. *J. Neurosci.* **2009**, *29*, 4442–4460. [\[CrossRef\]](#)
108. Varshavskaya, K.B.; Mitkevich, V.A.; Makarov, A.A.; Barykin, E.P. Synthetic, Cell-Derived, Brain-Derived, and Recombinant β -Amyloid: Modelling Alzheimer's Disease for Research and Drug Development. *Int. J. Mol. Sci.* **2022**, *23*, 15036. [\[CrossRef\]](#) [\[PubMed\]](#)
109. Chen, Z.Y.; Zhang, Y. Animal models of Alzheimer's disease: Applications, evaluation, and perspectives. *Zool. Res.* **2022**, *43*, 1026–1040. [\[CrossRef\]](#)
110. Drummond, E.; Wisniewski, T. Alzheimer's disease: Experimental models and reality. *Acta Neuropathol.* **2017**, *133*, 155–175. [\[CrossRef\]](#)
111. Yin, X.; Zhao, C.; Qiu, Y.; Zhou, Z.; Bao, J.; Qian, W. Dendritic/Post-synaptic Tau and Early Pathology of Alzheimer's Disease. *Front. Mol. Neurosci.* **2021**, *14*, 671779. [\[CrossRef\]](#)
112. Ittner, L.M.; Ke, Y.D.; Delerue, F.; Bi, M.; Gladbach, A.; van Eersel, J.; Wölfling, H.; Chieng, B.C.; Christie, M.J.; Napier, I.A.; et al. Dendritic function of tau mediates amyloid-beta toxicity in Alzheimer's disease mouse models. *Cell* **2010**, *142*, 387–397. [\[CrossRef\]](#) [\[PubMed\]](#)
113. Alfaro-Ruiz, R.; Aguado, C.; Martín-Belmonte, A.; Moreno-Martínez, A.E.; Merchán-Rubira, J.; Hernández, F.; Ávila, J.; Fukazawa, Y.; Luján, R. Different modes of synaptic and extrasynaptic NMDA receptor alteration in the hippocampus of P301S tau transgenic mice. *Brain Pathol.* **2023**, *33*, e13115. [\[CrossRef\]](#)
114. Ma, D.L.; Luo, Y.; Huang, R.; Zhao, Z.R.; Zhang, L.; Li, Y.L.; Wang, Q.; Li, L. Cornel Iridoid Glycoside Suppresses Hyperactivity Phenotype in rTg4510 Mice through Reducing Tau Pathology and Improving Synaptic Dysfunction. *Curr. Med. Sci.* **2020**, *40*, 1031–1039. [\[CrossRef\]](#)
115. Hering, H.; Sheng, M. Dendritic spines: Structure, dynamics and regulation. *Nat. Rev. Neurosci.* **2001**, *2*, 880–888. [\[CrossRef\]](#) [\[PubMed\]](#)
116. Regan, P.; Mitchell, S.J.; Kim, S.C.; Lee, Y.; Yi, J.H.; Barbati, S.A.; Shaw, C.; Cho, K. Regulation of Synapse Weakening through Interactions of the Microtubule Associated Protein Tau with PACSIN1. *J. Neurosci.* **2021**, *41*, 7162–7170. [\[CrossRef\]](#)
117. Tsai, Y.C.; Huang, S.M.; Peng, H.H.; Lin, S.W.; Lin, S.R.; Chin, T.Y. Imbalance of synaptic and extrasynaptic NMDA receptors induced by the deletion of CRMP1 accelerates age-related cognitive decline in mice. *Neurobiol. Aging* **2024**, *135*, 48–59. [\[CrossRef\]](#)
118. Nakamura, F.; Kumeta, K.; Hida, T.; Isono, T.; Nakayama, Y.; Kuramata-Matsuoka, E.; Yamashita, N.; Uchida, Y.; Ogura, K.; Gengyo-Ando, K.; et al. Amino- and carboxyl-terminal domains of Filamin-A interact with CRMP1 to mediate Sema3A signalling. *Nat. Commun.* **2014**, *5*, 5325. [\[CrossRef\]](#) [\[PubMed\]](#)
119. Quach, T.T.; Moutal, A.; Khanna, R.; Deems, N.P.; Duchemin, A.M.; Barrientos, R.M. Collapsin Response Mediator Proteins: Novel Targets for Alzheimer's Disease. *J. Alzheimer's Dis.* **2020**, *77*, 949–960. [\[CrossRef\]](#)
120. Pallas-Bazarra, N.; Draffin, J.; Cuadros, R.; Antonio Esteban, J.; Avila, J. Tau is required for the function of extrasynaptic NMDA receptors. *Sci. Rep.* **2019**, *9*, 9116. [\[CrossRef\]](#)
121. Goebel-Goody, S.M.; Davies, K.D.; Alvestad Linger, R.M.; Freund, R.K.; Browning, M.D. Phospho-regulation of synaptic and extrasynaptic N-methyl-d-aspartate receptors in adult hippocampal slices. *Neuroscience* **2009**, *158*, 1446–1459. [\[CrossRef\]](#)
122. Whiteman, I.T.; Minamide, L.S.; Goh, d.L.; Bamburg, J.R.; Goldsbury, C. Rapid changes in phospho-MAP/tau epitopes during neuronal stress: Cofilin-actin rods primarily recruit microtubule binding domain epitopes. *PLoS ONE* **2011**, *6*, e20878. [\[CrossRef\]](#)

123. Rosenberger, A.F.; Morrema, T.H.; Gerritsen, W.H.; van Haastert, E.S.; Snkhchyan, H.; Hilhorst, R.; Rozemuller, A.J.; Scheltens, P.; van der Vies, S.M.; Hoozemans, J.J. Increased occurrence of protein kinase CK2 in astrocytes in Alzheimer's disease pathology. *J. Neuroinflamm.* **2016**, *13*, 4. [\[CrossRef\]](#) [\[PubMed\]](#)
124. Shankar, G.M.; Bloodgood, B.L.; Townsend, M.; Walsh, D.M.; Selkoe, D.J.; Sabatini, B.L. Natural oligomers of the Alzheimer amyloid-beta protein induce reversible synapse loss by modulating an NMDA-type glutamate receptor-dependent signaling pathway. *J. Neurosci.* **2007**, *27*, 2866–2875. [\[CrossRef\]](#) [\[PubMed\]](#)
125. Goto, Y.; Niidome, T.; Akaike, A.; Kihara, T.; Sugimoto, H. Amyloid beta-peptide preconditioning reduces glutamate-induced neurotoxicity by promoting endocytosis of NMDA receptor. *Biochem. Biophys. Res. Commun.* **2006**, *351*, 259–265. [\[CrossRef\]](#) [\[PubMed\]](#)
126. Kurup, P.; Zhang, Y.; Xu, J.; Venkitaramani, D.V.; Haroutunian, V.; Greengard, P.; Nairn, A.C.; Lombroso, P.J. Abeta-mediated NMDA receptor endocytosis in Alzheimer's disease involves ubiquitination of the tyrosine phosphatase STEP61. *J. Neurosci.* **2010**, *30*, 5948–5957. [\[CrossRef\]](#)
127. Dinamarca, M.C.; Colombes, M.; Cerpa, W.; Bonansco, C.; Inestrosa, N.C. Beta-amyloid oligomers affect the structure and function of the postsynaptic region: Role of the Wnt signaling pathway. *Neurodegener. Dis.* **2008**, *5*, 149–152. [\[CrossRef\]](#)
128. Olajide, O.J.; Chapman, C.A. Amyloid- β (1-42) peptide induces rapid NMDA receptor-dependent alterations at glutamatergic synapses in the entorhinal cortex. *Neurobiol. Aging* **2021**, *105*, 296–309. [\[CrossRef\]](#) [\[PubMed\]](#)
129. Huh, K.H.; Wenthold, R.J. Turnover analysis of glutamate receptors identifies a rapidly degraded pool of the N-methyl-D-aspartate receptor subunit, NR1, in cultured cerebellar granule cells. *J. Biol. Chem.* **1999**, *274*, 151–157. [\[CrossRef\]](#)
130. Rammes, G.; Mattusch, C.; Wulff, M.; Seeser, F.; Kreuzer, M.; Zhu, K.; Deussing, J.M.; Herms, J.; Parsons, C.G. Involvement of GluN2B subunit containing N-methyl-d-aspartate (NMDA) receptors in mediating the acute and chronic synaptotoxic effects of oligomeric amyloid-beta ($A\beta$) in murine models of Alzheimer's disease (AD). *Neuropharmacology* **2017**, *123*, 100–115. [\[CrossRef\]](#)
131. Dodd, P.R.; Hardy, J.A.; Baig, E.B.; Kidd, A.M.; Bird, E.D.; Watson, W.E.; Johnston, G.A. Optimization of freezing, storage, and thawing conditions for the preparation of metabolically active synaptosomes from frozen rat and human brain. *Neurochem. Pathol.* **1986**, *4*, 177–198. [\[CrossRef\]](#)
132. Mishizen-Eberz, A.J.; Rissman, R.A.; Carter, T.L.; Ikonovic, M.D.; Wolfe, B.B.; Armstrong, D.M. Biochemical and molecular studies of NMDA receptor subunits NR1/2A/2B in hippocampal subregions throughout progression of Alzheimer's disease pathology. *Neurobiol. Dis.* **2004**, *15*, 80–92. [\[CrossRef\]](#) [\[PubMed\]](#)
133. Wang, Y.; TesFaye, E.; Yasuda, R.P.; Mash, D.C.; Armstrong, D.M.; Wolfe, B.B. Effects of post-mortem delay on subunits of ionotropic glutamate receptors in human brain. *Brain Res. Mol. Brain Res.* **2000**, *80*, 123–131. [\[CrossRef\]](#) [\[PubMed\]](#)
134. Lau, S.F.; Cao, H.; Fu, A.K.Y.; Ip, N.Y. Single-nucleus transcriptome analysis reveals dysregulation of angiogenic endothelial cells and neuroprotective glia in Alzheimer's disease. *Proc. Natl. Acad. Sci. USA* **2020**, *117*, 25800–25809. [\[CrossRef\]](#) [\[PubMed\]](#)
135. Hardy, J.A.; Dodd, P.R.; Oakley, A.E.; Perry, R.H.; Edwardson, J.A.; Kidd, A.M. Metabolically active synaptosomes can be prepared from frozen rat and human brain. *J. Neurochem.* **1983**, *40*, 608–614. [\[CrossRef\]](#) [\[PubMed\]](#)
136. Bayés, À.; Collins, M.O.; Galtrey, C.M.; Simonnet, C.; Roy, M.; Croning, M.D.; Gou, G.; van de Lagemaat, L.N.; Milward, D.; Whittle, I.R.; et al. Human post-mortem synapse proteome integrity screening for proteomic studies of postsynaptic complexes. *Mol. Brain* **2014**, *7*, 88. [\[CrossRef\]](#)
137. Bi, H.; Sze, C.I. N-methyl-D-aspartate receptor subunit NR2A and NR2B messenger RNA levels are altered in the hippocampus and entorhinal cortex in Alzheimer's disease. *J. Neurol. Sci.* **2002**, *200*, 11–18. [\[CrossRef\]](#)
138. Hynd, M.R.; Scott, H.L.; Dodd, P.R. Differential expression of N-methyl-D-aspartate receptor NR2 isoforms in Alzheimer's disease. *J. Neurochem.* **2004**, *90*, 913–919. [\[CrossRef\]](#)
139. Hynd, M.R.; Scott, H.L.; Dodd, P.R. Glutamate(NMDA) receptor NR1 subunit mRNA expression in Alzheimer's disease. *J. Neurochem.* **2001**, *78*, 175–182. [\[CrossRef\]](#)
140. Das, S.; Li, Z.; Wachter, A.; Alla, S.; Noori, A.; Abdourahman, A.; Tamm, J.A.; Woodbury, M.E.; Talanian, R.V.; Biber, K.; et al. Distinct transcriptomic responses to $A\beta$ plaques, neurofibrillary tangles, and APOE in Alzheimer's disease. *Alzheimer's Dement.* **2024**, *20*, 74–90. [\[CrossRef\]](#)
141. Mathys, H.; Davila-Velderrain, J.; Peng, Z.; Gao, F.; Mohammadi, S.; Young, J.Z.; Menon, M.; He, L.; Abdurrob, F.; Jiang, X.; et al. Single-cell transcriptomic analysis of Alzheimer's disease. *Nature* **2019**, *570*, 332–337. [\[CrossRef\]](#)
142. Bossers, K.; Wirz, K.T.; Meerhoff, G.F.; Essing, A.H.; van Dongen, J.W.; Houba, P.; Kruse, C.G.; Verhaagen, J.; Swaab, D.F. Concerted changes in transcripts in the prefrontal cortex precede neuropathology in Alzheimer's disease. *Brain* **2010**, *133*, 3699–3723. [\[CrossRef\]](#) [\[PubMed\]](#)
143. Qian, Z.; Qin, J.; Lai, Y.; Zhang, C.; Zhang, X. Large-Scale Integration of Single-Cell RNA-Seq Data Reveals Astrocyte Diversity and Transcriptomic Modules across Six Central Nervous System Disorders. *Biomolecules* **2023**, *13*, 692. [\[CrossRef\]](#) [\[PubMed\]](#)
144. Sze, C.; Bi, H.; Kleinschmidt-DeMasters, B.K.; Filley, C.M.; Martin, L.J. N-Methyl-D-aspartate receptor subunit proteins and their phosphorylation status are altered selectively in Alzheimer's disease. *J. Neurol. Sci.* **2001**, *182*, 151–159. [\[CrossRef\]](#) [\[PubMed\]](#)
145. Ortiz-Sanz, C.; Balantzategi, U.; Quintela-López, T.; Ruiz, A.; Luchena, C.; Zuazo-Ibarra, J.; Capetillo-Zarate, E.; Matute, C.; Zugaza, J.L.; Alberdi, E. Amyloid β /PKC-dependent alterations in NMDA receptor composition are detected in early stages of Alzheimer's disease. *Cell Death Dis.* **2022**, *13*, 253. [\[CrossRef\]](#) [\[PubMed\]](#)
146. Kravitz, E.; Gaisler-Salomon, I.; Biegon, A. Hippocampal glutamate NMDA receptor loss tracks progression in Alzheimer's disease: Quantitative autoradiography in postmortem human brain. *PLoS ONE* **2013**, *8*, e81244. [\[CrossRef\]](#)

147. Yeung, J.H.Y.; Walby, J.L.; Palpagama, T.H.; Turner, C.; Waldvogel, H.J.; Faull, R.L.M.; Kwakowsky, A. Glutamatergic receptor expression changes in the Alzheimer's disease hippocampus and entorhinal cortex. *Brain Pathol.* **2021**, *31*, e13005. [[CrossRef](#)]
148. Lee, H.G.; Wheeler, M.A.; Quintana, F.J. Function and therapeutic value of astrocytes in neurological diseases. *Nat. Rev. Drug Discov.* **2022**, *21*, 339–358. [[CrossRef](#)]
149. Krasnow, A.M.; Attwell, D. NMDA Receptors: Power Switches for Oligodendrocytes. *Neuron* **2016**, *91*, 3–5. [[CrossRef](#)]
150. Cao, N.; Yao, Z.X. Oligodendrocyte N-methyl-D-aspartate receptor signaling: Insights into its functions. *Mol. Neurobiol.* **2013**, *47*, 845–856. [[CrossRef](#)]
151. Liu, H.; Leak, R.K.; Hu, X. Neurotransmitter receptors on microglia. *Stroke Vasc. Neurol.* **2016**, *1*, 52–58. [[CrossRef](#)]
152. Hogan-Cann, A.D.; Anderson, C.M. Physiological Roles of Non-Neuronal NMDA Receptors. *Trends Pharmacol. Sci.* **2016**, *37*, 750–767. [[CrossRef](#)]
153. Tovar, K.R.; Westbrook, G.L. The incorporation of NMDA receptors with a distinct subunit composition at nascent hippocampal synapses in vitro. *J. Neurosci.* **1999**, *19*, 4180–4188. [[CrossRef](#)] [[PubMed](#)]
154. Lai, T.W.; Shyu, W.C.; Wang, Y.T. Stroke intervention pathways: NMDA receptors and beyond. *Trends Mol. Med.* **2011**, *17*, 266–275. [[CrossRef](#)] [[PubMed](#)]
155. Zhou, X.; Ding, Q.; Chen, Z.; Yun, H.; Wang, H. Involvement of the GluN2A and GluN2B subunits in synaptic and extrasynaptic N-methyl-D-aspartate receptor function and neuronal excitotoxicity. *J. Biol. Chem.* **2013**, *288*, 24151–24159. [[CrossRef](#)]
156. Jhou, J.F.; Tai, H.C. The Study of Postmortem Human Synaptosomes for Understanding Alzheimer's Disease and Other Neurological Disorders: A Review. *Neurol. Ther.* **2017**, *6*, 57–68. [[CrossRef](#)]
157. Höhn, L.; Hußler, W.; Richter, A.; Smalla, K.H.; Birkel-Toeglhofer, A.M.; Birkel, C.; Vielhaber, S.; Leber, S.L.; Gundelfinger, E.D.; Haybaeck, J.; et al. Extracellular Matrix Changes in Subcellular Brain Fractions and Cerebrospinal Fluid of Alzheimer's Disease Patients. *Int. J. Mol. Sci.* **2023**, *24*, 5532. [[CrossRef](#)] [[PubMed](#)]
158. Mueller, T.M.; Kim, P.; Meador-Woodruff, J.H. Fractionation of Subcellular Compartments from Human Brain Tissue. *Methods Mol. Biol.* **2019**, *1941*, 201–223. [[CrossRef](#)]
159. Luabeya, M.K.; Vanisberg, M.A.; Jeanjean, A.P.; Baudhuin, P.; Laduron, P.M.; Maloteaux, J.M. Fractionation of human brain by differential and isopycnic equilibration techniques. *Brain Res. Brain Res. Protoc.* **1997**, *1*, 83–90. [[CrossRef](#)]
160. Maloteaux, J.M.; Luabeya, M.K.; Vanisberg, M.A.; Jeanjean, A.P.; Baudhuin, P.; Scherman, D.; Laduron, P.M. Subcellular distribution of receptor sites in human brain: Differentiation between heavy and light structures of high and low density. *Brain Res.* **1995**, *687*, 155–166. [[CrossRef](#)]
161. Zhang, W.; Ross, P.J.; Ellis, J.; Salter, M.W. Targeting NMDA receptors in neuropsychiatric disorders by drug screening on human neurons derived from pluripotent stem cells. *Transl. Psychiatry* **2022**, *12*, 243. [[CrossRef](#)]
162. Lao, K.; Ji, N.; Zhang, X.; Qiao, W.; Tang, Z.; Gou, X. Drug development for Alzheimer's disease: Review. *J. Drug Target.* **2019**, *27*, 164–173. [[CrossRef](#)] [[PubMed](#)]

Disclaimer/Publisher's Note: The statements, opinions and data contained in all publications are solely those of the individual author(s) and contributor(s) and not of MDPI and/or the editor(s). MDPI and/or the editor(s) disclaim responsibility for any injury to people or property resulting from any ideas, methods, instructions or products referred to in the content.

9. Agradecimientos

Me encuentro en un cruce de caminos. Hacia atrás veo el sendero que me ha llevado hasta aquí, con sus luces y sus sombras, sus subidas y bajadas. Por delante sigue el sendero, aunque la vista no me alcanza a ver dónde me lleva. Como bien saben mis directores de tesis estoy ansioso de seguir construyendo ese sendero, de construirlo a la mayor velocidad posible. Pero ahora es momento de parar y mirar atrás para agradecer a tod@s aquell@s que me han ayudado a no flaquear, a confiar en mí mismo y a guiarme en estos años de viaje.

Llegué al laboratorio en 2018 para unas prácticas de verano, y madre mía para lo que ha dado. Me quedé para hacer el TFG, luego el TFM, y terminé haciendo los 4 años de tesis en el mismo laboratorio, el gran 241. Agradezco mi estancia en este grupo, ya que he disfrutado de una compañía agradable, he tenido la libertad que necesitaba y las oportunidades que merecía.

En primer lugar, quiero agradecer a Inma el haber confiado en mí y haberme dado la libertad que necesitaba para desarrollarme como investigador, pero también para enseñarme, guiarme y ayudarme siempre que lo he necesitado. No he tenido la sensación de tener en ella a una jefa, sino a una compañera a la que he podido comentar cualquier pifiada sin miedo a sentirme reprendido. Gracias también por haber trascendido la barrera de la compañera de trabajo y hablar de cosas personales, que han hecho del laboratorio un sitio más agradable y cómodo. También son de agradecer las innumerables conversaciones científicas que han estimulado mi pensamiento.

Creo que el segundo en la lista debe ser Javier. Gracias por ayudarme en todo lo que ha estado en su mano, por contestar mails importantes, aunque estuviese muy ocupado y por darme la oportunidad de poder entrar en varios trabajos. También es de agradecer su carácter afable, tranquilo y simpático, pero que no ha impedido tener un tono autoritario cuando ha sido conveniente. He aprendido cosas de él a nivel científico, pero también a cómo ser jefe.

Y gracias, por encima de todos, a Susana, mi señora esposa. Muchos conocidos me han dicho que no saben cómo puedo trabajar tanto, ser tan productivo o aguantar tanto la presión. La respuesta es ella. Sin Susana recibíendome con una sonrisa en casa tras un día de 11 horas de trabajo hubiera sido absolutamente imposible mantener este ritmo sin que me petara la cabeza. Ella es lo más importante de mi vida. Así que gracias por quererme, por entender mi modo de vida, y por acompañarme en esta futura aventura y seguir recorriendo el sendero conmigo.

Gracias a mis padres y mi hermano por apoyarme y estar orgullosos de mí. Por quererme incondicionalmente y sentir que en ellos tengo un núcleo, un refugio que siempre estará ahí, pase lo que pase. Os quiero mucho.

Gracias a Dani Tendero por ser un compañero de centro de trabajo convertido en uno de mis mejores amigos. Gracias a él el lugar de trabajo ha sido un lugar infinitamente más acogedor. Sin duda es la persona con la que más cafés he tomado (y los que nos quedan).

Gracias a Mari por ser la mejor compañera de laboratorio imaginable, y por haberte convertido en una buena amiga. Gracias por las conversaciones, las risas y las bronquitas. Sin duda eres de las personas que más cosas me ha enseñado y que todavía tiene por enseñar.

Gracias a Carlos por hacer de la investigación una cosa de intercambio de opiniones dinámico. He encontrado en él a un verdadero “colega” en el sentido original del término. Gracias por haber tomado el relevo de las células y enhorabuena, eres un crack. Gracias también al resto de compañeros de laboratorio que han hecho del lugar de trabajo un sitio acogedor.

Gracias a Joan, Javi y Dani por haberos convertido en algo más que amigos. Por estar ahí en los buenos y en los malos momentos. Y gracias por tantas conversaciones estimulantes. Sin haber estado vosotros ahí estimulando mis ideas quizás no estaría escribiendo esto.

Por último, gracias a Fede por haberme dado la oportunidad de ir a los EEUU a probarme a mí mismo. De esa fantástica aventura me llevé a un buen amigo y me dejé el síndrome del impostor que tanto atenazaba mi ser y mi futuro. Gracias por abrirme su casa y hacerme sentir como si fuese mía. Por apostar por mí y por tu generosidad, científica y personal. Y por darme la oportunidad que cambiará mi vida. Creo que no voy a defraudar a nadie, ni a él ni a mí mismo.